

BIO-HYDROGEN AND BIOMASS- SUPPORTED PALLADIUM CATALYST FOR ENERGY PRODUCTION AND WASTE- MINIMISATION

by

Mark D. Redwood

A thesis submitted to
The University of Birmingham
For the degree of
DOCTOR OF PHILOSOPHY

School of Biosciences
The University of Birmingham
September 2007

UNIVERSITY OF
BIRMINGHAM

University of Birmingham Research Archive

e-theses repository

This unpublished thesis/dissertation is copyright of the author and/or third parties. The intellectual property rights of the author or third parties in respect of this work are as defined by The Copyright Designs and Patents Act 1988 or as modified by any successor legislation.

Any use made of information contained in this thesis/dissertation must be in accordance with that legislation and must be properly acknowledged. Further distribution or reproduction in any format is prohibited without the permission of the copyright holder.

Abstract

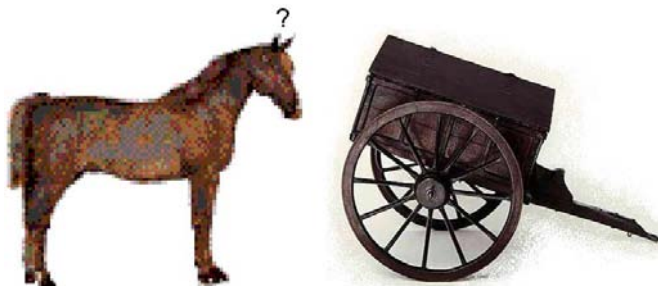
The project objective was to advance the development of the H₂ economy by improving biological H₂ production in a sustainable way. Pseudo-continuous H₂ production was achieved with improved efficiency, *via* the bacterial fermentation of sugars in a dual-bioreactor ('upstream system') comprising a dark fermentation coupled to a photofermentation. Excess biomass from the upstream system was used to recover palladium from solution, producing 'palladised biomass' (Bio-Pd(0)), which was useful in the construction of bioinorganic catalytic anodes for the electricity generation from bio-H₂ using a polymer electrolyte membrane fuel cell ('downstream system'). Furthermore, the catalytic usefulness of Bio-Pd(0) was confirmed in several reactions in comparison with other palladised biomasses and with Pd(0) made chemically.

The upstream modules: *Escherichia coli* dark fermentation and *Rhodobacter sphaeroides* photofermentation, were investigated and developed separately, before coupling the two stages by the novel application of electrodialysis (accelerated membrane separation). The biorecovery and testing of palladium bionanocatalyst are described, before the production of fuel cell catalyst using waste biomass. The technical challenges and potential benefits of biohydrogen production are discussed and contrasted with those of competing biofuel technologies.

Dedicated to my family

Acknowledgements

Foremost thanks to my supervisor, Professor Lynne E. Macaskie, for all she has taught me, for her leadership and patience, and for always putting the cart before the horse.



I owe a great debt to our collaborators Dr Frank Sargent, Dr Wolfgang Skibar, Mr Duncan Stratton-Campbell, and Dr Mike Wright for their contributing work (acknowledged where appropriate) and advice and to Mr Nick G May, Mr Graham D Burns and Mr Peter R Ashton for their assistance with chemical analysis.

I would like to thank Dr Frank S Yates, Prof Jeff Cole, Dr Doug Browning, and Miss Catherine Redwood for their helpful advice and discussions.

Special thanks to all my colleagues at the Unit of Functional Bionanomaterials, especially Mr Kevin (the Plank) Deplanche, Dr Marion (Hawkeyes) Paterson-Beedle, Dr Iryna (Mummy) Mikheenko, Dr David (the c**k) Penfold, Dr Ping (-aling) Yong, Dr Neil (Fontofallknowledge) Creamer, Dr Douglas (the face) Sanyahumbi, Ms Claire (Furryfruitophobe) Mennan, Ms Angela (Tartan chav) Murray, Ms Mitra (saary) Kashani, Ms Doro (source of Stöllen) Fiebiger, and Ms Virginie (Vivi) Marcadet. I would like to express my gratitude to the sadly deceased Dr 'Vic' Baxter-Plant, who is missed by all who knew her.

Thanks are also due to the BBSRC for funding me throughout my study.

Table of contents

| | |
|--|-----|
| 1 : Introduction | 1 |
| 1.0 Chapter contents | 1 |
| 1.1 Project concepts | 2 |
| 1.2 Integrating dark and light biohydrogen production: towards the hydrogen economy | 4 |
| 1.3 Downstream system: Biomass-supported palladium catalysts | 65 |
| 2 : Results | 76 |
| 2.0 Chapter contents | 76 |
| 2.1 Dissecting the roles of <i>Escherichia coli</i> hydrogenases in biohydrogen production..... | 78 |
| 2.2 Development of H ₂ production by <i>Escherichia coli</i> | 89 |
| 2.3 Development of photobiological H ₂ production by <i>Rhodobacter sphaeroides</i> | 113 |
| 2.4 A two-stage, two-organism process for biohydrogen from glucose..... | 130 |
| 2.5 Development of the electro dialysis technique for use in a dual system..... | 140 |
| 2.6 Linking dark and light H ₂ production by electro dialysis..... | 158 |
| 2.7 Biomass-supported palladium catalysts on <i>Desulfovibrio</i> and <i>Rhodobacter</i> | 175 |
| 2.8 Fuel cell anode construction to recycle biomass from biohydrogen production..... | 187 |
| 3 : Discussion | 199 |
| 3.0 Chapter summary and contents..... | 199 |
| 3.1 Dark fermentation by <i>Escherichia coli</i> | 201 |
| 3.2 Photofermentation by <i>Rhodobacter sphaeroides</i> | 203 |
| 3.3 Integrating the dual bioreactor by electro dialysis..... | 205 |
| 3.4 Biomass-supported palladium catalyst | 209 |
| 3.5 Environmental impacts | 210 |
| 3.6 Prominent technical challenges for future development | 213 |
| 4 : Appendices | 217 |
| 4.0 Chapter contents | 217 |
| 4.1 Methodology and validation | 218 |
| 4.2 Additional publications..... | 243 |
| 4.3 Video showing operational dual system..... | 284 |
| 5 : Bibliography | 285 |

Organisation of thesis

Each chapter begins with a Summary section, which defines the focus of the chapter in the context of the wider thesis, summarises conclusions and their significance to the wider project and acknowledges the inputs of colleagues into the study where appropriate. Due to the number of convergent themes of this project, each chapter of the results section is written in the form of a scientific paper, including a methods section and an independent reference list. Therefore, a single comprehensive methods section is not included methodology and validation are given in the appendices, along with other published work associated with this project to which the author contributed or which duplicates results described in the main body of this thesis. All work included in the body of the thesis was authored by myself and those in the appendices are accredited as appropriate.

List of illustrations

Section 1.2.1 (review article)

- Figure 1: Direct and indirect photolysis.
- Figure 2: Suitable dark fermentations for dual systems.
- Figure 3: Dual systems in co-culture and in sequential reactors.
- Figure 4: Spatial feasibility of de-centralized energy generation.

Section 2.1.1 (research letter published in FEMS Microbiology Letters)

- Fig. 1. Metabolic scheme for mixed acid fermentation.
- Fig. 2. H₂ production by *E. coli* strains deficient in HycA (A), and uptake hydrogenases (B).

| | |
|---|-----|
| Figure 1.1-a Project Concept..... | 2 |
| Figure 1.3-a Changes in the supply of palladium over the past decade. | 67 |
| Figure 1.3-b Palladised cells of <i>Desulfovibrio desulfuricans</i> | 68 |
| Figure 1.3-c Functioning of a polymer electrolyte membrane fuel cell (PEM-FC). | 70 |
| Figure 1.3-d <i>Rhodobacter capsulatus</i> grown in the presence of tellurite, showing needlelike granules of tellurium under electron microscopy. | 73 |
| Figure 2.1-a Fates of potential H ₂ in <i>Escherichia coli</i> strains deficient in HycA (A), and uptake hydrogenases (B). | 88 |
| Figure 2.2-a Phase 1: Batch mode with phosphate buffer. | 94 |
| Figure 2.2-b Phase 2: Effect of pH on mixed-acid fermentation. | 96 |
| Figure 2.2-c H ₂ production (A) and traces of organic acids and glucose (B) in phase 3 fermentations and division of the experiments into 4 stages (C). | 99 |
| Figure 2.2-d HPLC-MS analysis of butyrate. | 101 |
| Figure 2.2-e Elements of fermentation balance during mixed-acid fermentation (MAF) and butyrate-type fermentation, occurring in the 1 st and subsequent stages, respectively, of phase 3 fermentations. | 102 |
| Figure 2.2-f Generic hydrogenation of enoyl-CoA to acyl-CoA species. | 105 |
| Figure 2.2-g Putative <i>Escherichia coli</i> BCADs and their conserved functional domain topologies. | 108 |
| Figure 2.2-h Alignment of putative <i>Escherichia coli</i> K-12 BCAD (accession: AP_000876) and five representative bacterial BCAD sequences. | 109 |
| Figure 2.3-a A photobioreactor for the continuous culture of <i>Rhodobacter sphaeroides</i> | 118 |
| Figure 2.3-b The effect of initial acetate concentration on H ₂ production by <i>Rhodobacter sphaeroides</i> | 120 |
| Figure 2.3-c The effect of culture density on H ₂ production (A, B) and growth (C). | 122 |
| Figure 2.3-d H ₂ production (A), substrate conversion efficiency (B) and residual substrate in continuous cultures of <i>Rhodobacter sphaeroides</i> , diluted with synthetic organic acid medium. | 129 |

Section 2.4.1 (article published in the International Journal of Hydrogen Energy)

- Fig. 1. Overall scheme
- Fig. 2. Growth of *R. sphaeroides* on *E. coli* spent fermentation liquor and neutralization of pH
- Fig. 3. Removal of organic compounds from fermentation liquor by *R. sphaeroides*.

| | | |
|--|--|-----|
| Figure 2.5-a | An electro dialysis (ED) cell using a ‘BAC’ membrane configuration..... | 144 |
| Figure 2.5-b | Mass balances for organic acid transport from fermenting <i>Escherichia coli</i> cultures using the ‘high-intermittent’ approach. | 145 |
| Figure 2.5-c | Inhibition of fermentative H ₂ production by electro dialysis..... | 146 |
| Figure 2.5-d | The determination of limiting current density (LCD). | 147 |
| Figure 2.5-e | Variation in limiting current density in a sustained <i>Escherichia coli</i> fermentation..... | 148 |
| Figure 2.5-f | The effect of NH ₄ ⁺ concentration in the M chamber on the transfer of NH ₄ ⁺ ... | 149 |
| Figure 2.5-g | Dependence of NH ₄ ⁺ transfer on current. | 150 |
| Figure 2.5-h | Transport rates of organic acids related to anionic mass and pH in the MA chamber (pH _{MA}). | 151 |
| Figure 2.5-i | Mass balance for organic acid transport from a cell-free solution using the ‘low-constant’ approach..... | 153 |
| Figure 2.6-a | Process scheme (A) and configuration (B) for a dual system with integrated electro dialysis. | 161 |
| Figure 2.6-b | H ₂ production (A) glucose concentration (B) and organic acid concentration (C & D) in <i>Escherichia coli</i> fermentations. (Legend overleaf)..... | 164 |
| Figure 2.6-c | H ₂ production (A) and substrate conversion efficiency (B) by <i>Rhodobacter sphaeroides</i> | 167 |
| Figure 2.6-d | Efficiencies of organic acid transfer in experimental dual systems..... | 168 |
| Figure 2.6-e | H ₂ production by a dual system with integrated electro dialysis. | 169 |
| <u>Section 2.7.1 (article published in the Journal of Biotechnology and Bioengineering</u> | | |
| Figure 1. | TEM sections of <i>D. desulfuricans</i> (D) and <i>R. sphaeroides</i> (R) palladized to 0 % , 1 % , 5 % and 25 % Pd(0) w/w. | |
| Figure 2. | Rates of H ₂ release via hypophosphite by various catalytic preparations. | |
| Figure 3. | Reductive dehalogenation of pentachlorophenol (PCP) | |
| | | |
| Figure 2.8-a | Construction of polymer electrolyte membrane fuel cell with bio-fabricated Pd anode..... | 190 |
| Figure 2.8-b | Power output profiles of ‘bio-fabricated’ fuel cells..... | 192 |
| Figure 2.8-c | The effect of medium composition on the precipitation of Pd(0)..... | 194 |
| Figure 2.8-d | Production of <i>Escherichia coli</i> HD701 (A) and <i>Rhodobacter sphaeroides</i> (B) biomasses by a dual-bioreactor system for H ₂ production. | 197 |
| Figure 3-a | An hypothetical application combining electro dialysis and membrane dialysis for the non-specific transport of fermentation products..... | 208 |
| Figure 3-b | Prototype light focussing photobioreactor under development at Wageningen University, Netherlands..... | 214 |
| Figure 3-c | Conceptual design of a light-concentrating photosynthetic system, for light intensities below saturation. | 215 |
| Figure 4.1-a | Fluid displacement systems for the measurement of H ₂ production..... | 219 |
| Figure 4.1-b | Storage of gas samples for analysis. | 221 |
| Figure 4.1-c | Gas chromatogram showing the absence of CH ₄ and CO ₂ | 222 |
| Figure 4.1-d | Example growth curve for <i>Rhodobacter sphaeroides</i> O.U. 001..... | 224 |
| Figure 4.1-e | Growth kinetics and organic acid profile for the aerobic growth of <i>Escherichia coli</i> HD701 on nutrient broth with sodium formate. | 225 |
| Figure 4.1-f | The relationship between OD ₆₆₀ and culture density in <i>Rhodobacter sphaeroides</i> O.U. 001, grown on SyA medium. | 226 |

| | |
|---|-----|
| Figure 4.1-g Absorption spectrum of purple non-sulphur bacteria (solid line) and spectrum of daylight..... | 227 |
| Figure 4.1-h Emission spectrum of tungsten filament within a white light bulb. | 228 |
| Figure 4.1-i Sample calibration curve for Pd(II) assay by the SnCl ₂ method | 231 |
| Figure 4.1-j Sample calibration curves for the analysis of glucose..... | 232 |
| Figure 4.1-k Sample calibration curve for the analysis of NH ₄ ⁺ , validating the method for use in a background of 20 mM phosphate. | 234 |
| Figure 4.1-l Sample calibration curve for the analysis of chloride. | 235 |
| Figure 4.1-m Analysis of ethanol. | 237 |

List of Tables

Section 1.2.1 (review article)

Table 1 : Summary of dual systems employed for biohydrogen production

Table 2 : Bottlenecks to the application of anoxygenic photosynthetic bacteria in H₂ production.

Table 3 : Potential productivities of algal/cyanobacterial-driven dual systems

Section 2.1.1 (research letter published in FEMS Microbiology Letters)

Table 1 Bacterial strains and fermentation balances

Table 2.2-1 The effect of pH on rates of growth and glucose consumption 95

Table 2.2-2 Candidate enzymes in the pathway of butyrate formation..... 106

Table 2.3-1 Growth in 'resting' cultures of *Rhodobacter sphaeroides*..... 123

Table 2.3-2 Conditions for H₂-production by chemostat cultures of purple non-sulphur bacteria 127

Section 2.4.1 (article published in the International Journal of Hydrogen Energy)

Table 1 Conditions for anion chromatography

Table 2 Properties of fermentation liquor

Table 2.5-1 Properties of organic acids 151

Table 2.5-2 Potentially offset electrical input through electrolytically generated H₂ 155

Table 2.5-3 'Break-even' current efficiency (BCE) for organic acids 156

Table 2.6-1 Experiments 160

Section 2.7.1 (article published in the Journal of Biotechnology and Bioengineering)

Table 1. Chlorinated aromatic compounds used in catalytic dehalogenation testing

Table 2.8-1 Maximum power outputs from 'bio-fabricated' fuel cells..... 191

Table 3-1 Summary of outcomes..... 200

Table 3-2 Free-sugars content of apple 210

Table 3-3 Scenario for H₂ production from apple waste 211

Table 3-4 Technical aspects requiring development prior to an economic assessment of the dual system 212

Table 4.1-1 Media for the culture of *Rhodobacter sphaeroides* 223

Table 4.1-2 Additives to media for the culture of *Rhodobacter sphaeroides* 224

Table 4.1-3 Example analysis of Pd content in Bio-Pd(0) 231

Table 4.1-4 Assay range of DNSA method..... 232

Table 4.1-5 Reagents for the analysis of NH₄⁺ 233

Table 4.1-6 Sequences producing significant alignments – *Euglena gracilis*..... 240

Table 4.1-7 Sequences producing significant alignments – *Clostridium actobutylicum* 241

Abbreviations

ACT: acetoacetyl-CoA thiolase
ADH: alcohol dehydrogenase
Al-DH: aldehyde dehydrogenase
ASM: anion-selective membrane
BCAD: butyryl-CoA dehydrogenase
BCE: 'break-even' current efficiency
Bio-Pd(0): biomass-supported palladium catalyst. 0 denotes the fully reduced metallic state.
BLAST: basic local alignment search tool
BP membrane: bi-polar membrane (a bi-layer of ASM and CSM)
CE: current efficiency
CSM: cation-selective membrane
C/N: molar ratio of total carbon over total nitrogen
DC: direct current
ECH: enoyl-CoA hydratase
ED: electro dialysis
FHL: formate-hydrogen lyase
FR: fructuronate reductase
F/D: fill-and-draw
GHG: Greenhouse gas
HCDH: 3-hydroxyacyl-CoA dehydrogenase
HPLC: high performance liquid chromatography
HRT: hydraulic retention time
LCD: limiting current density
LDH: lactate dehydrogenase
MAF: mixed acid fermentation
MEA: membrane electrode assembly
MS: mass spectroscopy
NA: data not available
Org.: organic
PBR: photobioreactor
PEM: polymer electrolyte membrane (or proton-exchange membrane)
pH_i: internal pH of cell cytoplasm
pH_o: outside pH of culture medium
PFL: pyruvate-formate lyase
PM: precious metal
PGM: platinum group metals
Re: Reynolds number
R²: square of regression coefficient
Sp.: species
Subs. con. eff. (%) : substrate conversion efficiency
TER: trans-2-enoyl-CoA reductase (NAD⁺)
[x]: concentration of x
μ: specific growth rate

1 : INTRODUCTION

1.0 Chapter contents

| | |
|--|----|
| 1.1 Project concepts..... | 2 |
| 1.1.1 Upstream system: Hydrogen fuel from waste by a two-stage bioreactor..... | 2 |
| 1.1.2 Downstream system: Conversion of bio-hydrogen into electricity | 3 |
| 1.2 Integrating dark and light biohydrogen production: towards the hydrogen economy | 4 |
| 1.2.0 Summary..... | 4 |
| 1.2.1 Review article..... | 4 |
| Abstract | |
| Glossary & Abbreviations | |
| 1: Biofuels for sustainable energy production | |
| 2: The use of microorganisms for H ₂ production. | |
| 2.1: Photobiological H ₂ production | |
| 2.1.1: Photoautotrophs | |
| 2.1.2: Photoheterotrophs | |
| 2.2: Dark fermentation | |
| 2.2.1: Axenic cultures | |
| 2.2.2: Mixed fermentation | |
| 3: Hybrid hydrogen | |
| 3.1: Techniques for connecting the components of a dual system | |
| 3.2: Comparing diverse strategies | |
| 3.3: Selection of organisms for the 2 nd stage | |
| 3.4: Selection of organisms for the 1 st stage | |
| 3.4.1: Dual systems with photoautotrophic 1 st stage | |
| 3.4.2: Dual systems with dark fermentative 1 st stage | |
| 4: Conclusions and future perspectives | |
| 1.3 Downstream system: Biomass-supported palladium catalysts..... | 65 |
| 1.3.0 Summary..... | 65 |
| 1.3.1 Biomass-supported catalyst..... | 65 |
| 1.3.2 Palladium..... | 66 |
| 1.3.3 <i>Desulfovibrio</i> bio-Pd(0)..... | 68 |
| 1.3.4 Use of <i>Rhodobacter sphaeroides</i> in metal reduction and remediation technology. | 72 |

1.1 Project concepts

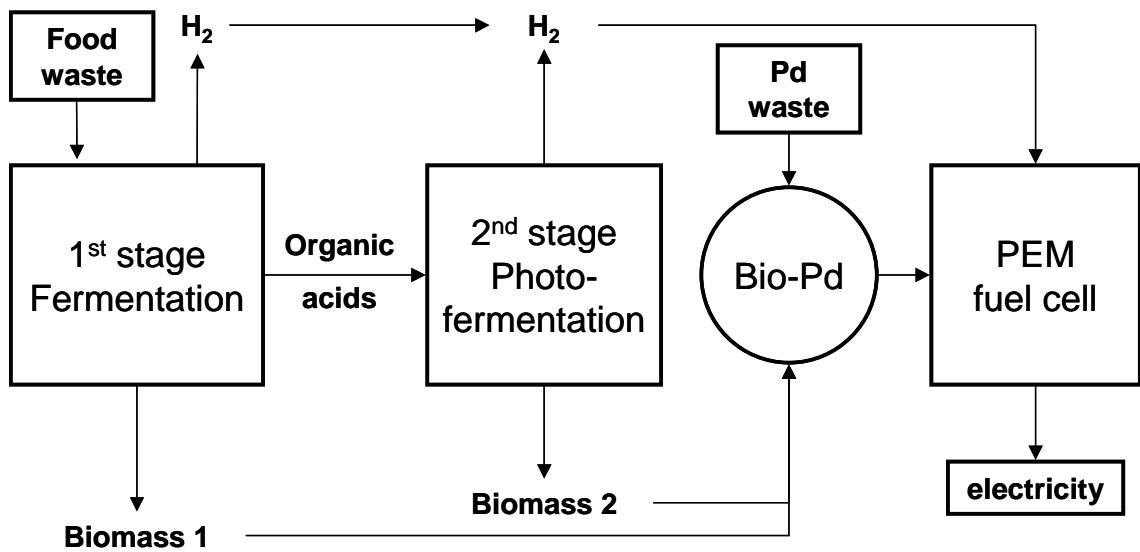


Figure 1.1-a Project Concept.

Hydrogen has potential value as a clean fuel. Further, if the system were applied using carbohydrate-rich wastes from industry, hydrogen could be used immediately on-site in industry (*via* combustion or electricity generation) to offset process and manufacturing costs. The development of hydrogen biotechnology is advancing rapidly as hydrogen gains recognition as a fuel of increasing importance, in parallel to the demise of fossil fuels. In this context, the concept of this project was to produce both H₂ and electricity using linked biosystems. Pd, palladium; Bio-Pd(0), biomass supported palladium catalyst; PEM, polymer electrolyte membrane.

The project is divided between the ‘upstream system’ for biohydrogen (bio-H₂) production and the ‘downstream system’ for electricity generation from bio-H₂ and excess biomass.

1.1.1 Upstream system: Hydrogen fuel from waste by a two-stage bioreactor

The primary aim of this project was to design and build a biological system capable of efficient hydrogen production from glucose. A dual system is proposed in which *Escherichia coli* first ferments glucose to produce hydrogen and organic acids (chapters 2.1 and 2.2). The organic acids are then consumed by *Rhodobacter sphaeroides* to produce further hydrogen, and to complete the conversion of glucose to hydrogen (chapters 2.3 and 2.4). A major technical constraint was the integration of *E. coli* and *R. sphaeroides* fermentations, which

was overcome by the application of a novel separation technique (chapters 2.5 and 2.6), which formed the subject of a patent application [159] (reproduced in appendix 4.2.1).

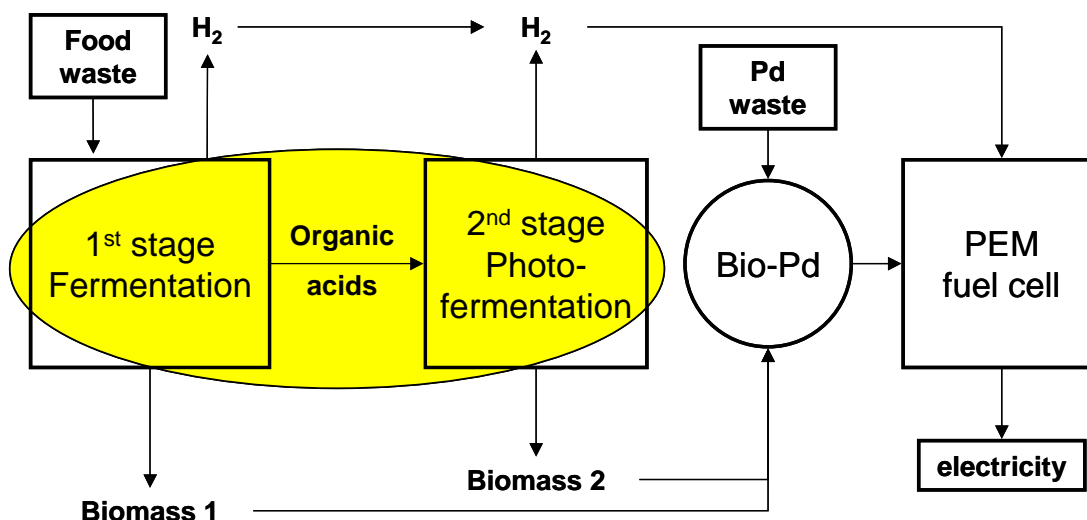
1.1.2 Downstream system: Conversion of bio-hydrogen into electricity

The upstream system (above) produced two types of biomass as co-products, which would be rich in high quality protein and B-vitamins, suggesting use as a protein supplement or as a fertiliser [138], but there may be a more profitable use for this biomass in the biomanufacture of supported palladium catalyst. Precious metal (PM) catalysts are the most costly components of fuel cells, which generate electricity from H₂ using PM catalytic electrodes (chapters 1.3.3b and 2.8).

Much of the global production of PMs currently supports the manufacture of automotive catalytic converters, which are now obligatory for atmospheric protection. A shift to H₂-fuelled vehicles over the coming decades is likely to increase the demand for fuel cell PM, making their recovery from secondary sources increasingly important, while scrapped automotive catalysts will become increasingly abundant. As described in section 1.3, the biorecovery of PM from spent automotive catalyst has been demonstrated [214] and catalytic activity of biorecovered PM catalyst has been demonstrated [111]. It has also been shown that palladised biomass can function in the generation of electricity using a fuel cell using *Desulfovibrio desulfuricans* as a model organism [215,216].

1.2 Integrating dark and light biohydrogen production: towards the hydrogen economy

1.2.0 Summary



This chapter comprises a review paper in submission to Reviews in Environmental Science and Biotechnology. The author researched and prepared the manuscript and performed the critical assessments (novel synthesis). Co-authors assisted by editing the manuscript and checking calculations.

As several focussed reviews were already available, this review provides a relatively brief description and comparison of the available biological approaches to H₂ production but provides for the first time, an exhaustive description, categorisation and evaluation of reported dual systems. The case is made for combining dark fermentation and photofermentation, and for achieving this *via* a dual bioreactor system rather than in co-culture. The potential for energy generation is evaluated and compared with alternative bioenergy strategies.

1.2.1 Review article

Review article

Title: Integrating dark and light biohydrogen production strategies: towards the hydrogen economy

Running head: Dual systems for Bio-H₂

Shortened title: Hybrid H₂

Authors: Mark D. Redwood, Marion Paterson-Beedle and Lynne E. Macaskie

Affiliation: School of Biosciences, University of Birmingham

Correspondence should be addressed to Prof. Lynne E. Macaskie, School of Biosciences, University of Birmingham, Edgbaston, Birmingham, B15 2TT, UK. Tel: +44 1214145889 ; Fax: +44 1214145925; e-mail: l.e.macaskie@bham.ac.uk

Keywords: biohydrogen, bioenergy, renewable energy, hydrogen economy, dark fermentation, dual systems, photosynthesis.

**Integrating dark and light biohydrogen production strategies:
Towards the hydrogen economy**

Mark D. Redwood, Marion Paterson-Beedle and Lynne E. Macaskie *

Corresponding author. Tel: +44 1214145434 ; fax: +44 1214145925; e-mail:

l.e.macaskie@bham.ac.uk

School of Biosciences, University of Birmingham, Edgbaston, Birmingham, B15 2TT, UK.

Abstract

Biological methods of hydrogen production are preferable over chemical methods because of the possibility to use sunlight, CO₂, and organic wastes as substrates for environmentally benign conversions, under moderate conditions. By uniting different microorganisms with individual capabilities, their individual strengths may be exploited and their weaknesses overcome, resulting in increased H₂ yields over single-organism systems. Available organisms for biohydrogen production are described and strategies to integrate them are discussed. This concept was described some decades ago and a review of progress is timely. This review focuses on 2-component H₂-producing systems (“dual systems”), in which the 1st stage entails the conversion of carbohydrates to organic residua, which are subsequently consumed in a light-dependent 2nd stage.

Dual systems can be divided broadly into wholly light-driven systems (with microalgae/cyanobacteria as the 1st stage) and partially light-driven systems (with a dark, fermentative initial reaction). By reviewing published data and evaluating potentials for energy generation, it is concluded that the latter type holds greater promise for industrial application. It is calculated that a wholly light-driven dual system has a land-requirement for light capture that would be too large for either centralised or decentralised energy generation. Partially light-driven dual systems, with a lower photosynthetic requirement and the capacity for organic waste utilisation hold greater promise for economic application. Research into partially light driven dual systems has focussed on the fermentative capabilities of strictly anaerobic bacteria. Other microorganisms such as enteric bacteria, lactic acid bacteria and

hyperthermophiles have significant potential, which is overviewed alongside other biofuels such as bio-methane and bioethanol.

Contents

- 1: Biofuels for sustainable energy production
- 2: The use of microorganisms for H₂ production.
 - 2.1: Photobiological H₂ production
 - 2.1.1: Photoautotrophs
 - 2.1.2: Photoheterotrophs
 - 2.2: Dark fermentation
 - 2.2.1: Axenic cultures
 - 2.2.2: Mixed fermentation
- 3: Hybrid hydrogen
 - 3.1: Techniques for connecting the components of a dual system
 - 3.2: Comparing diverse strategies
 - 3.3: Selection of organisms for the 2nd stage
 - 3.4: Selection of organisms for the 1st stage
 - 3.4.1: Dual systems with photoautotrophic 1st stage
 - 3.4.1.1: Energy generation potential with a photoautotrophic 1st stage
 - 3.4.2: Dual systems with dark fermentative 1st stage
 - 3.4.2.1: Selection of organisms for a dark fermentative 1st stage
 - 3.4.2.2: Distribution of H₂ between 1st and 2nd stages
 - 3.4.2.3: Energy generation potential with a dark fermentative 1st stage.
 - 3.4.2.4: Bio-H₂, bio-methane or bio-ethanol?
- 4: Conclusions and future perspectives
- 5: Bibliography

Glossary & Abbreviations

Akinete: Vegetative cyanobacterial cell accumulating carbohydrate. The main component of filaments, including heterocysts

Autotrophy: Metabolism with the synthesis of carbohydrate using light and/or inorganic substrates

Av. : Average

Axenic: Pure culture containing only one type of microorganism

BOD: Biological oxygen demand; the mass of oxygen consumed by microorganisms during the oxidation of organic compounds from a sample of water

COD: Chemical oxygen demand; the mass of oxygen consumed during the chemical oxidation of organic compounds from a sample of water

CSTR: Continuously stirred tank reactor

Direct Bio-photolysis: H₂ production from water; electrons liberated from H₂O by PSII recombine with H⁺ to form H₂, catalysed by hydrogenase or nitrogenase

DMFC: Direct methanol fuel cell, a type of PEM-FC using methanol fuel directly without reforming as in the indirect methanol fuel cell

dw: Dry cell weight

FHL: Formic hydrogen lyase

Fermentation: Microbial growth mode in which ATP is generated only by substrate level phosphorylation in the absence of exogenous electron acceptors (e.g. O₂, NO₃²⁻, NO₂²⁻, SO₄²⁻)

HRT: Hydraulic retention time. The total flow rate through a diluted system over its volume

Indirect bio-photolysis: H₂ production from water *via* the photosynthesis and fermentation of carbohydrates

Heterocyst: A cyanobacterial cell specialised for N₂ fixation

Heterotrophy: Microbial metabolism utilising organic carbon sources

HHV: higher heating value

Hyperthermophilic: (extreme thermophilic) Most active in the temperature range 80 – 110 °C

LDH: Fermentative lactate dehydrogenase

Light conversion efficiency: The percentage of available light energy converted to H₂, distinct from photosynthetic efficiency (PE)

1.2 Dual systems (review article)

Mesophilic: Most active in the temperature range 20 – 40 °C

Net energy ratio: The dimensionless ratio of the energy outputs to primary inputs for the entire operational lifetime of a system

Nitrogenase: Nitrogenase complex (reductase and nitrogenase)

PE: Photosynthetic efficiency. The percentage of photosynthetically active light energy converted to H₂. (includes only those wavelengths which interact with photopigments)

PEM-FC: Proton exchange membrane fuel cell; a type of low-temperature fuel cell considered most suitable for transport applications

PHB: Poly-β-hydroxybutyrate, a storage polymer

Photoheterotrophy: light-driven mode of anaerobic metabolism using organic substrates as electron donors.

Pi : inorganic phosphate

PFL: Pyruvate:formate lyase

PFOR: Pyruvate:ferredoxin oxidoreductase

Photopigments: Light harvesting proteins

PEM-FC: Proton-exchange membrane fuel cell

Phototrophy: Microbial metabolism using light energy

Photoautotrophy: Microbial metabolism using light energy for the synthesis of carbon sources

PNS bacteria: Purple non-sulfur bacteria

PSI: Photosystem I, possessed by all phototrophs, not powerful enough for photolysis of water

PSII: Photosystem II, possessed by photoautotrophs, responsible for photolysis of water

RV Missing

Reserve: The amount of a resource in place (e.g. oil in the ground) that is economically recoverable

SOFC: Solid oxide fuel cell, a high temperature alkaline fuel cell

SOT medium: Growth medium for cyanobacteria containing salts and trace elements but no carbon source

Thermophilic: Most active in the temperature range 40 – 60 °C

UASB: Upstream anaerobic sludge blanket reactor

1: Biofuels for sustainable energy production

An estimated 45 % of the identified world oil reserves has been combusted and atmospheric CO₂ has increased by 20 % since 1900 (Holmes & Jones 2003; Keeling & Whorf 2005). Conservative estimates suggest that demand for oil will outstrip supply by 2050 (Holmes & Jones 2003), while the Stern Review (Stern 2006) highlights the urgent need for reduction in greenhouse gas emissions. A sustainable energy economy is needed and this will require a different fuel; one that is not limited in supply and whose use is environmentally benign. Hydrogen is now recognised as a key energy vector in the future energy economy. H₂ storage technology and fuel cell efficiency continue to receive urgent attention and have advanced sufficiently for transport applications to approach commercial viability. For example, BMW's fleet of 100 "Hydrogen 7" cars, each having a material value of \$500,000 each, is now available for promotional purposes (carsguide.com.au, Nov 2006). A prototype H₂-powered boat is also opening the way to economic transport *via* inland waterways (A. Bevan, University of Birmingham, pers. comm.). Whereas the use of H₂ in transport applications is dependent upon such emerging technologies, its use in stationary applications, for electricity supply, is limited primarily by H₂ availability.

Biological approaches could contribute to large-scale H₂ production as various microorganisms can produce H₂ under moderate conditions from readily available, renewable substrates, making biological strategies potentially competitive with chemical process such as reforming and gasification. Biohydrogen processes are 'CO₂-neutral', being fuelled by carbohydrates originating from photosynthetic fixation of CO₂, and bio-H₂ is free of catalyst poisons (CO and H₂S), requiring no treatment before use in fuel cells for electricity generation (Macaskie et al. 2005).

Suitable feeds for biohydrogen generation processes can be found in agricultural residues (Banik et al. 2003), food wastes (Franchi et al. 2004) and effluents from industrial processes such as refining sugar (Yetis et al. 2000; Ren et al. 2006), distilling alcohol (Sasikala et al. 1992), olive processing (Eroğlu et al. 2004), and tofu production (Zhu et al. 1995; Zhu et al. 2002). Hence, microbial process could be employed to remediate wastes while simultaneously producing H₂ with the dual economic benefit of energy production and savings in the cost of waste disposal. In the UK the majority of waste is disposed by land-filling and the related environmental damage is being recognised in financial terms *via* landfill

tax; which is paid on top of normal landfill fees at an increasing rate (GBP 24/tonne for 2007/2008; www.businesslink.gov.uk/bdotg/action/) (Bartelings et al. 2005). The avoidance of waste disposal costs is, therefore, anticipated to be an important economic driver in the start-up of bioenergy processes.

The capability for H₂ formation is widespread among microorganisms, but only a few have been the focus of research with the aim of biohydrogen production. In particular, photosynthetic microorganisms such as microalgae, cyanobacteria and purple bacteria, along with various bacterial dark fermentations are of interest. Each of these candidates represents a potential method in its own right, but it has long been recognised that to realise the maximum potential for biohydrogen production would entail multi-organism systems, combining the capabilities of different species (Rocha et al. 2001; Wakayama & Miyake 2001; de Vrije & Claassen 2003; Nath et al. 2005; Basak & Das 2007). Several examples of dual systems are illustrated in Table 1. The purpose of this review is to advance the state of knowledge by comparing the successes of diverse strategies, by relating them to the methods employed, by evaluating the potentials for energy generation and by highlighting potential problems.

2: The use of microorganisms for H₂ production

The capacity for H₂ formation is a widespread property of microorganisms. This work does not attempt to review microbial hydrogen metabolism (for reviews see (Vignais et al. 1985; Blankenship et al. 1995; Sasikala et al. 1995; Nandi & Sengupta 1998; Das & Veziroglu 2001; Hallenbeck & Benemann 2002; Nath & Das 2004a, 2004b; Bae et al. 2005; Dutta et al. 2005; Hawkes et al. 2007; Tsygankov 2007), but provides a summary of those organisms which have been studied expressly for the purpose of H₂ production. In order to evaluate strategies for combining organisms to exploit the best facets of different metabolic strategies, they are first considered individually.

2.1: Photobiological hydrogen production

Many microorganisms have evolved the capacity to harness solar energy for growth, and several types of photosynthetic microorganism are potentially useful for biohydrogen production. Artificial light sources are often used as models for future applications with

sunlight, but solar biohydrogen projects have been successful despite the diurnal and seasonal variations in light intensity.

2.1.1: Photoautotrophic microorganisms

Photoautotrophs produce H₂ by two distinct mechanisms: “direct photolysis” and “indirect photolysis”, which can both occur in the same organism (Figure 1). Like higher plants, microalgae (green unicellular algae) and cyanobacteria (previously called blue-green algae) have two photosystems (Photosystems I and II: PSI and PSII), which produce H₂ by “direct photolysis” in which water is decomposed to H₂ and O₂ (oxygenic photosynthesis). PSII splits water, reducing electron carriers and exporting protons to generate a proton gradient for ATP generation (Miyake et al. 1999).

Hydrogenase and nitrogenase enzymes are found in cyanobacteria, but (as in purple bacteria, see section 2.1.2) self-sustained H₂ formation results from the activity of nitrogenase, which consumes ATP and re-oxidises electron carriers, whereas in microalgae a hydrogenase performs the reduction of 2H⁺ to H₂ without any ATP requirement. In “indirect photolysis”, CO₂ is fixed *via* the Calvin cycle to synthesise simple sugars and thence accumulate carbohydrates (starch in microalgae and glycogen in cyanobacteria). Stored carbohydrates can be subsequently metabolised through fermentative metabolism (section 2.2) to generate H₂ indirectly.

H₂ production by direct photolysis is limited by the inhibition of hydrogenase and nitrogenase by oxygen, generated from water, whereas indirect photolysis is sustainable because the production of O₂ and H₂ can be separated spatially (into compartments) or temporally (into aerobic and anaerobic phases) (Levin et al. 2004a).

Cyanobacteria are divided into non nitrogen-fixing varieties (e.g. *Synechococcus* spp), which form only one kind of cell (akinetes), and nitrogen-fixing varieties (e.g. *Nostoc*, *Anabaena* spp.), which form akinetes and also heterocysts arranged into filaments - chains of cells connected by channels for the exchange of nutrients (Tsygankov 2007). Heterocysts differ from akinetes due to the absence of O₂ generation by PSII, the increased rate of O₂ consumption by respiration, the presence of a thick envelope to limit the ingress of environmental O₂, and the expression of nitrogenase to fix N₂ as NH₄⁺, supporting the growth of the adjacent akinetes (Tamagnini et al. 2002). Heterocystous cyanobacteria separate H₂

production and O₂ production spatially (by compartmentalisation), accumulating glycogen in the vegetative akinetes and fermenting it to produce H₂ in the anaerobic heterocysts, whereas non N₂-fixing cyanobacteria and microalgae separate H₂ production and O₂ production temporally, producing H₂ by the dark anaerobic fermentation of photosynthesised carbohydrates. Upon transition to darkness, the generation of O₂ by the photosystem ceases and residual O₂ is consumed by respiration enabling H₂ production (Tsygankov 2007).

The capacity for sustained aerobic H₂ production in the light, is a beneficial property of heterocystous cyanobacteria (e.g. *Anabaena* spp.) achieving maximum H₂ production rates of ca. 100 µmol H₂/mg chlorophyll *a*/h, with light conversion efficiencies of up to 3.9 % (proportion of absorbed light energy converted to H₂) (Dutta et al. 2005; Yoon et al. 2006; Sakurai & Masukawa 2007). Rates were increased 3-7 fold in *Anabaena* mutants deficient uptake hydrogenase activity (Borodin et al. 2000; Happe et al. 2000; Masukawa et al. 2002; Yoshino et al. 2006), and this strategy was applied in outdoor culture, however the maximum light conversion efficiency was only 0.1 %, which has implications for the large scale application of this approach (Lindblad et al. 2002; Tsygankov et al. 2002).

Unicellular cyanobacteria have been studied with a view to dark fermentative H₂ production, being unsuitable for photoproduction of H₂ due to their high (competing) uptake hydrogenase activity in the light (Troshina et al. 2002). However, a mutant of *Synechocystis* deficient in uptake hydrogenase activity photoproduced H₂ at a rate of 6 µmol H₂/mg chlorophyll *a*/h (2 ml/L/h) (Cournac et al. 2004).

Like unicellular cyanobacteria, microalgae were originally studied for dark H₂ production by indirect photolysis (Miyamoto et al. 1987). The isolation of *Chlamydomonas* spp MGA161 having a high rate of H₂ photoproduction (6 mmol H₂/g chlorophyll *a*/h), high starch accumulation (18 % w/w) and unusually rapid and efficient dark fermentation (2 mol H₂/mol starch-glucose) prompted the study of a dual system (Miura et al. 1986) (Table 1).

The extent of metabolic engineering success in microalgae lags behind that of cyanobacteria due to the greater difficulty of eukaryotic genetic engineering. Work is ongoing to improve light conversion efficiency through the truncation of light-harvesting antenna complexes, an approach already proven using PNS bacteria (section 2.1.2) (Akkerman et al. 2002; Polle et al. 2002). Other approaches are to develop O₂-tolerant hydrogenases (Ghirardi et al. 2005) and to express clostridial hydrogenase in non-heterocystous cyanobacteria, the aim being to engineer the rapid and ATP-independent

(hydrogenase-mediated) H₂ production by direct photolysis in a fast-growing host organism, possibly overcoming O₂-inhibition through strong expression (Miyake et al. 1999).

A relatively new method to increase rates of H₂ production by direct photolysis is nutrient deprivation. Under conditions of sulfate-limitation the iron-sulfur clusters of PSII subunits cannot be maintained and PSII activity is selectively inhibited (Wykoff et al. 1998). The rate of O₂ production decreases, while the respiration rate remains high and establishes anoxia, which permits hydrogenase and/or nitrogenase expression. The result is sustained H₂ production *via* direct photolysis. The technique was pioneered using microalgae (Benemann 1996; Jo et al. 2006; Laurinavichene et al. 2006) and has been recently extended to cyanobacteria (Antal & Lindblad 2005).

2.1.2: Photoheterotrophs

Purple non-sulfur (PNS) bacteria are anoxygenic photosynthetic bacteria which, unlike the purple and green sulfur bacteria, do not produce H₂S (a powerful catalyst poison), and the off-gas is typically > 90 % H₂, hence it is suitable for use in PEM-fuel cells without purification (Nakada et al. 1995).

PNS bacteria produce H₂ under photoheterotrophic conditions (light, anaerobiosis, organic electron donor) although they are metabolic generalists capable of autotrophic and heterotrophic growth. The best-studied species belong to the genera *Rhodobacter*, *Rhodospseudomonas* and *Rhodospirillum*.

H₂ is produced by the nitrogenase enzyme, which is active anaerobically under nitrogen limitation (Vignais et al. 1985). In the absence of N₂ the production of H₂ occurs according to equation 1.

$$(1) \text{ (Koku et al. 2002).}$$

In this respect the reaction serves to dissipate excess ATP and reducing power where growth is nitrogen-limited. The nitrogenase complex must be saturated with ATP, and also NADH for optimal activity, hence H₂ photoproduction occurs most rapidly under saturating light intensity at the expense of organic electron donors.

Nitrogenase activity is strictly an anaerobic facet of metabolism since O₂ damages the photopigments needed to maintain ATP flux for nitrogenase activity and nitrogenase expression is strongly inhibited by oxygen (Koku et al. 2002). Sustained H₂ photoproduction is possible as the single photosystem (PSI) of these organisms does not generate O₂ (this is termed anoxygenic photosynthesis) and continuous H₂-producing cultures have been operated for up to several months (Liessens & Verstraete 1986; Weetall et al. 1989; Erođlu et al. 1997; Hassan et al. 1997; Fascetti et al. 1998; Tsygankov et al. 1998; Yokoi et al. 2001; Franchi et al. 2004; Shi & Yu 2006).

Rocha et al. (2001) analysed a large number of reports, indicating that the efficiency of light conversion to H₂ is variable for PNS bacteria, the average value being *ca.* 4 %. The theoretical maximum photosynthetic efficiency is considered to exceed 10 % (Akkerman et al. 2002) but the photosystems of PNS bacteria saturate at low light intensity, leading to low light conversion efficiency under high light intensity, e.g. in solar photobioreactors (Kondo et al. 2002). PNS bacteria are adapted to photosynthesis at low light intensities, requiring large light harvesting complexes to capture diffuse light energy and channel it into the reaction centre. Light conversion efficiency may be improved beyond 10 % by genetic manipulation to reduce the size of light-harvesting antennae, thereby increasing the saturating light intensity (Table 2). This would allow efficient H₂ production at higher light intensities, by deeper or denser cultures (Miyake et al. 1999; Vasilyeva et al. 1999; Kondo et al. 2002; Kim et al. 2004; Kim et al. 2006a) (Table 2).

Nitrogenase-mediated H₂ formation is irreversible (Hillmer & Gest 1977b), which is an advantageous property in relation to reversible hydrogenase-mediated H₂ production, which is inhibited under high partial pressure of H₂ (Valdez-Vazquez et al. 2006). However, in PNS bacteria, uptake hydrogenase activity can detract from H₂ yields (Sasikala et al. 1990), prompting the development of uptake hydrogenase deficient mutants with up to 70 % increased H₂ production efficiency (Willison et al. 1984; Jahn et al. 1994; Worin et al. 1996; Ozturk et al. 2006) (Table 2).

Nitrogenase re-oxidises electron carriers to reduce 2H⁺ to H₂, and any other reductive processes ('electron sinks') can compete with, and detract from H₂ production. The formation of storage polymer poly-β-hydroxybutyrate (PHB) from acetate is such a competing reductive reaction (equation 2) (Vincenzini et al. 1997; Khatipov et al. 1998).

(2) (Tabita 1995).

Mutagenesis of the PHB synthase gene yielded PHB deficient mutants, which were capable of H₂ production under conditions that would normally favour PHB synthesis (Hustede et al. 1993) (Table 2). In recent studies, double mutants lacking uptake hydrogenase and also PHB synthase produced H₂ at up to 2.5-fold higher rates compared to the parent strain (Lee et al. 2002; Kim et al. 2006b), while in a separate study a similar double mutant sustained H₂ production for over 45 days, while the wild-type ceased H₂ production after 10 days (Franchi et al. 2004).

Numerous simple organic molecules serve as suitable electron donors for PNS bacteria, including common fermentation products such lactate, acetate, butyrate, propionate, and succinate (Hillmer & Gest 1977a, 1977b), alcohols such as ethanol and propanol (Fuji et al. 1987) and other substrates such as aromatic acids (e.g. cinnamate, benzoate) (Sasikala et al. 1994b; Fissler et al. 1995). The biochemical pathways of assimilation are uncertain for many of these substrates, with the exception of acetate (a common fermentation product). In most bacteria acetate is assimilated using the glyoxylate cycle, but a diverse group of microorganisms (including *Rhodobacter sphaeroides* and *Rhodospirillum rubrum*) lack the key glyoxylate cycle enzyme, isocitrate lyase, while rapidly assimilating acetate. An alternative citramalate cycle is now thought to operate in these species (Ivanovskii et al. 1997; Filatova et al. 2005a; 2005b). The distinction is important in the context of H₂ production as species lacking the glyoxylate shunt generally require the availability (not the addition) of CO₂ during H₂ production from acetate, with the exception of *R. sphaeroides* which has a high capacity for acetate consumption (and hence CO₂ production) compared to other PNS bacteria and also has a thick capsule obstructing the diffusion of produced CO₂ (Table 2). Some uncertainty remains over the suitability of ethanol, a common fermentation product, as an electron donor for photoproduction of H₂. A *Rhodopseudomonas* species produced H₂ at the expense of various alcohols (Fuji et al. 1987) and ethanol was consumed simultaneously with acetate by *Rhodobium marinum* at ca. 50 % the rate of acetate, although the initial concentration of ethanol was ca. 25 % that of acetate (Ike et al. 2001). Ethanol was rapidly removed from an *Escherichia coli* fermentation effluent by *R. sphaeroides* O.U.001 after a delay of 96 h, although the induction of ethanol-utilising enzymes was not monitored

(Redwood & Macaskie 2006). Hence, it is plausible that other PNS bacteria would be capable of ethanol utilisation after an adaptation period.

PNS bacteria have significant potential for industrial application as mixed cultures can be maintained for extended periods (Liessens & Verstraete 1986; Ko & Noike 2002; Fang et al. 2005), industrial waste streams can make suitable feeds for the photoproduction of H₂ (Thangaraj & Kulandaivelu 1994; Fascetti et al. 1998; Yigit et al. 1999; Zhu et al. 1999a; Yetis et al. 2000), larger scale photobioreactors are under development (Hoekema et al. 2002; Claassen & de Vrije 2007) and outdoor projects using sunlight have been successful (Wakayama et al. 2000; Kondo et al. 2002).

The foremost limitation with PNS bacteria is the incompatibility of nitrogenase activity and the presence of NH₄⁺. Waste streams can only be used for H₂ production if they are of high C/N ratio, and many reports of this application are available (Sasikala et al. 1992; Turkarslan et al. 1997; Tsygankov et al. 1998; Yigit et al. 1999; Yetis et al. 2000; Eroğlu et al. 2004; Fang et al. 2005). Low C/N waste streams have been applied successfully for the purposes of biomass production and effluent remediation (Ensign 1977; Hassan et al. 1997; Cornet et al. 2003; Yun & Ohta 2005). H₂ production using low C/N feeds has been accomplished by the use of immobilisation matrices which exclude cations such as NH₄⁺ (Zhu et al. 1999b; Zhu et al. 2001) and the development of nitrogenase-derepressed strains (Wall & Gest 1979; Zinchenko et al. 1991; Yagi et al. 1994; Zinchenko et al. 1997) (Table 2). These approaches were not, however, tested at pilot-scale or in continuous culture and issues such as the economic viability of immobilisation and the long-term stability of nitrogenase-derepressed strains remain to be addressed.

PNS bacteria are capable, therefore, of efficient conversion of organic acids to H₂, providing a potentially applicable method for the remediation of wastes rich in organic acids, alcohols or aromatics. Excepting usual strains (Macler et al. 1979; Macler & Bassham 1988; Oh et al. 2004), PNS bacteria lack the capacity for the efficient conversion of sugars to H₂, and for this application a dark fermentation is the method of choice.

2.2 Dark Hydrogen fermentation

Large quantities of simple and complex carbohydrates are available as agricultural and food processing residues (Easterly & Burnham 1996; Filho & Badr 2004; Haq & Easterly 2006;

Mabee et al. 2006; Levin et al. 2007). Fermentative bacteria represent a promising means not only to reclaim energy from these wastes in the form of hydrogen but also to utilise the wastes as resources, a particularly valuable attribute given the escalating cost of landfill (Bartelings et al. 2005). Indeed, it was calculated that the savings in landfill tax would be the main economic driver, outweighing the value of the energy produced *via* dark-fermentative production of H₂ from confectionery waste (Macaskie 2004).

The anaerobic degradation of organic matter by heterotrophic microorganisms can liberate H₂ at high rates, depending on the particular organisms and conditions. Fermentation generates energy solely through substrate level phosphorylation. Substrates are converted to reduced compounds, which are excreted as waste products and the ATP yield is low, in comparison to respiration. The formation of relatively reduced organic molecules is an integral part of all dark fermentations, and some of these molecules (e.g. acetate) can inhibit H₂ production if allowed to accumulate (Roe et al. 1998; Kirkpatrick et al. 2001; Van Ginkel & Logan 2005).

In a minority of fermentative microorganisms (e.g. *Klebsiella* spp.) H₂ production is primarily mediated by nitrogenase (Vignais et al. 2001) but due to the high ATP requirement and low turnover rate of nitrogenase, the theoretical H₂ yield is only 0.5 mol H₂/mol hexose (Wakayama & Miyake 2001). Without the contribution of light energy through photosynthesis, hydrogenase is preferred for H₂ production due to its higher rate of turnover and lower metabolic cost. The highest fermentative H₂ yields have been achieved using clostridia, other enteric bacteria and hyperthermophiles (see reviews: (Hallenbeck 2005; Davila-Vazquez et al. 2007).

H₂ fermentations are restricted by the Thauer limit. Thermodynamically, no more than 4 mol H₂ can be produced from 1 mol hexose, because substrate level phosphorylation must produce whole numbers of ATP, and the yield of ATP from glucose must be at least 1 mol/mol for the cell to survive (Thauer 1977). However, microbial fermentation typically generates more than 1 mol ATP and less than 4 mol H₂/mol hexose, quantities that vary according to the metabolic system and conditions.

2.2.1 Axenic dark fermentations

Axenic cultures (pure cultures containing clonal microbial populations) have been used in the majority of fermentation research, creating a wealth of information regarding model organisms, and the understanding of their fermentative metabolism has facilitated and rationalised the optimisation of conditions for H₂ production.

Dark fermentations are united by the initial glycolytic generation of ATP, NADH and pyruvate. Three enzymes compete for pyruvate: pyruvate:ferredoxin oxidoreductase (PFOR), pyruvate formate lyase (PFL) and the fermentative lactate dehydrogenase (LDH). The realised H₂ yield is dependent upon the fate of pyruvate, which differs among species due to varying activities of PFL, PFOR and LDH, of which one or more may be present (Figure 2).

Mixed-acid fermentation, in which the key enzymes are PFL and the formic hydrogen lyase (FHL) complex (comprising a specific formate dehydrogenase and hydrogenase) (Figure 2B), is performed by facultative anaerobes such as *E. coli*. PFL converts pyruvate to acetyl-CoA and formate, which is cleaved to H₂ and CO₂ by FHL, while acetyl-CoA is divided between the formation of acetate (which generates ATP) and the formation of ethanol (which oxidises NADH to regenerate NAD). PFOR is expressed constitutively to a low level (Knappe 1987), but since H₂ is entirely formate-derived (Ordal & Halvorson 1939) PFOR is not thought to be involved in H₂ production in *E. coli*.

Ideally, mixed-acid fermentation yields 2 mol H₂/mol glucose (Figure 2B), but in batch mode a yield of *ca.* 50 % of this is usually obtained due to diversion of pyruvate into lactate formation. The latter can be suppressed by control of culture conditions or through metabolic engineering (Sode et al. 1999). While the cleavage of formate is irreversible, H₂ recycling is an issue, as suggested by the observation of 37 % increased H₂ yield in Hyd-2 mutants of *E. coli* (Redwood et al. 2007c). The rate of H₂ formation was also increased through the increased expression of FHL (Penfold et al. 2003; Yoshida et al. 2005).

Facultative anaerobes of the related genus *Enterobacter* also produce H₂ from formate but analysis of the fermentation balance implicated the simultaneous activity of the NADH pathway (Tanisho & Ishiwata 1995; Tanisho et al. 1998; Kurokawa & Shigeharu 2005), in which the regeneration of NAD⁺ is coupled to the reduction of ferredoxin by NADH:ferredoxin oxidoreductase (NFOR). Reduced ferredoxin subsequently transfers electrons onto H⁺ to produce additional H₂. The NADH pathway (operating simultaneously

with PFL/FHL) could theoretically achieve the Thauer limit (4 mol H₂/mol glucose). However, both electron transfer reactions, (from NADH onto oxidised ferredoxin and from reduced ferredoxin onto H⁺) are reversible and neither would be considered electrochemically feasible under standard conditions: i.e. the standard electrode potentials of the NAD and ferredoxin half-cells (-320 mV and -400 mV, respectively) are more positive than that of the H⁺ half-cell (-414 mV) (McCormick 1998). A very low H₂ partial pressure (pH₂) (theoretically <60 Pa or <0.0006 bar) is required to drive this reaction forwards and H₂ yields exceeding 2 mol H₂/mol glucose were obtained only under vacuum or with continuous gas purging to strip away H₂ (Park et al. 2005). Indeed, a maximum yield of 3.9 mol H₂/mol glucose was reported using *E. cloacae* under a vacuum of 330 torr (equivalent to 0.44 bar or 44 kPa) (Mandal et al. 2006).

Clostridia also use the NADH pathway. In this case PFOR cleaves pyruvate to acetyl-CoA and CO₂, transferring electrons to ferredoxin, which is coupled to a reversible hydrogenase to produce H₂. In this situation, all H₂ is produced by a single reversible reaction and it is even more important to maintain a low pH₂ (Kataoka et al. 1997; Mizuno et al. 2000). Advances in gas separation technology may permit a purge-gas recycle system to remove the need for large quantities of inert, anaerobic purge gas for H₂ removal (Nielsen et al. 2001; Liang et al. 2002; Teplyakov et al. 2002).

A positive pressure (*ca.* 1-1.5 bar at 25 °C) is needed for H₂ uptake by metal hydride H₂-stores (Züttel 2004). Therefore, to charge a H₂ store directly from a fermentation culture (without intermediary gas-pressurisation) would require an organism capable of sustaining H₂ production under high pH₂. This would require the absence of biological H₂ recycling and would preclude a reversible H₂-producing system, such as the NADH pathway occurring in enteric bacteria and clostridia, but may be possible using an uptake hydrogenase mutant of *E. coli* in which the FHL complex (involving hydrogenase-3) performs the irreversible oxidation of formate to form H₂ (and CO₂). However, a degree of reversibility is a common property of hydrogenases (van Haaster et al. 2005) and although hydrogenase-3 has no uptake role during fermentation (Redwood et al. 2007c), it is known to operate reversibly when coupled to redox dyes (e.g. Sauter et al. 1992). Therefore, the latter strategy may tolerate a higher pH₂, but regardless of the organism employed, a pressurisation step would be advantageous between the fermentation and the H₂-store.

Various *Clostridium* spp. have been investigated for biohydrogen production (Collet et al. 2004), of which *C. butyricum* is perhaps the best known. Like *E. coli* and *E. aerogenes*, this organism is mesophilic but unlike them, it is a strict anaerobe. Hence, clostridial growth media are usually supplemented with a reducing agent to ensure anaerobiosis. Alternatively, a facultative aerobe, added to the H₂-production culture, was effective as an O₂-scavenger (Yokoi et al. 2001).

The H₂ yield from *C. butyricum* could in theory reach 4 mol H₂/mol hexose (Figure 2C) although a detailed metabolic analysis of *C. butyricum* calculated a maximum of 3.26 mol H₂/mol hexose (Chen et al. 2006) and practical yields obtained using clostridia rarely exceed 2 mol H₂/mol hexose (Collet et al. 2004; Ferchichi et al. 2005).

The clostridial species selected for H₂ production produce acetate and butyrate rather than propionate but they sporulate in response to environmental stresses such as heat or nutrient depletion, hence, the feeding regimes used in continuous culture are designed to maintain excessive nutrient concentrations to minimise sporulation (Hawkes et al. 2002). Asporogenic mutants have proved advantageous in ethanol production from cellulose, but have not yet been applied to H₂ production (Taillez et al. 1983). Whereas mesophilic clostridia sporulate as temperature increases, certain clostridial species are moderately thermophilic. For example, *C. thermolacticum* prefers to grow at 54 °C (Collet et al. 2004). Recently, hyperthermophiles (normally archaea), which live and produce H₂ at temperatures above 60 °C have been studied. Little biochemical information is yet available (e.g. de Vrije et al. 2007) but it seems that hyperthermophiles are capable of H₂ production with higher yields than mesophiles (Hallenbeck 2005). For example, a yield of 2.8 mol H₂/mol glucose was reported for *Thermotoga elfii* and 3.2-3.7 mol/mol for *Caldicellulosiruptor saccharolyticus* (Van Niel et al. 2002; Kadar et al. 2004; de Vrije et al. 2007). Observations support the connection of H₂ production with the hydrogenase-linked oxidation of electron carriers (as in clostridia), rather than the decomposition of formate (as in enteric bacteria). A p_{H₂} of 10-20 kPa (0.1-0.2 bar) induced a metabolic shift to inhibit H₂ production in *C. saccharolyticus* (Van Niel et al. 2003) and a limiting H₂ pressure of 20 kPa (0.2 bar) was reported for a mixed hyperthermophilic culture (Van Groenestijn et al. 2002), while formate was not decomposed by *Thermotoga neapolitana* (Van Ooteghem et al. 2004).

Due to the necessity of growth on solid media for molecular work (i.e. at temperatures lower than the melting point of agar), hyperthermophiles are not readily amenable to genetic

engineering (Van Ooteghem et al. 2004). Thermophilic cultures are resistant to overgrowth by mesophilic contaminants, and although an economic analysis is not available, the energetic costs associated with maintaining 70 °C may mitigate against large-scale application.

Several mesophilic and thermophilic clostridia and hyperthermophiles have the capacity to utilise complex carbohydrates such as cellulose and starch, a valuable property widening the potential for the use of industrial waste streams and agricultural residues as feeds. For example, *T. neopolitana* can utilise dextrans (Van Ooteghem et al. 2004), and *C. thermocellum* produced 1.6 mol H₂/mol hexose from cellulosic substrate (Levin et al. 2006). Enteric bacteria generally lack the ability to metabolise complex carbohydrates although the necessary genes can be introduced in the case of *E. coli* (Dien et al. 2000).

2.2.2 Mixed dark fermentations

The use of mixed cultures offers real practical advantages over the use of pure cultures, such as the use of feedstocks without pre-treatment or sterilisation, and is already a proven, commercially available technology (Kyazze et al. 2007). Inocula for H₂ production can be obtained from soil, compost or anaerobic digestion sludge (Hawkes et al. 2002; Hawkes et al. 2007). H₂ was produced from sucrose using sewage sludge microflora with a yield of 1.7 mol H₂/mol hexose (Lin & Lay 2005) and from food processing effluent using a heat-treated (2 h, 104 °C) sludge inoculum with typical yields of 0.2-0.87 mol H₂/mol hexose (Oh & Logan 2005). Rice slurry was fermented by a heat-treated (30 min, 100 °C) clostridial community to produce up to 2.5 mol H₂/mol hexose (Fang et al. 2006). Paper sludge and cellulose powder were rapidly degraded by mesophilic anaerobic consortia, producing mixtures of CH₄ and H₂ (Ueno et al. 1995; Valdez-Vazquez et al. 2005).

For mixed cultures there is a tendency towards lower rates and yields of H₂ production, because non H₂-producing organisms (e.g. methanogens and sulfate-reducers) consume a proportion of the substrate and perform H₂ uptake using H₂ as an electron donor. Furthermore, H₂S (the product of dissimilatory sulfate reduction) is a potent catalyst poison requiring removal if the biohydrogen is intended for use in a fuel cell. Hence, for the efficient production of clean H₂, the microbial population must be controlled to some degree in order to select for H₂-producers. Methanogens can be suppressed by the addition of chemical inhibitors or by operating continuous cultures at low pH or HRT (Mizuno et al. 2000). The

microbial population is often manipulated by inoculating with a mixed population having been subject to some pre-selection (Valdez-Vazquez et al. 2005). A widely adopted strategy is to select for spore-forming clostridia using a heat-treated inoculum, and where this can be achieved the properties of clostridial fermentation are predominantly applicable (Kim et al. 2004; Van Ginkel & Logan 2005). However, heat treatment also eliminates non-sporulating H₂-producers (e.g. *Enterobacter* spp.) and selects for spore-forming H₂-consumers (e.g. some acetogens) (Kraemer & Bagley 2007). The metabolic switch from H₂ production to solventogenesis was avoided by the intermittent release of headspace pressure and N₂ purging (Valdez-Vazquez et al. 2006).

3: Hybrid hydrogen

As reviewed above, no single-stage system has been shown to produce H₂ beyond 4 mol H₂/mol hexose. Current research focuses on the possible use of two-component systems *via* a variety of strategies (Table 1). These dual systems are united by the conversion of carbohydrates into organic acids in the 1st stage (which may be mesophilic or thermophilic and may not necessarily produce H₂), followed by the conversion of fermentation products into H₂ in the 2nd stage (Figure 3). In some examples, algae or cyanobacteria initially photosynthesise carbohydrates, which are then fermented by the same organisms, while other systems use carbohydrates as the primary feed, either as artificial solutions or in the form of wastes or algal biomass.

3.1 Techniques for connecting the components of a dual system

Alongside the choice of organisms, dual systems have been implemented through a variety of strategies. The nature of the bridge connecting these two stages is a key part of the operational strategy affecting the overall productivity of the system. The simplest approach constitutes a co-culture in which different organisms are in direct contact and act simultaneously, under the same conditions (Figure 3A). However, it is necessary to seek a compromise between the optimal requirements of each microbial component. While increasing the complexity and cost, sequential reactors permit the operator to maintain different conditions in separate parts of the dual system, allowing a combination of

organisms, which may not be compatible in co-culture (Figure 3B). For example, (wild-type) microalgae/cyanobacteria and PNS bacteria were not compatible in co-culture since the photosynthetic generation of oxygen inhibited nitrogenase-mediated H₂ production by the PNS bacteria (Miyamoto et al. 1987; Weetall et al. 1989). Further, sequential reactor systems can be potentially more effective as either component can be optimised without compromise to the other, and may be preferred even for ‘compatible’ combinations of organisms.

Sequential reactors require some method to transport fermentation products from the 1st reactor to the 2nd (while retaining biomass), which presents an engineering challenge for future scale-up operations. The simplest and most common method is ‘batch-transfer’ in which spent medium is transferred between reactors in batches. Centrifugation followed by filtration or autoclaving is usually performed to generate a clear, sterile feed for the 2nd stage (e.g. Yokoi et al. 2002; Redwood & Macaskie 2006). For large-scale application, continuous processes are generally preferred over batch systems. Fermentation products could potentially be transferred continuously through the use of bi-phasic solvent extraction, by continuous centrifugation or by membrane systems (Banik et al. 2003; Emanuelsson et al. 2003; Splendiani et al. 2003), but these techniques have yet to be applied in a H₂-producing system.

3.2 Comparing diverse strategies

As explained above, the two components of a dual system may be bridged in several ways. To add to the difficulty of comparison, either part of the dual system may use free or immobilised cells and may operate in batch, fed-batch, repeated fed-batch, or continuous mode, and the two components may be linked continuously or discontinuously in an open (exit flow to waste) or recycling system.

In order to reach some conclusions about the efficacy of different strategies, a common comparator is needed. Rates of H₂ production are not always meaningful in this kind of comparison due to number of contributory factors and variables. A common parameter taking into account many factors can be useful, (e.g. H₂ volume / reactor volume / dry cell weight / mol substrate consumed / time) but it is rarely possible to interpret accurately so many factors from published accounts. The molar yield of H₂ from hexose (or monosaccharide) is the most appropriate measure for the comparison of dual systems, as it

can be applied regardless of organisms, scale, means of integration, and the chemical natures of substrates (Table 1). This factor can be misleading, however, in the case of complex feeds (e.g. algal biomass, tofu wastewater) containing organic acids or non-hexose substrates such as fats and proteins from the outset, which contribute to the fermentative yield of organic acids (Ike et al. 1997; Ike et al. 2001).

3.3 Selection of organisms for the 2nd stage

In a dual H₂ producing system, the 2nd stage functions to clean up the effluent from the 1st stage (i.e. to decrease its BOD) and to produce a secondary H₂ stream at the expense of stage 1 products (e.g. reduced organic molecules). An algal-PNS bacterial symbiosis was proposed but no experimental data is yet available (Melis & Melnicki 2006). Fermentation products (e.g. acetate) could be used as C-source for the growth of microalgae, cyanobacteria or PNS bacteria. While acetate is regularly used in algal growth media (Kim et al. 2006c), the authors are not aware of any published attempts to cultivate algae or cyanobacteria on fermentation effluents. PNS bacteria, conversely, have been cultivated to produce biomass, single-cell protein, or PHB (poly-β-hydroxybutyrate), using primary fermentation waste streams (Ensign 1977; Hassan et al. 1997). Reduced organic molecules are the preferred carbon source for PNS bacteria (Biebl & Pfennig 1981), suggesting that these species may be ecologically associated with fermentative, organic acid-producing organisms. There are many examples of the use of PNS bacteria for H₂ production from wastes (e.g. Thangaraj & Kulandaivelu 1994), many of which have similar characteristics to fermentation effluents.

Using PNS bacteria in the 2nd stage, organic fermentation products can be converted to H₂ with high efficiency (50-100 % of stoichiometric yield) (Rocha et al. 2001) and light conversion efficiencies could reach 10 % (Akkerman et al. 2002). Using both dairy and sugarcane wastewaters the PNS bacterium *Rhodospseudomonas capsulata* produced H₂ at a 10-fold higher rate than the cyanobacterium *Anacystis nidulans* (Thangaraj & Kulandaivelu 1994).

PNS bacteria are the popular choice for the conversion of organic fermentation products to H₂ in the 2nd stage of a dual system. Of the 36 reports summarised in Table 1, only one employed a purple sulfur bacterium for this purpose (Akano et al. 1996; Ikuta et al. 1997) and none employed microalgae or cyanobacteria.

3.4: Selection of organisms for the 1st stage

In this overview, dual systems are grouped broadly according to whether both 1st and 2nd stages or only the 2nd stage are light-driven.

3.4.1: Dual systems with photoautotrophic 1st stage

In this approach, the 1st stage entails the photoautotrophic production of H₂ and accumulation of carbohydrate during a light phase. The photoautotroph switches to fermentative metabolism during a dark phase, converting starch or glycogen to organic fermentation products, which are utilised by PNS bacteria to generate H₂ in the next light phase. Alternatively, the phototroph cell mass may be harvested to supply the feed for a dual system with dark fermentative 1st stage (section 3.4.2).

1st and 2nd stages may be joined in co-culture or sequentially with transfer of spent broth between stages. Co-culture was until recently unsuitable for this combination because the O₂ produced by microalgae/cyanobacteria would prevent photoproduction of H₂ by PNS bacteria. Microalgal strains exhibiting a decreased rate of photolysis relative to respiration (P/R ratio; i.e. decreased rate of O₂ production) have recently become available and work is ongoing to characterise H₂ production in co-cultures of attenuated microalgae and PNS bacteria (Melis & Happe 2004).

In this type of system, there is the possibility for H₂ production in 3 stages because microalgae/cyanobacteria can produce H₂ both at night and by day. While the production of H₂ through photolysis (or nitrogenase) is widely reported, there are no accounts of 3-stage systems in which H₂ production occurred in all 3 stages. In all cases, the accumulated biomass was the sole substrate from which H₂ was generated, by dark algal/cyanobacterial fermentation followed by photofermentation.

In most cases, algal fermentation produced no H₂. In the most successful example (Miura et al. 1992), the yield of microalgal fermentation from accumulated starch was *ca.* 1.3 mol H₂/mol hexose and the overall yield was maintained at a steady 10.5 mol H₂/mol hexose for 5 days under continuous illumination (8 mol/mol under diurnal illumination). *Chlamydomonas* spp. were found to accumulate higher levels of starch than other microalgae

(Ike et al. 2001) and strain MGA161 with a high fermentative H₂ yield was highlighted (Miura et al. 1986). Although the microalgal-based dual system achieved excellent H₂ yields based on the accumulated carbohydrate, the rate of carbohydrate accumulation limits the application of this strategy.

3.4.1.1: Energy generation potential with a photoautotrophic 1st stage

In the case of a dark-fermentative 1st stage fed by wastes or synthetic solutions, the feeding rate can easily be adjusted to control the overall rate of H₂ production, whereas an algal/cyanobacterial-driven system (dependent on light) is limited by the yield of photoautotrophic carbohydrate production (e.g. mol hexose/m² light capture area/day). Combined with the molar yield of H₂ per hexose in the dual system, this can indicate the potential rate of H₂ production from a given light capture area (Table 3). Using an 800 L pond-type pilot plant with CO₂ as the carbon source for cultivation of *Chlamydomonas* spp., Ikuta et al. (1997) achieved a maximum productivity of 92.6 mmol hexose/m²/d, and an average productivity of 24.4 mmol hexose/m²/d over 23 days. Using a closed photobioreactor, *Chlamydomonas reinhardtii* was grown under outdoor light conditions using CO₂ in addition to acetate as carbon sources, yielding 158 mmol starch-hexose/m²/d (Kim et al. 2006c). Assuming cultivation conditions can be optimised to maintain the highest rate of starch accumulation this value was used to calculate the potential productivities of algal/cyanobacterial-driven dual systems (Table 3).

Using the data provided by Levin et al. (2004a) (see legend to Table 3), it can be calculated that at least 436 m² of light capture area would be needed to generate sufficient H₂ to power one home with modest energy requirements (1 kW), discounting the energy costs of the process (e.g. mixing, pumping, medium supplements, pH control and maintenance). Thus, significant improvements in the rate and efficiency of light conversion to carbohydrate would be required to permit biological energy generation by a dual system reliant upon microalgal or cyanobacterial starch accumulation, which is rather overshadowed by the availability of significant quantities of starch and cellulose wastes (Yokoi et al. 2002; Haq & Easterly 2006).

As a best-case scenario, metabolic engineering will lead to significant improvements in the efficacy of direct photolysis, allowing significant H₂ production coupled to

carbohydrate accumulation. If productivity could be increased 20-fold and the required area compacted to 20 m², decentralised domestic energy generation might become spatially feasible (assuming parallel developments in process automation, and not accounting for operational energy costs). Large centralised hydrogen farms might be more efficiently run, but such an industry would be in direct competition with conventional agriculture, which currently accounts for 77 % of land in the UK (Anon 2005). However, H₂ farms would not require fertile soil and might be operated in inhospitable environments such as deserts or on contaminated land where remediation might not be economically attractive (Aldhous 2006). The cultivation of 'energy crops', is currently receiving widespread attention (de Vrije & Claassen 2003; Aldhous 2006; Schnoor 2006). For example, *Jatropha* sp. are proposed as energy crops suitable for cultivation on sparse, non-arable land for the production of seed oil, which can be esterified to produce biodiesel fuel with the co-production of 'press-cake' residues which are suitable substrates for bioconversion e.g. to H₂ (Staubmann et al. 1997; Gübitz et al. 1999; Martínez-Herrera et al. 2006; Tiwari et al. 2007). A comparison of the potential energy yields per hectare for crop farms and photo-energy farms would repay study.

As the most plentiful energy source, solar energy must be part of any vision of future energy generation. This is the case either in a wholly light-driven system (e.g. microalgae + PNS bacteria) or in a partially light driven system (fermentation + PNS bacteria) where the fermentation is fed on biomass residues. As world population and food-demand grow, the limited availability of non-agricultural land may discourage algal or cyanobacterial cultivation. While 'green roofs' are established as a means of improved insulation and storm water retention, the potential of rooftop agriculture remains to be widely exploited (Nowak 2004). At the same time, the availability of residues is set to increase from both food and energy crops. Therefore, with the current state of knowledge and technology development, a dual system with dark fermentative 1st stage has a greater potential for near-term application.

On a broader scale, the use of microbial photosynthesis will have to compete with photovoltaic (PV) technology, which although as yet economically unattractive, is also under parallel development (Avi 2007). Data are as yet unavailable to compare the energy yields from optimised PV and bio-systems as industrial-scale photobioreactors for H₂ production are still under development. The estimated net energy ratio (NER) was *ca.* 2 for a photobioreactor lasting 20 years, constructed using tubes of flexible polyethylene film (thickness 0.18 mm), under the assumptions of film replacement every 3 years, 80 % time on-

line, 20 % loss of H₂, and discounting the costs of nutrients, temperature control and water (Burgess & Fernandez-Velasco 2007).

3.4.2: Dual systems with a dark fermentative 1st stage

Dark fermentation represents a rapid and relatively simple method for the conversion of carbohydrates into hydrogen, but the accumulation of organic fermentation products can exert stress upon the fermenting microorganisms and generates a secondary waste, requiring disposal (Eiteman & Altman 2006). Concurrently, fermentation products are preferred substrates for PNS bacteria, which oxidise reduced organic molecules and dispose of the reducing power as H₂. It has long been recognised that dark fermentation and photo-fermentation should be coupled to create an efficient scheme for waste-free hydrogen production (Odom & Wall 1983; Miyake et al. 1984). In practice, the maximum yield reported was 8.3 mol H₂/mol hexose (Kim et al. 2006c), and indeed several independent results of *ca.* 7 mol H₂/mol hexose were generated by different methods (Table 1).

The dark fermentation-photofermentation (DF-PF) dual system can be operated in continuous mode over extended periods. The longest experiment reported sustained H₂ evolution for 45 days by coupling lactic acid fermentation and a continuous photofermentation, but the yield of H₂/mol hexose cannot be calculated from the available data (Franchi et al. 2004). Yokoi et al. (2001 and 2002) reported sustainable operation of a dual system for 30 days, maintaining a steady overall yield of 7 mol H₂/mol hexose, using sweet potato starch residue. This system was used in repeated-batch culture, the fermenter being partially drained daily, and the photobioreactor every 5 days. A fully continuous system is currently under development (Redwood & Macaskie 2007a, 2007b). A continuous *E. coli* CSTR and a continuous *R. sphaeroides* photobioreactor were integrated by anion-selective electro dialysis, simultaneously transferring anionic fermentation products, while retaining repressive ammonium ion, *E. coli* cells and suspended solids. This approach resulted in sustained H₂ production by *E. coli* with a yield of 1.6 mol H₂/mol hexose and sustained H₂ photoproduction by *R. sphaeroides* despite the presence of 15 mM ammonium ion in the initial feed. The overall yield was 2.4 mol H₂/mol glucose, attributable to a low efficiency in the PBR (38 %) and a proportion of *E. coli* products being uncharged species (ethanol), not transported by electro dialysis. An overall yield of 10.1 mol H₂/mol glucose

could be predicted based on a substrate conversion efficiency of 75 % in the photobioreactor and optimisation of the latter is in progress.

Therefore, with present approaches, a dual system can be sustained continuously, and achieves on average *ca.* 60 % of the hypothetical maximum, 12 mol H₂/mol hexose (Figure 2D). As a priority, research is needed to investigate techniques for the integration and rate-balancing of inter-dependent bioreactors, alongside further study of the conditions needed to sustain high H₂ production continuously in either component of DF-PF dual systems.

3.4.2.1 Selection of organism for dual systems with dark fermentative 1st stage

An ideal fermentation, coupled to an ideal photo-fermentation could approach the maximum stoichiometry of 12 mol H₂/mol hexose (Figure 2D). As different fermentations can theoretically be coupled to a photofermentation to achieve the same maximum yield (Figure 2), differences in practicality and experimental yields must be examined.

The distinction is made between the use of obligate anaerobes in stage 1 and facultative aerobes/anaerobes, because there are distinct differences between the biochemical mechanisms of H₂ production of these classes (section 2.2, Figure 2).

In the case described by Yokoi et al. (2001 and 2002), the facultative anaerobe *Enterobacter aerogenes* was included in the 1st stage in co-fermentation with the strict anaerobe *C. butyricum* (Table 1). This example is classed among the strict anaerobic dual systems because *Enterobacter*, being unable to utilise starch, did not contribute to the fermentation but provided a cheaper alternative to reducing agents to ensure anaerobiosis by scavenging O₂ (Yokoi et al. 2001; Yokoi et al. 2002).

Facultative anaerobes (e.g. *E. coli*) can be rapidly pre-cultured, are very amenable to metabolic engineering, and do not require the addition of a reducing agent to ‘poise’ the redox potential, while the biochemistry of mixed-acid fermentation has been well-studied (Stephenson & Stickland 1932; Knappe 1987; Alam & Clark 1989; Clark 1989; Bock & Sawers 1992). Nevertheless, obligate anaerobes have been preferred in the study of dual systems, perhaps due to the potentially higher H₂ yield. Table 1 shows 14 examples of strict anaerobe-driven dual systems, with an average overall yield (where given) of 5.73 mol H₂/mol hexose (or 47.8 %). Conversely only eight examples of dual systems could be found using other types of fermentation in the 1st stage, of which, systems based on lactic acid

fermentation were the most effective, producing (overall) up to 7.3 mol H₂/mol hexose entirely from the 2nd stage (Kawaguchi et al. 2001). High overall yield is, therefore, possible without H₂ production in the 1st stage. This can be explained by the fact that lactic acid fermentation has been optimised for the industrial production of lactic acid (Li et al. 2004) and because lactate is theoretically converted to 6 H₂ in the 2nd stage, which typically operates with high efficiency (section 2.1.2).

It is possible that researchers have disregarded mixed-acid fermentation for use in the 1st stage because of its theoretically lower H₂ yield (Figure 2). The fermentative yield of H₂ from hexose by living organisms is thermodynamically limited to 4 mol H₂/mol hexose (Thauer 1977). The metabolic pathways of strict anaerobes (e.g. *C. butyricum*) allow this to be achieved only under very low H₂ partial pressure, otherwise the reaction is stoichiometrically similar to mixed-acid fermentation, producing a maximum of 2 mol H₂/mol hexose (Figure 2). The yield from strict anaerobic fermentation in a dual system has not exceeded 2.6 mol/mol (Table 1), and the use of a non-sporulating facultative anaerobe would cause no theoretical sacrifice of yield and a certain increase in practicality (Figure 2D, section 3.4.2.1).

Hyperthermophilic fermentations may yield up to 3.8 mol H₂/mol hexose in practice (section 2.2.1), but no accounts describe dual systems using hyperthermophiles. Furthermore, they would not be compatible with PNS bacteria in co-culture, which produce H₂ optimally at *ca.* 30 °C and live at temperatures below 47 °C (Castenholz 1995). A hypothetical industrial-scale facility based on the sequential combination of a thermobioreactor and a photobioreactor was estimated to produce H₂ at a cost of €2.74 /kg H₂ (de Vrije & Claassen 2003). If the bio-H₂ were used to generate electricity in a fuel cell operating at 50 % efficiency and 95 % utilisation, the cost of the energy production would be €0.145 /kWh. The price of domestic electricity is *ca.* €0.15 /kWh (2006, DTI file 36184, www.dti.gov.uk). However a more extensive economic analysis of the bioprocess, suggested a cost of €4/kg H₂ (Davila-Vazquez et al. 2007). Continued research and development of biohydrogen systems is required preceding a reliable economic assessment.

Some information is available regarding the use of non-axenic fermentations in the 1st stage of a dual system (Table 1). This strategy takes advantage of the presence of suitable microorganisms in the feedstock, thus eliminating the need to sterilise inputs and to pre-culture specific organisms. However, in undefined mixtures of microorganisms it is more

difficult to repress unwanted reactions (section 2.2.2), H₂ yields are generally lower than in axenic dual systems (Table 1), and it would be difficult to ensure reproducibility between feedstock sources and locations.

3.4.2.2: Distribution of H₂ production among stages of a dual system

Ike et al. (1997) compared 3 different ways to generate H₂ from algal biomass rich in starch, of which the most effective (in terms of H₂ yield) utilised a lactic acid fermentation (producing no H₂) followed by photo-fermentation with PNS bacteria, showing that it is not essential to produce H₂ in both phases of the dual system.

Figure 2 illustrates that various different stage 1 fermentations (e.g. lactic acid, mixed-acid and clostridial-type fermentations) can be applied with different H₂ yields but with equal potential for H₂ production overall (12 mol H₂/mol hexose). The type of fermentation employed affects the theoretical distribution of H₂ between the 1st and 2nd stages. If lactic acid fermentation were used, all 12 moles of H₂ would arise from the 2nd stage; 10 for mixed-acid fermentation and 8-10 for *C. butyricum*.

It is possible that *C. butyricum*-based dual systems have been favoured by researchers in order to skew the distribution of H₂ production towards the 1st stage and thus to minimise the required transfer of organic fermentation products and the light capture area. Conversely, H₂ is generally produced by fermentations at *ca.* 50 % of the theoretical maximum, while the photo-fermentation typically operates at *ca.* 70 % efficiency, so a higher overall yield could be expected using lactic acid or mixed-acid fermentation in which more H₂ is produced in the more efficient 2nd stage. The gain in productivity would need to be offset against the increased costs of light capture area and transfer of fermentation products.

3.4.2.3 Energy generation potential with a dark fermentative 1st stage.

The increased productivity of a dual system over a single-stage system is significant. For example, a molasses-fed pilot fermentation plant generated 8240 L H₂ (342.5 mol H₂) and 3000 L effluent per day (Ren et al. 2006). The effluent contained primarily acetate and ethanol with a hydrogen production potential of 246.35 mmol H₂/L (authors' calculations).

Therefore the addition of a photoheterotrophic 2nd stage could maximally increase productivity by 317 %.

As a best-case scenario, a dual system capable of generating 12 mol H₂/mol hexose might be developed. Work is underway to meet a target of 10 mol H₂/mol hexose, which would make bio-H₂ economically viable, given low feedstock costs (Davila-Vazquez et al. 2007). Using reported values for the productivity of dual systems, the potential for energy generation can be estimated.

With the same assumptions as used in Table 3, a household might consume H₂ at a minimum rate of 573.6 mol/d (Levin et al. 2004a; Levin 2004b). The feasibility of the decentralised application of a sequential dual system was evaluated (in this study) by calculating the necessary reactor sizes and the feed requirements to meet this demand. The energy requirements of the process were not taken into account.

If the potential H₂ yield (12 mol H₂/mol hexose) were to be distributed 4:8 between the 1st and 2nd stages, respectively, then the dark fermentation would be required to produce 191.2 mol H₂/d and the photobioreactor 382.4 mol H₂/day (of which only *ca.* 12 h is light). Using published volumetric productivities (Levin et al. 2004a; Levin 2004b), it was calculated that a 79.6 L fermenter (containing an undefined mesophilic culture, *ca.* 0.1 mol H₂/L/h) would be needed. The productivity of the photobioreactor (PBR) would be constrained by several parameters: light conversion efficiency (up to 10 % energy basis (Akkerman et al. 2002)), light availability (1 kW/m² for 12 h/d (Miyake et al. 1999)), specific rate of H₂ production (*ca.* 0.1 L H₂/g dw/h, (Rocha et al. 2001)), culture depth (5 cm), culture density (*ca.* 1 g dry wt./L : OD *ca.* 2.5). To operate within these constraints a PBR volume of 7648 L would be required. The corresponding square panel PBR would be 5 cm deep and 12.4 m wide with a light capture area of 153.0 m². This area could potentially harvest 6.6 GJ per 12 h light period, indicating a comfortable light conversion efficiency of 1.65 % to meet the H₂ demand (Figure 4).

It is noteworthy that the limiting factor is the specific rate of H₂ production (necessitating a dense culture and limiting the PBR depth) rather than the light conversion efficiency even at the reasonable light intensity of 1 kW/m². Were specific rates to be increased (e.g. through improved strains or bioreactors), the light intensity and conversion efficiency would limit the productivity of the photobioreactor. At a light intensity of 1 kW/m² for 12 h per day, with 65.8 % of useful solar energy and 10 % a photosynthetic efficiency a

light capture area of 38.44 m² (6.2 m x 6.2 m) would be needed to produce 382.4 mol H₂ in 12 hours. A house might barely accommodate an 80 L fermenter and a 40 m² photobioreactor, along with H₂ storage, regulatory equipment and fuel cell (Figure 4), but even with a conversion efficiency of 12 mol H₂/mol hexose, the feed-demand would be 7.74 kg cellulose/d or 8.17 kg sucrose/d, which could be supplemented with organic household wastes for disposal, although the additional sugar would be negligible. Sugar production is an agricultural industry, so this option could not be applied in the long-term due to competition for farmland (as 3.4.1.1) but sugar-processing wastes could be exploited as feed substrates.

Whereas the use of energy crops would incur costs, it could be economically realistic to co-locate H₂ production with feed sources such as food processing plants. The UK food industry produces *ca.* 5.3 million ton biodegradable waste annually (UK food & drink processing mass balance, C-tech Innovation, 2004), a large fraction of which is disposed of by land-filling, which incurs a cost (Bartelings et al. 2005). Co-locating food-waste generation and conversion to H₂ would remove transport costs, while minimising spoilage of the residues to maintain their value. Bio-H₂ production could be optimised for the use of residues having relatively consistent composition and little H₂ storage or distribution would be required as produced energy could be used on-site to meet predictable energy demands and any excess production could be sold to the national grid to alleviate the demand for fossil fuel.

There are many accounts of biohydrogen production from non-synthetic substrates (i.e. wastes), and dual systems have been applied in several cases (Table 1) (Zhu et al. 1995; Fascetti et al. 1998; Kim et al. 2001; Zhu et al. 2002; Franchi et al. 2004). De Vrije and Claassen (2003) described a hypothetical process fed by lignocellulosic biomass, and calculated that 9 % of the domestic energy demand could be met using available biomass residues in the Netherlands.

3.4.2.4 Bio-H₂, bio-methane or bio-ethanol?

Biomass residues are available in significant quantities for use as feedstocks for bioenergy production (Easterly & Burnham 1996; Filho & Badr 2004; Haq & Easterly 2006; Mabee et al. 2006; Dawson & Boopathy 2007; Levin et al. 2007). Bioprocesses for the production of H₂, methane and ethanol can all utilise biomass residues as feeds, although currently, bio-ethanol and bio-methane processes are commercially more advanced than bio-H₂ processes.

Levin et al. (2007) calculated the energy potential of Canada's biomass residues for methane production by anaerobic digestion and H₂ production by anaerobic bacterial fermentation. The potential H₂ energy equated to only 41.4 % of the potential methane energy. However, this calculation was based on a H₂ yield of 1.3 mol H₂/mol hexose from a single-stage bacterial fermentation. Several authors report multi-organism systems for H₂ production producing in excess of 7 mol H₂/mol hexose (Weetall et al. 1989; Miura et al. 1992; Ike et al. 2001; Kawaguchi et al. 2001; Yokoi et al. 2001; Asada et al. 2006; Kim et al. 2006c). Therefore, bio-H₂ production could be more economically attractive than bio-methane production, if dual H₂-producing systems can be implemented.

Bio-ethanol is a major energy vector in Brazil, with a production of 16 billion L of ethanol *per year*, requiring *ca.* 3 million hectares of land. The total sugarcane crop area (for sugar and ethanol) is 5.6 million hectares (Goldemberg 2007). The average industrial yield during the crop 2004/2005 was 144.35 kg sucrose/tonne sugarcane, equivalent to 79.39 L anhydrous ethanol/tonne sugarcane or 82.86 L hydrous ethanol/tonne sugarcane (Nastari et al. 2005). Therefore, the process efficiency of bio-ethanol production is 80.5 % (of a biochemical maximum of 2 mol ethanol/mol hexose). Considering the higher heating value (HHV) of ethanol of 29.840 MJ/kg (<http://hydrogen.pnl.gov/cocoon/morf/hydrogen/article/401>), the bio-ethanol process produces 2,212 kJ energy/mol hexose (from sugar cane). To equal this energy yield a biohydrogen process must achieve *ca.* 7.8 mol H₂/mol hexose (HHV of H₂ = 141.88 MJ/kg, hydrogen.pnl.gov/cocoon/morf/hydrogen/article/401). This could not be achieved by a single-organism system, and a dual system would be required.

4: Conclusions and future perspectives

Biological hydrogen production is a promising avenue that should be pursued urgently as the world energy demand increases, fossil fuel resources dwindle and the need for greenhouse gas minimisation becomes increasingly pressing. Hydrogen biotechnology is poised to become increasingly prominent alongside, and eventually emerging as competitive with other sustainable biofuel processes and/or as an adjunct to them.

This review shows that (unlike with bioethanol production) no single microorganism can produce competitive yields of H₂. Multiple-organism systems offer increased H₂ yields over single organisms and would be mandatory for realistic future energy generation.

Examination of the properties of photosynthetic microorganisms revealed that purple non-sulfur (PNS) bacteria are the most suitable organisms for the 2nd stage of a dual system, while for the 1st stage dark fermentation, clostridia have been the most widely used but facultative aerobes may increase the ease of operation while detracting little from the overall H₂ yield. Advances in membrane separation technology (e.g. anion-selective electro dialysis) can overcome rate-limitations of substrate transfer between the 1st and 2nd stages (Redwood & Macaskie 2007a), which precludes the need for biomass immobilization and would allow high density, well mixed cultures. However the potential limitations of membrane fouling and the expense of membranes would need to be addressed.

A dual system combining anaerobic fermentation and photoheterotrophy could potentially result in high energy yields from industrial wastes or biomass residues, although it is unlikely that a domestic household would produce sufficient fermentable waste to make a significant contribution to its energy budget. For example, a molasses-fed pilot fermentation plant operated with a yield of 26.1 mol H₂/kg COD removed, generating 342.5 mol H₂/day (Ren et al. 2006), sufficient to produce an electrical power of 0.6 kW using a realistic PEM-FC (operating at 50 % efficiency and 95 % utilisation) (Levin et al. 2004a).

Even by increasing the output by several-fold by addition of the second stage PBR it is unlikely that a light-driven dual system would repay investment for single household domestic electricity generation. Furthermore, it can be calculated that for domestic self-sufficiency several tonnes of sugary waste would be required annually, therefore, substrate supply would be the limiting factor rather than spatial considerations. Hence, industrial, retail and agricultural waste producers would be the likely initial users of bio-H₂ systems.

In addition to food processing and retailing wastes, biomass residues are available in significant quantities for use as feedstocks for bioenergy production (Easterly & Burnham 1996; Filho & Badr 2004; Haq & Easterly 2006; Mabee et al. 2006; Levin et al. 2007). Bioprocesses for the production of H₂, methane and ethanol can all utilise biomass residues as feedstocks although, currently, bio-ethanol and bio-methane processes are commercially more advanced than bio-H₂ processes.

It was argued above (section 3.4.2.4) that a dual bio-H₂ system could be more productive than bio-methane and equally productive to bio-ethanol in terms of energy production. This calculation used values of combustion enthalpy for bio-CH₄ and bio-H₂ in both cases, making the assumption that energy can be recovered from H₂ and CH₄ with equal

efficiency, e.g. by coupling of the biogas-producing generation reactor to a fuel cell for electricity generation assuming a pure gas stream (e.g. see Macaskie *et al.*, 2005). The most efficient type, proton exchange membrane (PEM; also called polymer electrolyte membrane) fuel cells, achieve the highest power densities when H₂ is used as a fuel, whereas solid oxide fuel cells (SOFCs) are more suitable for the use of hydrocarbons such as methane (Larminie & Dicks 2003). However SOFCs use an oxide ion-conducting ceramic material as the electrolyte and require an operating temperature of 600-1100 °C and hence the necessary heat input detracts from the overall energy balance. In addition, any contamination of bio-methane with H₂S, the end product of dissimilatory sulfate metabolism by the sulfate-reducing bacteria present in anaerobic mixed cultures, would necessitate gas filtration, since sulphur compounds are powerful catalyst poisons affecting all types of fuel cells. The direct methanol fuel cell (DMFC) is a type of PEM-FC in which methanol reacts (slowly) at the anode according to: $\text{CH}_3\text{OH} + \text{H}_2\text{O} \rightarrow 6\text{H}^+ + 6\text{e}^- + \text{CO}_2$ (Larminie & Dicks 2003). For DMFC, the power density is relatively low compared to PEM-FC and SOFC, but this would not prevent application in portable devices such as laptop computers, where the power storage exceeds 25 Wh and the required DMFC unit would be significantly smaller in volume than the equivalent lithium-ion battery (see Larminie & Dicks, 2003).

The formation of methanol from methane via methane monooxygenase is very well established (Grosse *et al.* 1999; Dalton 2005) and a comparative study of the various biogas and fuel cell-coupling options would be worthwhile.

Fuels which are liquid at room temperature (e.g. methanol and ethanol) have higher volumetric energy densities than gaseous H₂. Apart from the consideration of land use the long-term economics of bioethanol production need to be considered (Rogers *et al.* 2005). Ethanol cannot be used efficiently in fuel cells (Larminie & Dicks 2003) and a major problem is the higher cost of bioethanol production (from cellulosic biomass) as compared to diesel or petrol; this cost is projected to become comparable to that of petrol by 2015, based on an oil price of \$35-\$40 a barrel (Chandel *et al.* 2007). The distillation cost is significantly higher at low ethanol concentrations (Zacchi & Axelsson 1989), and a membrane distillation process can be used as an efficient and cost effective option (see Chandel *et al.* 2007); molecular sieve techniques are now widely used in the industry (Rogers *et al.* 2005). A net energy balance (NEB) calculated by Hill *et al.* (2006) suggests that corn grain ethanol provides *ca.* 25 %

more energy than that consumed in its production; however almost all of the NEB can be attributed to the 'energy credit' for the animal feed co-product.

Brazil has certain comparative advantages in ethanol production. Unlike American or European processes based on crops (e.g. barley, corn or wheat) that must first be converted at significant expense into sugars, Brazilian processes are based on sugarcane, which its climate favours, obviating any need for conversion. Ethanol produced from sugarcane in Brazil has a net positive energy balance (renewable energy output versus fossil fuel input) of 10.2, whilst the energy balance for ethanol from corn (US) is 1.4 (Goldemberg 2007). Also, the production cost of ethanol from sugarcane (Brazil) (US\$ 0.81 *per* gallon, in 2006) is lower compared to ethanol from corn (US) (US\$ 1.03 *per* gallon, in 2006) and is competitive with gasoline in the US, even considering the import duty of US\$0.54 *per* gallon and energy-efficiency penalties (30 % or less with modern flexible fuel vehicle technologies) (Goldemberg 2007). Ethanol produced in Brazil has remained fully competitive with gasoline on the international markets, without government intervention, since 2004, i.e. subsidising ethanol production is a thing of the past. In addition to the production of ethanol, the industrial processing of sugarcane generates bagasse, another valuable product which adds to the industry's positive environmental differential because it has been used to replace fossil fuels in the production of industrial heat and electricity in the sugar mills and distilleries, thereby boosting the abatement potential of greenhouse gases emission (Macedo et al. 2004). Moreover, the competition for land use between food and fuel has not been substantial: sugarcane covers 10 % of total cultivated land and 1 % of total land available for agriculture in the country (Goldemberg 2007).

A recent review (Hill et al. 2006) has evaluated critically the long-term potential for bioethanol against emerging biodiesel technology. While ethanol is made by the fermentation of biomass substrates (cane sugar is ideal because no further processing is required), biodiesel is made *via* processing of plant material from 'energy crops'. For example, soybean biodiesel is sourced directly from long-chain triglycerides obtained from the seeds; in comparison corn-starch requires pre-enzymatic conversion into fermentable sugars for ethanol production. Critically, biodiesel yields 93 % more energy than that invested in its production and relative to the fossil fuels they displace, greenhouse gas emissions are reduced by 12 % and by 41 % by bioethanol and biodiesel, respectively. However, Hill *et al.* (2006) point out that 'even dedicating all U.S. corn and soybean production to biofuels would meet only 12 % of gasoline

demand and 6 % of diesel demand'. Lin & Tanaka (2006) suggest that any country with a significant agronomic-based economy could use technology for ethanol fuel production. However, this and many other critiques overlook the difficulty of achieving a positive energy balance for the production of bio-ethanol from crops such as corn and wheat rather than from sugarcane. An early analysis (Pimentel 2001) reported a negative energy balance for corn ethanol in the US, whereas the result of recent studies was a more favourable energy balance of 1.4 (Goldemberg 2007). Nevertheless, the cultivation area needed to support a US fuel economy based on corn-ethanol would equate to most of the nation's land area (Pimentel 2001), and the same argument applies to all 'energy crops' that compete for agricultural land with food supply, a very major factor, which is acknowledged but understated by Hill et al. (2006). These authors suggest the use of agriculturally marginal land or the use of waste biomass for bioethanol production; both are potentially more sustainable than outright energy crop cultivation. Assuming that the cost of ethanol recovery can be lowered by effective recovery technology, the use of large global reserves of lignocellulosic waste biomass as potentially fermentable feedstock is receiving widespread attention with respect to bioethanol production and also with respect to bio-H₂ production (de Vrije & Claassen 2003; Aldhous 2006; Schnoor 2006). The main problem lies in converting the recalcitrant woody material into readily fermentable substrate. This requires pre-treatment, which may be physico-chemical, enzymatic or combinations of these. An overview of upstream treatments is outside the scope of this review and the reader is referred to recent example reviews in this area (Rogers et al. 2005; Lin & Tanaka 2006; Chandel et al. 2007). Once a fermentable feedstock is generated there are several options for the downstream energy production process and the hydrolysate could be equally well used for biohydrogen production as for bioethanol production, without the attendant processing costs.

The use of energy crops for biodiesel production is particularly promising and the technological limitations have been reviewed by Abdullah et al. (2007). Chemically, 'biodiesel' is fatty acid methyl esters, produced by the transesterification of oils and fats with methanol in the presence of suitable catalysts. Here bio-methanol could find a large-scale application as an alternative to the niche market for fuel cell use. The disadvantages of biodiesel production are that large volumes of contaminated wastewater are produced and that homogeneous catalysis is employed for maximum processing efficiency; the catalyst is currently not retained and major research efforts are directed towards the development of

solid phase catalysts (Abdullah et al. 2007). Glycerol is produced in tonnage quantities as a by-product, which could be a suitable substrate for microbial fermentation to produce ethanol or H₂ as additional energy products. However the glycerol is obtained as an aqueous impure NaCl-solution which requires purification and its use as a fermentation substrate would compete with other potential uses in the pharmaceutical, cosmetic and food industries, and as animal feeds, polymers, surfactants and lubricants (Ma & Hanna 1999). Assuming that microorganisms resistant to the contaminants are developed, biohydrogen production could be attractive in this context since a gaseous product is easily separated from the fermentation liquor and hence the purity or otherwise of the starting material is largely irrelevant, assuming the product gas stream is free of volatile agents.

Biodiesel is made by pressing plant material (e.g. seeds) to extract the oils and hence plant residua could be a useful waste for fermentation to make a secondary ethanol or hydrogen fuel stream; however the problems of upstream treatment of the wastes are similar to those of other fibrous materials. However in at least one example waste from oil production (in this case olive oil) has been used as the substrate for biohydrogen production (Eroğlu et al. 2004). Clearly the use of edible oils from food-crops such as *Olea* sp. (olive) for biofuel production would be impractical, whereas attention has recently focused on the use of inedible oil for biodiesel production, obtained from the tropical oil seed plant *Jatropha curcas*, which is drought resistant and can grow on marginal, sub-arable or even waste land (Srivastava & Prasad 2000) in Central and South America, Mexico, South-East Asia, India and Africa. *J. curcas* is not suitable as animal feed without detoxification (Martínez-Herrera et al. 2006) but has many other applications and a transesterification process of the seed oil as a biofuel has been evaluated on an industrial scale (1500 tonnes per annum) (Gübitz et al. 1999). Due to its high free fatty acid content (*ca.* 14 % w/w) *Jatropha* oil requires pre-esterification using methanol before conventional transesterification to produce biodiesel, which was shown to give a high yield of biodiesel with satisfactory fuel properties (Tiwari et al. 2007). Bio-methane production from anaerobic digestion is a potential source of bio-methanol, which could find use in the pre-esterification reaction. Crushing *Jatropha* seeds to release the oil results in an equal mass of press-cake, which can be used as a substrate for further bioprocessing, e.g. methane production by anaerobic digestion (Staubmann et al. 1997).

In conclusion, the production of biofuels (biodiesel, bioethanol or biogases) from energy-dedicated crops appears to be unsustainable unless the plant occupies a niche other than agricultural land or provides a high yield of energy per area of cultivation. Agricultural residues (lignocellulosic biomass) are available as sources of fermentable substrate for biofuel production but these wastes form a common bottleneck in the conversion of wastes into fermentable feedstock. Biogases and bioethanol can both be made by the fermentation of sugars and sugary wastes but the processing costs of ethanol limit the energy output of this method.

The hydrogen economy *per se* is still some decades away but combination and hybrid technologies are appealing in the shorter term. Production of H₂ from food waste sources or from the wastes from biodiesel production is potentially a clean, and sustainable route to clean energy production.

Although the maximum yields of H₂ from sugar are being approached by fermentation this is only possible by the application of more than one microorganism. This review has attempted to identify the two-stage approaches by which maximum yields (and rates) of conversion can be obtained and it identifies that, as with energy crops, available land area for light capture is likely to be a major limiting factor in operation. Under-used, waste ground in sunny regions (as for *Jatropha*) could provide one solution but for most of the developed world arable land takes priority for food production. Process intensification is required to overcome the problem of light delivery to the second stage photofermentations, which would push bio-H₂ production to competitive levels. A review of photobioreactor designs to achieve effective light transfer into high-activity cultures is outside the scope of this overview; the reader is referred to recent reviews (Tsygankov 2001; Hoekema et al. 2002; Kondo et al. 2002; Claassen & de Vrije 2007).

5: Bibliography

- Abdullah AZ, Razali N, Mootabadi H & Salamatina B (2007). Critical technical areas for future improvements in biodiesel technologies. *Environ Res Lett* in press, online 2nd July 2007 doi:10.1088/1748-9326/2/3/034001.
- Akano T, Miura Y, Fukatsu K, Miyasaka H, Ikuta Y, Matsumoto H, Hamasaki A, Shioji N, Mizoguchi T, Yagi K & Maeda I (1996). Hydrogen production by photosynthetic microorganisms. *Appl Biochem Biotechnol* 57-8:677-688.
- Akkerman I, Janssen M, Rocha J & Wijffels RH (2002). Photobiological hydrogen production: photochemical efficiency and bioreactor design. *Int J Hydrogen Energy* 27(11-12):1195-1208.
- Alam KY & Clark DP (1989). Anaerobic fermentation balance of *Escherichia coli* as observed by *in vivo* nuclear magnetic resonance spectroscopy. *J Bacteriol* 171(11):6213-6217.

- Aldhous P (2006). Green gold. *New Sci* 25 Feb:37-40.
- Anon. (2005). Agriculture in the United Kingdom. Retrieved Aug 2007, 2007, from statistics.defra.gov.uk/esg/publications/auk/2005/default.asp.
- Antal TK & Lindblad P (2005). Production of H₂ by sulphur-deprived cells of the unicellular cyanobacteria *Gloeocapsa alpicola* and *Synechocystis* sp. PCC 6803 during dark incubation with methane or at various extracellular pH. *J Appl Microbiol* 98(1):114-20.
- Aoyama K, Uemura I, Miyake J & Asada Y (1997). Photosynthetic bacterial hydrogen production with fermentation products of cyanobacterium *Spirulina platensis*. International Conference on Biological Hydrogen Production, Waikoloa, Hawaii, Plenum Press, New York.
- Asada Y, Tokumoto M, Aihara Y, Oku M, Ishimi K, Wakayama T, Miyake J, Tomiyama M & Kohno H (2006). Hydrogen production by co-cultures of *Lactobacillus* and a photosynthetic bacterium, *Rhodobacter sphaeroides* RV. *Int J Hydrogen Energy* 31(11):1509-1513.
- Avi S (2007). Photovoltaics literature survey (No. 51). *Progress in Photovoltaics: Research and Applications* 15(1):87-91.
- Bae J-H, Bardiyia N & Reddy MRVP (2005). Bio-hydrogen: technology and future prospects. Wealth from waste: trends and technologies. Lal B & Reddy MRVP, (Eds). New Delhi, India, TERI Press: 87-132.
- Banik RM, Santhiagu A, Kanari B, Sabarinath C & Upadhyay SN (2003). Technological aspects of extractive fermentation using aqueous two-phase systems. *World J Microbiol Biotechnol* 19(4):337-348.
- Bartelings H, van Beukering P, Kuik O, Linderhof V, Oosterhuis F, Brander L & Wagtendonk A (2005). Effectiveness of landfill taxation, Report prepared for the Dutch Ministry of Housing, Spatial Planning and the Environment, Institute for Environmental Studies, Vrije Universiteit, R-05/05, Amsterdam. Available at www.ivm.falw.vu.nl/research_output/index.cfm/home_subsection.cfm/subsectionid/FF91BCBD-EAFE-426A-ABB8184073A39BBF.
- Basak N & Das D (2007). The prospect of purple non-sulfur (PNS) photosynthetic bacteria for hydrogen production: the present state of the art. *World J Microbiol Biotechnol* 23:31-42.
- Benemann JR (1996). Hydrogen biotechnology: Progress and prospects. *Nat Biotechnol* 14:1101-1103.
- Biebl H & Pfennig N (1981). Isolation of members of the family *Rhodospirillaceae*. The Prokaryotes. Starr MP, Stolp H, Truper HG, Balows A & Schlegel HG, (Eds). Springer. 1: 267-273.
- Blankenship RE, Madigan MT & Bauer CE (1995). Anoxygenic photosynthetic bacteria. Dordrecht, The Netherlands, Kluwer Academic.
- Bock A & Sawers G (1992). Fermentation. *Escherichia coli* and *Salmonella Typharium*. Niedhardt FC, (Ed.). Washington DC, ASM Press. 1: 262-282.
- Borodin VB, Tsygankov AA, Rao KK & Hall DO (2000). Hydrogen production by *Anabaena variabilis* PK84 under simulated outdoor conditions. *Biotechnol Bioeng* 69(5):478-485.
- Burgess G & Fernandez-Velasco JG (2007). Materials, operational energy inputs, and net energy ratio for photobiological hydrogen production. *Int J Hydrogen Energy* 32:1255-1234.
- Castenholz RW (1995). Ecology of thermophilic anoxygenic phototrophs. Anoxygenic photosynthetic bacteria. Blankenship RE, Madigan MT & Bauer CE, (Eds). Dordrecht, The Netherlands, Kluwer Academic: 87-103.
- Chandel AK, Chan ES, Rudravaram R, Narusu ML, Rao LV & Ravindra P (2007). Economics and environmental impact of bioethanol production technologies: an appraisal. *Biotechnol Mol Biol Rev* 2(1):14-32.
- Chen X, Sun Y, Xiu Z, Li X & Zhang D (2006). Stoichiometric analysis of biological hydrogen production by fermentative bacteria. *Int J Hydrogen Energy* 31:539-549.
- Claassen PAM & de Vrije GJ (2007). Hydrogen from biomass. Public report, BWP II project, Agrotechnology and Food Sciences Group, Wageningen. 2007.
- Clark DP (1989). The fermentation pathways of *Escherichia coli*. *FEMS Microbiol Rev* 5(3):223-234.
- Collet C, Adler N, Schwitzgubel J-P & Peringer P (2004). Hydrogen production by *Clostridium thermolactum* during continuous fermentation of lactose. *Int J Hydrogen Energy* 29:1479-1485.

- Cornet JF, Favier L & Dussap CG (2003). Modeling stability of photoheterotrophic continuous cultures in photobioreactors. *Biotechnol Prog* 19:1216-1227.
- Cournac L, Guedeney G, Peltier G & Vignais PM (2004). Sustained photoevolution of molecular hydrogen in a mutant of *Synechocystis* sp. strain PCC 6803 deficient in the type I NADPH-dehydrogenase complex. *J Bacteriol* 186:1737-1746.
- Dalton H (2005). The Leeuwenhoek Lecture 2000 The natural and unnatural history of methane-oxidizing bacteria. *Phil Trans R Soc B* 360(1458):1207-1222.
- Das D & Veziroglu TN (2001). Hydrogen production by biological processes: a survey of literature. *Int J Hydrogen Energy* 26:13-28.
- Davila-Vazquez G, Arriaga S, Alatrliste-Mondragon F, de Leon-Rodriguez A, Rosales-Colunga LM & Razo-Flores E (2007). Fermentative biohydrogen production: trends and perspectives. *Rev Environ Sci Biotechnol* in press.
- Dawson L & Boopathy R (2007). Use of post-harvest sugarcane residue for ethanol production. *Bioresour Technol* 98(9):1695-1699.
- de Vrije T & Claassen PAM (2003). Dark hydrogen fermentations. *Bio-methane & Bio-hydrogen*. Reith JH, Wijffels RH & Barten H, (Eds). Petten, Netherlands, Dutch Biological Hydrogen Foundation: 103-123.
- de Vrije T, Mars AE, Budde MAW, Lai MH, Dijkema C, de Waard P & Claassen PAM (2007). Glycolytic pathway and hydrogen yield studies of the extreme thermophile *Caldicellulosiruptor saccharolyticus*. *Appl Microbiol Biotechnol* 74:1358-1367.
- Dien BS, Nichols NN, O'Bryan PJ & Bothast RJ (2000). Development of new ethanologenic *Escherichia coli* strains for fermentation of lignocellulosic biomass. *Appl Biochem Biotechnol* 84-6:181-196.
- Dutta D, De D, Chaudhuri S & Bhattacharya SK (2005). Hydrogen production by cyanobacteria. *Microb Cell Fact* 4:36.
- Easterly JL & Burnham M (1996). Overview of biomass and waste fuel resources for power production. *Biomass Bioenergy* 10(2-3):79-92.
- Eiteman MA & Altman E (2006). Overcoming acetate in *Escherichia coli* recombinant protein fermentations. *Trends Biotechnol* 24(11):530-536.
- Emanuelsson EAC, Arcangeli JP & Livingston AG (2003). The anoxic extractive membrane bioreactor. *Water Res* 37(6):1231-1238.
- Ensign JC (1977). Biomass production from animal wastes. *Microbial Energy Conversion*. Schlegel HG & Barnea J, (Eds). Oxford, Pergamon: 455-483.
- Eroğlu E, Gündüz U, Yücel M, Türker L & Eroğlu I (2004). Photobiological hydrogen production by using olive mill wastewater as a sole substrate source. *Int J Hydrogen Energy* 29:163-171.
- Eroğlu I, Aslan K, Gündüz U, Yücel M & Türker L (1997). Continuous hydrogen production by *R. sphaeroides* O.U 001. International Conference on Biological Hydrogen Production, Waikoloa, Hawaii, Plenum Press, New York.
- Fang HHP, Liu H & Zhang T (2005). Phototrophic hydrogen production from acetate and butyrate in wastewater. *Int J Hydrogen Energy* 30:785-793.
- Fang HHP, Li C & Zhang T (2006). Acidophilic biohydrogen production from rice slurry. *Int J Hydrogen Energy* 31:683-692.
- Fascetti E, D'Addario E, Todini O & Robertiello A (1998). Photosynthetic hydrogen evolution with volatile organic acids derived from the fermentation of source selected municipal solid wastes. *Int J Hydrogen Energy* 23(9):753-760.
- Ferchichi M, Crabbe E, Hintz W, Gil GH & Almadidy A (2005). Influence of culture parameters on biological hydrogen production by *Clostridium saccharoperbutylacetonicum* ATCC 27021. *World J Microbiol Biotechnol* 21(6-7):855-862.
- Filatova LV, Berg IA, Krasil'nikova EN, Tsygankov AA, Laurinavichene TV & Ivanovskii RN (2005a). A study of the mechanism of acetate assimilation in purple nonsulfur bacteria lacking the glyoxylate shunt: Acetate assimilation in *Rhodobacter sphaeroides*. *Microbiol* 74(3):265-269.

- Filatova LV, Berg IA, Krasil'nikova EN & Ivanovskii RN (2005b). A study of the mechanism of acetate assimilation in purple nonsulfur bacteria lacking the glyoxylate shunt: Enzymes of the citramalate cycle in *Rhodobacter sphaeroides*. *Microbiol* 74(3):270-278.
- Filho PA & Badr O (2004). Biomass resources for energy in north-eastern Brazil. *Appl Energy* 77:51-67.
- Fissler J, Kohring GW & Giffhorn F (1995). Enhanced hydrogen production from aromatic acids by immobilized cells of *Rhodopseudomonas palustris*. *Appl Microbiol Biotechnol* 44:43-46.
- Franchi E, Tosi C, Scolla G, Penna GD, Rodriguez F & Pedroni PM (2004). Metabolically engineered *Rhodobacter sphaeroides* RV strains for improved biohydrogen photoproduction combined with disposal of food wastes. *Mar Biotechnol* 6:552-565.
- Fuji T, Tarusawa M, Miyanaaga M, Kiyota S, Watanabe T & Yabuki M (1987). Hydrogen production from alcohols, malate and mixed electron donors by *Rhodopseudomonas* sp. No. 7. *Agric Biol Chem* 51(1):1-7.
- Ghirardi ML, King PW, Posewitz MC, Maness PC, Fedorov A, Kim K, Cohen J, Schulten K & Seibert M (2005). Approaches to developing biological H₂-photoproducing organisms and processes. *Biochem Soc Trans* 33:70-72.
- Goldemberg J (2007). Ethanol for a sustainable energy future. *Science* 315:808-810.
- Gosse JL, Engel BJ, Rey FE, Harwood CS, Scriven LE & Flickinger MC (2007). Hydrogen production by photoreactive nanoporous latex coatings of nongrowing *Rhodopseudomonas palustris* CGA009. *Biotechnol Prog* 23(1):124-130.
- Grosse S, Laramee L, Wendlandt K-D, McDonald IR, Miguez CB & Kleber H-P (1999). Purification and characterization of the soluble methane monooxygenase of the type II methanotrophic bacterium *Methylocystis* sp. strain WI 14. *Appl Environ Microbiol* 65(9):3929-3935.
- Gübitz GM, Mittelbach M & Trabi M (1999). Exploitation of the tropical oil seed plant *Jatropha curcas* L. *Bioresour Technol* 67:73-82.
- Hallenbeck PC & Benemann JR (2002). Biological hydrogen production; fundamentals and limiting processes. *Int J Hydrogen Energy* 27(11-12):1185-1193.
- Hallenbeck PC (2005). Fundamentals of the fermentative production of hydrogen. *Water Sci Technol* 52(1-2):21-29.
- Happe T, Schutz K & Bohme H (2000). Transcriptional and mutational analysis of the uptake hydrogenase of the filamentous cyanobacterium *Anabaena variabilis* ATCC 29413. *J Bacteriol* 182(6):1624-31.
- Haq Z & Easterly JL (2006). Agricultural residue availability in the United States. *Appl Biochem Biotechnol* 129-132:3-21.
- Hassan MA, Shirai Y, Kusubayashi N, Karim MIA, Nakanishi K & Hashimoto K (1997). The production of polyhydroxyalkanoate from anaerobically treated palm oil mill effluent by *Rhodobacter sphaeroides*. *J Ferment Bioeng* 83(5):485-488.
- Hawkes FR, Dinsdale R, Hawkes DL & Hussy I (2002). Sustainable fermentative hydrogen production: challenges for process optimisation. *Int J Hydrogen Energy* 27:1339-1347.
- Hawkes FR, Hussy I, Kyazze G, Dinsdale R & Hawkes DL (2007). Continuous dark fermentative hydrogen production by mesophilic microflora: Principles and progress. *Int J Hydrogen Energy* 32:172-184.
- Hill J, Nelson E, Tilman D, Polasky S & Tiffany D (2006). Environmental, economic, and energetic costs and benefits of biodiesel and ethanol biofuels. *Proc Nat Acad Sci USA* 103:11206-11210.
- Hillmer P & Gest H (1977a). H₂ metabolism in the photosynthetic bacterium *Rhodopseudomonas capsulata*: H₂ production by growing cultures. *J Bacteriol* 129(2):724-731.
- Hillmer P & Gest H (1977b). H₂ metabolism in the photosynthetic bacterium *Rhodopseudomonas capsulata*: Production and utilisation of H₂ by resting cells. *J Bacteriol* 129(2):732-739.
- Hoekema S, Bijmans M, Janssen M, Tramper J & Wijffels RH (2002). A pneumatically agitated flat-panel photobioreactor with gas re-circulation: anaerobic photoheterotrophic cultivation of a purple non-sulfur bacterium. *Int J Hydrogen Energy* 27(11-12):1331-1338.
- Holmes B & Jones N (2003). Brace yourself for the end of cheap oil. *New Sci* 179(2406):9.

- Hustede E, Steinbuchel A & Schlegel HG (1993). Relationship between the photoproduction of hydrogen and the accumulation of PHB in nonsulfur purple bacteria. *Appl Microbiol Biotechnol* 39(1):87-93.
- Ike A, Toda N, Murakawa T, Hirata K & Miyamoto K (1997). Hydrogen photoproduction from starch in CO₂-fixing microalgal biomass by a halotolerant bacterial community. *Biohydrogen*, Hawaii, Plenum Press, New York and London.
- Ike A, Kawaguchi H, Hirata K & Miyamoto K (2001). Hydrogen photoproduction from starch in algal biomass. *Biohydrogen II : An Approach to Environmentally Acceptable Technology*. Miyake J, Matsunaga T & San Pietro A, (Eds). Pergamon: 53-61.
- Ikuta Y, Akano T, Shioji N & Maeda I (1997). Hydrogen production by photosynthetic microorganisms. *International Conference on Biological Hydrogen Production*, Waikoloa, Hawaii, Plenum Press, New York.
- Ivanovskii RN, Krasil'nikova EN & Berg IA (1997). The mechanism of acetate assimilation in the purple nonsulfur bacterium *Rhodospirillum rubrum* lacking isocitrate lyase. *Microbiol* 66(6):621-626.
- Jahn A, Keuntje B, Dorffler M, Klipp W & Oelze J (1994). Optimizing photoheterotrophic H₂ production by *Rhodobacter capsulatus* upon interposon mutagenesis in the *hupL* gene. *Appl Microbiol Biotechnol* 40:687-690.
- Jo JH, Lee DS & Park JM (2006). Modeling and optimization of photosynthetic hydrogen gas production by green alga *Chlamydomonas reinhardtii* in sulfur-deprived circumstance. *Biotechnol Prog* 22(2):431-437.
- Kadar Z, de Vrije T, van Noorden GE, Budde MAW, Szengyel Z, Reczey K & Claassen PAM (2004). Yields from glucose, xylose, and paper sludge hydrolysate during hydrogen production by the extreme thermophile *Caldicellulosiruptor saccharolyticus*. *Appl Biochem Biotechnol* 113-116:497-508.
- Kataoka N, Miya A & Kiriya K (1997). Studies on hydrogen production by continuous culture system of hydrogen-producing anaerobic bacteria. *Water Sci Technol* 36(6-7):41-47.
- Kawaguchi H, Hashimoto K, Hirata K & Miyamoto K (2001). H₂ production from algal biomass by a mixed culture of *Rhodobium marinum* A-501 and *Lactobacillus amylovorus*. *J Biosci Bioeng* 91(3):277-282.
- Keeling CD & Whorf TP (2005). Atmospheric CO₂ records from sites in the SIO air sampling network. *Trends: A Compendium of Data on Global Change*. Carbon Dioxide Information Analysis Center, Oak Ridge National Laboratory, U.S. Department of Energy, Oak Ridge, Tenn., U.S.A.
- Kern M, Koch HG & Klemme JH (1992). EDTA activation of H₂ photoproduction by *Rhodospirillum rubrum*. *Appl Microbiol Biotechnol* 37(4):496-500.
- Khatipov E, Miyake M, Miyake J & Asada Y (1998). Accumulation of poly- β -hydroxybutyrate by *Rhodobacter sphaeroides* on various carbon and nitrogen substrates. *FEMS Microbiol Lett* 162:39-45.
- Kim E-J, Kim J-S, Kim M-S & Lee JK (2006a). Effect of changes in the level of light harvesting complexes of *Rhodobacter sphaeroides* on the photoheterotrophic production of hydrogen. *Int J Hydrogen Energy* 31:531-538.
- Kim M-S, Lee TJ, Yoon YS, Lee IG & Moon KW (2001). Hydrogen production from food processing wastewater and sewage sludge by anaerobic dark fermentation combined with photo-fermentation. *Biohydrogen II : An Approach to Environmentally Acceptable Technology*. Miyake J, Matsunaga T & San Pietro A, (Eds). Pergamon: 263-272.
- Kim M-S, Baek J-S & Lee JK (2006b). Comparison of H₂ accumulation by *Rhodobacter sphaeroides* KD131 and its uptake hydrogenase and PHB synthase deficient mutant. *Int J Hydrogen Energy* 31:121-127.
- Kim M-S, Baek J-S, Yun Y-S, Sim SJ, Park S & Kim S-C (2006c). Hydrogen production from *Chlamydomonas reinhardtii* biomass using a two-step conversion process: Anaerobic conversion and photosynthetic fermentation. *Int J Hydrogen Energy* 31:812-816.
- Kim NJ, Lee JK & Lee CJ (2004). Pigment reduction to improve photosynthetic productivity of *Rhodobacter sphaeroides*. *J Gen Microbiol* 1692(28):607-16.

- Kim S-H, Han S-K & Shin H-S (2004). Feasibility of biohydrogen production by anaerobic co-digestion of food waste and sewage sludge. *Int J Hydrogen Energy* 29:1607-1616.
- Kirkpatrick C, Maurer LM, Oyelakin NE, Yoncheva YN, Maurer R & Slonczewski JL (2001). Acetate and formate stress: Opposite responses in the proteome of *Escherichia coli*. *J Bacteriol* 183(21):6466-6477.
- Knappe J (1987). Anaerobic dissimilation of pyruvate. *Escherichia coli* and *Salmonella Typharium*. Niedhardt FC, (Ed.). Washington DC, Am. Soc. Microbiol. 1: 151-155.
- Ko IB & Noike T (2002). Use of blue optical filters for suppression of growth of algae in hydrogen producing non-axenic cultures of *Rhodobacter sphaeroides* RV. *Int J Hydrogen Energy* 27(11-12):1297-1302.
- Koku H, Eroglu I, Gunduz U, Yucel M & Turker L (2002). Aspects of the metabolism of hydrogen production by *Rhodobacter sphaeroides*. *Int J Hydrogen Energy* 27:1315-1329.
- Kondo T, Arakawa M, Wakayama T & Miyake J (2002). Hydrogen production by combining two types of photosynthetic bacteria with different characteristics. *Int J Hydrogen Energy* 27(11-12):1303-1308.
- Kraemer JT & Bagley DM (2007). Improving the yield from fermentative hydrogen production. *Biotechnol Lett* 29:685-695.
- Kurokawa T & Shigeharu T (2005). Effects of formate on fermentative hydrogen production by *Enterobacter aerogenes*. *Mar Biotechnol* 7:112-118.
- Kyazze G, Dinsdale R, Guwy AJ, Hawkes FR, Premier GC & Hawkes DL (2007). Performance characteristics of a two-stage dark fermentative system producing hydrogen and methane continuously. *Biotechnol Bioeng* 97(4):759-770.
- Larminie J & Dicks A (2003). Fuel cell systems explained, 2nd ed., John Wiley & Sons, Chichester, Sussex, UK.
- Laurinavichene TV, Fedorov AS, Ghirardi ML, Siebert M & Tsygankov AA (2006). Demonstration of sustained hydrogen production by immobilised, sulfur-deprived *Chlamydomonas reinhardtii* cells. *Int J Hydrogen Energy* 31:659-667.
- Lee CM, Chen PC, Wang CC & Tung YC (2002). Photohydrogen production using purple nonsulfur bacteria with hydrogen fermentation reactor effluent. *Int J Hydrogen Energy* 27(11-12):1309-1313.
- Levin DB, Pitt L & Love M (2004a). Biohydrogen production: prospects and limitations to practical application. *Int J Hydrogen Energy* 29:173-185.
- Levin DB (2004b). Re: Biohydrogen production: prospects and limitations to practical application-Erratum. *Int J Hydrogen Energy* 29:1425-1426.
- Levin DB, Islam R, Cicek N & Sparling R (2006). Hydrogen production by *Clostridium thermocellum* 27405 from cellulosic biomass substrates. *Int J Hydrogen Energy* 31(11):1496-1503.
- Levin DB, Zhu H, Beland M, Cicek N & Holbein BE (2007). Potential for hydrogen and methane production from biomass residues in Canada. *Bioresour Technol* 98:654-660.
- Li H, Mustacchi R, Knowles CJ, Skibar W, Sunderland G, Dalrymple I & Jackman S, A. (2004). An electrokinetic bioreactor: using direct electric current for enhanced lactic acid fermentation and product recovery. *Tetrahed* 60:655-661.
- Liang TM, Cheng SS & Wu KL (2002). Behavioral study on hydrogen fermentation reactor installed with silicone rubber membrane. *Int J Hydrogen Energy* 27(11-12):1157-1165.
- Liessens J & Verstraete W (1986). Selective inhibitors for continuous non-axenic hydrogen production by *Rhodobacter capsulatus*. *J Appl Bacteriol* 61(6):547-557.
- Lin C-Y & Lay CH (2005). A nutrient formation for fermentative hydrogen production using anaerobic sewage sludge microflora. *Int J Hydrogen Energy* 30:285-292.
- Lin Y & Tanaka S (2006). Ethanol fermentation from biomass resources: current state and prospects. *Appl Microbiol Biotechnol* 69(6):627-642.
- Lindblad P, Christensson K, Lindberg P, Fedorov A, Pinto F & Tsygankov A (2002). Photoproduction of H₂ by wildtype *Anabaena* PCC 7120 and a hydrogen uptake deficient mutant: From laboratory experiments to outdoor culture. *Int J Hydrogen Energy* 27(11-12):1271-1281.
- Ma F & Hanna MH (1999). Biodiesel production: a review. *Bioresour Technol* 70:1-15.

- Mabee WE, Fraser EDG, McFarlane PN & Saddler JN (2006). Canadian biomass reserves for biorefining. *Appl Biochem Biotechnol* 129-132:22-40.
- Macaskie LE (2004). Biological hydrogen production from crops & sugar wastes. Final Report, EPSRC Project GR/S62406/01.
- Macaskie LE, Baxter-Plant VS, Creamer NJ, Humphries AC, Mikheenko IP, Mikheenko PM, Penfold DW & Yong P (2005). Applications of bacterial hydrogenases in waste decontamination, manufacture of novel bionanocatalysts and in sustainable energy. *Biochem Soc Trans* 33(Pt 1):76-9.
- Macedo IC, Leal MRLV & Silva JEAR (2004). Assessment of greenhouse gas emissions in the production and use of fuel ethanol in Brazil, available at www.unica.com.br/i_pages/files/gee3.pdf.
- Macler BA, Pelroy RA & Bassham JA (1979). Hydrogen formation in nearly stoichiometric amounts from glucose by a *Rhodospseudomonas* mutant. *J Bacteriol* 138(2):446-452.
- Macler BA & Bassham JA (1988). Carbon allocation in wild-type and Glc⁺ *Rhodobacter sphaeroides* under photoheterotrophic conditions. *Appl Environ Microbiol* 54(11):2737-2741.
- Mandal B, Nath K & Das D (2006). Improvement of biohydrogen production under decreased partial pressure of H₂ by *Enterobacter cloacae*. *Biotechnol Lett* 28:831-835.
- Martínez-Herrera J, Siddhuraju P, Francis G, Dávila-Ortíz G & Becker K (2006). Chemical composition, toxic/antimetabolic constituents, and effects of different treatments on their levels, in four provenances of *Jatropha curcas* L. from Mexico. *Food Chem* 96:80-89.
- Masukawa H, Mochimaru M & Sakurai H (2002). Disruption of the uptake hydrogenase gene, but not of the bidirectional hydrogenase gene, leads to enhanced photobiological hydrogen production by the nitrogen-fixing cyanobacterium *Anabaena* sp. PCC 7120. *Appl Microbiol Biotechnol* 58(5):618-24.
- McCormick DB (1998). Oxidation–reduction reactions. *Encyclopedia of Life Sciences*. Chichester, John Wiley & Sons, Ltd.
- Melis A & Happe T (2004). Trails of green alga hydrogen research - from Hans Gaffron to new frontiers. *Photosynth Res* 80(1-3):401-409.
- Melis A & Melnicki MR (2006). Integrated biological hydrogen production. *Int J Hydrogen Energy* 31(11):1563-1573.
- Miura Y, Ohta S, Mano M & Miyamoto K (1986). Isolation and characterisation of a unicellular green alga exhibiting high activity in dark hydrogen production. *Agric Biol Chem* 50(11):2837-2844.
- Miura Y, Saitoh C, Matsuoka S & Miyamoto K (1992). Stably sustained hydrogen production with high molar yield through a combination of a marine green alga and a photosynthetic bacterium. *Biosci Biotechnol Biochem* 56(5):751-754.
- Miyake J, Mao X-Y & Kawamura S (1984). Photoproduction of hydrogen from glucose by a co-culture of a photosynthetic bacterium and *Clostridium butyricum*. *J Ferment Technol* 62(6):531-535.
- Miyake J, Miyake M & Asada Y (1999). Biotechnological hydrogen production: research for efficient light conversion. *J Biotechnol* 70:89-101.
- Miyamoto K, Ohta S, Nawa Y, Mori Y & Miura Y (1987). Hydrogen production by a mixed culture of a green alga *Chlamydomonas reinhardtii* and a photosynthetic bacterium *Rhodospirillum rubrum*. *Agric Biol Chem* 51(5):1391-1324.
- Mizuno O, Dinsdale R, Hawkes FR, Hawkes DL & Noike T (2000). Enhancement of hydrogen production from glucose by nitrogen gas sparging. *Bioresour Technol* 73:59-65.
- Nakada E, Asada Y, Arai T & Miyake J (1995). Light penetration into cell suspensions of photosynthetic bacteria and relation to hydrogen production. *J Ferment Bioeng* 80(1):53-57.
- Nandi R & Sengupta S (1998). Microbial production of hydrogen: An overview. *Crit Rev Microbiol* 24(1):61-84.
- Nastari PM, Macedo IC & Szwarc A (2005). Observations on the draft document entitled "Potential for Biofuels for transport in developing countries". The World Bank, Air Quality Thematic Group, p. 8. http://www.unica.com.br/i_pages/files/ibm.pdf.
- Nath K & Das D (2004a). Biohydrogen production as a potential energy source - Present state-of-art. *J Sci Indust Res* 63(9):729-738.

- Nath K & Das D (2004b). Improvement of fermentative hydrogen production: various approaches. *Appl Microbiol Biotechnol* 65(5):520-529.
- Nath K, Kumar A & Das D (2005). Hydrogen production by *Rhodobacter sphaeroides* strain O.U.001 using spent media of *Enterobacter cloacae* strain DM11. *Appl Microbiol Biotechnol* 68:533-541.
- Nielsen AM, Amandusson H, Bjorklund R, Dannetun H, Ejlertsson J, Ekedahl L-G, Lundstrom I & Svensson BH (2001). Hydrogen production from organic waste. *Int J Hydrogen Energy* 26:547-550.
- Nowak M (2004). Urban Agriculture on the Rooftop, Cornell University, available at www3.telus.net/public/a6a47567/roofgarden_thesis.pdf.
- Odom JM & Wall JD (1983). Photoproduction of H₂ from cellulose by an anaerobic bacterial culture. *Appl Environ Microbiol* 45(4):1300-1305.
- Oh SE & Logan BE (2005). Hydrogen and electricity production from a food processing wastewater using fermentation and microbial fuel cell technologies. *Water Res* 39(19):4673-4682.
- Oh Y-K, Seol E-H, Kim M-S & Park S (2004). Photoproduction of hydrogen from acetate by a chemoheterotrophic bacterium *Rhodospseudomonas palustris* P4. *Int J Hydrogen Energy* 29:1115-1121.
- Ordal EJ & Halvorson HO (1939). A comparison of hydrogen production from sugars and formic acid by normal and variant strains of *Escherichia coli*. *J Bacteriol* 38:199-220.
- Ozturk Y, Yucel M, Daldal F, Mandaci S, Gunduz U, Turker L & Eroglu I (2006). Hydrogen production by using *Rhodobacter capsulatus* mutants with genetically modified electron transfer chains. *Int J Hydrogen Energy* 31(11):1545-1552.
- Park W, Hyun SH, Oh SE, Logan BE & Kim IS (2005). Removal of headspace CO₂ increases biological hydrogen production. *Environ Sci Technol* 39(12):4416-4420.
- Penfold DW, Forster CF & Macaskie LE (2003). Increased hydrogen production by *Escherichia coli* strain HD701 in comparison with the wild-type parent strain MC4100. *Enz Microb Technol* 33(2-3):185-189.
- Pimentel D (2001). The limitations of biomass energy. in *Encyclopedia of Physical Science and Technology*, 3rd edition. Meyers R, (Ed.), Academic Press, San Diego, CA: p.159-171.
- Polle JEW, Kanakagiri S, Jin E, Masuda T & Melis A (2002). Truncated chlorophyll antenna size of the photosystems - a practical method to improve microalgal productivity and hydrogen production in mass culture. *Int J Hydrogen Energy* 27(11-12):1257-1264.
- Redwood MD & Macaskie LE (2006). A two-stage, two-organism process for biohydrogen from glucose. *Int J Hydrogen Energy* in press.
- Redwood MD & Macaskie LE (2007a). Method and apparatus for biohydrogen production. British Patent Application No. 0705583.3. 0705583.3. UK
- Redwood MD & Macaskie LE (2007b). Efficient bio-H₂ and PEM-FC catalyst. Proceedings of the 7th Hydrogen - Power and Theoretical Engineering Solutions International Symposium (HyPoThESIS VII), Merida, Mexico. CICY ISBN:968-6114-21-1.
- Redwood MD, Mikheenko IP, Sargent F & Macaskie LE (2007c). Dissecting the roles of *E. coli* hydrogenases in biohydrogen production. *FEMS Microbiol Lett* in press.
- Ren N, Li J, Wang Y & Liu S (2006). Biohydrogen production from molasses by anaerobic fermentation with a pilot-scale bioreactor system. *Int J Hydrogen Energy* 31:2147-2157.
- Rocha JS, Barbosa MJ & Wijffels RH (2001). Hydrogen production by photoheterotrophic bacteria: Culture media, yields and efficiencies. *Biohydrogen II : An Approach to Environmentally Acceptable Technology*. Miyake J, Matsunaga T & San Pietro A, (Eds). Pergamon: 3-32.
- Roe AJ, McLaggan D, Davidson I, O'Byrne C & Booth IR (1998). Perturbation of anion balance during inhibition of growth of *Escherichia coli* by weak acids. *J Bacteriol* 180(4):767-722.
- Rogers PL, Jeon YJ & Svensson CJ (2005). Application of biotechnology to industrial sustainability. *Trans IChemE Part B* 83(B6):499-503.
- Sakurai H & Masukawa H (2007). Promoting R & D in photobiological hydrogen production utilizing mariculture-raised cyanobacteria. *Mar Biotechnol* 9:128-145.
- Sasikala C, Ramana CV & Prasad GS (1994a). H₂ production by mixed cultures. *World J Microbiol Biotechnol* 10(2):221-223.

- Sasikala C, Ramana CV & Rao PR (1994b). Nitrogen fixation by *Rhodospseudomonas palustris* OU 11 with aromatic compounds as carbon source / electron donors. FEMS Microbiol Lett 122:75-78.
- Sasikala K, Ramana CV, Rao PR & Subrahmanyam M (1990). Effect of gas phase on the photoproduction of hydrogen and substrate conversion efficiency on the photosynthetic bacterium *Rhodobacter sphaeroides* O.U. 001. Int J Hydrogen Energy 15(11):795-797.
- Sasikala K, Ramana CV & Subrahmanyam M (1991). Photoproduction of hydrogen from wastewater of a lactic acid fermentation plant by a purple non-sulfur photosynthetic bacterium *Rhodobacter sphaeroides*. Indian J Exp Biol 29(74-75).
- Sasikala K, Ramana CV & Rao PR (1992). Photoproduction of hydrogen from the waste water of a distillery by *Rhodobacter sphaeroides* O.U. 001. Int J Hydrogen Energy 17(1):23-27.
- Sasikala K, Ramana CV, Rao PR & Kovacs KL (1995). Anoxygenic Phototrophic Bacteria : Physiology and Advances in Hydrogen Production Technology. Adv Appl Microbiol 38:211-295.
- Sauter M, Bohm R & Bock A (1992). Mutational analysis of the operon (*hyc*) determining hydrogenase-3 formation in *Escherichia coli*. Mol Microbiol 6(11):1523-1532.
- Schnoor JL (2006). Biofuels and the environment. Environ Sci Technol 40(13):4024.
- Shi X-Y & Yu Q-H (2006). Continuous production of hydrogen from mixed volatile fatty acids with *Rhodospseudomonas capsulata*. Int J Hydrogen Energy 31:1641-1647.
- Sode K, Watanabe M, Makimoto H & Tomiyama M (1999). Construction and characterisation of fermentative lactate dehydrogenase *E. coli* mutant and its potential for bacterial hydrogen production. Appl Biochem Biotechnol 77-79:317-323.
- Sode K, Yamamoto S & Tomiyama M (2001). Metabolic engineering approaches for the improvement of bacterial hydrogen production based on *Escherichia coli* mixed acid fermentation. Biohydrogen II : An Approach to Environmentally Acceptable Technology. Miyake J, Matsunaga T & San Pietro A, (Eds). Pergamon: 195-204.
- Splendiani A, Nicoletta C & Livingston AG (2003). A novel biphasic extractive membrane bioreactor for minimization of membrane-attached biofilms. Biotechnol Bioeng 83(1):8-19.
- Srivastava A & Prasad R (2000). Triglycerides-based diesel fuels. Renew Sustain Energy Rev 4(2):111-133.
- Staubmann R, Foidl G, Foidl N, Guebitz GM, Lafferty R, Valencia-Arbizu VM & Walter S (1997). Biogas production from *Jatropha curcas* press-cake. Appl Biochem Biotechnol 63-65(0):457-467.
- Stephenson M & Stickland LH (1932). Hydrogenlyases: Bacterial enzymes liberating molecular hydrogen. Bacteriol J 26:712-724.
- Stern N. (2006). Stern review executive summary. New Economics Foundation. Available at news.bbc.co.uk/1/shared/bsp/hi/pdfs/30_10_06_exec_sum.pdf.
- Tabita FR (1995). The biochemistry and metabolic regulation of carbon metabolism and CO₂ fixation in purple bacteria. Anoxygenic Photosynthetic Bacteria. Blankenship RE, Madigan MT & Bauer CE, (Eds). 885-914.
- Taillez P, Girard H, Longin R, Beguin P & Millet J (1983). Cellulose fermentation by an asporogenic mutant and an ethanol-tolerant mutant of *Clostridium thermocellum*. Appl Environ Microbiol 55(1):203-206.
- Tamagnini P, Axelsson R, Lindberg P, Oxelfelt F, Wunschiers R & Lindblad P (2002). Hydrogenases and hydrogen metabolism in cyanobacteria. Microb Mol Biol Rev 66(1):1-20.
- Tanisho S & Ishiwata Y (1995). Continuous hydrogen production from molasses by fermentation using urethane foam as a support of flocks. Int J Hydrogen Energy 20(7):541-545.
- Tanisho S, Kuromoto M & Kadokura N (1998). Effect of CO₂ removal on hydrogen evolution by fermentation. Int J Hydrogen Energy 23(7):559-563.
- Tao Y, Chen Y, Wu Y, He Y & Zhou Z (2007). High hydrogen yield from a two-step process of dark and photo-fermentation of sucrose. Int J Hydrogen Energy 32:200-206.
- Tepljakov VV, Gassanova LG, Sostina EG, Slepova EV, Modigell M & Netrusov AI (2002). Lab-scale bioreactor integrated with active membrane system for hydrogen production: experience and prospects. Int J Hydrogen Energy 27:1149-1155.
- Thangaraj A & Kulandaivelu G (1994). Biological hydrogen photoproduction using dairy and sugarcane wastewaters. Bioresour Technol 48:9-12.

- Thauer R (1977). Limitation of microbial H₂-formation via fermentation. *Microbial Energy Conversion*. Schlegel HG & Barnea J, (Eds). Oxford, Pergamon: 201-204.
- Tiwari AK, Kumar A & Raheman H (2007). Biodiesel production from jatropha oil (*Jatropha curcas*) with high free fatty acids: An optimized process. *Biomass Bioenergy* 31:569-575.
- Troshina O, Serebryakova L, Sheremetieva M & Lindblad P (2002). Production of H₂ by the unicellular cyanobacterium *Gloeocapsa alpicola* CALU 743 during fermentation. *Int J Hydrogen Energy* 27(11-12):1283-1289.
- Tsygankov A (2007). Nitrogen-fixing cyanobacteria: A review. *Appl Biochem Microbiol* 43(3):250.
- Tsygankov AA, Fedorov AS, Laurinavichene TV, Gogotov IN, Rao KK & Hall DO (1998). Actual and potential rates of hydrogen photoproduction by continuous culture of the purple non-sulphur bacterium *Rhodobacter capsulatus*. *Appl Microbiol Biotechnol* 49(1):102-107.
- Tsygankov AA (2001). Laboratory scale photobioreactors. *Appl Biochem Microbiol* 37(4):333-341.
- Tsygankov AA, Fedorov AS, Kosourov SN & Rao KK (2002). Hydrogen production by cyanobacteria in an automated outdoor photobioreactor under aerobic conditions. *Biotechnol Bioeng* 80(7):777-83.
- Tsygankov AA (2007). Biological generation of hydrogen. *Russ J Gen Chem* 77(4):685-693.
- Turkarlan S, Yigit OD, Aslan K, Eroglu I & Gunduz U (1997). Photobiological hydrogen production by *R. sphaeroides* O.U 001 by utilisation of waste water from milk industry. *International Conference on Biological Hydrogen Production*, Waikoloa, Hawaii, Plenum Press, New York.
- Ueno Y, Kawai T, Sato S, Otsuka S & Morimoto S (1995). Biological production of hydrogen from cellulose by natural anaerobic microflora. *J Ferment Bioeng* 97(4):395-397.
- Valdez-Vazquez I, Sparling R, Risbey D, Rinderknecht-Seijas N & Poggi-Varraldo HM (2005). Hydrogen generation via anaerobic fermentations of paper mill wastes. *Bioresour Technol* 96:1907-1913.
- Valdez-Vazquez I, Rios-Leal E, Carmona-Martinez A, Munoz-Paez KM & Poggi-Varaldo HM (2006). Improvement of biohydrogen production from solid wastes by intermittent venting and gas flushing of batch reactors headspace. *Environ Sci Technol* 40:3509-3415.
- Van Ginkel S & Logan BE (2005). Inhibition of biohydrogen production by undissociated acetic and butyric acids. *Environ Sci Technol* 39:9350-9356.
- Van Groenestijn JW, Hazewinkel JHO, Nienoord M & Bussmann PJT (2002). Energy aspects of biological hydrogen production in high rate bioreactors operated in the thermophilic temperature range. *Int J Hydrogen Energy* 27(11-12):1141-1147.
- van Haaster DJ, Hagedoorn PL, Jongejan JA & Hagen WR (2005). On the relationship between affinity for molecular hydrogen and the physiological directionality of hydrogenases. *Biochem Soc Trans* 33(1):12-14.
- Van Niel EWJ, Budde MAW, de Haas GG, van der Wal FJ, Claassen PAM & Stams AJM (2002). Distinctive properties of high hydrogen producing extreme thermophiles, *Caldicellulosiruptor saccharolyticus* and *Thermotoga elfii*. *Int J Hydrogen Energy* 27(11-12):1390-1398.
- Van Niel EWJ, Claassen PAM & Stams AJM (2003). Substrate and product inhibition of hydrogen production by the extreme thermophile, *Caldicellulosiruptor saccharolyticus*. *Biotechnol Bioeng* 81(3):255-262.
- Van Ooteghem SA, Jones A, van der Lelie D, Dong B & Mahajan D (2004). H₂ production and carbon utilization by *Thermotoga neapolitana* under anaerobic and microaerobic growth conditions. *Biotechnol Lett* 26(15):1223-1232.
- Vasilyeva L, Miyake M, Khatipov E, Wakayama T, Sekine M, Hara M, Nakada E, Asada Y & Miyake J (1999). Enhanced hydrogen production by a mutant of *R. sphaeroides* having an altered light-harvesting system. *J Biosci Bioeng* 87(5):619-624.
- Vignais PM, Colbeau M, Willison JC & Jouanneau Y (1985). Hydrogenase, nitrogenase, and hydrogen metabolism in the photosynthetic bacteria. *Adv Microb Physiol* 26:155-234.
- Vignais PM, Billoud B & Meyer J (2001). Classification and phylogeny of hydrogenases. *FEMS Microbiol Rev* 25(4):455-501.
- Vincenzini M, Marchini A, Ena A & DePhilippis R (1997). H₂ and poly-β-hydroxybutyrate, two alternative chemicals from purple non sulfur bacteria. *Biotechnol Lett* 19(8):759-762.

- Wakayama T, Nakada E, Asada Y & Miyake J (2000). Effect of light/dark cycle on bacterial hydrogen production by *Rhodobacter sphaeroides* RV - From hour to second range. *Appl Biochem Biotechnol* 84-6:431-440.
- Wakayama T & Miyake J (2001). Hydrogen from biomass. *Biohydrogen II : An Approach to Environmentally Acceptable Technology*. Miyake J, Matsunaga T & San Pietro A, (Eds). Pergamon: 3-32.
- Wall JD & Gest H (1979). Derepression of Nitrogenase Activity in Glutamine Auxotrophs of *Rhodospseudomonas capsulata*. *J Bacteriol* 137(3):1459-1463.
- Weetall HH, Sharma BP & Detar CC (1989). Photometabolic production of hydrogen from organic substrates by free and immobilised mixed cultures of *Rhodospirillum rubrum* and *Klebsiella pneumoniae*. *Biotechnol Bioeng* 23:605-614.
- Willison JC, Madern D & Vignais PM (1984). Increased photoproduction of hydrogen by non-autotrophic mutants of *Rhodospseudomonas capsulata*. *Biochem J* 219(2):593-600.
- Worin NA, Lissolo T, Colbeau A & Vignais PM (1996). Increased H₂ photoproduction by *Rhodobacter capsulatus* strains deficient in uptake hydrogenase. *J Mar Biotechnol* 4:28-33.
- Wykoff DD, Davies JP, Melis A & Grossman AR (1998). The regulation of photosynthetic electron-transport. *Plant Physiol* 117:129-139.
- Yagi K, Maeda I, Idehara K, Miura Y, Akano T, Fukatu K, Ikuta Y & Nakamura HK (1994). Removal of inhibition by ammonium ion in nitrogenase-dependent hydrogen evolution of a marine photosynthetic bacterium, *Rhodospseudomonas* sp strain W-1s. *Appl Biochem Biotechnol* 45-6:429-436.
- Yetis M, Gunduz U, Eroglu I, Yucel M & Turker L (2000). Photoproduction of hydrogen from sugar refinery wastewater by *Rhodobacter sphaeroides* O.U. 001. *Int J Hydrogen Energy* 25:1035-1041.
- Yigit OD, Gunduz U, Turker L, Yucel M & Eroglu I (1999). Identification of by-products in hydrogen producing bacteria; *Rhodobacter sphaeroides* O.U. 001 grown in the waste water of a sugar refinery. *J Biotechnol* 70:125-131.
- Yokoi H, Mori S, Hirose J, Hayashi S & Takasaki Y (1998). H₂ production from starch by a mixed culture of *Clostridium butyricum* and *Rhodobacter* sp. M-19. *Biotechnol Lett* 20(9):895-899.
- Yokoi H, Saito A, Uchida H, Hirose J, Hayashi S & Takasaki Y (2001). Microbial hydrogen production from sweet potato starch residue. *J Biosci Bioeng* 91(1):58-63.
- Yokoi H, Maki R, Hirose J & Hayashi S (2002). Microbial production of hydrogen from starch-manufacturing wastes. *Biomass Bioenergy* 22:389-395.
- Yoon JH, Shin JH, Kim M-S, Sim SJ & Park TH (2006). Evaluation of conversion efficiency of light to hydrogen energy by *Anabaena variabilis*. *Int J Hydrogen Energy* 31:721 – 727.
- Yoshida A, Nishimura T, Kawaguchi H, Inui M & Yukuwa H (2005). Enhanced hydrogen production from formic acid by formate hydrogen lyase-overexpressing *Escherichia coli* strains. *Appl Environ Microbiol* 71(11):6762-6768.
- Yoshino F, Ikeda H, Masukawa H & Sakurai H (2006). Photobiological production and accumulation of hydrogen by an uptake hydrogenase mutant of *Nostoc* sp PCC 7422. *Plant Cell Physiol* 47:S56-S56.
- Yun S-I & Ohta Y (2005). Removal of volatile fatty acids with immobilised *Rhodococcus* sp. B261. *Bioresour Technol* 96:41-46.
- Zacchi G & Axelsson A (1989). Economic evaluation of preconcentration in product and of ethanol from dilute sugar solutions. *Biotechnol Bioeng* 34:223-233.
- Zhu H, Miyake J, Tsygankov AA & Asada Y (1995). Hydrogen production from highly concentrated organic wastewater by photosynthetic bacteria & anaerobic bacteria. *Water Treatment* 10:61-68.
- Zhu H, Suzuki T, Tsygankov AA, Asada Y & Miyake J (1999a). Hydrogen production from tofu wastewater by *Rhodobacter sphaeroides* immobilised in agar gels. *Int J Hydrogen Energy* 24:305-310.
- Zhu H, Wakayama T, Suzuki T, Asada Y & Miyake J (1999b). Entrapment of *Rhodobacter sphaeroides* in cationic polymer/agar gels for hydrogen production in the presence of NH₄⁺. *J Biosci Bioeng* 88(5):507-512.

1.2 Dual systems (review article)

- Zhu H, Wakayama T, Asada Y & Miyake J (2001). Hydrogen production by four cultures with participation by anoxygenic photosynthetic bacterium and anaerobic bacterium in the presence of NH_4^+ . *Int J Hydrogen Energy* 26(11):1149-1154.
- Zhu HG, Ueda S, Asada Y & Miyake J (2002). Hydrogen production as a novel process of wastewater treatment - Studies on tofu wastewater with entrapped *R. sphaeroides* and mutagenesis. *Int J Hydrogen Energy* 27(11-12):1349-1357.
- Zinchenko VV, Kopteva AV, Belavina NV, Mitronova TN, Frolova VD & Shestakov SV (1991). The study of *Rhodobacter sphaeroides* mutants of different type with derepressed nitrogenase. *Genetika* 27(6):991-999.
- Zinchenko VV, Babykin M, Glaser V, Mekhedov S & Shestakov SV (1997). Mutation in *ntrC* gene leading to the derepression of nitrogenase synthesis in *Rhodobacter sphaeroides*. *FEMS Microbiol Lett* 147:57-61.
- Zurrer H & Bachofen R (1979). Hydrogen production by the photosynthetic bacterium *Rhodospirillum rubrum*. *Appl Environ Microbiol* 37(5):789-793.
- Züttel A (2004). Hydrogen storage methods. *Naturwissenschaften* 91(4):157-172.

Table 1 : Summary of dual systems employed for biohydrogen production

| Feeds, substrates, supplements | 1 st stage | | Integration strategy | 2 nd stage | | Overall productivity | Notes, limitations, caveats | Source |
|---|---|--|----------------------------|--|---|---|---|--|
| | Inoculum and mode | Productivity | | Organism and mode | Productivity | | | |
| Microalgae – Anoxygenic photosynthetic bacteria | | | | | | | | |
| CO ₂ (sole C source) | <i>Chlamydomonas</i> MGA161 Batch | ca. 1.3 mol H ₂ / hexose + acetate and ethanol | Sequential, Batch-transfer | Photosynthetic bacterium W-1S Fed-batch | ca. 6.7 mol H ₂ / mol hexose | 8 mol H ₂ / mol hexose for (7 d) ^a | 12 h day/night cycle | (Miura et al. 1992) |
| | | | | | ca. 9.2 mol H ₂ / mol hexose | | | |
| CO ₂ , NG | <i>Chlamydomonas</i> sp. strain MGA161 Repeated batch, 30 °C | Av. 24.4 mmol hexose/d 80% conversion to glycerol, acetate, ethanol | Sequential, Batch-transfer | <i>Rhodovulum sulfidophilum</i> Purple sulfur bacteria Fed-batch | Average: 3.4 L H ₂ / d | 5.8 mol H ₂ / mol hexose ^b 23 d operation | Pilot scale. Difficulty with contamination of the 2 nd stage | (Akano et al. 1996; Ikuta et al. 1997) |
| NG | <i>C. reinhardtii</i> , batch | NG | Co-culture ratio NG | <i>Rhodospirillum rubrum</i> PNS bacteria Batch | NG | NG | Qualitative success, data NG | (Melis & Melnicki 2006) |
| Cyanobacteria – Anoxygenic photosynthetic bacteria | | | | | | | | |
| Glucose | <i>Synechococcus cedrorum</i> Batch | mol H ₂ / mol hexose free: 0.013 immob. : 0.01 | Co-culture 1:1 (vol) | <i>Rhodobacter sphaeroides</i> O.U.001 PNS bacteria Batch | mol H ₂ / mol hexose free: 0.186 immob. : 3.82 | Mol H ₂ / mol hexose free: 0.702 ^a immob. : 0 | Continuous illumination (2.4 klux) | (Sasikala et al. 1994a) |

| | | | | | | | | |
|---|---|--|--------------------------------------|---|--|--|--|------------------------|
| SOT medium lacking nitrate | <i>Spirulina platensis</i> Batch N-starvation | Light phase: 1.03 mmol hexose/L/d Dark phase: 1 hexose → 0.68 H ₂ + 0.4 acetate + 0.15 formate | Sequential, Batch-transfer | <i>R. sphaeroides</i> RV PNS bacteria batch | Nearly stoichiometric | ca. 2 mol H ₂ / mol hexose ^b 2 mmol H ₂ /day/L | Light-dark cycle (72 h light, 24 h dark) | (Aoyama et al. 1997) |
| Obligate anaerobic fermenters – Anoxygenic photosynthetic bacteria | | | | | | | | |
| glucose | <i>Clostridium butyricum</i> Batch | 16 % of total H ₂ 1.1 mol H ₂ /mol hexose ^a | Immobilised co-culture 1:5 (mass) | <i>R. sphaeroides</i> RV PNS bacteria batch | 84 % of total H ₂ ^a est. 70.4 % efficiency ^b | 7.0 mol H ₂ / mol hexose ^a | Continuous illumination, > 300 h | (Miyake et al. 1984) |
| Tofu or alcohol wastewater | <i>C. paraputrificum</i> Batch, 30 °C | <u>mL/h/L</u> 10 % Tofu: 68 50 % Alcohol: 90 | Sequential, batch-transfer | <i>R. sphaeroides</i> RV PNS bacteria batch | <u>μmol/h</u> 10 % Tofu: 2 50 % Alcohol: 4 | Pre-treatment by fermentation improved photosynthetic H ₂ production | | (Zhu et al. 1995) |
| Glucose | <i>C. butyricum</i> SC-E1 Continuous | 2.0-2.3 mol H ₂ /mol hexose | Sequential, Continuous | <i>Rhodobacter</i> | - | 1.4-5.6 mol H ₂ /mol hexose (predicted) ^a | Hypothetical study | (Kataoka et al. 1997); |
| Starch + yeast extract + glutamate | <i>C. butyricum</i> Batch | 1.9 mol H ₂ /mol hexose ^a | Sequential, batch-transfer | <i>Rhodobacter</i> sp. M-19 PNS bacteria | 1.7 mol H ₂ /mol hexose 32.4 % efficiency ^b | <u>mol H₂/mol hexose</u> 3.6 ^a | Medium included glutamate | (Yokoi et al. 1998) |
| | | - | Co-culture 1:10 (mass) | | - | Batch: 4.5 ^a Repeated fed-batch: 6.4 ^a | Fed-batch performed for 30 days | |
| glucose | | 1.29 mol H ₂ / mol hexose ^b | | | 0.36 mol H ₂ / mol hexose ^b | 1.64 mol H ₂ /mol hexose ^b | - | |
| Rice-wine wastewater | <i>C. butyricum</i> NCIB 9576 semi-continuous | 1 L H ₂ /L wastewater/18h ^a | Sequential, batch-transfer | <i>R. sphaeroides</i> E151 Immobilised in hollow fibres Fed-batch | 0.44 L H ₂ /L broth/ day for 10 days ^a | 1.44 H ₂ /L broth/day ^a | - | (Kim et al. 2001) |
| Tofu wastewater | | 0.9 L H ₂ /L wastewater/26h ^a | | | 0.2 L H ₂ /L broth/day for 30 days ^a | 1.1 L H ₂ /L broth/day ^a | - | |

| | | | | | | | | |
|---|--|--|--|--|--|--|--|--|
| Glucose | <i>C. butyricum</i> | NG 62% of H ₂ | Immobilised co-culture ca. 1:1 (mass) | <i>R. sphaeroides</i> RV batch, immobilised | NG 38% of H ₂ | NG | H ₂ produced for for ca. 24h | (Zhu et al. 2001) |
| Tofu wastewater | batch, immobilised | - | | | - | 2.2 L H ₂ /L wastewater | H ₂ produced for for ca. 48h | (Zhu et al. 2002) |
| Sweet potato starch residue + polypepton or corn steep liquor | <i>C. butyricum</i> & <i>Enterobacter aerogenes</i> co-culture initially ca. 2:1 (w:w) ^b Repeated-batch HRT: 2 d | 2.7 mol H ₂ /mol hexose ^a | Sequential, batch- transfer | <i>Rhodobacter</i> sp. M-19 + 20µg/l Na ₂ MoO ₄ + 10 mg/l EDTA Repeated-batch HRT: 6.25 d | 4.5 mol H ₂ /mol hexose ^a | 7.2 mol H ₂ /mol hexose ^a | Performed for >30 days | (Yokoi et al. 2001; Yokoi et al. 2002) |
| hydrolysed lignocellulosic biomass | Extreme thermophiles* Continuous | 80 % efficiency ^a i.e. 3.2 mol H ₂ and 1.6 mol acetate/ mol hexose | sequential continuous (planned) | PNS bacteria | 80 % efficiency ^a i.e. 3.2 mol H ₂ /mol acetate | 8.32 mol H ₂ /mol hexose (hypothetical) ^b | Hypothetical study, estimate cost of H ₂ : 0.93 Euro/kg | (de Vrije & Claassen 2003) |
| algal biomass (starch) <i>C. reinhardtii</i> | <i>C. butyricum</i> Batch | 2.6 mol H ₂ /mol hexose ^a | Sequential Batch- transfer | <i>R. sphaeroides</i> KD131 PNS bacteria + glutamate, batch | 88 % efficiency ^b | 8.3 mol H ₂ /mol hexose ^a | Starch was not the sole substrate in algal biomass | (Kim et al. 2006c) |
| Glucose | Anaerobic bacteria Continuous, 37 °C | 1.36 mol H ₂ /mol hexose, + acetate, propionate, butyrate ^a | Sequential Batch- transfer | <i>Rhodopseudomonas capsulata</i> 35 °C, continuous | 3.2 mol H ₂ /mol hexose ^a 40 % efficiency | 4.56 mol H ₂ /mol hexose ^a | Glutamate added to stage-1 effluent. 1 st stage maintained for over 6 months, 2 nd for over 10 days. | (Shi & Yu 2006) |
| Facultative aerobes/anaerobes – Anoxygenic photosynthetic bacteria | | | | | | | | |
| Dextrose | <i>Streptococcus faecalis</i> | lactate (0.35 M) No H ₂ | Sequential Batch- transfer | <i>Rhodospirillum rubrum</i> S-1 Fed-batch, 30 °C | 99 % efficiency 16-24 ml H ₂ /g/h | NG | 1 st stage was industrial yoghurt production | (Zurrer & Bachofen 1979) |
| Cellulose | <i>Cellulomonas</i> sp. Batch | Hexose → organic acids (no H ₂) | Co-culture 1:1 (vol) | <i>Rhodopseudomonas. capsulata</i> B100 (WT) batch <i>R. capsulata</i> ST410 batch | - - | 1.2-4.3 mol H ₂ /mol hexose ^a 4.6-6.2 mol H ₂ /mol hexose ^a | 20 ml scale. All H ₂ from 2 nd stage. ST410 is a H ₂ uptake deficient mutant | (Odom & Wall 1983) |

| | | | | | | | | |
|---|--|--|-----------------------------------|---|---|--|---|-------------------------|
| Glucose | | | | | | 1.3-5.3 mol H ₂ /mol hexose ^b 10 days | | |
| Sawdust hydrolysate | <i>Klebsiella pneumoniae</i> Continuous 18-19 °C | NG | Immobilised co-culture (ratio NG) | <i>Rhodospirillum rubrum</i> Continuous 18-19 °C | NG | 6.6-8.4 mol H ₂ /mol hexose ^b 30 days | <i>K. pneumoniae</i> was a contaminant | (Weetall et al. 1989) |
| Cellulose hydrolysate | | | | | | NG 46 days | | |
| Molasses | NG Industrial lactic acid production | No H ₂ 3.4 mM lactate in wastewater | Sequential Batch-transfer | <i>Rhodobacter sphaeroides</i> O.U.001 Batch, 30 °C | > 100% based on lactate content of wastewater | 4480 ml H ₂ /L wastewater | Wastewater contained non-lactate substrates and was diluted 10-fold | (Sasikala et al. 1991) |
| algal biomass (starch) <i>C. reinhardtii</i> | Mixed bacterial community enriched on succinate | - | Co-culture | Consortium: <i>Rhodobium marinum</i> , <i>Vibrio fluvialis</i> and <i>Proteus vulgaris</i> | - | 1.13 mol H ₂ /mol hexose ^a | Algal biomass may contain substrates other than starch | (Ike et al. 1997) |
| | <i>Lactobacillus amylovorus</i> Batch | Hexose → lactic acid 70-80% (no H ₂) | Sequential, batch-transfer | <i>Rhodobacter sphaeroides</i> RV batch + 10 mM glutamate | 41.7 % efficiency ^b | 4.6 mol H ₂ /mol hexose ^a | | |
| Starch | <i>Vibrio fluvialis</i> Batch | Acetate & ethanol (no H ₂) | Sequential, batch-transfer | | 100 % of H ₂ 95 % efficiency | 2.4 mol H ₂ /mol hexose ^b | - | |
| algal biomass (starch) <i>C. reinhardtii</i> | <i>L. amylovorus</i> batch | Lactate (no H ₂) | Co-culture | <i>Rhodobium marinum</i> A-501 (halophile) | 100 % of H ₂ | 7.9 mol H ₂ /mol hexose ^a | Starch was not the sole substrate in algal biomass | (Ike et al. 2001) |
| | <i>V. fluvialis</i> | No H ₂ | ca. 1:2 (mass) | | 100% of H ₂ | 6.2 mol H ₂ /mol hexose ^a | | |
| algal biomass (starch) <i>C. reinhardtii</i> & <i>Dunaleilla tertiolecta</i> | <i>Lactobacillus amylovorus</i> batch, 30 °C | No H ₂ 1.6 mol lactate/mol starch-hexose | Co-culture ca. 5:6 (mass) | <i>R. marinum</i> PNS bacteria batch, 30 °C + 1.5 g/L NaHCO ₃ | 100% of H ₂ | 7.3 mol H ₂ /mol hexose, 60.8 % ^a | stable pH, 13 days | (Kawaguchi et al. 2001) |
| | | | Sequential batch-transfer | | 3.4 mol H ₂ /mol lactose (57 %) | 5.4 mol H ₂ /mol hexose, 45.3 % ^a | - | |

| | | | | | | | | |
|--|--|---|--|---|---|--|--|--|
| Glucose | <i>Rhodopseudomonas palustris</i> P4 Dark-adapted | 0.041 mol H ₂ and 5.7 mol organic carbon/mol hexose ^b | Sequential, batch- transfer | <i>Rhodopseudomonas palustris</i> P4 Light-adapted | 10 % efficiency on fermentation broth | 2-fold increase over dark fermentation alone ^a | Rate of H ₂ photoproduction too low to be economically practical | (Oh et al. 2004) |
| Glucose | <i>Enterobacter cloacae</i> DM11 Batch, 37 °C | 1.86 mol H ₂ /mol hexose ^a | Sequential, batch- transfer | <i>Rhodobacter sphaeroides</i> O.U.001 Batch, 30 °C | 37.5-43.0 % efficiency ^a | NG | <i>est.</i> : 0.63 Euro/kg H ₂ ^a | (Nath et al. 2005) |
| Glucose | <i>Lactobacillus delbrueckii</i> Batch, 30 °C | Lactate, acetate No H ₂ | Immobilised co-culture 4:11 (mass) | <i>R. sphaeroides</i> RV Batch, 30 °C | 100 % of H ₂ | 7.1 mol H ₂ /mol hexose ^a | - | (Asada et al. 2006) |
| Glucose | <i>E. coli</i> HD701 Batch, 30 °C | 0.4 mol H ₂ /mol hexose | Sequential, batch- transfer | <i>R. sphaeroides</i> O.U.001 Batch, 30 °C | Acetate and ethanol consumed No H ₂ | 0.4 mol H ₂ /mol hexose ^a | Inhibitory N-source in primary substrate | (Redwood & Macaskie 2006) |
| Glucose (60 mmol/day) | <i>E. coli</i> HD701 Continuous, 30 °C HRT=30 days | 1.6 mol H ₂ /mol hexose ^a | Sequential, Continuous transfer by Electro- dialysis | <i>R. sphaeroides</i> O.U.001 Continuous, 30 °C HRT=3 days | 0.83 mol H ₂ /mol hexose 38 % efficiency | 2.4 mol H ₂ /mol hexose ^a | Predicted yield: 10.1 mol H ₂ /mol hexose 2 stages not balanced | (Redwood & Macaskie 2007a, 2007b) |
| Non-axenic dark fermentation – Anoxygenic photosynthetic bacteria | | | | | | | | |
| Cow manure | Mixed bacterial culture from digester | H ₂ , CH ₄ , acetate, propionate, butyrate | Sequential, batch- transfer | Mixed, predominantly <i>Rhodopseudomonas</i> spp. | 10 g dry biomass/L | Disposal of wastes & generation of biomass | Biomass produced rather than H ₂ | (Ensign 1977) |
| Poultry manure | Extant feed microbes | acetate, propionate, butyrate | | | 11 g dry biomass/L | | | |
| Palm oil mill effluent | Palm oil sludge | Main products: Acetate and propionate, no H ₂ , no NH ₄ ⁺ | Sequential, batch- transfer | <i>Rhodobacter sphaeroides</i> + NH ₄ Cl to 0.25 g/l continuous | No H ₂ PHB | 1 g PHB/l feed | Valuable alternative product | (Hassan et al. 1997) |

| | | | | | | | | |
|--|--|---|----------------------------|---|--|---|---|------------------------|
| Fruit & vegetable waste | Extant feed microorganisms, batch, ambient temperature | Main product: lactate, no H ₂ | Sequential, batch-transfer | <i>Rhodobacter sphaeroides</i> RV + Mo, 30 °C cont. chemostat | 100 ml H ₂ /g dry weight/h for 10 days | NG | 2 nd stage produced H ₂ for 10 days, then switched to PHB | (Fascetti et al. 1998) |
| | | | | <i>R. sphaeroides</i> RV WT, 30 °C cont. chemostat | Max. 100 mL H ₂ g dry weight/h (1 st 24 h) | NG | 10 days H ₂ , then PHB | (Franchi et al. 2004) |
| | | | | Strain SMV087 PHB ⁻ , H ₂ uptake ⁻ cont. chemostat | | NG | > 45 days H ₂ | |
| Glucose UASB | NG anaerobic bacteria Batch, > 43 °C | Main product: butyrate, no H ₂ | Sequential, batch-transfer | Contents of 1 st stage + <i>Rhodopseudomonas palustris</i> Batch, 35 °C | <u>Headspace gas</u> | | toxic products from 1 st stage: H ₂ S and ethanol | (Lee et al. 2002) |
| Glucose CSTR | | | | | 7 % H ₂ 4 % CH ₄ | NG | | |
| Glucose & beef extract CSTR | | | | | ca. 14 % H ₂ ca. 2 % CH ₄ | NG | | |
| | | | | | ca. 55 % H ₂ 0 % CH ₄ | NG | | |
| Olive Mill Wastewater (Diluted 50 %) | Acclimated sludge Batch, 30 °C | No H ₂ | Sequential, batch-transfer | <i>Rhodobacter sphaeroides</i> O.U.001 Batch, 30 °C | 100 % of H ₂ | 29 L H ₂ /L feed | Pre-treatment of the feed lessened the need for dilution | (Ozturk et al. 2006) |
| Sucrose | Cattle dung Batch, 38 °C | 1.285 mol H ₂ /mol hexose | Sequential, batch-transfer | <i>Rhodobacter sphaeroides</i> SH2C Batch, 30 °C | 63-70 % efficiency ^a | 3.315 mol H ₂ /mol hexose ^a | - | (Tao et al. 2007) |
| Non-biological – Anoxygenic photosynthetic bacteria | | | | | | | | |
| algal biomass (starch) <i>C. reinhardtii</i> | Heat-HCl treatment | Glucose, fatty acids and NH ₄ ⁺ | Sequential, batch-transfer | <i>R. sphaeroides</i> RV batch + 10 mM glutamate | 0.02 mol H ₂ / mol hexose ^a | 0.02 mol H ₂ /mol hexose ^a | - | (Ike et al. 1997) |

Free cells (and not immobilised) were used unless otherwise stated. NG: not given in source and/or cannot be calculated from given data. ^a Value given in original cited source; ^b Authors calculations from source data *Thermophiles are classed tentatively as strict anaerobes; *Thermotoga* spp. may in fact be microaerophiles (Van Ooteghem et al. 2004). Accounts are sorted according to the type of organism used in the 1st stage and then by date, grouping work by the same authors). Some accounts have been omitted due to insufficient data.

Table 2 : Bottlenecks to the application of anoxygenic photosynthetic bacteria in H₂ production.

| Limitation | Effect | Solutions | Progress | Source |
|---|---|--|-----------------------|--|
| Low light conversion efficiency due to unsuitable light intensity | Large land area needed due to low intensity of solar illumination and shallow cultures | Develop strains with truncated light harvesting antenna | Proven at lab-scale | (Miyake et al. 1999; Vasilyeva et al. 1999; Kondo et al. 2002; Kim et al. 2004; Kim et al. 2006a) |
| | | Improved photobioreactor design | Ongoing | (Tsygankov 2001; Hoekema et al. 2002; Kondo et al. 2002; Claassen & de Vrije 2007) |
| | | Immobilisation; adaptation to a more constant light intensity | Proven at lab-scale | (Zhu et al. 2002; Gosse et al. 2007) |
| Sub-optimal conversion of substrates to H ₂ | Diversion of carbon, reductant and ATP into PHB synthesis detracts from H ₂ production | Develop PHB deficient strains | Proven at pilot-scale | (Husted et al. 1993; Lee et al. 2002; Franchi et al. 2004; Kim et al. 2006b) |
| Requirement for CO ₂ (species- and substrate-dependent, see text) | Limited substrate uptake; continuous gas purging prevents cycling of produced CO ₂ | Recirculation of headspace gas | Proven at pilot-scale | (Hoekema et al. 2002) |
| | | Use of species not requiring CO ₂ e.g. <i>R. sphaeroides</i> , <i>R. capsulatus</i> | Proven at lab-scale | (Ivanovskii et al. 1997; Filatova et al. 2005a; Filatova et al. 2005b) |
| H ₂ uptake detracts from net H ₂ production | Decreased net H ₂ production | Develop strains deficient in uptake Hydrogenases | Proven at pilot-scale | (Willison et al. 1984; Jahn et al. 1994; Worin et al. 1996; Lee et al. 2002; Ozturk et al. 2006; Kim et al. 2006b) |
| | | Metal limitation (e.g. using EDTA) to prevent synthesis of active uptake hydrogenases | Proven at lab-scale | (Kern et al. 1992) |
| Culture contamination | Loss of PNS bacteria due to overgrowth of contaminants | Selective chemical inhibitors | Proven at lab-scale | (Liessens & Verstraete 1986) |
| | | Blue light-filters prevent algal growth | Proven at lab-scale | (Ko & Noike 2002) |
| Nitrogenase 'switch-off' in response to fixed sources of N (esp. NH ₄ ⁺) | Limited to using substrates with high C/N ratio | Use of NH ₄ ⁺ -insensitive strains (derepression of nitrogenase) | Proven at lab-scale | (Wall & Gest 1979; Zinchenko et al. 1991; Yagi et al. 1994; Zinchenko et al. 1997) |
| | | Anion-selective immobilisation matrices | Proven at lab-scale | (Zhu et al. 1999b; Zhu et al. 2001) |
| | | Electroreparation of NH ₄ ⁺ | Proven at lab-scale | (Redwood & Macaskie 2007a) |

Table 3 : Potential productivities of algal/cyanobacterial-driven dual systems

| Organism | 1 st stage | | Dual system yield (mol H ₂ /mol hexose) | Theoretical rate of H ₂ production (mol H ₂ /m ² /day) * | Light capture area needed to power 1 home (m ²) ** | Source |
|---------------------------------|--|--|---|---|--|--|
| | Photoautotrophic productivity (mol hexose/m ² /day)* | | | | | |
| <i>Chlamydomonas</i> sp. | NG Assume 0.158 | | 8 | 1.27 | 451.7 | (Miura et al. 1992) |
| <i>Chlamydomonas</i> sp. | Av. : 0.0244 Max. : 0.0926 | | 5.8 | Av. : 0.142 Max. : 0.537 | Av. : 4039.4 min. : 1068.2 | (Akano et al. 1996; Ikuta et al. 1997) |
| <i>Synechococcus cedrorum</i> | NG Assume 0.158 | | 0.702 (free cells) | 0.111 | 5167.6 | (Sasikala et al. 1994a) |
| <i>Spirulina platensis</i> | NG Assume 0.158 | | 2 | 0.317 | 1809.5 | (Aoyama et al. 1997) |
| <i>Clostridium butyricum</i> | 0.158 microalgal starch | | 8.3 | 1.315 | 436.2 | (Kim et al. 2006c) |
| <i>Lactobacillus amylovorus</i> | NG Assume 0.158 cyanobacterial glycogen | | 4.6 | 0.729 | 786.8 | (Shi & Yu 2006) |
| <i>Lactobacillus amylovorus</i> | NG Assume 0.158 microalgal starch | | 7.3 (co-culture) | 1.157 | 495.8 | (Ike et al. 2001) |
| | | | 5.4 (sequential) | 0.856 | 670.1 | |

NG: The productivity of carbohydrate accumulation was not given and could not be calculated from given data. The assumed value of 0.158 mol hexose/m²/day was calculated from published data (Kim et al. 2006c). Photoautotrophic productivity was assumed to be similar after scale-up and under dual system conditions but may be less e.g. due to light limitation in co-culture.

* by multiplying the photoautotrophic productivity with the dual system yield.

** Assuming a home can be powered by a 1 kW PEM fuel cell demanding 23.9 mol H₂/h and operating at 50 % efficiency and 95 % H₂ utilisation (Levin et al. 2004a).

Values are authors' calculations from data given in the published sources shown.

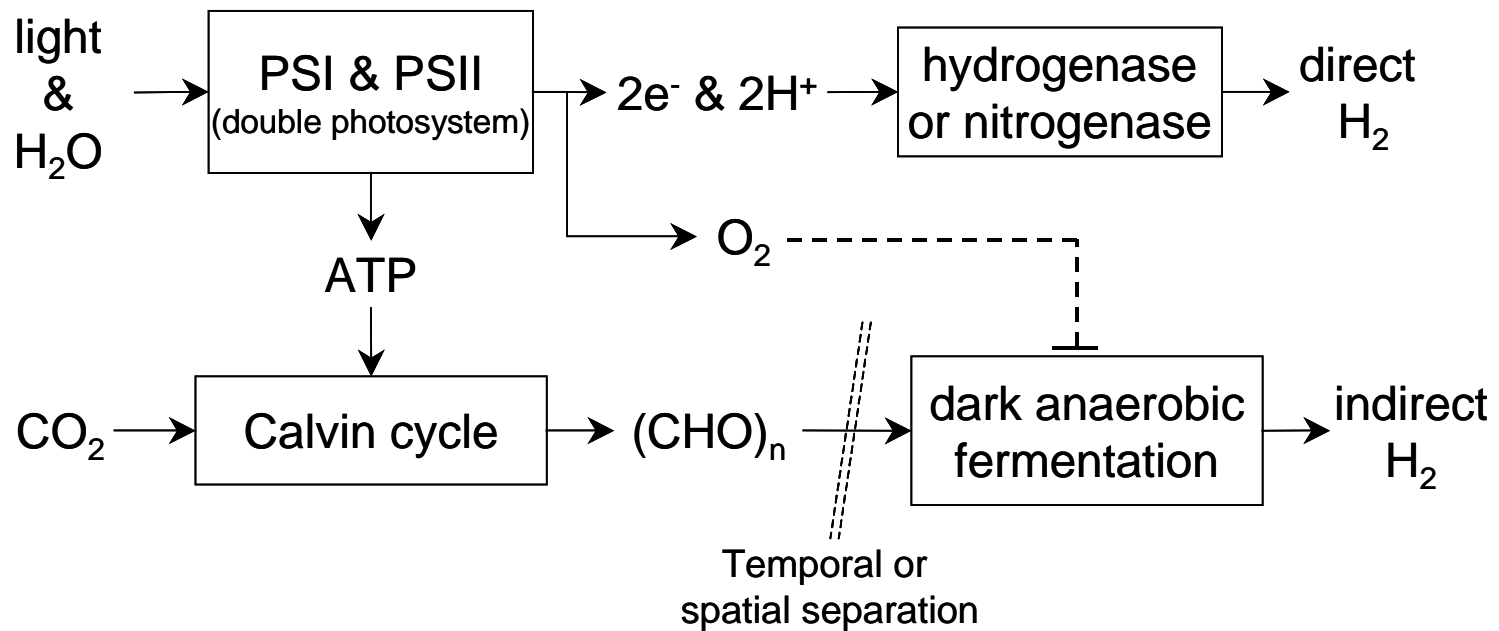
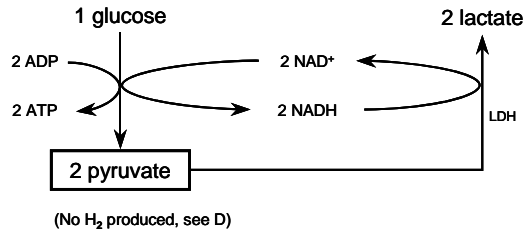
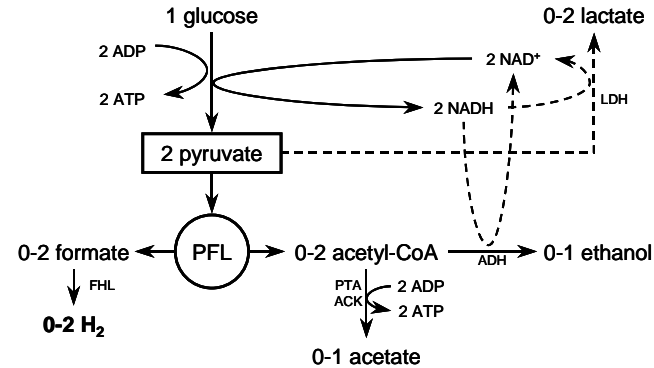


Figure 1: Direct and indirect photolysis. Through direct photolysis, the H₂ evolving enzyme is hydrogenase in microalgae and nitrogenase in cyanobacteria (see text). The dotted line represents the avoided inhibition of dark fermentation by O₂ via indirect photolysis.

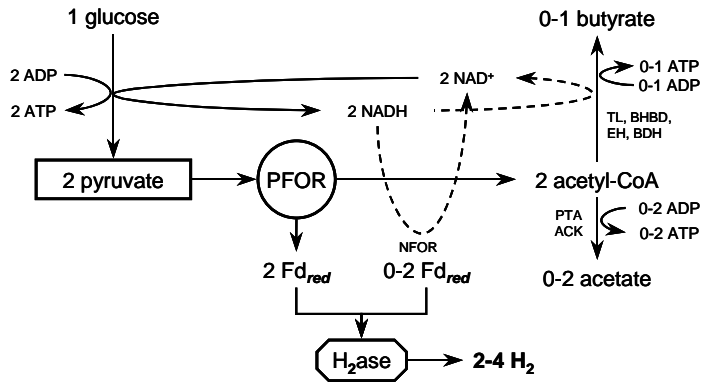
A: Lactic acid fermentation e.g. *Lactobacillus amylovorus*



B: Mixed-acid fermentation e.g. *Escherichia coli*



C: Anaerobic fermentation e.g. *Clostridium butyricum*



D: Effect of fermentation-type on hypothetical dual systems

Ideal fermentations

A: *L. amylovorus*

1 glucose \rightarrow 2 lactate

2 lactate \rightarrow 12 H₂
 0 H₂ + 12 H₂ = 12 H₂

B: *E. coli*

1 glucose \rightarrow 2 H₂ + 1 ethanol + 1 acetate

1 ethanol + 1 acetate \rightarrow 10 H₂
 2 H₂ + 10 H₂ = 12 H₂

C: *C. butyricum* (a mixture of two reactions)

1 glucose \rightarrow 4 H₂ + 2 acetate

2 acetate \rightarrow 8 H₂

4 H₂ + 8 H₂ = 12 H₂

1 glucose \rightarrow 2 H₂ + 1 butyrate

1 butyrate \rightarrow 10 H₂

2 H₂ + 10 H₂ = 12 H₂

Ideal photo-fermentations

Figure 2: Suitable dark fermentations for dual systems. Pathways are abridged to highlight the overall balances. Dotted lines indicate alternative/competing pathways. Abbreviations: LDH lactate dehydrogenase, PFL pyruvate:formate lyase, ACK acetate kinase, FHL formic hydrogen lyase, PTA phosphotransacetylase, ADH alcohol dehydrogenase, NFOR NADH:ferredoxin oxidoreductase, TL thiolase, BHBD hydroxybutyryl-CoA dehydrogenase, EH enoyl-CoA hydratase, BDH butyryl-CoA dehydrogenase. Compiled from (Sode et al. 2001; Chen et al. 2006).

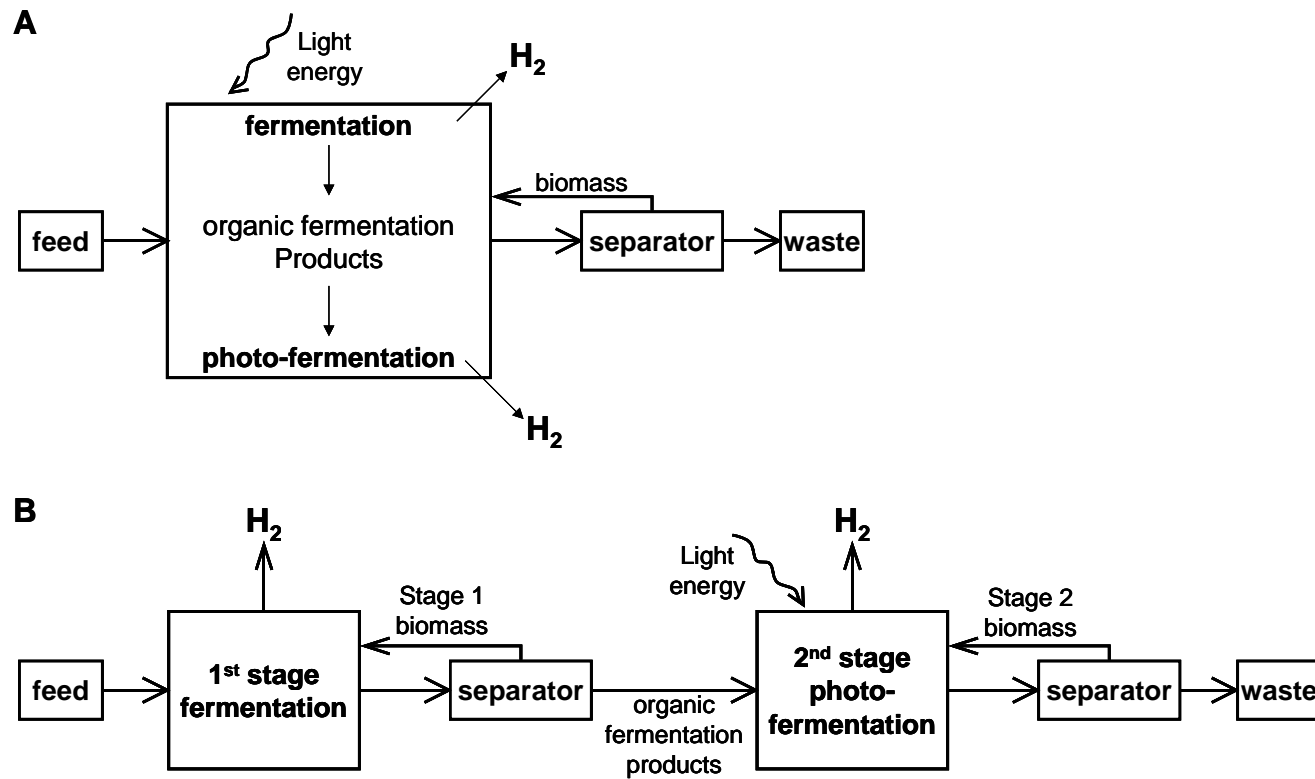


Figure 3: Dual systems in co-culture and in sequential reactors.

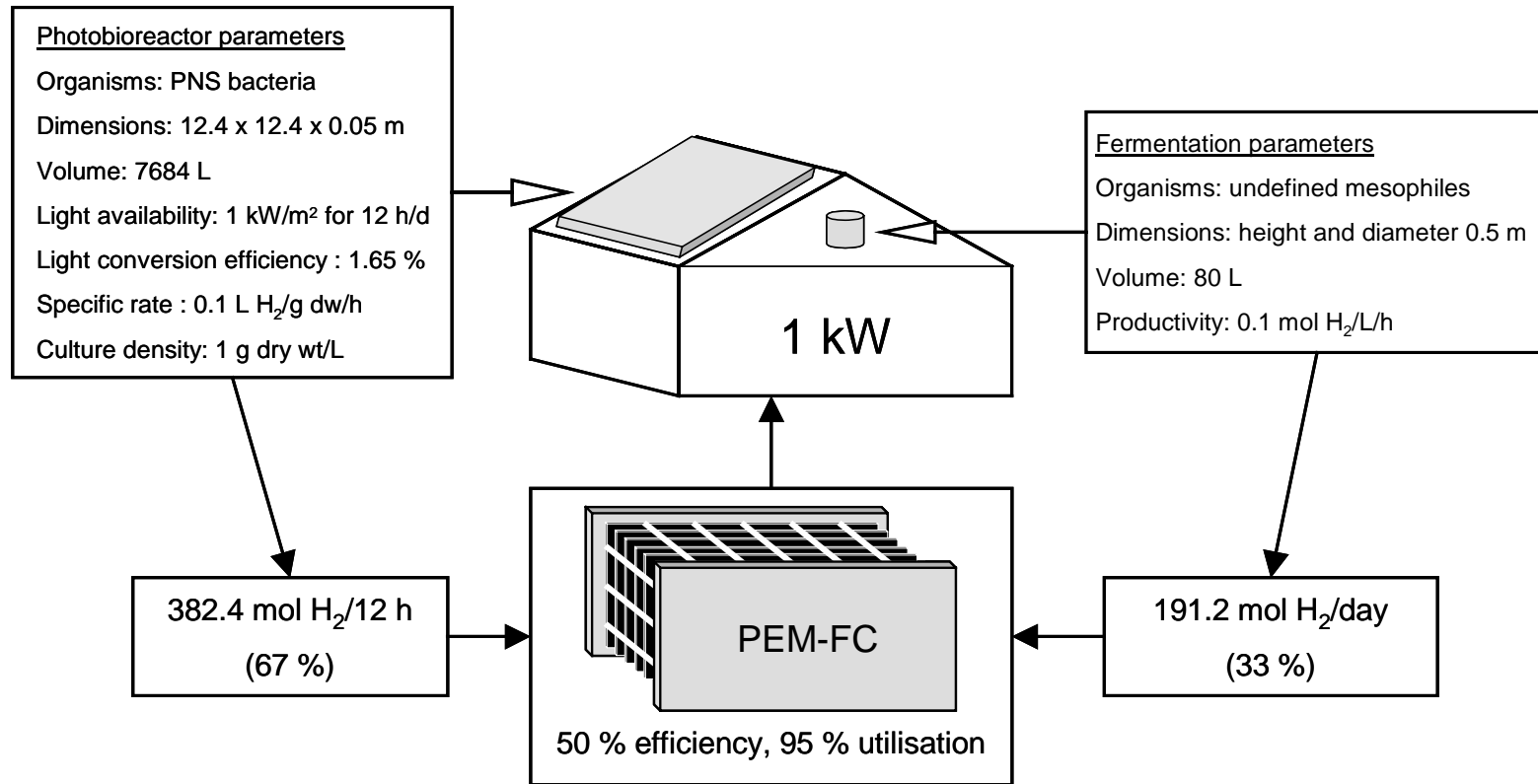
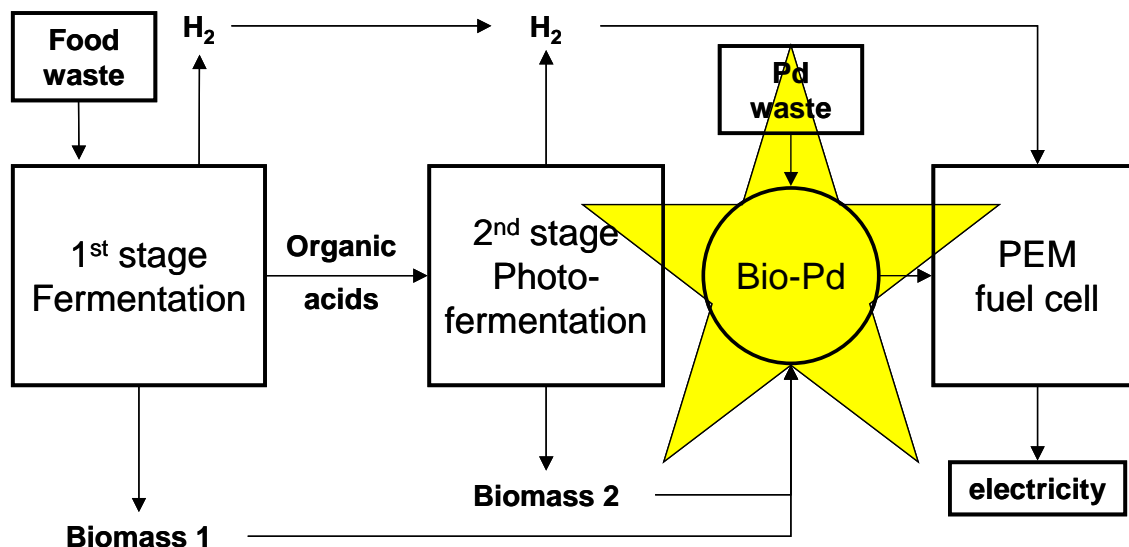


Figure 4: Spatial feasibility of de-centralized energy generation. The cartoon depicts one possible configuration of a sequential dual system combining dark fermentation and PNS bacteria. Detailed explanation is given in section 3.4.2.3.

1.3 Downstream system: Biomass-supported palladium catalysts

1.3.0 Summary



This section overviews the state of knowledge surrounding biomass-supported metallic catalysts, focussing on palladium, and discusses the potential for catalyst production using *Rhodobacter sphaeroides*. Chapter 2.7 describes the production of such a catalyst and the comparison of its activity to the previously-characterised *Desulfovibrio desulfuricans*-supported catalyst using a simple test reaction. In chapter 2.8, it is shown that *R. sphaeroides*-supported catalyst can be used in the fabrication of effective fuel cell anodes.

1.3.1 Biomass-supported catalyst

A dual system for H_2 production incorporating *Escherichia coli* and *Rhodobacter sphaeroides* would produce significant quantities of biomass as a consequence of culture growth (see chapter 2.8.4b). Simultaneously, the fuel cell envisioned to generate electricity from the bio- H_2 would require platinum group metal (PGM) catalyst. Potentially, excess biomass from the bioreactors could be used to reclaim PGM from waste leachates to generate a useful fuel-cell catalyst.

It was shown previously that *E. coli* and *Desulfovibrio* spp. can reclaim PGM from dilute solution, facilitating the reduction of soluble oxidised PGM (e.g. Pd(II)) to the insoluble metallic state (e.g. Pd(0)). Due to the involvement of cellular hydrogenases in initiating metal

reduction the resultant PGM particles are located at the cell surface creating a material with high catalytic activity (e.g. palladised biomass; bio-Pd(0)) [123]. Further, Pd(0) biorecovered from wastes can be used to make an effective catalyst without need for further processing [111].

There is significant interest in bio-Pd(0) because its catalytic activity is comparable to conventional chemically produced palladium catalyst, because it could be produced economically from palladium-containing waste streams, and because it has been shown to function in a PEM fuel cell [215,216]. Bio-Pd(0) consists of bacterial cells coated in a layer of small palladium particles. *Desulfovibrio desulfuricans*, *D. fructosovorans*, *Ralstonia metallireducans*, *Arthrobacter oxydans*, *Micrococcus luteus*, *Shewanella oneidensis*, *Proteus vulgaris*, *Serratia marscecens* and *E. coli* have been investigated in this context (K. Deplanche, personal communication). Other species may offer improvements and *R. sphaeroides* is a promising candidate because of its high-level intrinsic resistance to many toxic metal compounds, and because of its metal-reducing capabilities (section 1.3.4) and because, unlike *Desulfovibrio*, *R. sphaeroides* produces no H₂S, a potent catalyst poison. Further, the genetic manipulation of hydrogenase expression in *D. fructosovorans* and *E. coli* can affect the properties of the resultant catalysts and there is significant potential for similar work using *R. sphaeroides* as its hydrogenases are well-characterised [199].

1.3.2 Palladium

Palladium metal (Pd(0)) occurs naturally in mixed ores with other PGM (platinum, rhodium, iridium, ruthenium and osmium) and nickel. Demand for palladium is linked primarily with the chemical industry, where it has various applications as catalyst, from the automotive industry, where it is used in automotive catalytic converters and from the jewellery sector [82].

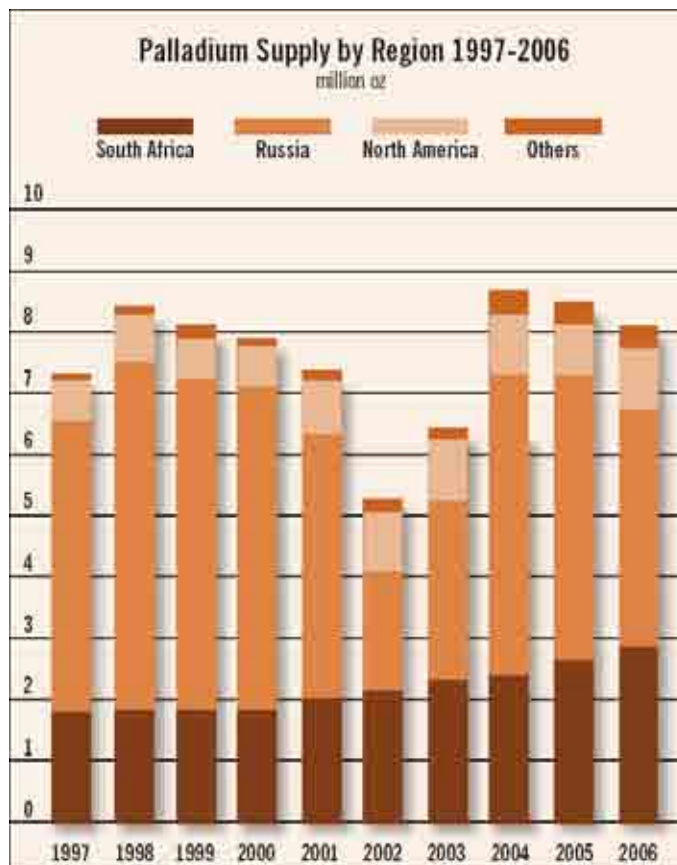


Figure 1.3-a Changes in the supply of palladium over the past decade. Taken from [82].

Recently, the demand for PGM has stabilised and supply and demand are in balance. However, continued growth in the fuel cell industry (20 % in 2006 [1]) is likely to create new demand. In the past, increases in the price of palladium (currently *ca.* US\$ 11.5/g) and recognition of its role as a strategic metal and limited ore resources prompted research into reclamation from scrap catalytic converters and circuit boards [214]. For example, 22.7 tonne Pd and 24.2 tonne Pt were recovered from scrapped autocatalyst in 2006, equivalent to *ca.* 10 % of the supply for Pd (Figure 1.3-a) [82]. Recovery involves a leaching process using *aqua regia* (a 3:1 mixture of concentrated hydrochloric acid and nitric acid) to oxidise PGM to soluble forms, (e.g. $[\text{PdCl}_4]^{2-}$). In order to recover metals from the leachate, a reducing mechanism is required. After partial neutralization of the leachate, microorganisms can promote reduction, depositing metallic nanoparticles on their surfaces.

1.3.3 *Desulfovibrio* bio-Pd(0)

1.3.3a Bio-Pd in bioremediation

The high catalytic activity of palladium coated (palladized) cells of *Desulfovibrio* species was demonstrated previously [9,10,107]. An important factor affecting catalytic activity is the available catalytic surface, rather than the total mass of catalyst (i.e. the number and size of palladium particles).

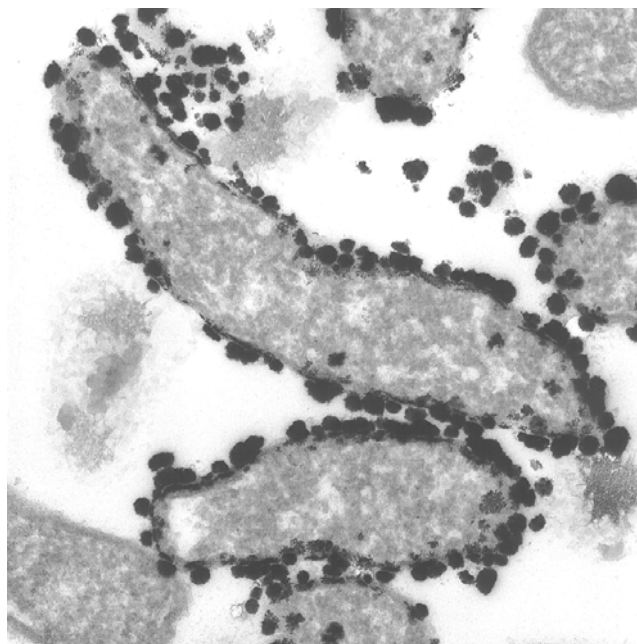


Figure 1.3-b Palladised cells of *Desulfovibrio desulfuricans*.

In this example the biomass is loaded at 25 % Pd (w/w). The dark black areas are Pd(0) particles as identified by X-ray diffraction [114].

Palladization is initiated as $[\text{PdCl}_4]^{2-}$ ions adsorb onto protonated ligand groups (on the bacterial cell surface), forming nucleation sites [38], where an initial reduction to Pd(II) may be facilitated by a bacterial enzyme such as a hydrogenase. Subsequently, the autocatalytic properties of Pd(0) permit further reduction and crystal growth at the expense of exogenous reductant [123,212,213]. This process is abiotic after the initial nucleation and initial crystal growth.

A study using X-ray photoelectron spectroscopy (XPS) was unable to identify conclusively the endogenous reduction of Pd(II) but reduction of Pt(IV) and Pt(0) species was clearly observed [39].

The examination of *D. desulfuricans* bio-Pd(0), by transmission electron microscopy (TEM), revealed that the periplasm was the primary site of nucleation [123]. It was hypothesised that periplasmic (or periplasmic-orientated) hydrogenase could govern nucleation and the XPS study also suggested metal coordination to biomass amino groups. A hydrogenase deletion mutant of *D. fructosovorans* showed a loss of reducing capacity for technetium (VII), which was regained after complementation with hydrogenase genes. This confirmed the involvement of hydrogenases in Tc (VII) reduction [37]. A similar conclusion was reached for Pd(II) reduction as Pd(0) particle formation was restricted to the cytoplasmic membrane in mutants of *D. fructosovorans* containing only cytoplasmic membrane-bound hydrogenase with no soluble periplasmic hydrogenase [124]. This evidence indicates a key role for *D. fructosovorans* hydrogenases in the initial formation of Pd(0).

1.3.3b Bio-Pd(0) and fuel cells

Fuel cells are widely regarded as the most promising technology for the release of energy stored in H₂ and, therefore, represent a key consumer-operated device in the future H₂ economy. H₂ combustion engines could also be used but fuel cell technology offer advantages in terms of energy efficiency, while the absence of moving parts (Figure 1.3-c) permits silent operation and potentially extended lifespan [154]. Demonstrator projects have shown fuel cells to be ready for stationary applications such as lighthouses or road signs [163], but H₂ storage and fuel cell volume currently limit transport applications [188]. Several types of fuel cell are under development but the proton exchange membrane fuel cells (also called polymer electrolyte membrane fuel cells; PEM-FC) may be the most suitable for small-scale and mobile applications. As PEM-FC work at low temperatures (*ca.* 80 °C) they require little ‘warming up’ and offer relatively high convenience to the user [98].

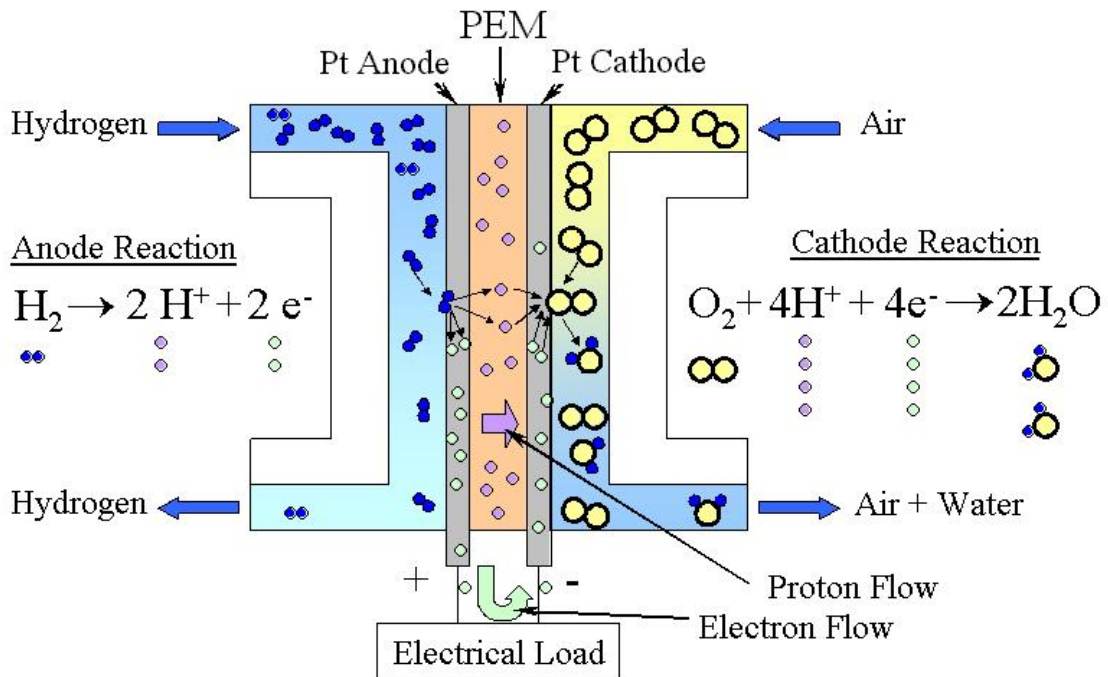


Figure 1.3-c Functioning of a polymer electrolyte membrane fuel cell (PEM-FC).

At the anode, which is typically platinum-coated carbon, H_2 is oxidized to H^+ ions (protons), which pass through a PEM (proton-exchange membrane) to the cathode, where combination with O_2 from the air produces H_2O . The impermeability of the PEM to electrons is the key feature of the system. A voltage is generated across the PEM, which can create a current to power a load. Multiple cells are stacked in series to increase power. Diagram provided by D. Brook, University of Birmingham.

The original fuel cell, Grove's 'gas voltaic battery', used platinum electrodes and catalysis by platinum-group metals (PGM) remains a fundamental aspect of modern PEM-FC [58]. The catalyst electrodes remain among the most costly components of fuel cells [180] and although supply and demand are currently in balance [81], PGM resources are limited. Therefore, the advent of a fuel cell-based 'hydrogen economy' could significantly affect the price of fuel cell construction and alternative sources of PGM are sought.

The functional unit of a PEM-FC is the membrane electrode assembly (MEA), which consists of a proton-conductive polymer electrolyte (e.g. Nafion®) flanked by catalytic electrode layers (PGM particles fixed in supporting matrices e.g. carbon), in turn flanked by conductive gas diffusion layers (e.g. carbon paper or cloth) (Figure 2.8-a) [105].

The performance of the MEA depends on the optimisation of each component. For example, the PGM catalyst support of choice was PTFE, but is now Nafion, and the best results are achieved by casting catalyst slurry onto the Nafion membrane instead of onto the gas diffusion layer [105]. PEM-FC electrode preparation methods are subject to intensive development, and tend to be proprietary. Catalyst slurries may be applied manually onto supports, by painting (this study, section 2.8.2b), spraying, screen-printing or transfer-printing. While manual-methods lack speed and reproducibility, advanced methods such as cold-rolling, electrodeposition, and vacuum deposition are under development [105,155,207]. Research has focussed on improving the efficiency of catalyst use. Early PEM-FC used 4 mg Pt/cm² [105] (which is unsustainable), while advanced ‘sputtering’ techniques reportedly produced functional electrodes using as little as 0.027 mg Pt/cm² [204].

In early studies on the use of bio-Pd(0) as a fuel cell catalyst [215,216] painting bio-Pd(0) slurry onto the gas diffusion layer resulted in an electrically resistant and ineffective MEA. High electrical conductivity is an important property of fuel cell electrode materials, but dried and compressed bio-Pd(0) was found (as expected) to have a high electrical resistance (*ca.* 2 Ohm-cm), due to the propensity of organic material. Incinerating bio-Pd at 700 °C was found to be effective in oxidising the organic matter to leave a material with a Pd content above 90 % (w/w), which was effective as a fuel cell catalyst due to its increased electrical conductivity.

However, incineration also affected the size-distribution of the Pd particles. Bulk palladium (like platinum) is paramagnetic; it becomes magnetised when exposed to a magnetic field, and the magnetism disappears when the field is removed. Ferromagnetism (permanent magnetism) would be a desirable property in heterogeneous catalysis as it could facilitate the manipulation of catalyst within a reactor or the downstream recovery and recycling of catalyst, while in an experimental context, the observed ferromagnetism of *D. desulfuricans* bio-Pd(0) was interpreted as indicative of particles of Pd in the range of 4-12 nm in diameter (nanoparticles) [122,185]. For magnetism to be exploited practically it must be retained at useful temperatures. Ferromagnetic substances have an associated Curie temperature; the temperature above which a ferromagnetic material loses its permanent magnetism. Although inconsistent, the Curie temperatures of preparations of *Desulfovibrio* bio-Pd(0) have been

comparable with temperatures used in catalytic reactions (up to ~500 K) [123]. However, incineration at 700 °C resulted in a significantly decreased ferromagnetic component, indicating the agglomeration of Pd(0) nanoparticles. Nevertheless, incinerated bio-Pd(0) catalyst was effective as a fuel cell anode catalyst (see section 2.8.3a).

1.3.4 Use of *Rhodobacter sphaeroides* in metal reduction and remediation technology

The chemical properties of cell surfaces have been shown to influence nucleation of Pd(II), which depends upon the initial biosorption to a large extent [213]. Variations among bacterial species may render one species a more effective matrix than another, according to the nanoparticles ‘patterning’ they promote. The investigation of this process in a variety of species and strains may, therefore, repay study. *R. sphaeroides* represents a particularly interesting organism for study, because of its known metal interactions and potential availability from a H₂ producing dual system.

Moore and Kaplan (1992) [130] first suggested photosynthetic bacteria (including *R. sphaeroides*) as promising candidates for remediation technology. These bacteria have high-level intrinsic resistance to various metal-containing pollutants such as tellurite/tellurate [20,130,209], selenite/selenate [83,130,197], rhodium sesquioxide [130] and chromate [135].

Bacterial metal reduction can function in energy conservation to support growth, and metals can act as the primary or sole terminal electron acceptor in a form of anaerobic respiration called dissimilatory metal reduction, requiring the oxidation of simple organics, aromatics or H₂. For example, *Geobacter metallireducens* can oxidise various simple organics and alcohols (e.g. acetate) to reduce Fe(III) to Fe(II) or U(VI) to U(IV) as principal if not sole terminal electron acceptors [108].

Where PNS (purple non-sulphur) bacteria have been studied, there is a consensus that metal reduction is not primarily involved in energy metabolism, but serves to detoxify compounds containing metals in an oxidised state. However, the mechanisms of metal reduction are not well understood and the roles are speculative. The reduction of chromate, for example, is clearly a mechanism of detoxification, as an extended lag-period was observed relative to chromate-free controls, during which the cells detoxified their environment in order to permit

growth [108]. Detoxification was achieved by the reduction of the highly soluble Cr(VI) to the relatively insoluble Cr(III), which was then exported from the cells. Nepple *et al.* (2000) [108] reported a MIC (minimum inhibitory concentration) of 43 μM Cr(VI) for *R. sphaeroides* grown under either light/anaerobic or dark/aerobic conditions.

The situation is more complex in the cases of tellurite and selenite. Tellurium and Selenium are semi-metallic elements, periodically grouped with oxygen and sulphur, which are key respiratory electron acceptors. The oxyanions of selenium and tellurium are distributed widely in nature at trace concentrations, but may reach toxic concentrations as a result of industry or volcanic activity. Due to their increased solubility, the most toxic forms of these elements are the oxyanions selenite (SeO_3^{2-}) and tellurite (TeO_3^{2-}), and detoxification is achieved *via* reduction to the insoluble elemental state [197]. Borsetti *et al.* (2003) [20] reported reduction of tellurite to elemental tellurium by *R. capsulatus*, with the formation of needle-like black inclusions associated with the intracytoplasmic membrane (Figure 1.3-d).

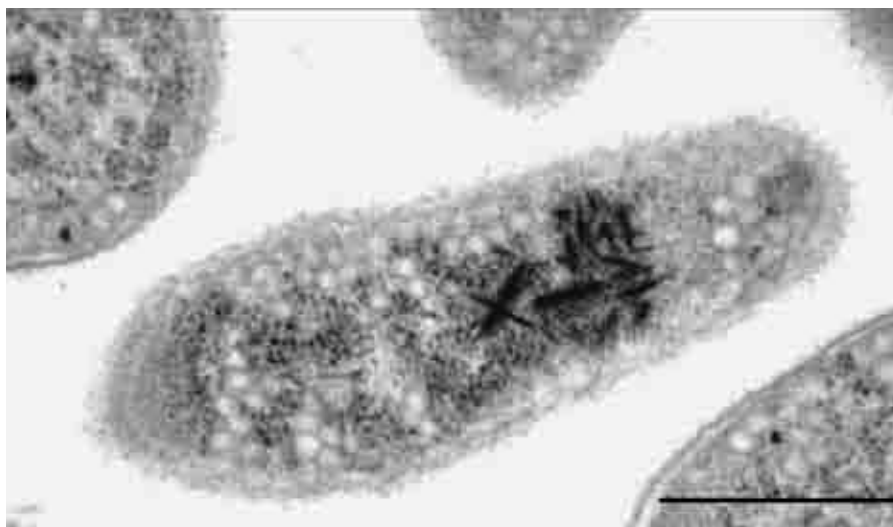


Figure 1.3-d *Rhodobacter capsulatus* grown in the presence of tellurite, showing needlelike granules of tellurium under electron microscopy. Scalebar shows 0.2 μm . Adapted from [20].

Borsetti *et al.* (2003) also observed a 30-50% decrease in the levels of c-type cytochromes as a result of growth under photoheterotrophic conditions with 50 mg/l potassium tellurite, and hypothesised that this played a functional role in resistance to tellurite. However, the level of resistance was also shown to be directly proportional to the incident light intensity [130].

Differences could, therefore, relate to shading by the black tellurium intrusions, or to direct influences of the oxyanion or element on gene expression. Moore and Kaplan (1992) [130] reported normal growth by *R. sphaeroides* 2.4.1 and WS8 in Siström's succinate medium supplemented with 600 mg/l $K_2TeO_3^{2-}$. Other PNS (purple non-sulfur) bacteria (*Rhodobacter capsulatus* and *Rhodopseudomonas palustris*) showed similar resistance. Interestingly, an increased rate of tellurite reduction was observed during growth in the presence of more reduced carbon sources such as succinate or butyrate and toxicity was severely increased in the presence of cysteine. Similar results were found when testing selenium- and rhodium-containing compounds, although selenite was found to be slightly less toxic to *R. sphaeroides* than tellurite.

There are several accounts of bacterial selenite reduction, but reports concerning the location of reduced elemental Se(0) differ, as do the suggested mechanisms. Macy *et al.* (1989) [115] reported reduction of selenate to selenite as a new mode of anaerobic respiration in *Pseudomonas* species. Elemental selenium was released but was unclear whether this was a detoxification response or an energetic mechanism. Van Praag *et al.* (2002) [197] reported selenite resistance in the PNS bacterium *Rhodospirillum rubrum*. Selenite was reduced to elemental selenium concomitantly with growth at initial selenite concentrations of up to 2 mM. A distinct increase in the rate of selenite reduction occurred after the onset of stationary phase. Were reduction simply a mechanism of detoxification, reduction would be expected to occur as a prerequisite to growth, as was observed with chromate. The observed association with stationary phase suggests that selenite may act as a non-preferential terminal electron acceptor under these conditions.

Given the apparent robustness of *R. sphaeroides* (and PNS bacteria in general) in challenging chemical environments, it is reasonable to expect some resistance to palladium compounds. Remediation of palladium-containing wastes is important for environmental reasons, and the high value of palladium and limited ore resources prompts research into economical methods of reclamation and catalyst preparation.

R. sphaeroides is hypothetically capable of palladium reduction during growth on reduced substrates (see above). This may occur as a detoxification mechanism as Pd(II) is highly

soluble whereas elemental Pd(0) is insoluble. However, the catalytic properties of palladium, which give it its value, could affect the mechanism of reduction in a biological context, making the process very different from previous observations of metal/metalloid reduction (see above). Soluble Pd(II) readily undergoes chemical reduction to Pd(0) in the presence of a suitable electron donor such as formate or hydrogen (although this occurs much more rapidly in the presence of bacterial cells). In photoheterotrophic cultures of *R. sphaeroides*, hydrogen formation occurs at the expense of reduced electron carriers (such as ferredoxin, NADH, and FADH). Palladium reduction could take the place of H₂ evolution, using reduced electron carriers as electron donors. Alternatively the evolved H₂ could act as an exogenous reductant.

A dual bioreactor system for H₂ production would produce significant quantities of biomass as a by-product (quantities estimated in chapter 2.8.4b), which could provide a suitable matrix for reductive precipitation of Pd(0) in an application with two aims: the remediation of Pd(II) containing waste, and the production of valuable bioinorganic catalyst, which could be used as fuel cell catalyst. Utilising the spent biomass within the energy generating system would be an important step towards a closed, 'zero emission' system for energy generation from wastes.

2 : RESULTS

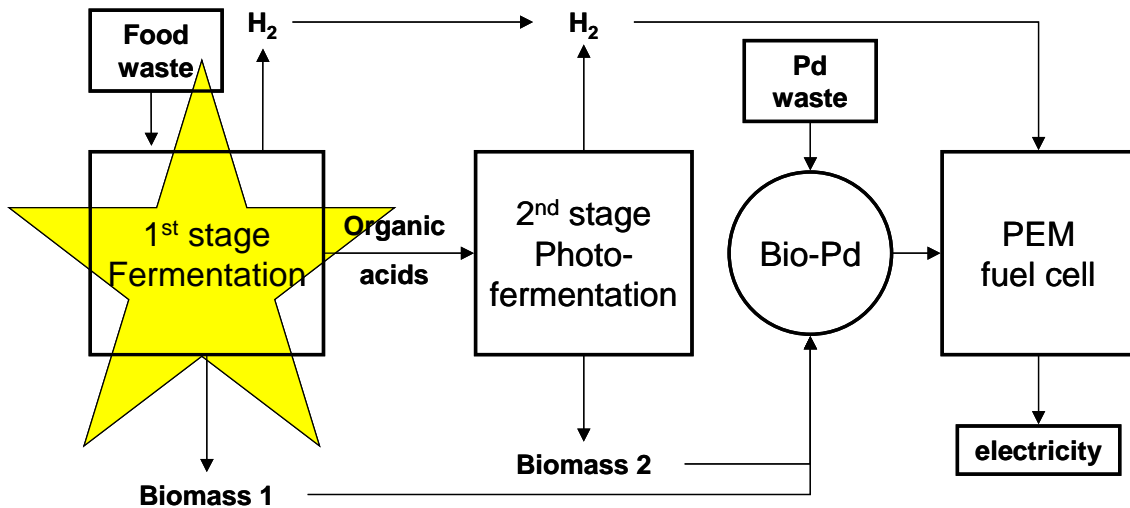
2.0 Chapter contents

| | |
|--|-----|
| 2.1 Dissecting the roles of <i>Escherichia coli</i> hydrogenases in biohydrogen production..... | 78 |
| 2.1.0 Summary..... | 78 |
| 2.1.1 Research letter published in FEMS Microbiology Letters..... | 79 |
| 2.1.2 Supplementary figure | 88 |
| 2.2 Development of H ₂ production by <i>Escherichia coli</i> | 89 |
| 2.2.0 Summary..... | 89 |
| 2.2.1 Introduction | 90 |
| 2.2.2 Methods | 91 |
| 2.2.2a Bacterial strains and growth conditions..... | 91 |
| 2.2.2b Phase 1 | 91 |
| 2.2.2c Phase 2..... | 92 |
| 2.2.2d Phase 3 | 92 |
| 2.2.2e Phase 4..... | 93 |
| 2.2.2f Analyses | 93 |
| 2.2.3 Results | 94 |
| 2.2.3a Phase 1: Batch mode with phosphate buffer | 94 |
| 2.2.3b Phase 2: Batch mode, un-buffered with pH control..... | 95 |
| 2.2.3b-I Optimisation of pH (Phase 2) | 95 |
| 2.2.3b-II H ₂ production with controlled pH (Phase 2) | 97 |
| 2.2.3c Phase 3: Fed-batch mode with pH control | 97 |
| 2.2.3d Phase 4: Fed-batch (semi-continuous), with pH control and electro dialysis.... | 98 |
| 2.2.3e Butyrate-type fermentation in <i>Escherichia coli</i> HD701 | 98 |
| 2.2.4 Discussion..... | 103 |
| 2.2.4a The effect of pH on mixed-acid fermentation (MAF) | 103 |
| 2.2.4b Butyrate formation during the anaerobic fermentation of <i>E. coli</i> | 105 |
| 2.2.4b-I The pathway of butyrate formation in <i>Escherichia coli</i> HD701 | 105 |
| 2.2.4b-II Butyrate-type fermentation balance..... | 110 |
| 2.2.5 Conclusions | 111 |
| 2.3 Development of photobiological H ₂ production by <i>Rhodobacter sphaeroides</i> | 113 |
| 2.3.0 Summary..... | 113 |
| 2.3.1 Introduction | 114 |
| 2.3.2 Materials and Methods | 115 |
| 2.3.2a Microorganisms, media and culture conditions..... | 115 |
| 2.3.2b Measurement of H ₂ production | 115 |
| 2.3.2c The effects of acetate and NH ₄ ⁺ concentrations | 116 |
| 2.3.2d The effect of culture density | 116 |
| 2.3.2e Operation of a continuous photobioreactor (PBR) | 117 |
| 2.3.3 Results and Discussion | 119 |
| 2.3.3a The effect of acetate concentration..... | 119 |
| 2.3.3b The effect of NH ₄ ⁺ | 121 |
| 2.3.3c The effect of culture density | 121 |
| 2.3.3d Validation of gas analysis..... | 124 |
| 2.3.3e Continuous H ₂ production by <i>Rhodobacter sphaeroides</i> | 125 |

| | |
|--|-----|
| 2.4 A two-stage, two-organism process for biohydrogen from glucose..... | 130 |
| 2.4.0 Summary..... | 130 |
| 2.4.1 Article published in the International Journal of Hydrogen Energy | 131 |
| 2.5 Development of the electro dialysis technique for use in a dual system..... | 140 |
| 2.5.0 Summary..... | 140 |
| 2.5.1 Electrodialysis in extractive fermentations | 141 |
| 2.5.2 Studies on the application of electro dialysis | 143 |
| 2.5.2a Operating modes: the hare or the tortoise? | 143 |
| 2.5.2b Operating modes: limiting current density (LCD)..... | 147 |
| 2.5.2c Retention of ammonium ion | 149 |
| 2.5.2d The effect of pH on organic acid transport..... | 151 |
| 2.5.2e Mass balances for organic acid transport..... | 153 |
| 2.5.2f The capacity for organic acid transfer..... | 154 |
| 2.5.2g Energetic analysis of a dual system using electro dialysis | 154 |
| 2.5.3 Conclusions | 157 |
| 2.6 Linking dark and light H ₂ production by electro dialysis..... | 158 |
| 2.6.0 Summary and introduction | 158 |
| 2.6.1 Materials & Methods..... | 159 |
| 2.6.1a Dual system set-up..... | 159 |
| 2.6.1b Electro dialysis | 162 |
| 2.6.2 Results | 162 |
| 2.6.2a H ₂ production by <i>Escherichia coli</i> | 162 |
| 2.6.2b H ₂ production by <i>Rhodobacter sphaeroides</i> | 166 |
| 2.6.2c Electro dialysis..... | 168 |
| 2.6.3 Discussion..... | 170 |
| 2.6.3a Productivity of the dual system | 170 |
| 2.6.3b Potential application of the system with alternative fermentations..... | 172 |
| 2.6.3c The effect of electro dialysis on <i>Escherichia coli</i> | 172 |
| 2.6.3d The effect of direct current on <i>Escherichia coli</i> | 173 |
| 2.6.3e Further development and application | 173 |
| 2.7 Biomass-supported palladium catalysts on <i>Desulfovibrio</i> and <i>Rhodobacter</i> | 175 |
| 2.7.0 Summary..... | 175 |
| 2.7.1 Article published in the Journal of Biotechnology and Bioengineering | 176 |
| 2.8 Fuel cell anode construction to recycle biomass from biohydrogen production..... | 187 |
| 2.8.0 Summary..... | 187 |
| 2.8.1 Introduction to study..... | 188 |
| 2.8.2 Materials & Methods..... | 189 |
| 2.8.2a Preparation of Bio-Pd(0)..... | 189 |
| 2.8.2b Construction of fuel cell anode..... | 189 |
| 2.8.2c Fuel cell testing..... | 190 |
| 2.8.3 Results | 191 |
| 2.8.3a Power generation by fuel cell with ‘bio-fabricated’ anodes..... | 191 |
| 2.8.3b Harvesting biomass from a continuous system | 193 |
| 2.8.4 Discussion..... | 195 |
| 2.8.4a Bio-fabricated Pd(0) fuel cell anode..... | 195 |
| 2.8.4b Catalyst productivity estimate | 195 |

2.1 Dissecting the roles of *Escherichia coli* hydrogenases in biohydrogen production

2.1.0 Summary



This chapter is presented in the form of a published research letter, which discusses the effects of culture conditions and deletions of HycA and hydrogenases on H₂ formation in 100 ml-scale *E. coli* batch fermentations. Pre-growth in the presence of formate caused pre-adaptation to anaerobic H₂ production (by inducing the expression of formate hydrogen lyase), since formate-grown cultures were able to produce H₂ without a lag phase under N-limitation. Conversely, broth-grown cultures failed to produce H₂ under N-limitation (author's observations) while in a rich medium broth-grown cultures produced H₂ after a lag of 5 h [148,182].

Nitrogen limitation is preferred for two reasons:

- (i) Limitation of overgrowth by extraneous microorganisms introduced via non-sterile waste feedstocks (commercial substrates for H₂ production).
- (ii) Minimisation of carry-over of inhibitory nitrogenous material into the secondary photobioreactor (see chapter 2.5)

E. coli strains (see Table 1) were provided by Dr. F. Sargent (formerly University of East Anglia and currently University of Dundee) except for strains HD701 and MC4100, which were provided by Prof. A. Böck (Lehrstuhl für Mikrobiologie der Universität, Munich, Germany). Experimental work was performed under the guidance of Dr. I.P. Mikheenko, while data analysis and preparation of the manuscript were undertaken by the author.

The deletion of hydrogenase-2 (uptake hydrogenase) caused a 37 % increase in H₂ yield, while the deletion of hydrogenase-1 had no effect, whether alone or in addition to the hydrogenase-2 deletion. Hydrogen uptake was absent in strains lacking hydrogenases 1 and 2. The theoretical maximum (2 mol H₂/mol glucose) was not reached in the uptake hydrogenase mutants because of the activity of competing pathways. In particular, lactate and succinate formation detracted from H₂ production and this was addressed by the control of pH in 3 L cultures, while lactate formation was completely suppressed due to a switch to butyrate-type fermentation in continuous culture (chapters 2.2 and 2.6).

This study showed that there is significant potential to increase H₂ production by *E. coli* through molecular techniques. Further work is needed to evaluate hydrogenase-deficient strains under conditions representative of industrial-scale application. Therefore, the development studies on *E. coli* fermentation (chapter 2.2) and dual system experiments (chapter 2.6) proceeded to focus on *E. coli* strain HD701 despite the activity of H₂ uptake in this strain, as it had already been tested at 5-L scale.

2.1.1 Research letter published in FEMS Microbiology Letters

2.1.2 Supplementary figure

The supplementary figure was removed from the publication at the request of the editor and it is included here for clarity.

The figure illustrates that the sum of H₂ formed and H₂ uptake was reasonably constant, whereas Hyd-2 activity affected the distribution of potential H₂ between these two fates, whereas the effects on other aspects of fermentation balance were relatively minor.

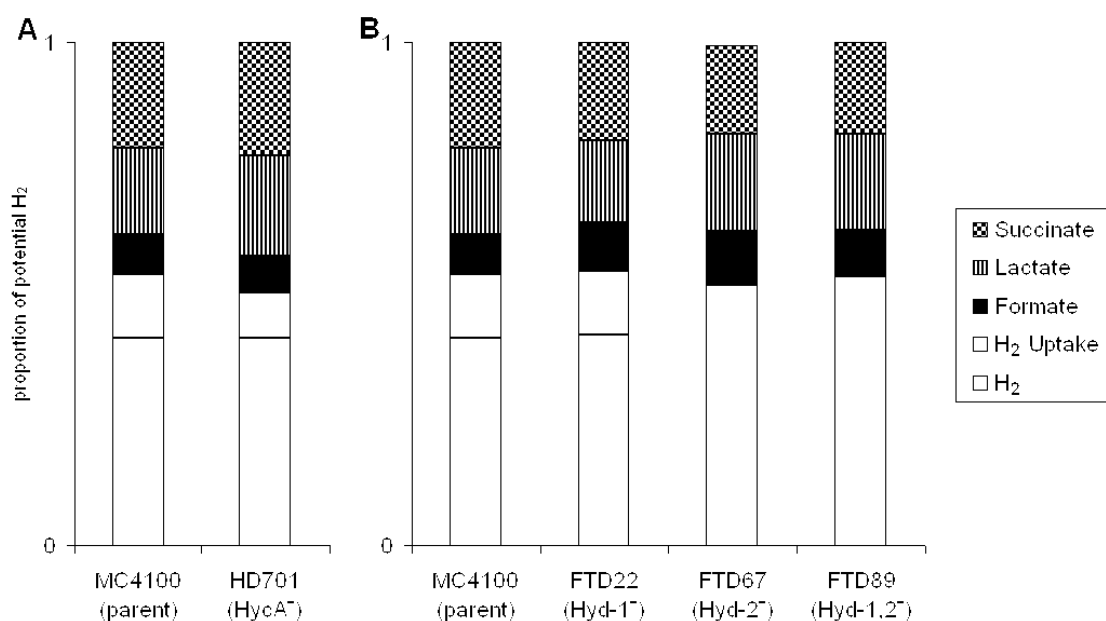
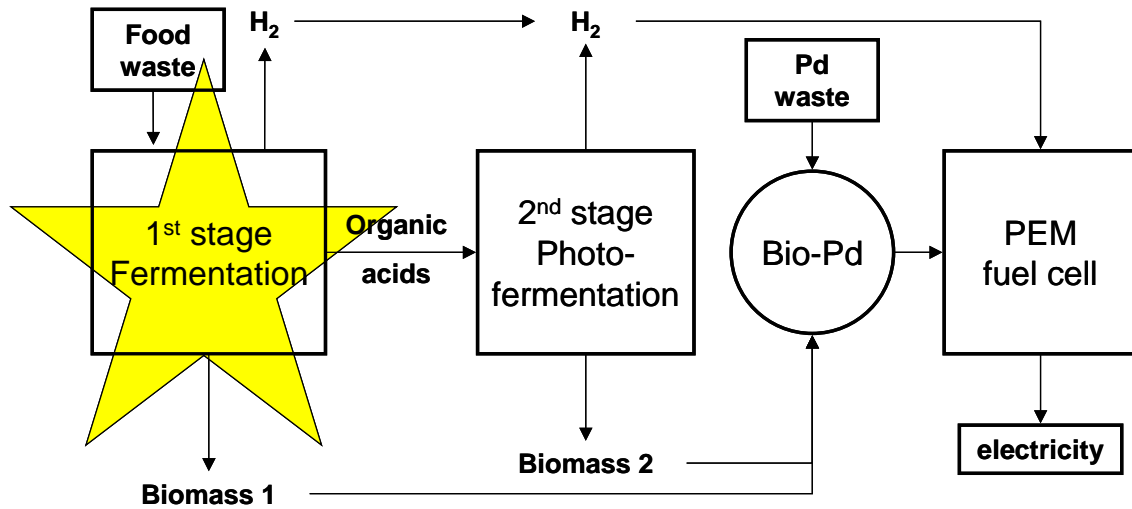


Figure 2.1-a Fates of potential H₂ in *Escherichia coli* strains deficient in HycA (A), and uptake hydrogenases (B).

In accordance with the scheme of mixed acid fermentation (Fig. 1), one mole of lactate, succinate, formate or ‘H₂ uptake’ represents one mole of potential H₂ production, whereas acetate and ethanol are produced concomitantly with H₂. Data are the normalised means of at least four replicate experiments. Means and standard errors (pre-normalisation) are given in Table 1 (section 2.1.1). For each strain the sums of potential H₂ and measured H₂ were not significantly different from 2 mol H₂/mol glucose and did not vary significantly between strains.

2.2 Development of H₂ production by *Escherichia coli*

2.2.0 Summary



This chapter describes the development of fermentation using *E. coli* HD701 from batch mode to continuously fed-batch ('pseudo-continuous') mode with pH control and integrated product and fluid extraction by electro dialysis. Overall the *E. coli* fermentation was developed from a batch culture achieving 16 % efficiency for 20 h, to a stable and pseudo-continuous culture achieving 80 % efficiency, generating a feedstock for a linked *R. sphaeroides* culture.

The H₂-overproducing *E. coli* strain HD701 was employed in pilot-scale studies of H₂ production *via* fermentation of glucose. Methods were developed through 4 phases:

phase 1: Batch mode with phosphate buffer

phase 2: Batch mode, un-buffered with pH control

phase 3: Fed-batch mode, with pH control

phase 4: Fed-batch (semi-continuous), with pH control and electro dialysis

In *phase 1* H₂ was produced for ~20 h with a yield of 0.32 mol H₂/mol glucose (16 % of the maximum) and the fermentation was limited by acidic pH, necessitating pH control. In *phase 2* the optimum pH of 5.5 was found and the H₂ yield was increased to 0.57 mol H₂/mol glucose (over 48 h), due to the suppression of lactate formation (a competing pathway to H₂ formation) and the promotion of formate hydrogenlyase (FHL) activity. With pH control, H₂

production was limited by substrate availability, which was overcome by the continuous addition of glucose in *phase 3*, where H₂ was produced for ~5 days with a yield of 1.65 mol H₂/mol glucose (82.5 %), but was ultimately limited due to the accumulation of inhibitory end-products. In *phase 4 in situ* product removal (ISPR) was incorporated *via* electro dialysis to relieve organic acid toxicity, resulting in stable H₂ production sustained for 20 days with a yield of 1.6 mol H₂/mol glucose (80 %). Instead of a ‘fill-and-draw’ fed-batch fermentation, a pseudo-chemostat mode of operation occurred due to continuous fluid removal *via* electro dialysis (ED). A butyrate-type fermentation occurred in long-term cultures, which although noted previously has been little-studied. The biochemistry and fermentation balance of butyrate-type fermentation are discussed. Butyrate is especially favoured with respect to its high ratio of potential H₂ production by *R. sphaeroides* to its charge (calculated in section 2.5.2g).

Phase 1 refers to fermentations performed by DW Penfold, while the analysis of samples from *phase 1* and all other work were carried out independently by the author. The author would like to thank D Browning and C Redwood for their advice on sequence analysis.

2.2.1 Introduction

E. coli produces H₂ during mixed acid fermentation of sugars such as glucose. H₂ is derived entirely from formate through the action of the formate hydrogenlyase system (FHL) [141,174]. FHL is a membrane-associated complex containing hydrogenase-3, formate dehydrogenase-H, and several electron transporters in unknown stoichiometry.

FHL expression is induced in response to the intracellular concentration of formate [168] and repressed by HycA by an unknown mechanism [177]. *E. coli* strains devoid of HycA showed increased FHL expression and increased rates of H₂ production in comparison to parent strains [146,172,179,217]. The HycA-deficient H₂-overproducing strain HD701 was used throughout this study, in which the effects of pH on H₂ production were observed.

E. coli is neutrophilic; it is able to maintain cytoplasmic pH in the range 7.5–8.0, while growing in media with pH in the range 5.0-9.0 [72]. The effect of pH on *E. coli* has been studied under aerobic and anaerobic conditions and three primary acid-resistance mechanisms

are known [161]. Anaerobically, the effect of pH on H₂ production by whole-cell *E. coli* cultures has not been subjected to detailed examination previously, however the seminal study of FHL [182] showed that extracts containing FHL from *E. coli* (at that time termed “*Bact. coli* (Escherich)”) dissimilated formate with an optimum pH of 7.0. *Hyc* operon expression increased with decreasing pH, but was absolutely dependent upon the presence of formate [168]. H₂ production from glucose was studied in batch mode at controlled pH values of 6.0 and 7.8. The accumulation of acetate, ethanol and lactate were not affected by pH, while H₂ was produced at pH 6.0 but formate and butyrate accumulated at pH 7.8 [17].

E. coli performs mixed acid fermentation with a maximum theoretical yield of 2 mol H₂/mol glucose, dependent upon the activity of competing pathways such as H₂ uptake and the production of lactate, succinate and butyrate (see Figure 1, section 2.1.1) [179].

In this study, the optimum pH for H₂ production from glucose by *E. coli* HD701 was determined and the rate and yield of H₂ production were improved in continuously fed-batch operation. The pH affected both H₂ production not only through its effects on FHL activity but also through its effects on the fermentation balance. The development of fermentative H₂ production by *E. coli* HD701 from glucose, from batch mode to continuously fed-batch mode is described. The continuous operation of an anaerobic, H₂ producing *E. coli* fermentation is a novel aspect of this study. This method may be preferable over batch-fermentation in a future scale up operation.

2.2.2 Methods

2.2.2a Bacterial strains and growth conditions

The H₂-overproducing strain *Escherichia coli* HD701 was cultured as described in section 2.1.1 unless otherwise indicated.

2.2.2b Phase 1

Media were autoclaved before use. 2.5 L late-logarithmic phase pre-culture was added to 2.5 L pre-warmed (30 °C) phosphate buffered saline (PBS: 1.43 g Na₂HPO₄, 0.2 g KH₂PO₄, 0.8 g NaCl, 0.2g KCl per L, pH 7.0) and 0.55 L glucose solution (1 M autoclaved separately) in a non-sterile vessel (5.5 L, Fermac200-series, Electrolab UK). The initial glucose concentration

was 100 mM and the initial biomass concentration was *ca.* 0.4 g/l. The mixture was stirred continuously at 300 rpm and made anaerobic by purging with argon for 1 hour. H₂ was measured by displacement of 1 M NaOH (which trapped CO₂) from a graduated cylinder. Other than CO₂, H₂ was the only gas found in the off-gas from the culture (Gas chromatographic analysis, see appendix 4.1.1e). *Phase 1* fermentations were performed by DW Penfold, providing samples for analysis in this study. Results were obtained from three replicate experiments.

2.2.2c Phase 2

The procedure was as *Phase 1* except that 1.5 L *E. coli* HD701 culture was added to 1.5 L pre-warmed saline-glucose solution (36.07 g glucose, 0.8 g NaCl, 0.2 g KCl per L, pH 7.0). The initial glucose concentration was 100 mM. The culture was purged with oxygen-free nitrogen (OFN) for 30 min, and the pH was adjusted immediately. Produced gas was bubbled through a scrubbing solution of 2 M NaOH containing universal indicator (Sigma) before measurement by displacement of water from a graduated cylinder. The pH was controlled automatically by the addition of 1 M NaOH (FerMac 260 pH controller, Electrolab UK). At each pH, two replicate experiments were carried out. H₂ production was monitored automatically by time-lapse photography.

2.2.2d Phase 3

The procedure was as *Phase 2* except that *E. coli* HD701 was pre-grown in nutrient broth with added sodium formate (to 0.5 % w/v). 1.5 L cultures were harvested (4435 x g, 20 °C, 10 min), washed twice in PBS and pellets were resuspended to 0.2 L in sterile PBS. For prolonged operation, the fermentation vessel was autoclaved containing 2.8 l aqueous fermentation medium (42.6 g Na₂SO₄, 10.456g K₂HPO₄, 0.204 g KH₂PO₄, 0.297 g (NH₄)₂SO₄, and 0.5 ml polyethylene glycol pH 5.5). Subsequently, the following were added aseptically: 6 ml 1 M MgSO₄, 30 ml 2 M glucose, 9 ml trace elements solution [64]. The solution was warmed to 30 °C before 0.2 L cell suspension was added to give a final volume of 3 L, and a final concentration of 20 mM glucose. The pH was immediately adjusted to 5.5 and maintained automatically (as *phase 2*).

Feeding began after 24 h operation. The feed (0.6 M glucose, 0.3 M NH₄Cl, pH 5.5) was autoclaved and rendered anaerobic by purging with OFN before being pumped into the reactor at a constant rate of 100 ml/d to provide 60 mmol glucose/d and 30 mmol NH₄Cl/d. The feed-bottle and vessel headspaces were connected so that the feed input would not affect the measurement of H₂ production.

At intervals, the culture was checked for contamination by dilution plating. As a derivative of strain MC4100, *E. coli* HD701 cannot utilise lactose [150] and produced white colonies on MacConkey agar (Sigma).

2.2.2e Phase 4

For experiments using electrodialysis, the fermentation was performed as *phase 3* except that 0.3 M NH₄Cl in the feed solution was replaced by 0.15 M (NH₄)₂SO₄ to minimise the formation of hypochlorite from chloride during ED. The fermentation culture was circulated continuously through the M chamber of a thin-cell electrodialysis stack (EKB Technology) at a rate of 450 ml/min. The specification and operation of the ED system are given in chapters 2.2, 2.5 and 2.6 and in [89]. A constant current of 400 mA was applied over a membrane area of 200 cm². The stack resistance was typically 10 Ω.

2.2.2f Analyses

Samples were filtered (32 mm Acrodisc, 0.2 µm pore) and stored at -20 °C before analysis. Organic acids were measured by anion HPLC using a Dionex-600 series system as described in chapter 2.4 [158]. The identification of organic acids was validated using a Waters/Micromass ZMD mass spectrometer using electrospray ionisation (operated by N. May, University of Birmingham and analysed by the author). The samples were run in negative ion using HPLC grade methanol as the mobile phase (source 130 °C, desolvation gas 300 °C). Analysis of glucose, ethanol and biomass concentrations are described in appendices 4.1.5c, 4.1.5f and 4.1.3 respectively.

2.2.3 Results

2.2.3a Phase 1: Batch mode with phosphate buffer

60 % of the glucose supplied was consumed while 3 L H₂ was produced over the first 10 h (Figure 2.2-a).

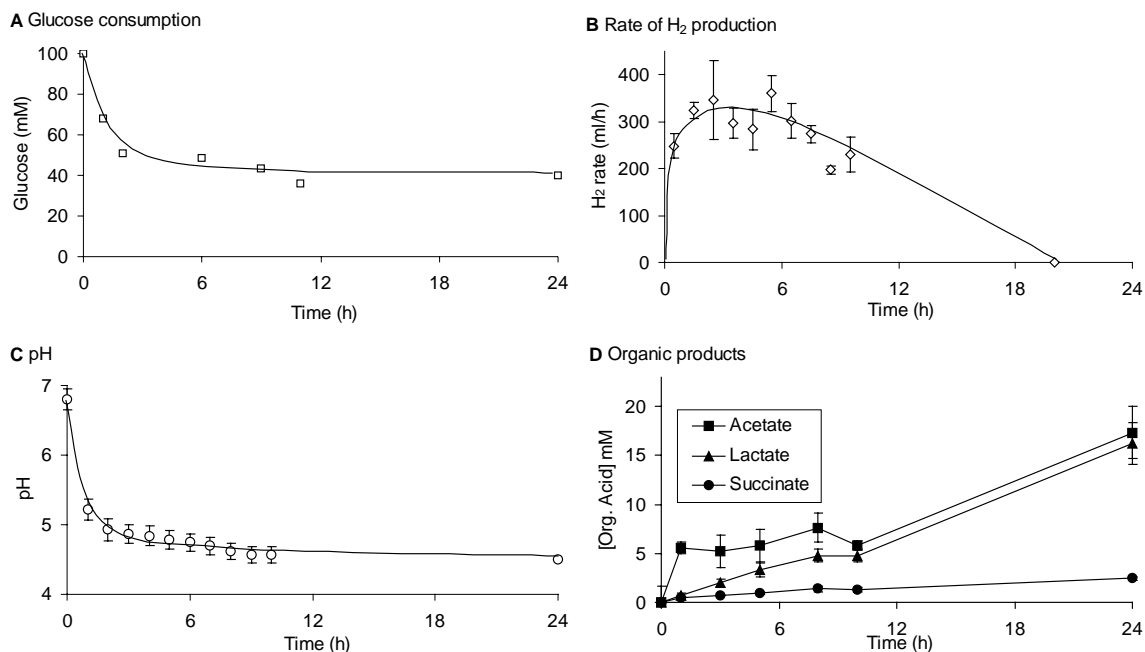


Figure 2.2-a Phase 1: Batch mode with phosphate buffer.

Values are means of three replicate experiments. Bars represent standard errors.

H₂ was produced at a high rate (54.5 ml/h/L) but at a low yield (0.32 mol/mol glucose: 16 %). The low yield is attributed primarily to the production of lactate (0.25 mol/mol glucose, equal to acetate) and to H₂ recycling by uptake hydrogenases (0.35 mol/mol glucose, calculated from fermentation products in chapter 2.1). The duration of H₂ production was *ca.* 20 h overall and H₂ production ceased with 40 % of glucose remaining unused. Given an observed rapid decrease in pH over the first few hours (Figure 2.2-a, part C) it was suggested that the main limiting factor was acidic pH, therefore pH control was incorporated in *phase 2*.

2.2.3b Phase 2: Batch mode, un-buffered with pH control**2.2.3b-1 Optimisation of pH (Phase 2)**

Fermentations were sustained for 24 h at constant pH to investigate the effect of pH in the range 5.0-7.0. The rates of growth and glucose consumption were generally lowest at pH 5.0, increasing with increasing pH (Table 2.2-1).

Table 2.2-1 The effect of pH on rates of growth and glucose consumption

| pH | Specific growth rate, μ (/h) ^a | Glucose consumption (mmol/h) |
|-----|---|------------------------------|
| 5.0 | -0.0030 | 0.438 |
| 5.5 | 0.0341 | 1.157 |
| 6.0 | 0.0725 | 1.522 |
| 6.5 | 0.0292 | 1.616 |
| 7.0 | 0.0591 | 2.595 |

Data represent the initial 6 h of fermentation. ^aSpecific rate (μ) was determined using linear regression from plots of the natural logarithm of biomass concentration against time. R^2 values were greater than 0.9 in all cases other than pH 5.0.

The rate and yield of H₂ production decreased below pH 5.5 and above pH 6.5; and varied little in the range pH 5.5-6.5 (Figure 2.2-b). Examination of the fermentation products lactate and formate provided explanations for the pattern of H₂ production. Lactate accumulation, which detracts from H₂ production, was only significant below pH 5.5, while formate accumulation, which indicates decreased FHL activity, increased with increasing pH in the range 5.5-7.0. The rate and yield of H₂ production were lowest at pH 7.0, corresponding to an accumulation of formate in the medium. It is likely that the toxicity of formate is not perceived until significant undissociated acid forms and re-enters the cell, which occurs at pH < 6.8 [173]. As the pK_a of formate is 3.75, the acid would be more than 99.95 % dissociated at pH 7.0, in which form it is unable to freely cross lipid bi-layers [166]. Although little variation in the rate and yield of H₂ production was observed between pH 5.5 and pH 6.5, a pH of 5.5 was chosen for further experiments, because of the low concentration of formate in the medium. In batch culture, the extracellular formate has the potential to re-enter the cell and contribute to H₂ production whereas in a dual system employing electrodialysis (see chapter 2.6), extracellular formate would be transported out of the *E. coli* culture preferentially over larger organic acids (Figure 2.5-h) detracting from the overall H₂ yield in a dual system.

2.2 Results - Dark fermentation development

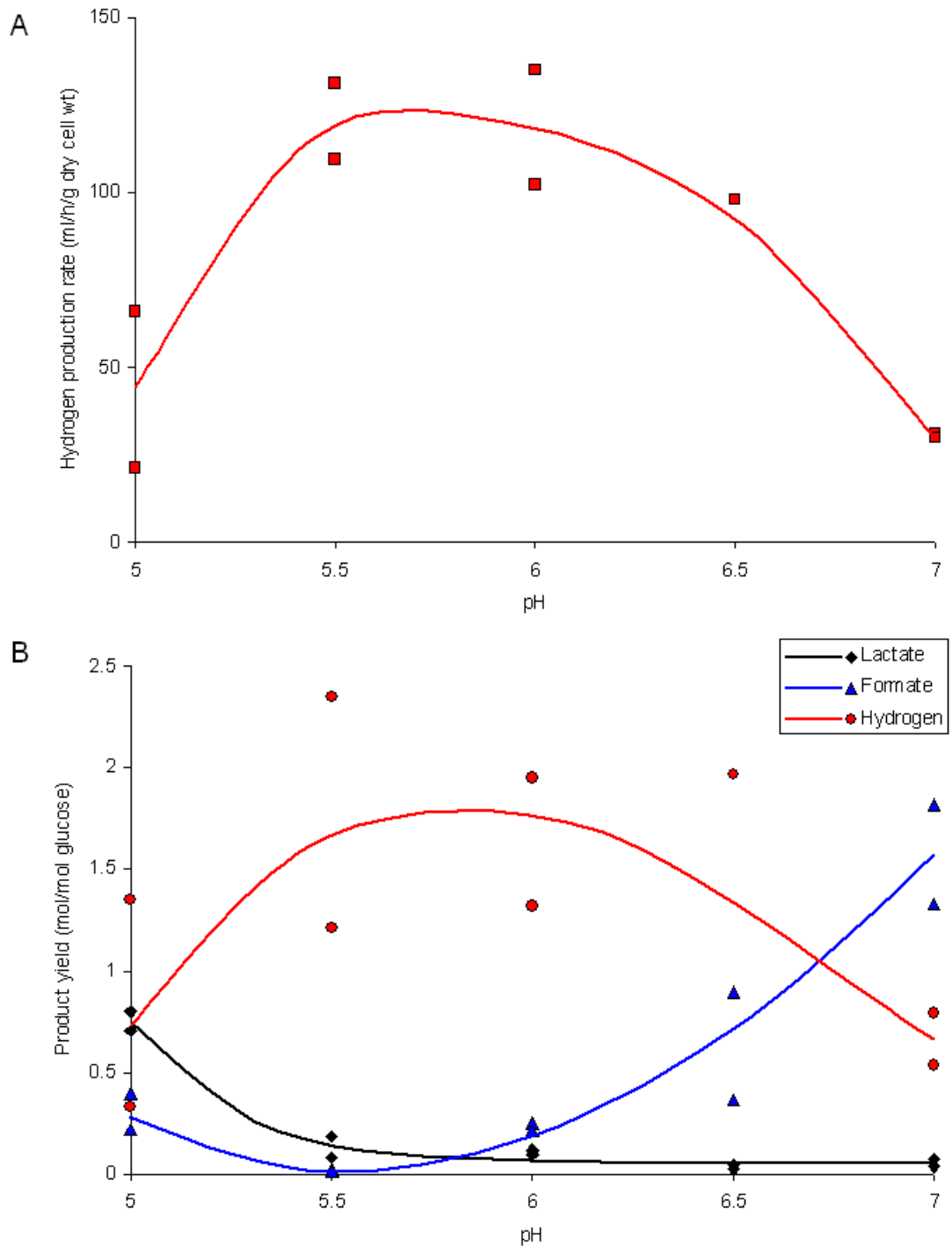


Figure 2.2-b Phase 2: Effect of pH on mixed-acid fermentation.

Datapoints represent individual experiments. Rates (A) and yields (B) of metabolite accumulation were calculated over the initial 6 h to mediate against the potential effects of end-product accumulation.

2.2.3b-II H₂ production with controlled pH (Phase 2)

In batch mode, with pH controlled at 5.5, the initial rate of H₂ production was higher than that in phase 1 (110.7 ml/h/L over the first 3 h), but the rate gradually decreased as glucose was depleted. Over the first 48 hours the H₂ yield was almost twice that in phase 1 (0.57 mol H₂/mol glucose). After 48 hours, the rate of H₂ production was almost zero and the concentration of glucose was below the limit of assay sensitivity (<1 mM). Glucose was added (to 100 mM) and the rate of H₂ production increased to 36.9 ml/h/L (i.e. 30 % of the initial rate) and was sustained for a further 24 hours with a yield of 0.12 mol H₂/mol glucose. This prompted the investigation of H₂ production in continuously fed-batch mode (phase 3).

2.2.3c Phase 3: Fed-batch mode with pH control

Feeding was started at 24 h post-inoculation at a constant rate of 60 mmol glucose/day and, for the following 5 days of fed-batch operation, cultures consumed all added glucose and produced H₂ with an average yield of 1.6 mol H₂/mol glucose, 80 % of the theoretical maximum for mixed acid fermentation (2 mol H₂/mol glucose). The progress of the fermentation was divided into 4 distinct stages (Figure 2.2-c, part C):-

1. During the initial 24 h > 95 % of glucose was consumed in a standard mixed-acid fermentation producing lactate, succinate, acetate and H₂ with a yield of < 2 mol H₂/mol glucose.
2. Following the introduction of glucose 24 h post-inoculation, there was a change of fermentation type. Acetate and succinate accumulated at decreased rates and butyrate accumulated rapidly, coinciding with the depletion of the initially formed lactate. For a brief period, H₂ was produced at rates of up to 320 ml/h. Since glucose was supplied at a rate of 60 mmol/day, the maximum H₂ production rate (corresponding to 2 mol H₂/mol glucose) would be 120.3 ml/h. The additional H₂ was attributed to the re-assimilation of lactate and its metabolism into a H₂ producing pathway (see section 2.2.4b).
3. Following the depletion of lactate (after 2 days), the rate of H₂ production stabilised at *ca.* 100 ml/h, equivalent to a yield of 1.6 mol H₂/mol glucose (80 %).
4. Finally, the fermentation products accumulated to high concentrations (39.3 mM butyrate, 25.1 mM acetate, 15.1 mM succinate) and the fermentation reached

completion. The accumulation of organic acids and H₂ ceased and glucose was detected increasingly in the medium. It is known that ethanol is also produced during *E. coli* fermentation but the concentration was not monitored and therefore a mass balance analysis was not possible in this study.

2.2.3d Phase 4: Fed-batch (semi-continuous), with pH control and electro dialysis

With the incorporation of electro dialysis, the fermentation progressed through stages 1, 2 and 3 as phase 3 but stage 4 was not reached within 20 days. This was attributed to the removal of fermentation products from the culture, resulting in the relief of organic acid toxicity, as shown and discussed in chapter 2.6.

2.2.3e Butyrate-type fermentation in *Escherichia coli* HD701

The shift from mixed acid fermentation to butyrate-type fermentation occurring in phase 3 and phase 4 was unexpected as butyrate formation by *E. coli* is scarcely reported [17], but analysis confirmed that the novel product was butyrate and that it was produced by *E. coli* HD701. Butyrate formation was confirmed by HPLC-MS (Figure 2.2-d). HPLC analysis (as chapter 2.4) showed the presence of an anion with a retention-time identical to a butyrate standard and distinctly different from pyruvate (Figure 2.2-d, part A). Conclusive qualitative analysis cannot be based on retention time alone as different anions may hypothetically elute with equal speed. Therefore the 'butyrate' fraction was collected from the HPLC outlet and analysed by MS, which detected an anion with a mass of 87, corresponding to butyrate, making an alternative conclusion highly unlikely (Figure 2.2-d, part C).

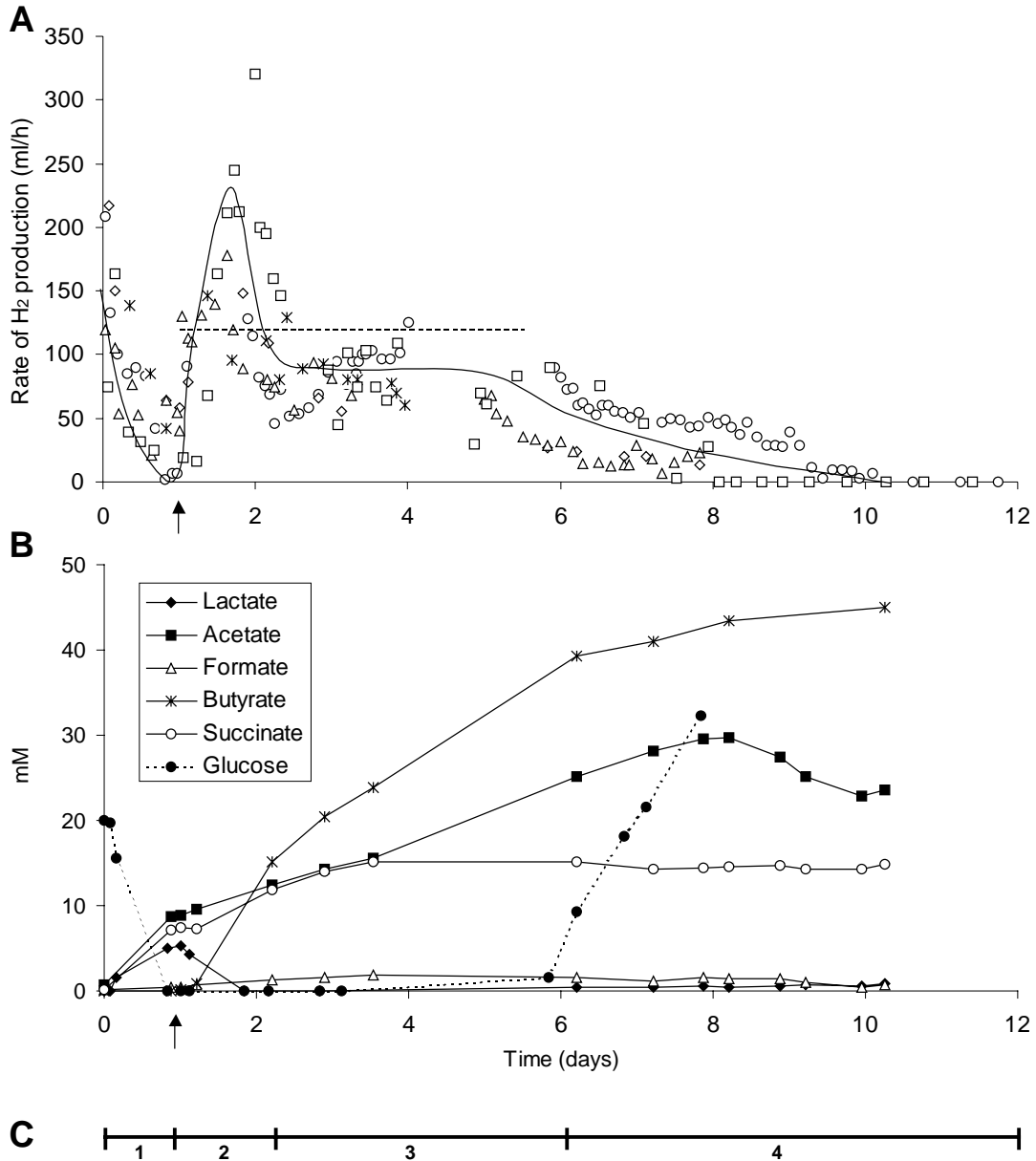


Figure 2.2-c H₂ production (A) and traces of organic acids and glucose (B) in *phase 3* fermentations and division of the experiments into 4 stages (C).

Phase 3 fermentations were fed-batch mode, unbuffered with pH control. Data from 5 replicate experiments are shown in A, whereas typical data is shown in B. For reproducibility see Figure 2.2-e. Arrows indicate the introduction of glucose 24 h post-inoculation. The dotted line (A) indicates a rate of 120.3 ml H₂/h, corresponding to a yield of 2 mol H₂/mol glucose (100 %).

It may be suggested that contaminants such as clostridia were responsible for the butyrate formation. As strict anaerobes, clostridia would not be detected by dilution plating. However, the fermentation medium was autoclaved before inoculation with a concentrate of aerobically grown *E. coli* and the onset of rapid butyrate formation occurred consistently 24 h post-inoculation, and always corresponding to lactate depletion. The following calculation shows that without a substantial inoculum (significantly beyond contamination), a clostridial culture capable of producing butyrate at the observed rate could not become established. Data produced using *Clostridium butyricum* ZJUCB were considered maximal as this strain was selected for its high capacity for butyrate production. *C. butyricum* produced 5.7 mmol butyrate/h/g bacterial dry weight under optimal conditions, with a specific growth rate (μ) of up to 0.2/h [63]. Assuming that this activity could be achieved under the conditions of the *E. coli* fermentation, 0.34 g clostridial dry cell weight would be required to produce butyrate at the observed rate (1.9 mmol butyrate/h; Figure 2.2-c, part B). Assuming clostridial spores were destroyed by autoclaving [116], the growth of the required cell mass in 24 h ($\mu = 0.2$ /h) would require an initial inoculum of 2.8 mg clostridial dry weight, which equates to *ca.* 7 ml of a rich culture (OD=1). Accidental contamination would be unlikely to introduce more than a few thousand cells/spores, leading to a μ -value several orders of magnitude higher than the reported rate for optimal conditions. Therefore, the formation of butyrate is not easily attributed to clostridial contamination although further investigation is required to rule it out completely. Also, the culture was only fed with glucose/ NH_4^+ solution, and no additional sources of amino acids, P or micronutrients. Therefore, a contaminant would have to compete with *E. coli* for traces of these nutrients in order to persist in long-term culture.

2.2 Results - Dark fermentation development

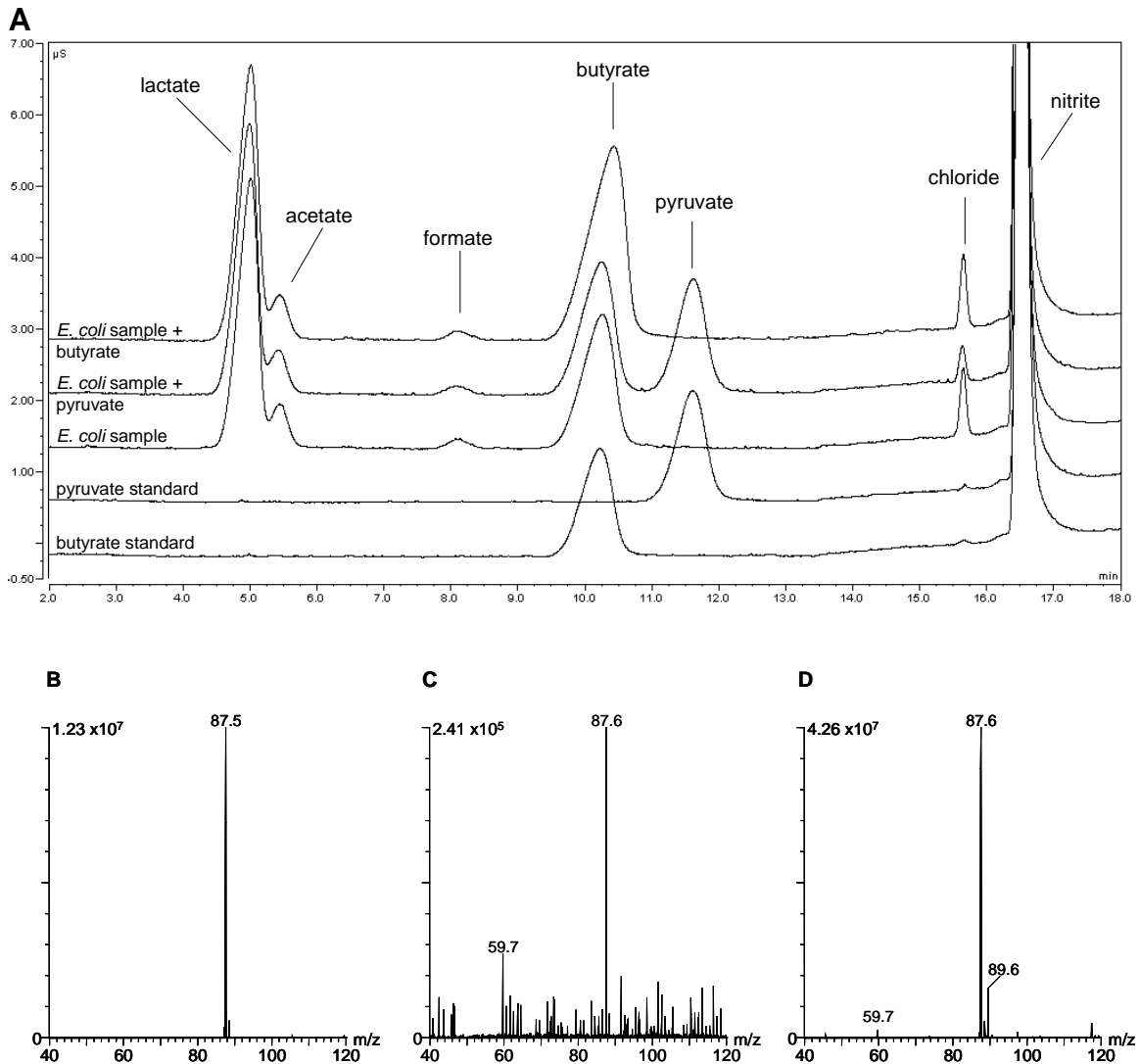


Figure 2.2-d HPLC-MS analysis of butyrate.

A, HPLC chromatogram showing the spiking of an *E. coli* sample with butyrate and pyruvate standards. Nitrite was added as an internal standard (1 mM); **B**, Mass spectrum of butyrate standard. Mass=87.5 corresponds to butyrate anion; **C**, Mass spectrum of “butyrate” fraction collected from RT 9.5-10.5 min (part A). Mass=59.7 corresponds to acetate anion; **D**, Mass spectrum of the *E. coli* sample (part A). Mass=89.6 corresponds to lactate anion.

Butyrate-type fermentation is under-reported in the context of *E. coli*, although in the current work it formed the major product in long-term fermentations (Figure 2.2-c, part B and Figure 2.2-e). Butyrate was identified as a product previously [17], and this study provides the impetus for a preliminary analysis of butyrate-type fermentation in *E. coli* (Figure 2.2-e).

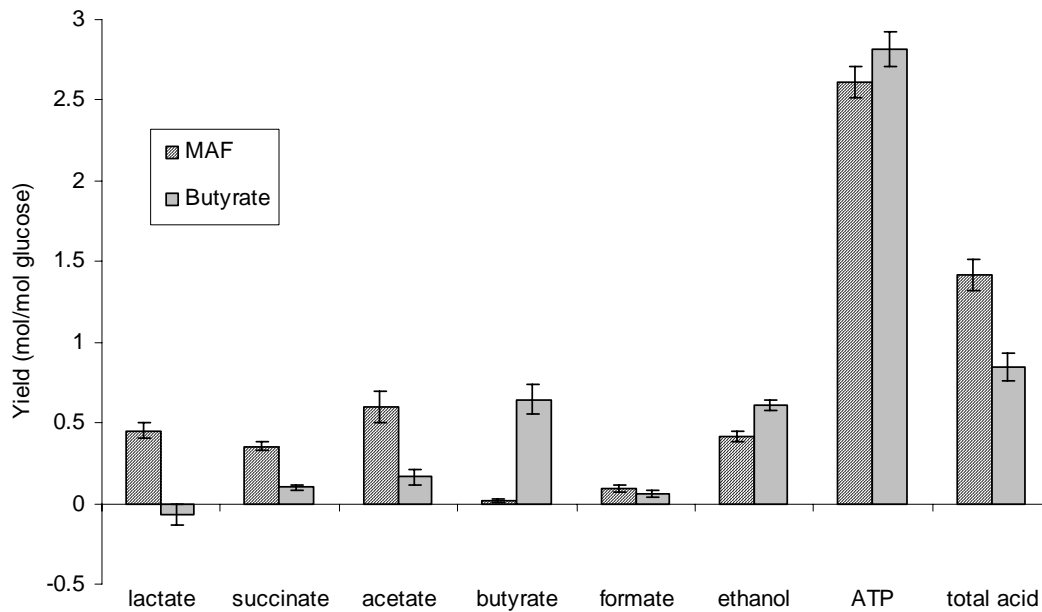


Figure 2.2-e Elements of fermentation balance during mixed-acid fermentation (MAF) and butyrate-type fermentation, occurring in the 1st and subsequent stages, respectively, of phase 3 fermentations.

Mixed acid fermentation (MAF) occurred during the initial 24 h and was followed by butyrate-type fermentation (Figure 2.2-c, part C). Values are means \pm SEM from at least 8 experiments. The yield of ATP was estimated as sum of the molar yields of acetate and butyrate, plus the yield of glycolysis (2). Ethanol was estimated on the basis of NADH balance, confirmed by analysis in chapter 2.1.

The environmental stimuli to butyrate production are unclear as small quantities of butyrate were detected in the fermentation medium slightly earlier than t-24h (Figure 2.2-c, part B). This is interpreted as evidence against the introduction of glucose as a stimulatory factor. Rather it is speculated that butyrate-synthetic machinery was up-regulated *ca.* t-20 h, with the onset of glucose depletion, and the subsequent addition of glucose was permissive to increased activity.

Given the scarcely precedent observation of a novel mode of fermentation in biochemistry's most extensively studied model organism, some consideration is given (section 2.2.4b) to the possible biochemical mechanisms of butyrate-type fermentation and its consequences on the fermentation balance.

2.2.4 Discussion

2.2.4a The effect of pH on mixed-acid fermentation (MAF)

The optimum pH for H₂ production by *E. coli* was found to be *ca.* 5.5. The rate, yield and duration of H₂ production were significantly improved by the incorporation of pH control. As an additional advantage, buffering was not required under these conditions. The addition of buffers would add a significant cost upon scale up and would introduce an unacceptable environmental contaminant into the waste-stream.

Organic acid toxicity is the product of three mechanisms by which organic acids can cause stress. Firstly, at low pH organic acids exist in their protonated forms (the proportion of which depends on the dissociation constant, pK_a), which are membrane-permeable [173]. Organic acids can cross the cell envelope and dissociate in the neutral cytoplasm, releasing H⁺ and causing acid stress. Secondly, organic anions may exert specific inhibition on the activity of cytoplasmic enzymes [88,120,166,200,202]. Finally, organic acids cause osmotic stress. Organic anions accumulate in the cytoplasm due to the concentration gradient and the pH gradient (membrane potential) between the cytoplasm and the external medium. For example, with an external pH (pH_o) of 6.0 and an external acetate concentration of 8 mM, acetate accumulated in the cytoplasm to at least 240 mM causing the cell to export useful molecules (e.g. glutamate) in order to maintain osmotic balance, resulting in a 50 % decrease in specific growth rate [165,166]. It is the active maintenance of internal pH (pH_i) within a narrow range that prevents equilibrium and drives the continual accumulation of organic acids. Decreasing pH_o results in lesser but proportional decrease in pH_i . In the case of *E. coli*, growth cannot occur when the pH_i is forced below 6.6-6.8 [18,72].

E. coli cells respond to unfavourable pH and osmolarity through well-characterised mechanisms [120,161]. Lactate production and formate breakdown can both be interpreted as additional mechanisms of acid resistance, which are active during anaerobic fermentation. Formic acid can be eliminated by FHL activity (with the co-incidence of H₂ production) and lactate can be produced instead of acetate, which is advantageous because lactic acid has a lower dissociation constant than acetic acid (3.86 and 4.76 respectively) [32].

Lactic acid fermentation would produce no H₂ (Figure 1, section 2.1.1) so in a H₂ producing system the pH must be maintained above the threshold for the induction of lactic acid production, which was between pH 5.0 and pH 5.5 (Figure 2.2-b) in accordance with previous reports [77,119,183]. FHL activity increased progressively with decreasing pH (Figure 2.2-b). Thus, for efficient H₂ production, the pH was maintained as low as possible without inducing significant lactate production (*ca.* pH 5.5).

A proportional increase in the yield of lactate with decreasing pH was reported previously [183], whereas the results of this study (Figure 2.2-b) suggest a threshold for the induction of lactate production in the region of pH 5.0-5.5. This discordance is attributed to methodological differences. In the previous work the initial pH was controlled (with phosphate buffer) and pH decreased over the course of fermentation, whereas in this work, the pH was controlled accurately and constantly.

The response of FHL activity to external pH may result from the direct effect of cytoplasmic pH on FHL activity [182], or from the increasing cytoplasmic concentration of formate with decreasing medium pH, which could affect both the rate of formate breakdown and the regulated expression of FHL components [168].

Organic acid toxicity is known to inhibit bacterial growth [28,41,88,96] and would be expected to inhibit H₂ production. An experiment was performed to confirm this. In batch-mode with excess glucose and controlled pH (6.0) (as *phase 2*), H₂ was produced at a steady rate of 44.5 ml/h after 48 h of operation. The concentration of organic acids in the 3 L culture was artificially increased by adding of a mixture of lactate, acetate and succinate (45:45:10 mol proportions respectively, 0.1 L, 0.3 mol total). The concentration of organic acids in the medium increased from 81.9 mM to 181.9 mM (~2-fold), and over the subsequent 10 h, the rate of H₂ production was constant at 25.0 ml/h, half of the earlier value. Organic acid toxicity may affect H₂ production proportionally, although further experiments would be required to confirm this. The reduction in rate can be attributed to the added organic acids and not to the possible introduction of O₂. As a control, the same method of addition was used in *phase 2* for the addition of glucose with no marked reduction in rate.

2.2.4b Butyrate formation during the anaerobic fermentation of *E. coli*

2.2.4b-I The pathway of butyrate formation in *Escherichia coli* HD701

Butyrate was not produced in batch cultures (*phase 1*, 2 and chapter 2.1). Traces of butyrate were first detected in the medium at *ca.* t-22 h (2 h prior to the onset of glucose addition), immediately preceding the highest rate of H₂ production, the depletion of lactate from the medium and the decreased rate of acetate accumulation (Figure 2.2-c). Since butyrate formation did not detract from H₂ production, it is proposed that the precursor to butyrate is a product of pyruvate formate-lyase, rather than a higher intermediate, such as phosphoenolpyruvate or pyruvate whose pools are drained by the formation of lactate and succinate, respectively, detracting from H₂ production (Figure 1, section 2.1.1). The product of PFL and precursor to ethanol and acetate is acetyl-CoA, which is a butyrate precursor in *Clostridium acetobutylicum* [13]. In clostridia 2 acetyl-CoA are condensed to form one butyrate consuming one NADH and producing 1 ATP [106].

The pathway from acetyl-CoA to butyrate is composed of five reactions, of which, enzymes known in *E. coli* can catalyse all but one. The hydrogenation of butenoyl-CoA (or crotonoyl-CoA) to butanoyl-CoA, carried out by an enoyl-CoA dehydrogenase (Figure 2.2-f, part B), is not an established function of any enzyme known in *E. coli*. However, two enzymes are known to perform this function in other organisms; trans-2-enoyl-CoA reductase (TER) and butyryl-CoA dehydrogenase (BCAD) (Table 2.2-2).

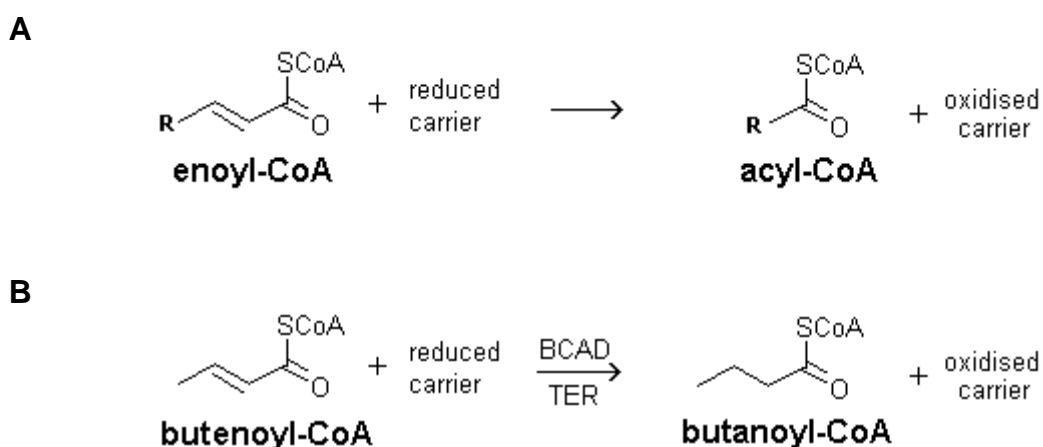


Figure 2.2-f Generic hydrogenation of enoyl-CoA to acyl-CoA species.

Generic reactions are catalysed by acyl-CoA dehydrogenases (A), for example the hydrogenation of butenoyl-CoA (B) as part of the pathway of butyrate formation (Table 2.2-2). BCAD, butyryl-CoA dehydrogenase; TER, trans-2-enoyl-CoA reductase.

Table 2.2-2 Candidate enzymes in the pathway of butyrate formation

| Reaction step | Candidate enzymes ^a | | | |
|-----------------------------------|--------------------------------|---|--------------------------|----------|
| | EC | Enzyme name (and abbrev.) | Status in <i>E. coli</i> | Source |
| acetyl-CoA ↓ | 2.3.1.9 | acetoacetyl-CoA thiolase (ACT) | known | [46] |
| Acetoacetyl-CoA ↓ ^b | 1.1.1.35 | 3-hydroxyacyl-CoA dehydrogenase (HCDH) | known | [16,145] |
| (S)-3-hydroxy-butanoyl-CoA ↓ | 1.1.1.57 | fructuronate reductase (FR) | known | [152] |
| butenoyl-CoA ↓ ^b | 4.2.1.17 | enoyl-CoA hydratase (ECH, MaoC) | known | [4,143] |
| butanoyl-CoA ↓ | 1.3.99.2 | butyryl-CoA dehydrogenase (BCAD) | putative | [171] |
| butanoyl-CoA ↓ | 1.3.1.44 | trans-2-enoyl-CoA reductase (NAD ⁺) (TER) | unknown | [68] |
| butyrate (butanoate) | 2.8.3.8 | acetate CoA-transferase (ACT) | known | [95] |

^aEnzyme function and species distribution data were assembled from the BRENDA database (www.brenda.uni-koeln.de).

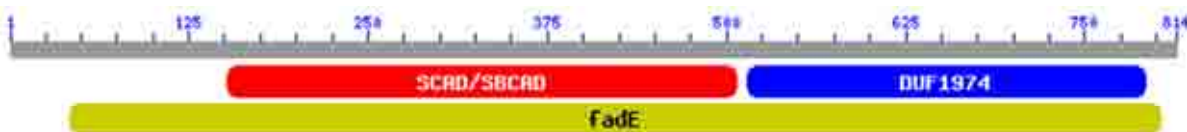
^bAny of the listed enzymes can perform the reaction alone

Butyryl-CoA dehydrogenases (BCAD) (EC 1.3.99.2) are known among bacteria, archaea, eukaryotic microorganisms, and higher organisms (www.brenda.uni-koeln.de). Conversely, trans-2-enoyl-CoA reductases (TER) (EC 1.3.1.44) are known only among mycobacteria and the mitochondria of eukaryotes such as *Euglena gracilis* and mammals (www.brenda.uni-koeln.de). Hoffmeister *et al.* (2005) identified several TER homologues in γ -proteobacteria (the same group as *E. coli*) annotated as putative acyl-CoA dehydrogenases, sometimes located in the proximity of genes involved in fatty acid synthesis [68].

Three putative *E. coli* BCADs (see Figure 2.2-g) were identified (on the basis of sequence analysis) within *E. coli* K-12 strains W3110 and MG1655, for which complete genome nucleotide sequences are available. Each of the three putative BCADs contains high homology (E-value threshold: 0.010) to conserved functional domains, identified by a conserved domain database [118].

Based on this analysis the most promising putative BCAD (AP_000876) is homologous to FadE, part of the *fad* operon, encoding enzymes involved in β -fatty acid oxidation in *E. coli* and *Salmonella enterica* [73]. Furthermore, its N-terminal domain is homologous to the SCAD domain, which is common to the FAD-dependent eukaryotic TER enzymes, the eukaryotic short/branched chain acyl-CoA dehydrogenase (SBCAD), the bacterial butyryl-CoA dehydrogenase (BCAD) and 2-methylbutyryl-CoA dehydrogenase (isoleucine catabolism). DUF1974 is predominantly found in various prokaryotic acyl-CoA dehydrogenases and may be considered indicative of bacterial BCAD (Figure 2.2-g, part A), although it is interesting that this C-terminal domain was not present in representative bacterial BCAD sequences. Conversely, close homologues to AP_002315 are most commonly annotated as crotonobetainyl-CoA dehydrogenases, functionally related to but not clearly functional as BCADs. NP_415757 homologues, however function as aldehyde and alcohol dehydrogenases and it seems unlikely that this protein functions as a BCAD in *E. coli*. The evidence suggests that the *E. coli* protein AP_000876 is a FadE homologue functioning as an acyl-CoA dehydrogenase, although further investigation would be needed to confirm its activity as a BCAD, specific to butyryl-CoA.

A: AP_000876: putative acyl-CoA dehydrogenase



B: AP_002315: acyl-CoA dehydrogenase



C: NP_415757: fused acyl-CoA dehydrogenase/Fe-dependent ADH/PFL deactivase

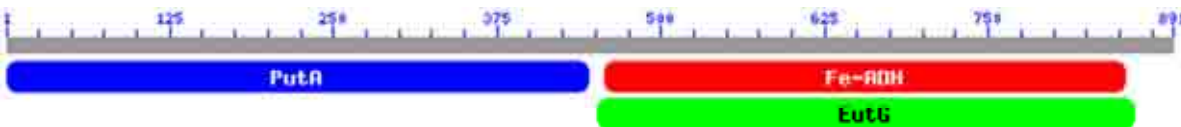


Figure 2.2-g Putative *Escherichia coli* BCADs and their conserved functional domain topologies.

Conserved domains were identified on the basis of close homology (E-value threshold: 0.010) with the query sequence using a conserved domain database [118]. SCAD/SBCAD, short chain acyl-CoA dehydrogenase (SCAD); DUF1974, domain of unknown function predominantly found in various prokaryotic acyl-CoA dehydrogenases; FadE; acyl-CoA dehydrogenase; ACAD, mitochondrial and peroxisomal acyl-CoA dehydrogenase; PRK12341, putative acyl-CoA dehydrogenase; PutA PutA, NAD-dependent aldehyde dehydrogenases; Fe-ADH, iron-containing alcohol dehydrogenase; EutG, Alcohol dehydrogenase, class IV.

Furthermore, the putative *E. coli* K-12 BCAD (AP_000876) aligns closely with representative BCADs from several bacterial species and retains a specific glutamate residue (and its context) known to be catalytically important to acyl-CoA dehydrogenase activity (Figure 2.2-h) [8,11,42,189]. Conserved domains were found near the N-terminal (SCAD domain), which are thought to be responsible for substrate specificity and binding [85], whereas the C-terminal (DUF 1974 domain) was missing from representative bacterial BCAD sequences.

In conclusion, the enzymes necessary for the operation of the pathway shown in Table 2.2-2 can be found in *E. coli* K-12, although detailed investigation would be necessary to establish the operation of this pathway and to confirm the involvement of specific enzymes.

2.2 Results - Dark fermentation development

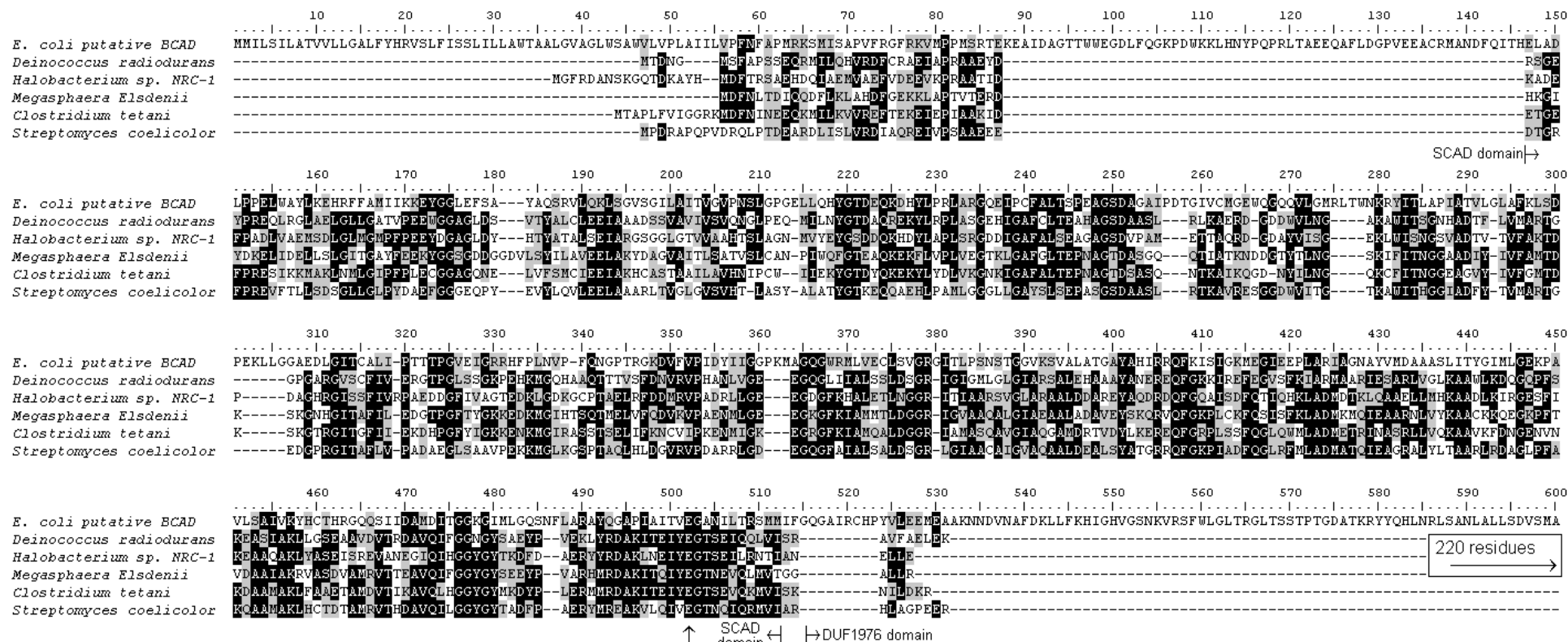


Figure 2.2-h Alignment of putative *Escherichia coli* K-12 BCAD (accession: AP_000876) and five representative bacterial BCAD sequences.

Organisms and sequences: *Deinococcus radiodurans* R1 (accession: NP_294979), *Halobacterium* sp. NRC-1 (accession: NP_279692), *Megasphaera Elsdenii* (accession: 1BUC_A), *Clostridium tetani* E88 (accession: NP_782646), *Streptomyces coelicolor* A3(2) (accession: NP_625710). The Alignment was performed using ClustalW (BLOSUM62 matrix). Background shading: Black: 100 % identity, grey: > 50 % identity, none: < 50 % [60]. Arrow represents a conserved active site catalytic residue (see text). The C-terminal domain (DUF1974, not shown) failed to align with representative BCAD sequences (see text).

2.2.4b-II Butyrate-type fermentation balance

A theoretical analysis of butyrate-type fermentation was performed based on the following axioms:-

1. Standard pathways of mixed acid fermentation [32] (Figure 1, section 2.1.1) with the additional pathway of butyrate production by the condensation of 2 acetyl-CoA to form 1 butyrate with the oxidation of 1 NADH and the phosphorylation of 1 ADP, as occurs in clostridia [106].
2. For balanced electron flow, the 2 mol NAD/mol glucose reduced during glycolysis is re-oxidised by the formation of end-products. Therefore, the sum of 2*ethanol, 2*succinate, lactate and butyrate must equal 2 (molar yields).
3. For balanced carbon flow, the sum of lactate, succinate, ethanol, acetate and 2*butyrate must equal 2 (molar yields).
4. The molar yields of all products other than lactate cannot be negative, in accordance with observations (Figures 2.2-c and 2.2-e).

Under these provisions, carbon and electron flow can be balanced, dependent upon the formation of feasible proportions of fermentation products. For example, lactate cannot be formed during butyrate production and the yields of succinate and butyrate must be in the range $0\text{-}\frac{2}{3}$ mol/mol glucose. Theoretically, the consequences of butyrate-type fermentation are decreased yields of acetate, ethanol and ATP, while the yield of H_2 is not directly affected. For example, an additional 0.5 mol butyrate/mol glucose would result in losses of -0.25 total acid, -0.25 ATP, -0.75 acetate and -0.25 ethanol (mol/mol glucose), according to the metabolic pathway and rules set out above. The cost of a lower ATP yield may be offset by the relief of organic acid toxicity due to the decreased overall acid production. *E. coli* is known to up-regulate lactic acid production as a response to acidic pH [32,183], which results in a lower proportion of the acid pool that is protonated and membrane-permeable, lactate having a lower dissociation constant than acetate ($\text{p}K_a$ values of 3.86 and 4.76, respectively). However, this reasoning cannot account for the switch to butyrate production because butyric and acetic acids are alike in terms of $\text{p}K_a$ values (4.81 and 4.76, respectively). Rather, butyrate-type fermentation resulted in a decreased quantity of acid formed (Figure 2.2-e).

In practice the switch to butyrate formation was associated with lactate re-assimilation, which would theoretically contribute to the pools of NADH and pyruvate allowing the yield of butyrate to exceed $\frac{2}{3}$ mol/mol glucose, increasing the yield of ATP, and allowing the yield of H₂ to appear to exceed 2 mol/mol glucose (Figure 2.2-c, part A).

The effects of butyrate-type fermentation were analysed by comparing the proportions of products during the first 24 h of fermentations (mixed acid fermentation) with the proportions observed subsequently (butyrate-type fermentation). By producing butyrate at the expense of lactate, acetate and succinate, the formation of acid was decreased by 40 % (Figure 2.2-e).

2.2.5 Conclusions

H₂ production by *E. coli* fermentation was developed through four phases, resulting in a continuous and sustainable system producing H₂ at 80 % efficiency.

The reaction was initially limited by pH. After a pH optimum of 5.5 was determined and applied, substrate limitation occurred prompting the investigation of fed-batch mode. The final limitation was organic acid toxicity, which was overcome by the incorporation *in situ* product removal (ISPR) by electrodialysis, which also provided water transport to balance the input of feed solution.

With pH control and continuous feeding, H₂ was produced for a total of 13 days. The rate and yield of H₂ production were initially high but began to decline after 4 days. It is speculated that the accumulated organic acids exerted stress upon the cells, bringing about the cessation of fermentation, which was avoided by the incorporation *in situ* product removal by electrodialysis.

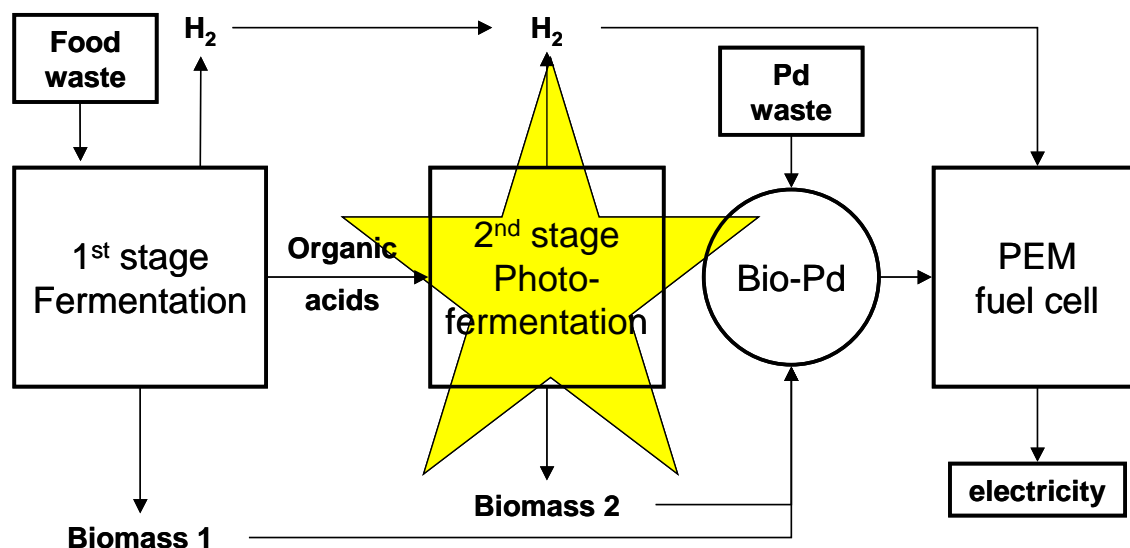
A novel form of *E. coli* fermentation was observed. Under the conditions of *phase 3* and *phase 4* *E. coli* took up the previously formed lactate and produced butyrate, temporarily producing H₂ at a high rate. Previous reports confirm the ability of *E. coli* to produce butyrate and the biochemical capability can be confirmed with the exception of one reaction step, for which putative enzymes were identified in *E. coli* K-12, from which strain HD701 was

2.2 Results - Dark fermentation development

derived. Further work would be required to confirm the presence and activity of these enzymes and to further characterise butyrate-type fermentation in *E. coli*.

2.3 Development of photobiological H₂ production by *Rhodobacter sphaeroides*

2.3.0 Summary



Environmental conditions for the production of H₂ by *R. sphaeroides* were investigated both practically and through the analysis of published data. Small-scale batch reactors (100 ml) were used to examine the effects of acetate availability, culture density, ammonium ion inhibition, and CO₂ availability on H₂ production by *R. sphaeroides*. Headspace gas composition analysis and a fluid-displacement system were employed for the measurement of H₂ production in experiments using acetate as the sole carbon source. The maximum concentration of NH₄⁺ permissive to H₂ evolution was *ca.* 1 mM in a background of 40 mM acetate. The concentration of acetate (substrate) directly affected the extent and duration of H₂ evolution, the minimum substrate concentration being *ca.* 10 mM. Substrate inhibition was absent at substrate concentrations up to 90 mM, and in an excess of acetate, the rate of H₂ evolution was proportional to culture density up to 0.65 g dry weight/l.

These data, coupled with information gathered from the literature were used in the design of a continuous *R. sphaeroides* photobioreactor achieving stable and continuous H₂ production, which was employed subsequently in a dual system combining *R. sphaeroides* and *E. coli* (chapter 2.6),

in which the composition of the medium supplied to *R. sphaeroides* was dependent upon the preceding dark fermentation.

Of particular relevance was the study of repression of H₂ production by *ca.* 1 mM NH₄⁺, even in an excess of acetate. This bottleneck prevented the production of H₂ from *E. coli* fermentation effluent (see chapter 2.4) and the problem shown in this chapter was subsequently overcome through the application of electro dialysis (chapters 2.5 and 2.6).

2.3.1 Introduction

The light stage of a dual system for H₂ production could be carried out by a variety of APB, of which the purple non-sulphur (PNS) bacteria are preferred owing to the lack of H₂S formation. For this study *Rhodobacter sphaeroides* O.U. 001 was selected because of the wealth of information available regarding this organism. Information is available regarding the metabolism [48,49,90] and kinetics [91] of H₂ production by this organism, which has been applied in the utilisation of wastes and pollutants for H₂ production [169,194,210], cultured in advanced photobioreactors [66], and cultured continuously [43].

Several factors affect H₂ production. Under photoheterotrophic conditions (anaerobiosis, light, absence of fixed or molecular nitrogen) nitrogenase consumes ATP and reoxidises electron carriers in the production of H₂ [86]. *R. sphaeroides* carries out anoxygenic photosynthesis to generate ATP, a requirement for nitrogenase activity and H₂ production. Nitrogenase activity is also dependent upon an excess of reduced electron carriers, generated by the assimilation of reduced carbon sources such as organic acids. H₂ production competes with other reductive processes for reducing power (and for ATP), such as the formation of storage materials, particularly poly-β-hydroxybutyrate (PHB) [70]. The nitrogenase of APB is a complex tetramer, containing Mo-Fe centres. Due to its complexity, high ATP requirement and low specific turnover rate, nitrogenase places an exceptional demand upon metabolism [61], but nitrogenase plays an essential role in normal growth by fixing N₂ (as NH₃), to allow growth in the absence of a fixed N-source. Normal nitrogenase activity produces NH₃ with H₂ formation as a wasteful side-reaction which disposes of excess reducing power, but in the absence of N₂ nitrogenase

continues to turn over, producing only H₂ [170]. The key factor is the nitrogenase, which is expressed and active only in the absence of O₂ and NH₄⁺; nitrogenase is not directly regulated in response to the availability of its substrate (N₂).

In order to maximise H₂ production by *R. sphaeroides*, the influences of environmental factors, particularly the concentrations of acetate and NH₄⁺, were investigated to determine the limits of operation. Based on this data, and information gathered from the literature, a continuous, H₂ producing *R. sphaeroides* culture was established, for use in further studies.

2.3.2 Materials and Methods

2.3.2a Microorganisms, media and culture conditions

The wild-type *Rhodobacter sphaeroides* strain O.U. 001 (DSM 5864), well-documented to produce H₂ [44,61,91,169,194,210], was studied in axenic culture. Cultures were grown using the SyA medium of Hoekema *et al.* (2002) [66], which contained 1 g/l yeast extract (Merck) as a source of N and Mo, and succinate as the primary carbon source (30 mM), which is standard for the growth of APB [15]. *R. sphaeroides* was cultured in full, sealed bottles, at 30 °C under 40 μE m²/s of photosynthetically active radiation (PAR) (wavelengths 400-700 nm; PAR light meter SKP200, *Skye Instruments*). Cells were harvested from late exponential phase (see Figure 4.1-d) by centrifugation (4435 × g; 4 °C; 10 min) and pellets were resuspended in HP (H₂ production) medium to the required volume. The HP medium was derived from the AA-b medium of Hoekema *et al.* (2002) [66] omitting sources of NH₄⁺ and using 50 mg/l MgSO₄•7H₂O and 25 mg/l CaCl₂•2H₂O (see appendix 4.1.2a). Aliquots of cell suspension (50 ml) were sealed in serum bottles using butyl rubber stoppers and aluminium tear-seals, and purged with argon for at least 20 min to displace air. H₂ production was monitored during incubation at 30 °C under 100 μE PAR/m²/s. Biomass concentration was estimated from measurements of optical density (1 OD₆₆₀ : 0.36 g dry weight/l).

2.3.2b Measurement of H₂ production

Two methods of H₂ measurement were employed in these experiments: composition analysis and fluid-displacement (see appendix 4.1.1).

For composition analysis 0.2 ml headspace samples were withdrawn from closed reactors using a gas-tight syringe (Hamilton) fitted with a 27-G needle. Samples were analysed immediately using a combustible gas meter (CGM, Gas surveyor 2, Gas Measurement Instruments, Ltd.). The CGM gave a numerical output related to the concentration of combustible gas in the injected sample. The data was normalised to show the estimated concentration of H₂ (% v/v) in the reactor headspace.

The fluid-displacement system provided volumetric measurements of gas *via* measuring the displacement of a scrubbing solution (1 M NaOH) from a graduated 5 ml pipette. The scrubbing solution absorbed CO₂ from the evolved gas, as confirmed by GC analysis (see appendix 4.1.1e).

2.3.2c The effects of acetate and NH₄⁺ concentrations

Composition analysis was used to examine the effects of acetate and NH₄⁺ concentrations on H₂ production. Acetate was selected as the substrate for H₂ production by *R. sphaeroides* in this study as previous work on *E. coli* fermentation suggested that acetate would be the primary organic acid produced by *E. coli* [32,146]. The effect of acetate concentration was examined in the absence of NH₄⁺ with acetate concentrations in the range 0-90 mM. Cells were resuspended in HP medium lacking acetate and dispensed into reactors in 50 ml aliquots, to which volumes of 1 M acetate were dispensed to give the required final concentrations.

The effect of NH₄⁺ was examined in a background of 40 mM acetate and ammonium concentrations in the range 0-10 mM. Duplicate 50 ml suspensions were supplemented with small volumes of sterile 1 M NH₄⁺ solution, to the required final concentrations. In accordance with Hoekema's AA-b medium the 1M NH₄⁺ solution was 93 % NH₄Cl and 3.5 % (NH₄)₂SO₄.

2.3.2d The effect of culture density

Fluid displacement was employed to measure the effect of culture density on H₂ production. Composition analysis was also employed as a qualitative test for H₂. Concentrated suspensions were prepared by harvesting late-exponential phase (see Figure 4.1-d) cultures (4435 x g; 4 °C;

10 min) and resuspending to the required OD₆₆₀ in HP medium, containing 100 mM acetate. A series of cultures (50 ml) was prepared by serial dilutions of the concentrate using HP medium.

2.3.2e Operation of a continuous photobioreactor (PBR)

Photofermentation was carried out in a cylindrical glass photobioreactor (internal diameter, 105 mm) (Figure 2.3-a). The illuminated surface area was 0.107 m² and the average intensity of photosynthetically active radiation (400-950 nm) at the culture surface was 334.3 μE/m²/s, provided by 3 tungsten filament bulbs arranged externally along the length of the cylinder, which was encased in a reflective tube (diameter, 35 cm). The culture (3.0±0.5 litre) was stirred using a magnetic stirrer and follower (1200 rpm) located at the base of the PBR. A temperature of 30.0±0.2 °C was maintained using a submerged cooling coil.

The vessel was autoclaved and filled with 3 l of a modified SyA medium [66] containing 16 mM acetate, 14 mM succinate, 8 mM lactate, 5 mM butyrate and 1 g/l yeast extract. The medium was inoculated with 30 ml late-exponential phase pre-culture and purged with argon for 30 min before H₂ production was measured by fluid-displacement. After growing for 72 h, the culture was diluted constantly (41.67 ml/h i.e. 1 l/day) and the photobioreactor (PBR) was constantly drained into an outflow vessel at the same rate, keeping the culture volume constant.

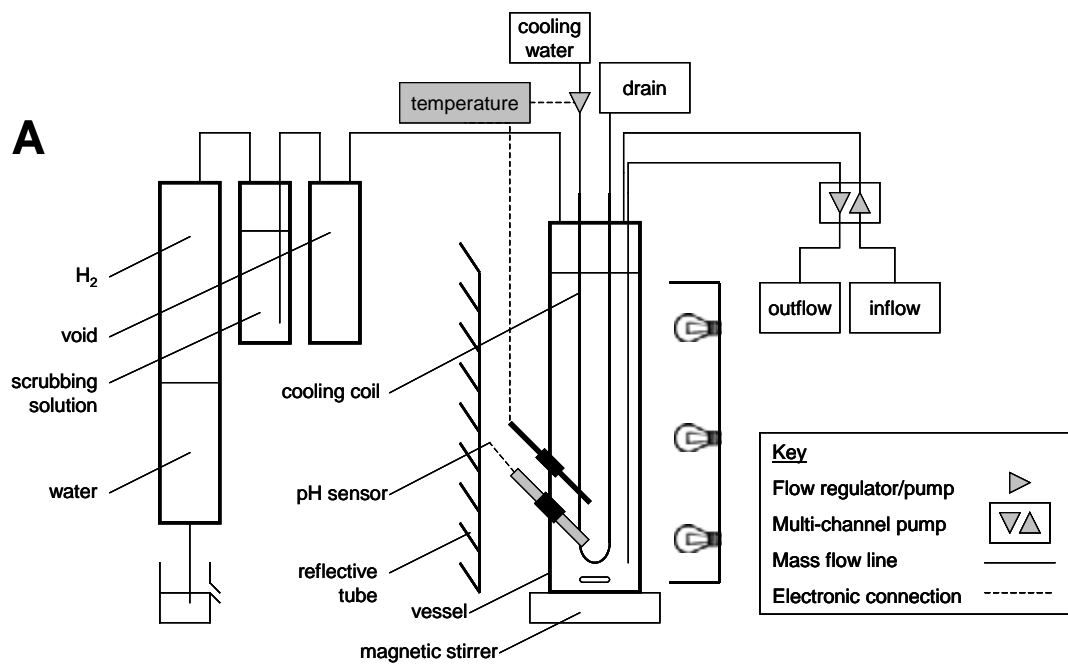


Figure 2.3-a A photobioreactor for the continuous culture of *Rhodobacter sphaeroides*. Schematic diagram (A) and operational system shown with the reflective tube unfurled (B).

The diluents consisted either of basal medium (0.366 g K_2HPO_4 , 0.433 g KH_2PO_4 , 0.05 g $MgSO_4 \cdot 7H_2O$, 0.025 g $CaCl_2 \cdot 2H_2O$, 1 g yeast extract per litre) or a mixed organic acid medium consisting of basal medium supplemented with simulated products of *E. coli* mixed acid fermentation; lactate (36.97 mM), acetate (31.42 mM), formate (3.56 mM) and succinate (20.18 mM). The simulated effluent was based on measurements of organic acid production in batch-mode ‘*phase 3*’ fermentations (see chapter 2.2). Culture purity was inspected regularly by serial dilution plating on nutrient agar (Oxoid, UK). Light conversion efficiency was calculated by dividing the combustion enthalpy of the produced H_2 by the supplied light energy (400-950 nm) [2] (appendix 4.1.4).

2.3.3 Results and Discussion

2.3.3a The effect of acetate concentration

In these experiments composition analysis (using a combustible gas meter) proved a simple and effective technique for the estimation of H_2 production, allowing factors affecting H_2 production to be compared within individual experiments (see appendix 4.1.1a). These results should be interpreted only in relative terms as the analysis could not be calibrated reproducibly.

The experiment aimed to determine the minimum concentration of acetate permissive to H_2 evolution by *R. sphaeroides*. H_2 was not detected using 0-5 mM acetate, traces of H_2 were detected using 10 mM, and prolific H_2 production was observed only at 20 mM and above (Figure 2.3-b, part A). Concentrations between 10 mM and 20 mM were not tested. The lower limit was, therefore, 10 mM, under these conditions. Higher concentrations (40-90 mM acetate) did not further promote H_2 production (Figure 2.3-b, part B) and no substrate inhibition was observed. 40 mM was selected as a standard acetate concentration for the investigation of the effect of NH_4^+ . Resting cultures such as these were not capable of long-term H_2 production and ceased H_2 production (after *ca.* 10 days) with a simultaneous change in appearance from yellow/brown to pink, indicative of the destruction of photopigments. Attempts to rescue exhausted cultures by the addition of further acetate were unsuccessful, suggesting the exhaustion of some other essential nutrient such as a N-source or vitamin.

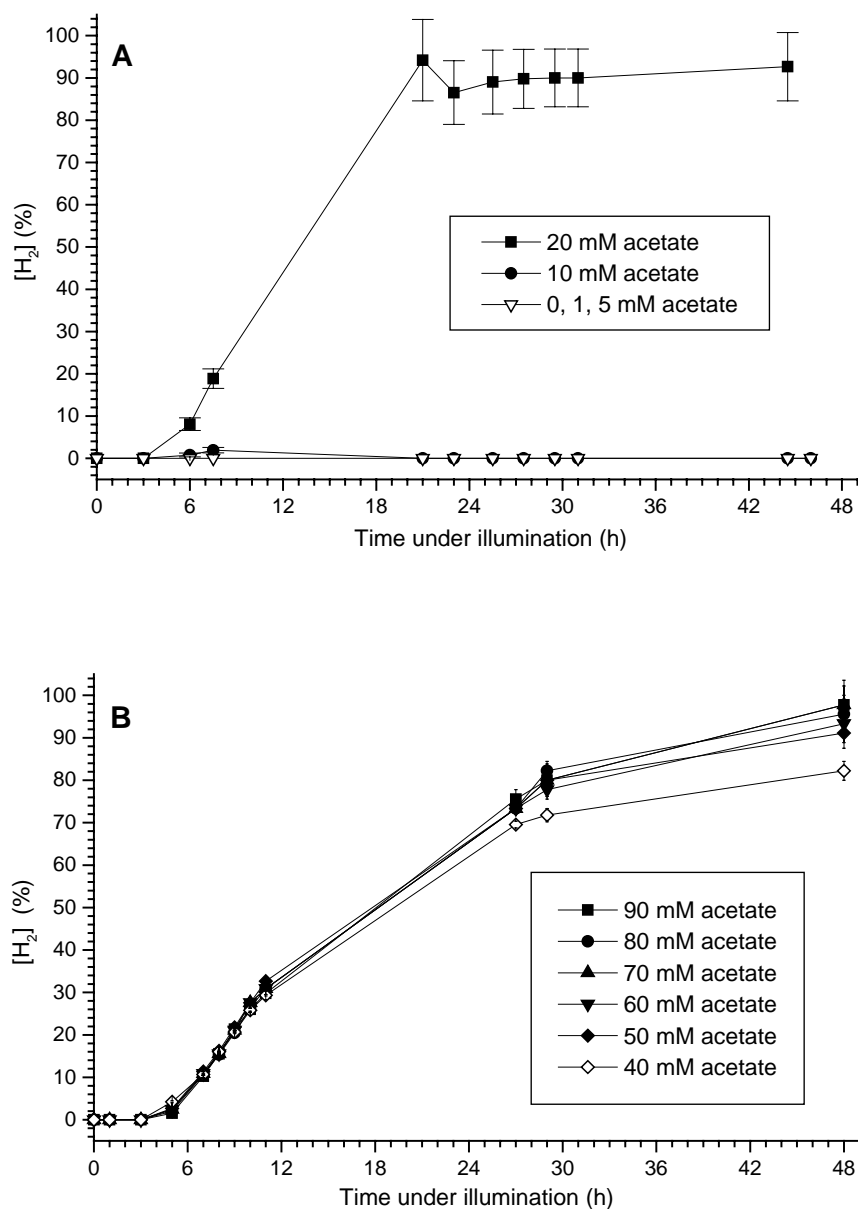


Figure 2.3-b The effect of initial acetate concentration on H₂ production by *Rhodobacter sphaeroides*.

H₂ was evolved using HP medium with acetate as the sole carbon source. H₂ production was monitored by headspace composition analysis. Concentrations of acetate below 10 mM were not permissive to H₂ production (A). No significant difference in H₂ production was observed in the range 40 mM to 90 mM acetate (B). A and B should not be compared directly due to limitations of gas composition analysis (see text).

2.3.3b The effect of NH_4^+

Experiments were conducted to determine the maximum NH_4^+ concentration permissive to H_2 production by *R. sphaeroides*, in the absence of any other added nitrogen source and with an excess of acetate (40 mM) as the sole carbon source. In the absence of NH_4^+ , H_2 was detected within 12 hours incubation, whereas at 2 mM and above no H_2 was detected over 11 days incubation. The maximum tolerable concentration of NH_4^+ was *ca.* 1 mM under these conditions, as traces of H_2 were detected. This result is in accordance with published reports documenting the repression of H_2 production by NH_4^+ concentrations as low as 20 μM [90]. These observations suggest that some nitrogen source is required for culture health, yet excess nitrogen is inhibitory to H_2 production. This paradox is addressed in chapter 2.5.

2.3.3c The effect of culture density

Although useful for the comparison of environmental conditions, composition analysis using the combustible gas meter was unsuitable for longer-term experiments and provided no absolute quantities for H_2 production. Therefore, a fluid displacement system was employed in the investigation of the effect of culture density on the rate of H_2 evolution, in which 100 mM acetate was the sole carbon source. Using this method, steady rates of gas evolution (up to 0.75 ml/h/50 ml culture) were maintained for 100 h (Figure 2.3-c, part A).

Cells were harvested rapidly (and not washed) to minimise the aerobic degradation of nitrogenase [110]. Therefore, the observed culture growth (Table 2.3-1) can be explained by the carry-over of residual and endogenous substrates from the growth medium, which supported less than one population doubling at the highest concentration. OD_{660} measurements recorded at the end of experiments were considered representative under the assumption that growth occurred principally during the initial part of the experiment. After an initial lag period, perhaps attributable to the consumption of residual or endogenous N-sources, H_2 evolution occurred at constant rates, which were proportional to culture density (Figure 2.3-b, part B). The maximum volumetric rate was 10 ml H_2 /l culture/h, which compares well with published rates in the range 7-18 ml H_2 /l culture/h production by cultures of *R. sphaeroides* O.U. 001 [91,169].

2.3 Results –*Rhodobacter sphaeroides* photofermentation

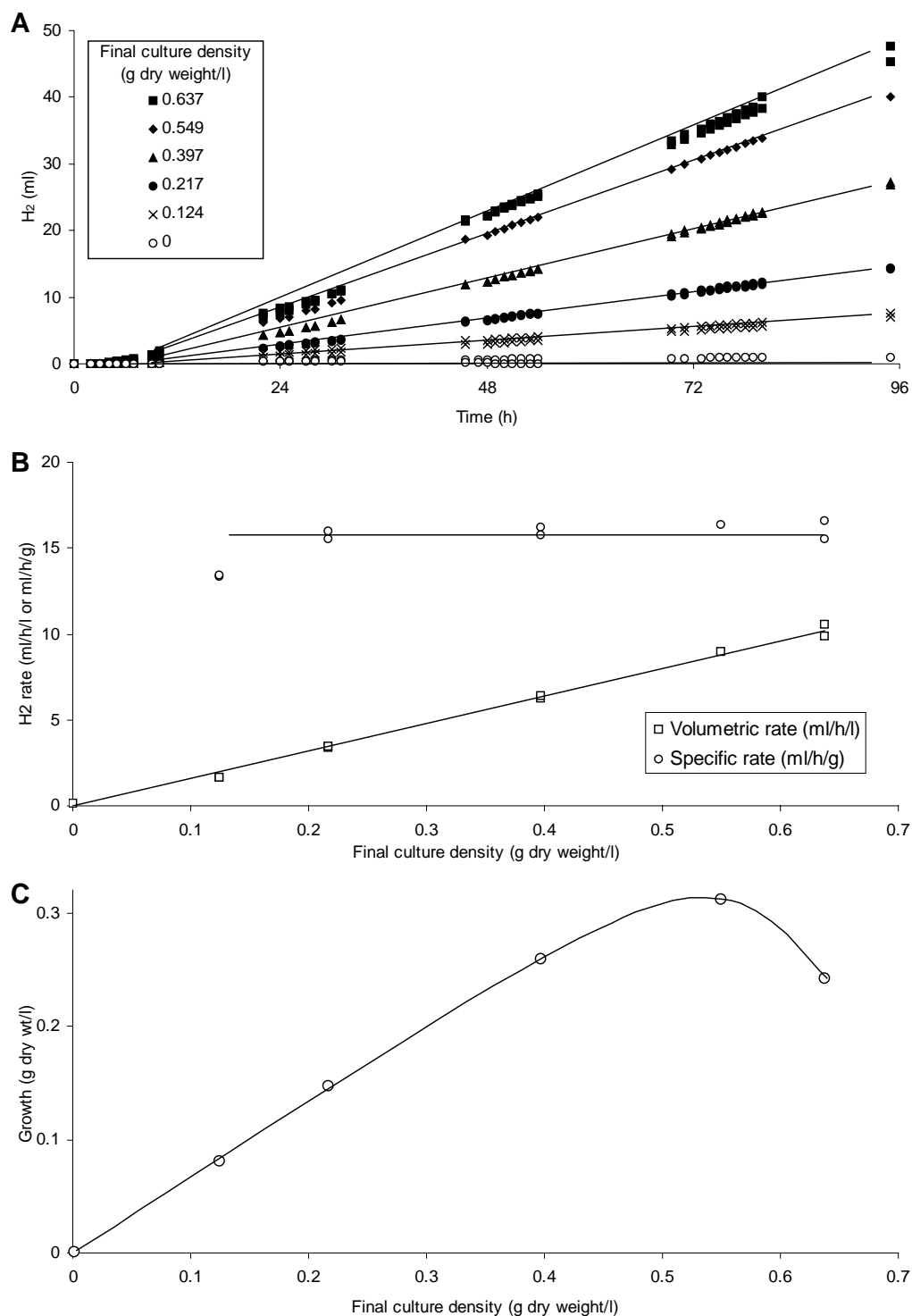


Figure 2.3-c The effect of culture density on H₂ production (A, B) and growth (C). The experiment was performed in duplicate under acetate excess (100 mM). H₂ production was measured by fluid displacement. Final culture densities are shown.

Table 2.3-1 Growth in ‘resting’ cultures of *Rhodobacter sphaeroides*

| Initial culture density (g dry weight/l) | Culture density after 95 h (g dry weight/l) | Residual population doublings |
|---|--|----------------------------------|
| 0.000 | 0.001 | - |
| 0.043 | 0.124 | 2.9 |
| 0.069 | 0.217 | 3.1 |
| 0.137 | 0.397 | 2.9 |
| 0.237 | 0.549 | 2.3 |
| 0.395 | 0.637 | 1.6 |

Data correspond to the investigation of culture density (Figure 2.3-c) and represent means of duplicate experiments. For interpretation see Figure 2.3-c, part C.

The volumetric rate of gas evolution (ml H₂/l culture/h) increased linearly with final culture density in the range 0–0.65 g dry weight/l and the specific rate of gas evolution was constant at *ca.* 35 ml H₂/h/mg dry weight (Figure 2.3-c, part B). Light is required for H₂ production, as the photosynthetic apparatus uses light energy to generate a proton motive force, which is used for ATP synthesis. In darkness the ATP flux is insufficient to meet the high demands of nitrogenase activity and H₂ production ceases. As culture density increases, the specific rate of H₂ production would be expected to decrease as the proportion of the culture receiving sufficient light decreases, but this relationship was not observed (Figure 2.3-c, part B), suggesting that light-limitation did not occur in these experiments.

As the HP medium contained no source of nitrogen, the extent of growth would be expected to relate directly to the size of the inoculum – the source of carried-over N-source. This relationship was observed for the lower culture densities, but growth was limited when the culture density exceeded *ca.* 0.5 g dry weight/l (Figure 2.3-c, part C), indicating a possible light limitation of growth in the absence of an effect on H₂ production. The expected effect on H₂ production was reported previously [140], and the penetration of light through photosynthetic bacterial cultures has been modelled [79,133]. Light intensity decreases logarithmically with respect to culture depth, and in dense cultures, the efficiency of H₂ production would be low as only cells located in a narrow region would receive a light intensity sufficient for H₂ evolution and below the saturation point. Light availability affects both the efficiency of light conversion and the efficiency of substrate conversion. At low light intensity, light conversion efficiency is high but

substrate conversion efficiency is low, and the inverse relationship occurs under high light intensity [133]. Therefore the optimum culture density for light conversion efficiency is higher than the optimum culture density for substrate conversion, requiring a compromise. As the objective of this project was to improve the efficiency of H₂ production from glucose, substrate conversion efficiency was prioritised over light conversion efficiency. Various approaches are available to increase the efficiency of light conversion to H₂, permitting denser cultures (see section 3.6.1).

In this experiment, culture densities were insufficient to reveal the previously described effects of light limitation. In larger continuous cultures, culture density may be controlled via the supply of nitrogen source. Therefore, the knowledge that light limitation did not occur using culture densities of up to 0.65 g dry weight/l was useful, although the extrapolation of these results to larger cultures with deeper light paths may be unreliable.

2.3.3d Validation of gas analysis.

The fluid displacement system operated on the basis of produced gas displacing a ‘scrubbing’ solution (1 M NaOH) from a cylinder. The evolved gas was a mixture of H₂ and CO₂, the latter dissolving in scrubbing solution (confirmed by GC, see section 4.1.1e). Concerns regarding the effect of scrubbing solution on *R. sphaeroides* were addressed.

R. sphaeroides cultures were in indirect contact (*via* the headspace) with a strongly basic solution, which could potentially strip dissolved CO₂ from the medium by disturbing the equilibrium between dissolved and gaseous CO₂. This phenomenon was observed by Hillmer and Gest (1977) [65] who observed the inhibition of H₂ production by *R. capsulatus* when alkali was present in the centre well of a Warburg flask. Furthermore, the removal of CO₂ by continuous argon purging was inhibitory to growth and H₂ production by a *Rhodospseudomonas* spp. [66]. Despite the net production of CO₂ during the photo-assimilation of acetate, there was a clear requirement for the *non-removal* of CO₂ in these species. It is emphasised that this is not equivalent to a requirement for CO₂ input.

In general, acetate assimilation occurs by the glyoxylate cycle [94] but the mechanism varies among anoxygenic photosynthetic bacteria [5]. Hoekema *et al.* [66] suggested that an alternative citramalate cycle [75] could explain the phenomenon. The citramalate cycle relies upon cycling of CO₂ and cannot operate in the absence of dissolved CO₂. The species in which a CO₂ requirement was detected (e.g. *Rhodospirillum rubrum*, *Phaespirillum fulvum*) lack isocitrate lyase (ICL) the key enzyme in the glyoxylate cycle, and hence the alternative citramalate cycle operates in these cases. *R. sphaeroides* also lacks ICL [3], therefore the question of exposure to scrubbing solution was addressed. A fluid break was added between the culture and the scrubbing solution, but this resulted in no significant increase in H₂ production. This was explained by recent work [48,49], which confirmed the operation of the citramalate cycle in *R. sphaeroides* and attributed the absence of a CO₂-dependence to an unusually high capacity for acetate assimilation (i.e. CO₂ production, 6-fold greater than that of *R. rubrum*) and to the presence of a mucous capsule, by which CO₂/HCO₃⁻ may be retained.

Therefore, the fluid displacement method, using strong alkaline solutions (NaOH), was effective in the measurement of H₂ production, without causing indirect adverse effects on H₂ production by *R. sphaeroides*.

2.3.3e Continuous H₂ production by *Rhodobacter sphaeroides*

A continuous culture (or chemostat) is typically operated by continuous dilution of the culture with fresh medium at a constant rate. Alternative approaches may be employed for photobioreactors such as dilution only during light periods or by using fill-and-draw (F/D), intermittently replacing a proportion of the culture with fresh medium. It was suggested that F/D operation is preferable due to the relatively low growth rate of PNS bacteria [25], however many reports are available describing chemostat cultures of PNS bacteria. To construct a manageable dual-bioreactor experiment, it was preferable to operate the photobioreactor as a continuously illuminated chemostat, although industrial application would entail the adaptation of the method to diurnal solar illumination.

A survey of literature revealed extensive variation in the conditions of continuous H₂-producing cultures of APB (Table 2.3-2).

A high relative supply of carbon over nitrogen (C/N) is required for nitrogenase-mediated H₂ production. The literature survey showed that C/N <10 only where hydraulic retention time (HRT) was very long, allowing N-sources to be consumed before H₂ production commenced. This study found that the minimum C/N permissive to H₂ production by resting cells, was *ca.* 80 (1 mM NH₄⁺; 40 mM acetate), which is significantly higher than most reported values (Table 2.3-2). However, NH₄⁺ is a more potent inhibitor of nitrogenase activity than complex N-sources such as glutamate and yeast extract, whose presence results in the formation of NH₄⁺ only after the C-source is exhausted [90]. Yeast extract was found to be an effective source of N and vitamins in the continuous culture of *R. sphaeroides* O.U. 001 [91] and was selected for use in this study. Yeast extract has a N-content of 8.85 % w/w [91] and PNS bacteria are composed of *ca.* 8.7 % N w/w [66], hence a medium designed to support a culture density of 1 g dry cell weight/l contained 1 g/l yeast extract, which when supplemented with mixed organic acids (see 2.3.3e) resulted in a C/N of 41.6 in this study. HRTs as short as 10 hours were reported previously (Table 2.3-2) but to increase the potential substrate loading a HRT of 3 days was selected.

Table 2.3-2 Conditions for H₂-production by chemostat cultures of purple non-sulphur bacteria

| Organism | C-source (mM) | N-source (mM) | C/N | Operation | HRT | Subs. con. eff. (%) | Source |
|---|---|--|----------|-----------|--------------------------------------|----------------------|---|
| <i>Rhodobacter sphaeroides</i> O.U. 001 | malate, 7.5 | glutamate, 10 yeast extract, 0.2 g/l | 7.1 | batch | - | 36 | [91] |
| <i>R. capsulatus</i> | lactate, 30 butyrate, 30 | glutamate, 7 | 18 22 | F/D | 3 days | 14-43 | [103] |
| <i>R. sphaeroides</i> O.U. 001 | malate, 7.5 | glutamate, 2 | 40 | F/D | 17 days (400 h) | NA | [43] |
| <i>Rhodopseudomonas palustris</i> WP3-5 | acetate, 32.5 | glutamate, 2.72 | 12 | F/D | 2 days | 72.5 | [25] |
| <i>R. sphaeroides</i> RV | lactate, 56 | NH ₄ Cl, 4.75 yeast extract, 0.25 g/l | 31 | chemostat | 1.25 days (30 h) | 31-36 | [52] |
| <i>R. capsulatus</i> B10 | lactate, 42 | (NH ₄) ₂ SO ₄ , 4 | 16 | chemostat | 1.39 days (33 h) | 43 | [191] |
| <i>Rhodopseudomonas capsulata</i> | acetate, 9.14 propionate, 1.67 butyrate, 13.6 | glutamate, 2.94 NH ₄ ⁺ , 9.14 | 7.6 | chemostat | 2 days 3 days 4 days 5 days | 34 39 36 32 | [175] |
| <i>R. sphaeroides</i> RV | lactate, 100 mM | NH ₄ ⁺ , 4.7 Yeast extract, 0.5 g/l | 38 | chemostat | 0.42 days (10 h) | 50-70 | [45] |
| <i>R. sphaeroides</i> O.U. 001 | lactate, 36.97 acetate, 31.42 formate, 3.56 succinate, 20.18 | yeast extract, 1 g/l | 41.6 | chemostat | 3 days | 32 38 | <u>This study</u> chapter 2.3 chapter 2.6 |

C/N: molar ratio of total carbon over total nitrogen; F/D: fill-and-draw; HRT: hydraulic retention time; NA: data not available.

The culture was maintained in batch-mode for the initial 3 days to allow growth. H₂ production commenced after 1 day, reaching a maximum substrate conversion efficiency of 60 % (Figure 2.3-d, part B). Subsequently, dilution with basal medium displaced residual substrate resulting in the cessation of H₂ production. Conversely, when organic acids were supplied in the diluent, H₂ production became stable and continuous after day-4 with a rate of 18 ml H₂/h/l culture, a light conversion efficiency of 3 % and substrate conversion efficiency of 14 % based on supplied substrates, or 32 % based on consumed substrates. Substrate conversion efficiency was low due to overloading of the culture; i.e. substrate was supplied at a rate higher than it was consumed. As a result 64.2 % of supplied organic acid carbon was accounted for in the outflow (i.e. not consumed), representing 75.4 % of the supplied potential for H₂ production (Figure 2.3-d, part C). Optimisation would be required to balance the supply of substrate with the capacity for consumption and in an industrial system the residual substrate could be recycled to the inlet after cell separation (Figure 2.6-e).

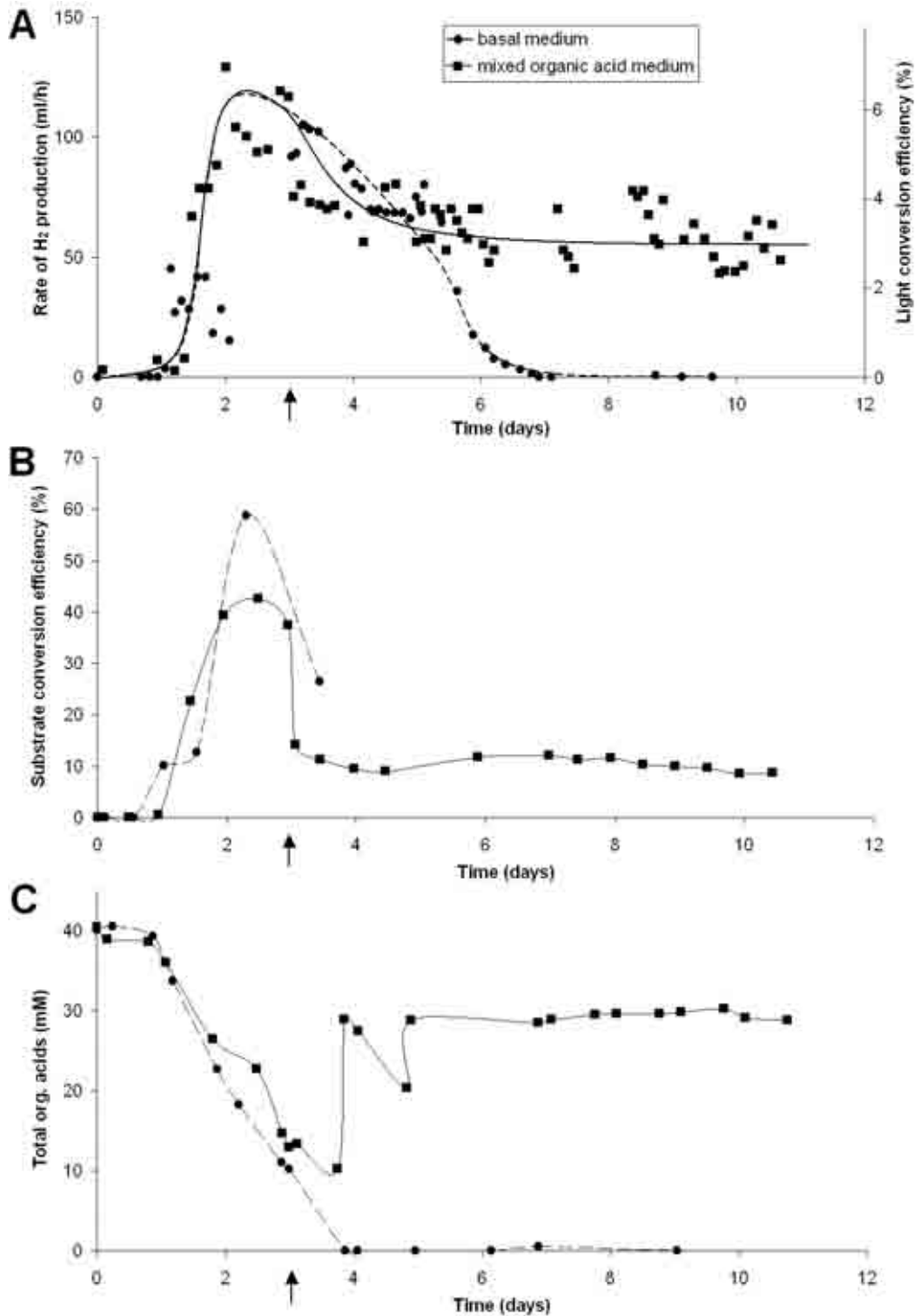
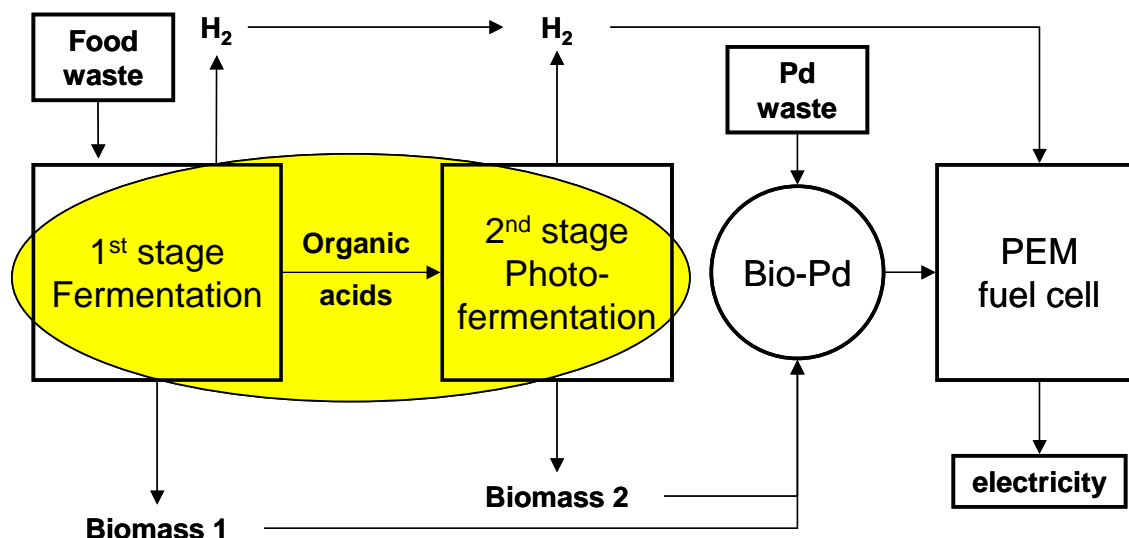


Figure 2.3-d H₂ production (A), substrate conversion efficiency (B) and residual substrate in continuous cultures of *Rhodobacter sphaeroides*, diluted with synthetic organic acid medium.

The H₂ production rate of 150 ml/h (A) corresponded to a light conversion efficiency of 7.84 % (appendix 4.1.4). Substrate conversion efficiency (B) was calculated using the theoretical maxima of 4 mol H₂/mol acetate, 6 mol H₂/mol lactate, 7 mol H₂/mol succinate and 10 mol H₂/mol butyrate [170], and calculation was based on total substrate supplied rather than the proportion consumed. Arrows indicate the onset of dilution after 3 days growth. Data from single experiments are shown.

2.4 A two-stage, two-organism process for biohydrogen from glucose

2.4.0 Summary



The content of this chapter was originally presented at the International Hydrogen Energy Congress (IHEC-2005), Istanbul. The paper has been published in a special issue of the International Journal of Hydrogen Energy and is reproduced in full.

This article describes the initial investigations into the photoproduction of H_2 using effluent from *E. coli* fermentations (sequential batch mode). While *Rhodobacter sphaeroides* grew well, consuming fermentation products (acetate, lactate, ethanol and residual glucose), the quantity of ammonium ion in the *E. coli* effluent was inhibitory to nitrogenase-mediated photoproduction of H_2 by *R. sphaeroides*. This result illustrated that the sensitivity to nitrogen sources is a major obstacle to overcome in the photoproduction of H_2 when feeds such as wastewaters of fermentation broths are to be used. It also showed that effluent from an *E. coli* glucose fermentation could at least be remediated *via* the cultivation of *R. sphaeroides*, which is itself a potentially useful product used for the production of biodegradable plastic from accumulated poly- β -hydroxybutyrate. These results also confirm that ethanol and glucose can be consumed by *R. sphaeroides* O.U. 001.

Hence, the principle of cross-feeding *E. coli* products to *R. sphaeroides* was demonstrated and the need to prevent the transfer of NH_4^+ was identified, prompting the investigation of

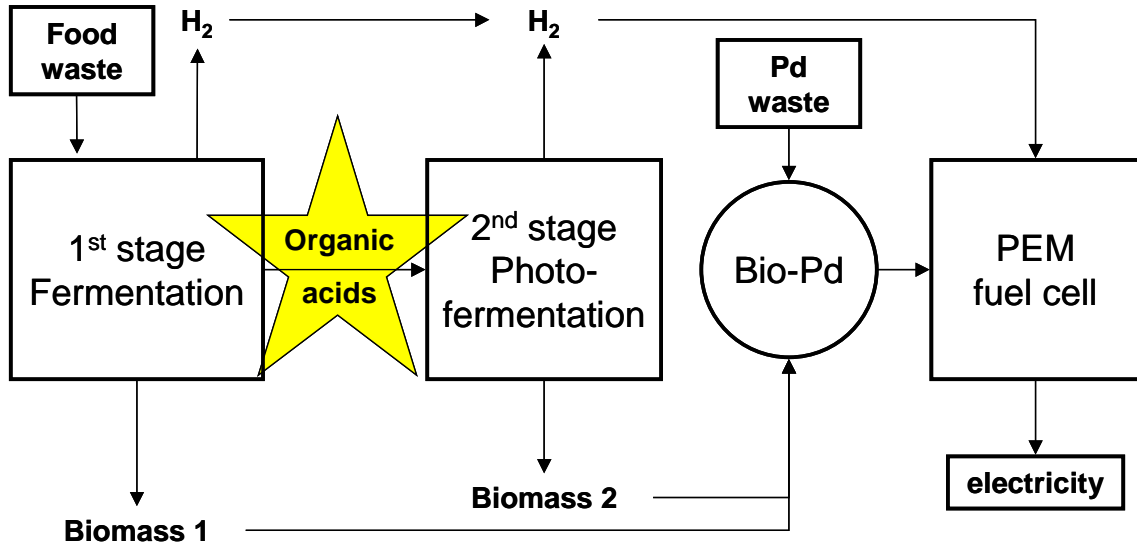
electrodialysis (chapter 2.5) and justifying its subsequent incorporation into the dual system (chapter 2.6).

The fermentation effluent (used as the feed in these experiments) was provided by DW Penfold, while analysis of the effluent and all other work, including authorship of the paper, were performed by the author.

2.4.1 Article published in the International Journal of Hydrogen Energy

2.5 Development of the electrodialysis technique for use in a dual system

2.5.0 Summary



Having identified the unwanted co-transfer of N-sources as a primary bottleneck to the successful operation of a dual system (chapter 2.4), the selective transfer of organic acids was investigated.

This chapter describes the development of an electrodialysis technique as a potential means to enable a dual system combining fermentation by *E. coli* and photofermentation by *R. sphaeroides*. This novel application is the subject of a patent application [159] (reproduced in appendix 4.2.1). Preliminary studies on the electrodialysis technique are described, which provided a basis for the introduction of electrodialysis into *E. coli* fermentation and a complete dual system (chapter 2.6).

To avoid repetition, a methods section is omitted from this chapter. Relevant details are given in figure legends and references are made to full details found in adjacent chapters and appendices.

2.5.1 Electrodialysis in extractive fermentations

Electrodialysis (ED) was identified as a promising technique for coupling the *E. coli* and *R. sphaeroides* reactors, for which the key function is the selective transport of *E. coli* fermentation products such as organic acids. Fermentation products including benzoic acid, lactic acid, acetic acid, propionic acid and pyruvic acid have been actively extracted from fermentations [30,53,76,102,131,132,137,203,220,221] but no previous studies address the novel application of electro-separation to the production of H₂.

ED techniques employ cation-selective (CSM), anion-selective (ASM) and bi-polar (BP) membranes, to achieve the charge-selective separation of valuable products or unwanted contaminants and the generation of acid and alkali, applicable in processes such as seawater desalination [156], and organic acid production [69]. Both ASM and CSM consist of a co-polymer matrix (various formulations, e.g. vinyl compounds), which provides physical support for charged functional groups conferring selectivity. These may be positive in the case of CSM (e.g. $-\text{SO}_3^-$, $-\text{COO}^-$, $-\text{PO}_3^{2-}$, $-\text{PO}_3\text{H}^-$, $-\text{C}_6\text{H}_4\text{O}^-$), or negative in the case of ASM (e.g. $-\text{NH}_3^+$, $-\text{NRH}_2^+$, $-\text{NR}_2\text{H}^+$, $-\text{NR}_3^+$, $-\text{PR}_3^+$) [208]. The industrial usefulness of ion-selective membranes expanded in 1973, with the advent of Nafion® by DuPont, having improved chemical and thermal stability due to its perfluorinated ionomer composition [57]. Further desirable qualities of ion-selective membranes include high electrical conductivity, low water content (swelling), high anion selectivity under applied current and low diffusivity without current. A second significant development was the BP membrane, consisting of a CSM-ASM bi-layer [29]. An ASM composed of Neosepta AHA was selected for use in this study. Neosepta AHA is characterised by its high mechanical strength and alkali resistance, and tolerates higher concentrations of solvents than earlier formulations (e.g. 7 % phenol, 30 % acetone, 30 % dioxane and 50 % ethanol), but remains sensitive to strong oxidising agents (www.astom-corp.jp). Little information is available on the function of Neosepta membranes and formulations are proprietary (Tokuyama Co., Japan). Monoselective ASM and CSM (e.g. Neosepta ACS or CMS) are also available, having specificity to monovalent ions [129,208], whereas Neosepta AHA transports anions of various valences, which is advantageous as the products of dark fermentation include monovalent and divalent organic acids.

The application of ED in the dual system involves separating the two cultures with an anion selective membrane (ASM), which permits the passage of anions (such as organic acids) by diffusion in either direction. Under a direct current (DC) the migration of anions is unidirectional and rapid. The previous chapter (2.4) demonstrated a limitation to the applicability of dual systems utilising PNS bacteria; the initial feed must be low in N-sources in order to permit nitrogenase activity, and hence H₂ production by PNS bacteria. As the ASM is relatively impermeable to cations including NH₄⁺, the application of ED results in a versatile system, able to utilise feeds with high N-content since NH₄⁺ and other cations are retained on the dark side of the ASM. The electrodialysis technique is, therefore, bifunctional in that it feeds organic acids to *R. sphaeroides* while at the same time excluding inhibitory NH₄⁺.

The ED cell was composed of four chambers (C, M, MA and A, from cathode to anode) (Figure 2.5-a). The two outermost compartments were named C and A, being in contact with the cathode and anode, respectively. The two innermost compartments were named M and MA, M representing the ‘main’ compartment (source of anions for recovery), and MA representing the space separating compartments M and A into which anions were recovered. These four compartments were divided by three membranes (BP, ASM and CSM). In the ED cell, CSM and BP membranes prevent direct contact between bacterial cells and the electrodes, as the extremes of pH at the electrode surfaces would result in unwanted reactions [102,131,132]. The BP membrane also lyses water, generating H⁺ on the cathode side and OH⁻ on the anode side. This function has been exploited to provide pH control simultaneously during extractive fermentations [102,137]. The CSM also functions to transport Na⁺ from the C chamber, resulting in the formation of sodium salts in the MA chamber.

2.5.2 Studies on the application of electrodialysis

Preliminary work was carried out to evaluate the application of ED to the integration of *E. coli* and *R. sphaeroides* cultures. The operating conditions were established by examining the transfer of organic acids, the retention of ammonium ion and the long-term stability of the system.

2.5.2a Operating modes: the hare or the tortoise?

ED could operate either to transport organic acids slowly and steadily (low-constant mode) or rapidly for short periods (high-intermittent mode). The latter strategy was examined initially as it would facilitate regular cleaning of the cell and would not require unattended operation. Initially, short periods of high current (10 A, 5-15 V) were studied. With this approach, organic acids were successfully transported from *E. coli* fermentation cultures (Figure 2.5-b).

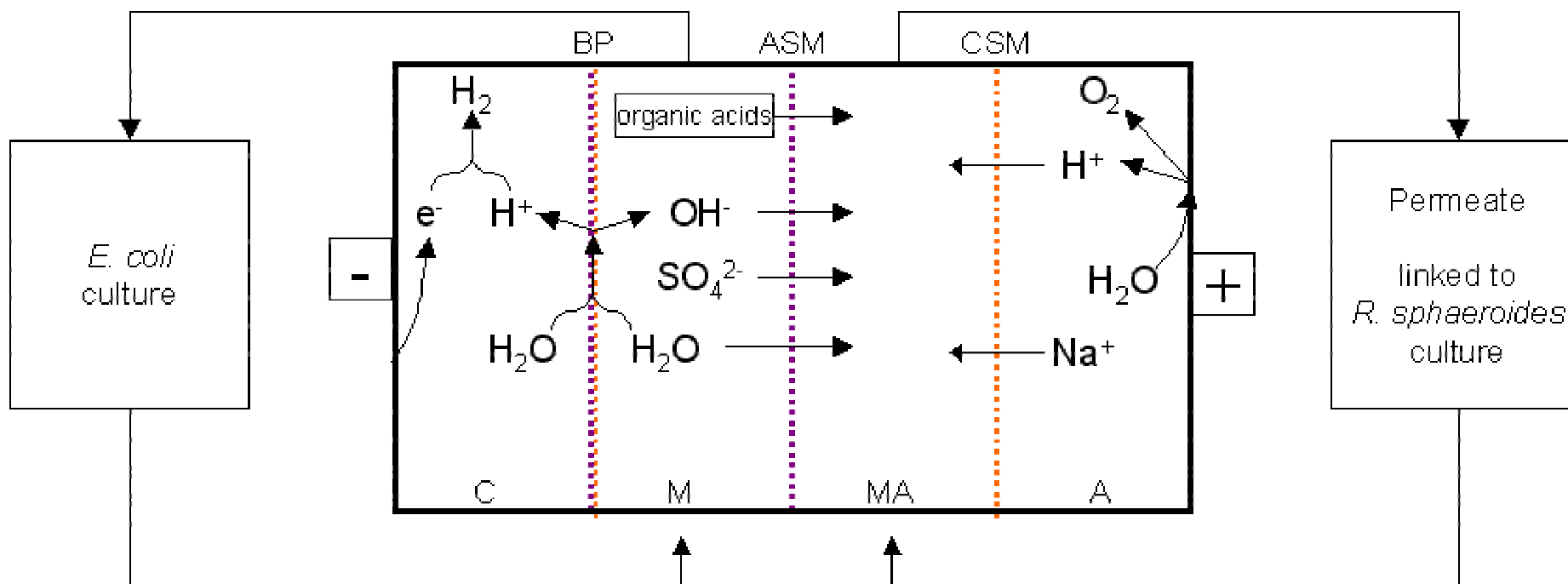


Figure 2.5-a An electro dialysis (ED) cell using a ‘BAC’ membrane configuration.

BP, bi-polar membrane; ASM, anion-selective membrane; CSM, cation-selective membrane; C, cathode chamber; M, main chamber; MA, permeate chamber; A, anode chamber; -, cathode; +, anode. In use, an organic acid-producing *E. coli* culture was circulated through the M chamber and the permeate was harvested for use by *R. sphaeroides* (see Figure 2.6-a). As described in sections 2.5.2f and chapter 2.6, additional features of the ED cell include electrolysis and water-transport; O_2 is evolved at the anode and H_2 at the cathode to be used as a tertiary H_2 stream, while water is transferred with organic acids from the main chamber to the permeate chamber, balancing the fluid volume input into the *E. coli* vessel.

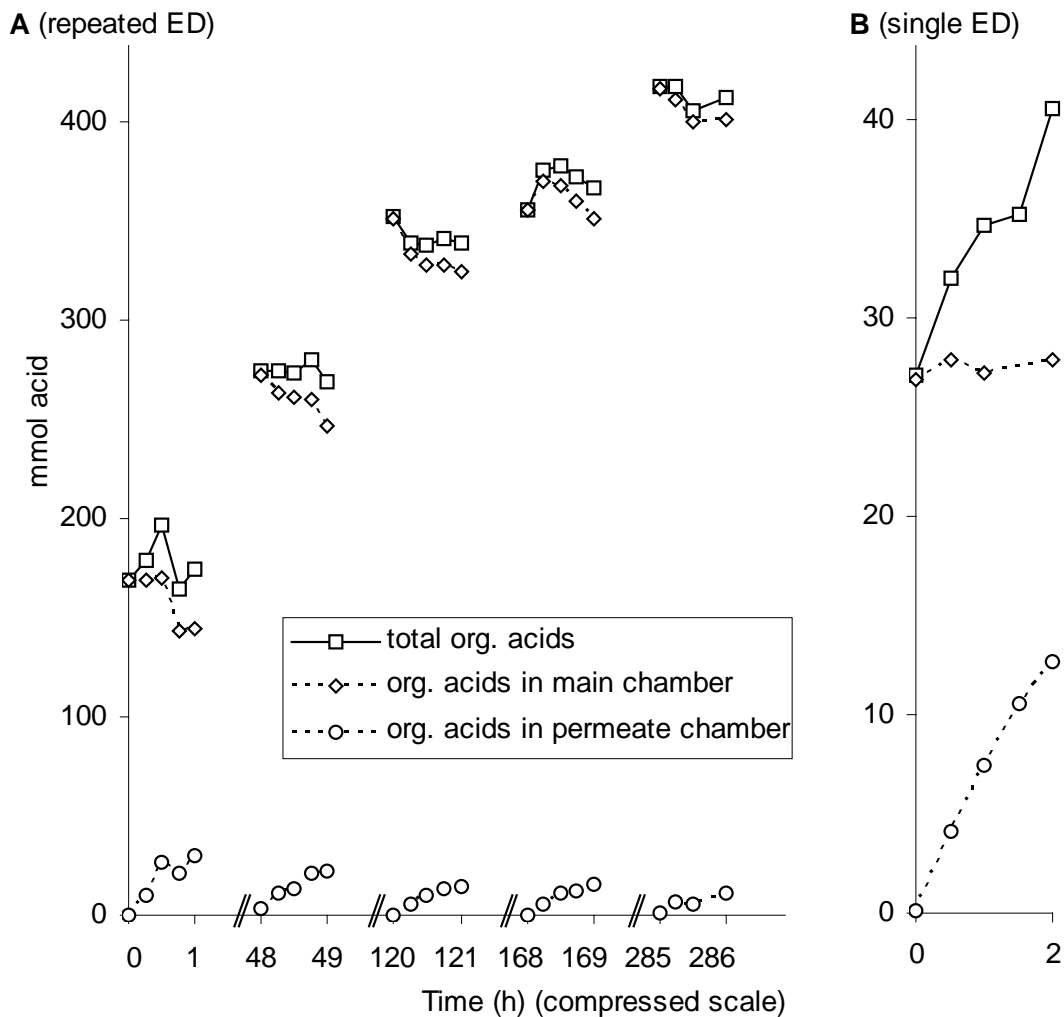


Figure 2.5-b Mass balances for organic acid transport from fermenting *Escherichia coli* cultures using the ‘high-intermittent’ approach.

A current of 10 A was applied over a membrane area of 200 cm² (50 mA/cm²) for 1 h periods separated by intervals of *ca.* 48 h. The M chamber contained a long-term glucose-fed *E. coli* HD701 culture (A) or the effluent from a batch fermentation fed with simulated fruit waste, as described in [149] (B), and was maintained constantly at 30 °C and pH 5.50 by the automatic addition of 2M H₂SO₄. The MA chamber contained initially 1L of basal salts (0.366 g K₂HPO₄, 0.433 g KH₂PO₄, 0.05 g MgSO₄·7H₂O, 0.025 h CaCl₂·2H₂O per litre) and the pH was not controlled. The apparently positive mass balance is due to the presence of cells as described in section 2.5.2e.

However several limitations of the rapid-intermittent mode were identified. Firstly, Figure 2.5-b (part A) shows a progressive decrease in the rate of organic acid transport (flux), which cannot be attributed to the exhaustion of organic acids from the fermentation culture (M), which increased over the course of the experiment. The decline in activity may be attributed to the negative effects of excessive current density on the activity of the ASM (section 2.5.2b). Secondly, H₂ production (by *E. coli*) ceased when the current was applied and resumed *ca.* 2 h after it was removed (Figure 2.5-c).

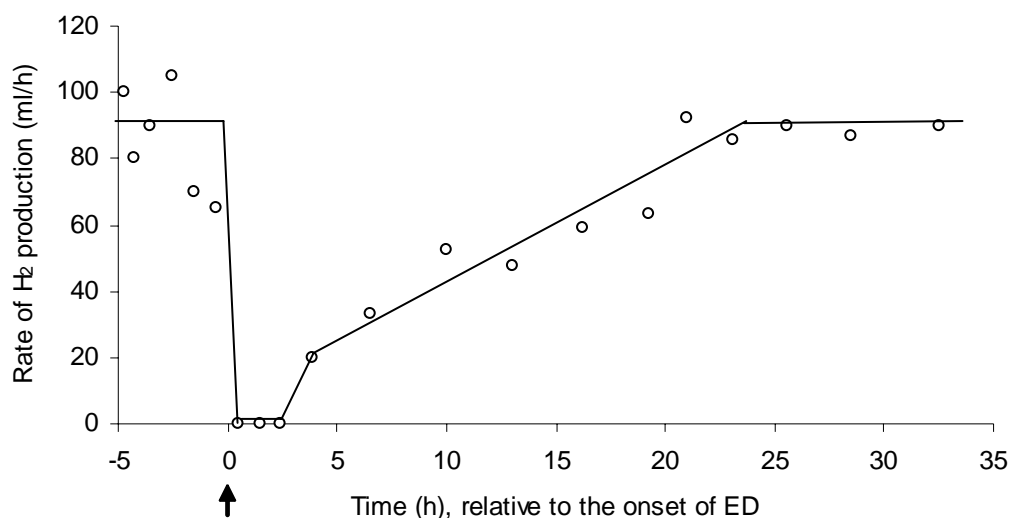


Figure 2.5-c Inhibition of fermentative H₂ production by electrodesialysis.

A high current (10 A) was applied for 1 hour from T=0. The *E. coli* fermenter was assembled as described in chapter 2.2 (*phase 4*).

H₂ production recovered to initial rates after *ca.* 24 h, suggesting that the use of intermittent periods of high-current electrodesialysis would be restrictive. During ED OH⁻ was generated rapidly by the BP membrane (see Figure 2.5-a), resulting in the consumption of large quantities of acid titrant and the creation of local extremes of pH, to which the cessation of H₂ production may be attributed. The effect on cell viability was not tested, however, the loss of viability of acidophilic bacteria subjected to direct current was reported previously [76]. Thirdly, heat was generated while current was applied and cooling was required to maintain cultures at 30 °C and to prevent heating beyond 50 °C, which would be damaging to the membranes (D. Stratton-Campbell, C-Tech Innovation Ltd, pers. comm.).

These limitations were overcome by operating continuous electrodesialysis with low current. An operating current density of 2 mA/cm² was selected based on the limiting current density

(LCD) (see 2.5.2.1b), the effectiveness of NH_4^+ retention (see 2.5.2.1c) and the capacity for organic acid extraction (see 2.5.2.5).

2.5.2b Operating modes: limiting current density (LCD)

Limiting current density (LCD) is defined as the maximum current density that can be applied without causing negative effects [129]. Exceeding LCD can cause decreased current efficiency, increased rates of side-reactions (e.g. water dissociation), membrane fouling and damage. LCD was determined by the method shown in Figure 2.5-d.

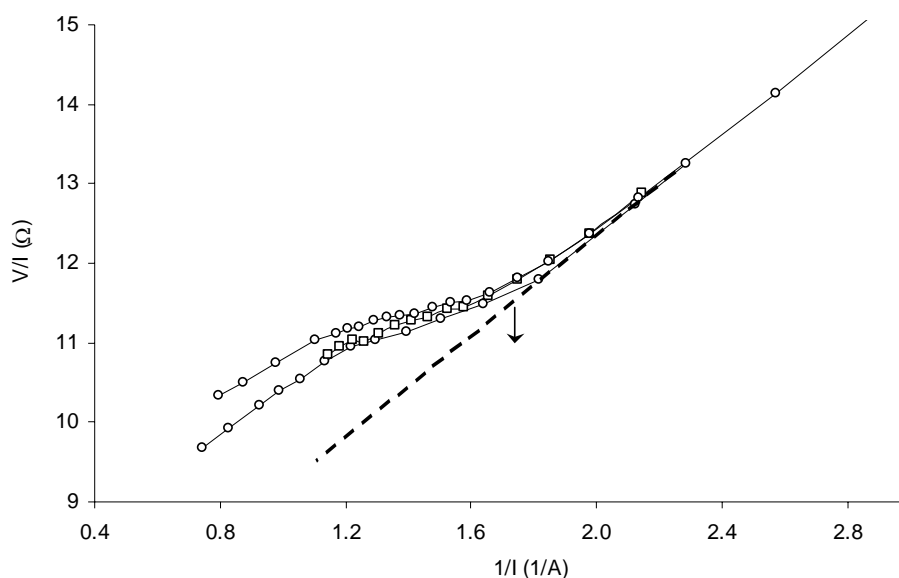


Figure 2.5-d The determination of limiting current density (LCD).

Power was supplied and measured using a power supply (Thurlby Thandar Instruments, 32V-2A). As described previously [47] current was increased gradually and voltage was measured. Resistance (V/I) was plotted over the reciprocal current ($1/I$) to highlight the point of departure from a linear (Ohmic) relationship (arrow). In this example, three repeats are shown and the point of divergence from a linear relationship corresponds to $1/I=1.67$; $I=0.6$ A for a membrane area of 200 cm^2 . Hence the LCD was 3 mA/cm^2 .

In a sustained *E. coli* fermentation ('phase 4' see chapter 2.2) the LCD was measured repeatedly over a period of 10 days, revealing a decreasing trend in LCD (Figure 2.5-e).

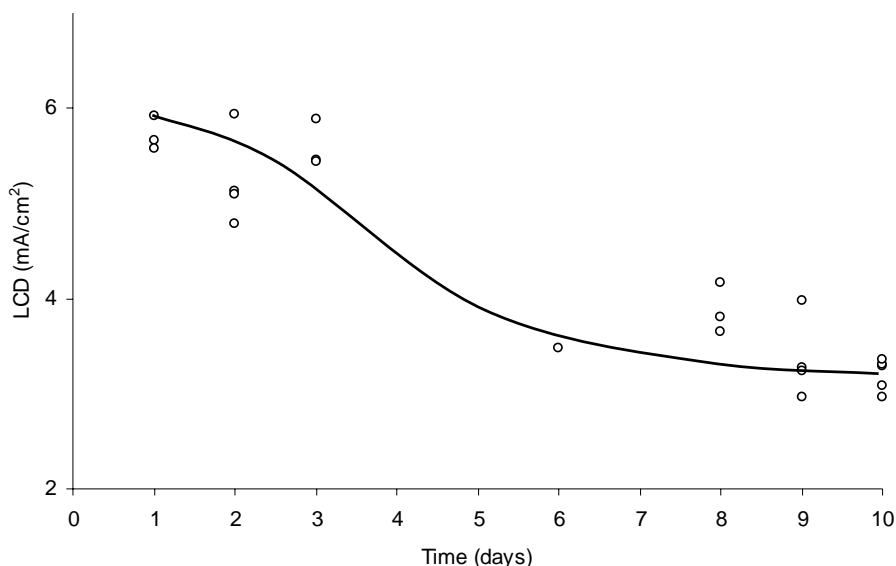


Figure 2.5-e Variation in limiting current density in a sustained *Escherichia coli* fermentation.

The fermentation was assembled as described in chapter 2.2 (*phase 4*). The current density was 2 mA/cm² except during measurements of LCD.

The LCD decreased initially and, after 6 days, stabilised at *ca.* 3.5 mA/cm². Operating close to LCD or higher would reduce the longevity of the membrane, therefore a maximum current density of 2.8 mA/cm² (80 % of LCD) was employed in subsequent work. The initial decrease in LCD equates to a decreasing capacity of the ED cell for efficient activity, which may be attributed to progressive fouling of the cell or membranes. The development of de-fouling techniques or anti-fouling methods was beyond the remit of this work, and all de-fouling was performed off-line by dismantling the ED cell. On-line de-fouling could be performed intermittently by flushing the ED cell at a high fluid flow rate, which could be coordinated with an interruption to the applied voltage, which drives electronegative cells towards the anode. In the absence of bi-polar membranes (which would be destroyed) the electric polarity could be reversed to remove cells actively from fouled membranes. Alternatively, anti-fouling methodology could be adopted such as the modification of culture medium to render cells electroneutral (e.g. by the addition of metal cations) or by the addition of surfactants to the bacterial culture to inhibit biofilm formation.

2.5.2c Retention of ammonium ion

Anion selective membranes (ASM) are not usually 100 % selective for anions and some cation leakage can occur (W. Skibar, C-Tech Innovation, pers. comm.). The NH_4^+ -permeability of the ASM used in this study (Neosepta AHA, described in section 2.5.1) was tested by placing varying concentrations of NH_4^+ in chamber M and measuring the transfer into chamber MA after 15 min. A linear relationship was found between the concentration of NH_4^+ in the M chamber and the rate of transfer into the MA chamber under a current density of 2 mA/cm^2 (Figure 2.5-f).

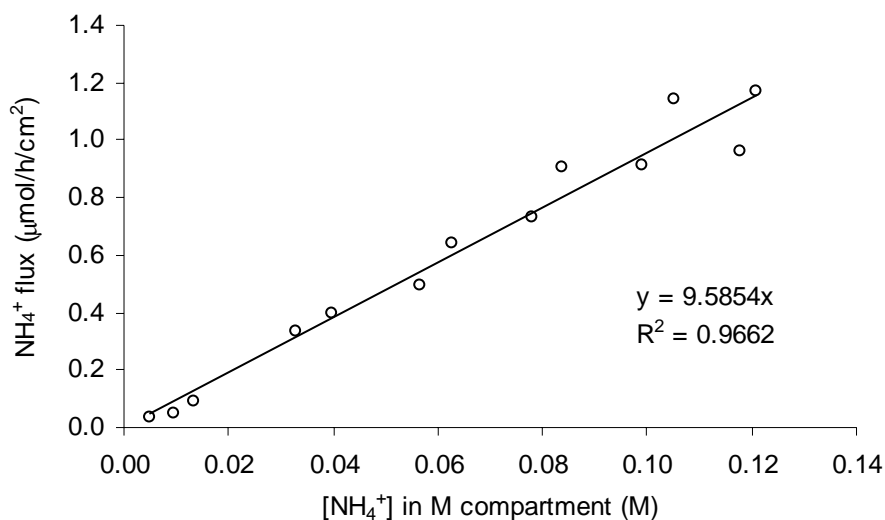


Figure 2.5-f The effect of NH_4^+ concentration in the M chamber on the transfer of NH_4^+ . A current density of 2 mA/cm^2 was applied constantly across a membrane area of 200 cm^2 . M and MA solutions contained (per l) $0.366 \text{ g K}_2\text{HPO}_4$, $0.433 \text{ g KH}_2\text{PO}_4$, $0.05 \text{ g MgSO}_4 \cdot 7\text{H}_2\text{O}$, $0.025 \text{ g CaCl}_2 \cdot 2\text{H}_2\text{O}$ supplemented with $(\text{NH}_4)_2\text{SO}_4$ in the M chamber to the concentrations stated.

The observed relationship suggests that the NH_4^+ concentration of 1.5 mM used in dual system experiments (chapter 2.6) resulted in a flux of *ca.* $2.87 \text{ µmol NH}_4^+/\text{h}$ ($0.014 \text{ µmol/h/cm}^2$; 200 cm^2). The MA compartment was diluted with NH_4^+ -free medium at a rate of 1 L/day , hence the concentration of NH_4^+ in the feed to *R. sphaeroides* would be estimated at 68.9 µM , which would be permissive to H_2 production by *R. sphaeroides* in a background of 40 mM acetate, as shown in chapter 2.1.

Figure 2.5-g shows a reproducible relationship between the applied current density and the transfer of NH_4^+ . The transfer of NH_4^+ would decrease by half, relative to no current, at a current density of 1.205 mA/cm^2 . The observation of a dependence of NH_4^+ transport on applied current suggests the possibility to control NH_4^+ transport, providing a metered N-supply to *R. sphaeroides*. This could replace the need for additional N-source, required in chemostat culture to support *de novo* biomass synthesis and prevent washout, as the careful supply of ammonium was shown previously to promote H_2 production [125]. In current work nitrogen (0.0885 g/l) was supplied by yeast extract (1 g/l) in ‘basal medium’ (appendix 4.1.2a). The replacement of yeast extract by the ED-controlled supply of NH_4^+ is a matter for future investigation.

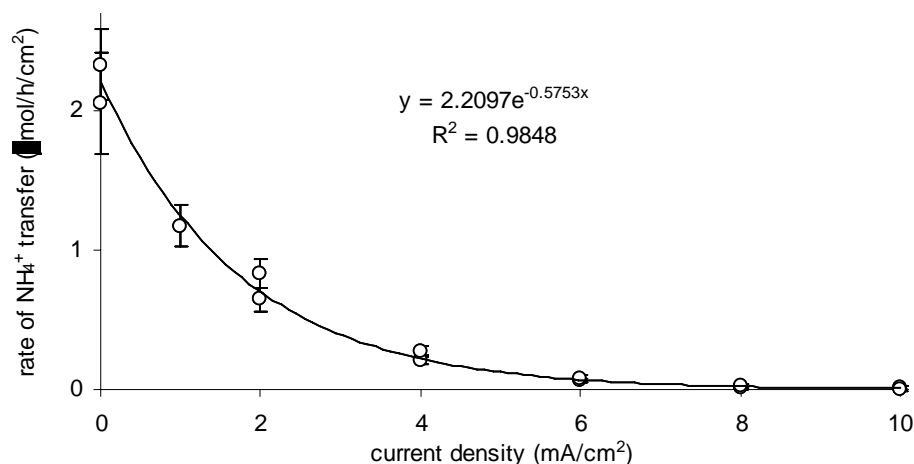


Figure 2.5-g Dependence of NH_4^+ transfer on current.

The NH_4^+ concentration in the M chamber was 0.02 M . Data were collected from two independent experiments. Points represent, means \pm standard errors of at least 3 results. Other details as Figure 2.5-f.

2.5.2d The effect of pH on organic acid transport

Electrodialysis typically generated an acidic (~pH 1) solution of sodium salts in the MA chamber. The pH of the transported organic acids solution would preferably be neutral so that the supply of substrate to the *R. sphaeroides* culture would not cause pH stress. The effects of maintaining neutral pH in the MA chamber on organic acid transport were investigated using an autotitrator. The transport of organic acids was measured while maintaining the pH in the MA chamber (pH_{MA}) at 2 or 7.5, while the pH in the M chamber (pH_{M}) was constantly 5.5.

Table 2.5-1 Properties of organic acids

| Organic acid | No. C | pK_a^α | Valence | Anion MW |
|--------------|-------|----------------------|---------|----------|
| Formate | 1 | 3.75 | 1 | 45 |
| Acetate | 2 | 4.76 | 1 | 59 |
| Butyrate | 4 | 4.81 | 1 | 87 |
| Lactate | 3 | 3.86 | 1 | 89 |
| Succinate | 4 | 4.19, 5.57 | 2 | 117 |

$^\alpha \text{pK}_a$ values were reproduced from [186].

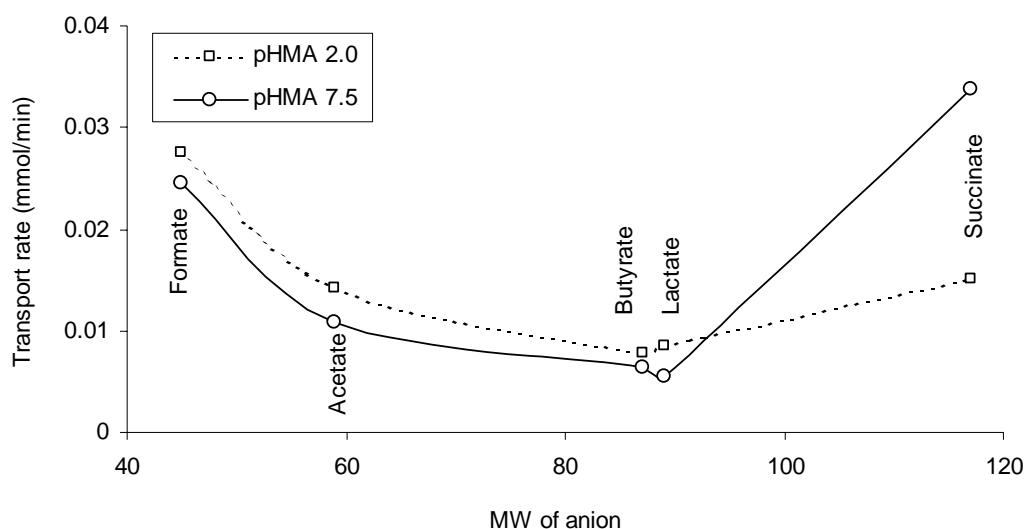


Figure 2.5-h Transport rates of organic acids related to anionic mass and pH in the MA chamber (pH_{MA}).

The M chamber initially contained 5 L of simulated fermentation products containing 20 mM each of sodium lactate, sodium acetate, formic acid, sodium butyrate, succinic acid and sodium sulphate maintained at 30 °C and pH 5.50 by automatic titration with 2 M H_2SO_4 . The MA chamber contained initially 1 L of basal salts (0.366 g K_2HPO_4 , 0.433 g KH_2PO_4 , 0.05 g $\text{MgSO}_4 \cdot 7\text{H}_2\text{O}$, 0.025 g $\text{CaCl}_2 \cdot 2\text{H}_2\text{O}$ per litre) maintained either at pH 2.0 or pH 7.5 by automatic titration with 5 M NaOH. A current density of 400 mA was applied over a membrane area of 200 cm^2 .

For monovalent organic acids (formate, acetate, butyrate and lactate), the transport rates were not significantly affected by pH_{MA} but were inversely related to their differing anionic molecular weights (Table 2.5-1), consistent with the theory that smaller molecules are more mobile in solution and more readily transported by the ASM (Figure 2.5-h). Conversely, the behaviour of succinate (a divalent acid) did not fit this pattern as it was transported more than twice as rapidly under neutral pH_{MA} relative to acidic pH_{MA} . These observations can be explained in terms of the ionisation of organic acids with differing $\text{p}K_{\text{a}}$ values and valence numbers (Table 2.5-1). As the pH_{M} was constant, the strong effect of pH_{MA} on succinate transport was unexpected. At pH 5.5 (in the M chamber), its first acid group ($\text{p}K_{\text{a}}$ 4.19) would be almost completely dissociated, while the second acid group ($\text{p}K_{\text{a}}$ 5.57) would be close to 50 % dissociated. It is speculated that incomplete mixing, proximal to the anion-selective membrane, would result in a localised divergence of pH_{M} from 5.5 and towards pH_{MA} . Therefore, under neutral pH_{MA} , the proportion of dissociated succinate would be significantly increased at the membrane surface on the M-side, resulting in a higher charge/mass ratio and a higher transport rate. The same effect may not be observed for monovalent organic acids due to their relatively low $\text{p}K_{\text{a}}$ values and resultant complete dissociation under both conditions.

A neutral pH_{MA} was, therefore, beneficial to the *R. sphaeroides* culture and marginally beneficial in terms of succinate transport and was used in subsequent work.

2.5.2e Mass balances for organic acid transport

Mass balances were attempted for electrodialysis experiments transporting organic acids from synthetic solutions and fermentation broths. Figure 2.5-i shows a successful mass balance for the transfer of organic acids from a cell-free solution containing 20 mM each of lactate, acetate, formate, butyrate, succinate and sulphate.

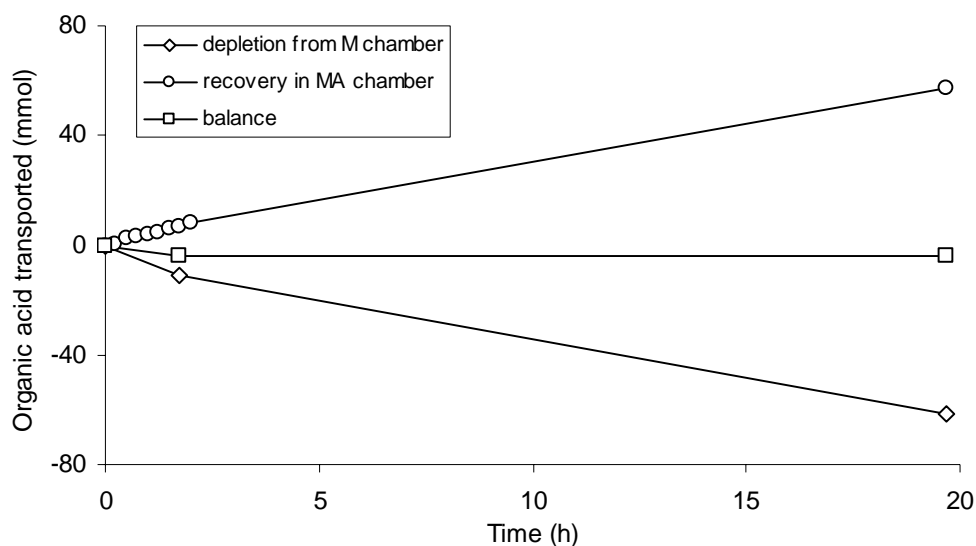


Figure 2.5-i Mass balance for organic acid transport from a cell-free solution using the ‘low-constant’ approach.

Conditions were as Figure 2.5-h (using a pH_{MA} of 7.5). The ‘low-constant’ approach is described in section 2.5.2a. In this experiment, the initial concentration of organic acids in chamber M was *ca.* 10-fold greater than the transport capacity in order to minimise the change in concentration in the M chamber.

Mass balances were also performed using *E. coli* cultures (Figure 2.5-b). Organic acids were transported from glucose-fed fermentations (Figure 2.5-b, part A) and also from fermented fruit waste obtained from a batch fermentation performed by Dr D. W. Penfold [149] (Figure 2.5-b, part B). For these samples, the mass balances appeared positive. This was attributed to the presence of cells, which concentrate organic acids internally (see section 2.2.4a) and may release them as the apparent (external) concentration decreases.

2.5.2f The capacity for organic acid transfer

Rates of organic acid transfer were measured in order to assess the ability of organic acid transfer to balance production by *E. coli* fermentation. The transport of a mixture of organic acids and Na₂SO₄ (all 20 mM) was studied (Figures 2.5-h and 2.5-i). Current efficiency (CE) was calculated according to equation 1 [117]:-

$$CE (\%) = \frac{100NF}{i} \quad (\text{equation 1})$$

CE current efficiency (%)
 N charge flux as organic acid in mol/s/m²
 F Faraday constant, 96485.38
 i current density in A/m²

In the example (Figure 2.5-i) the total charge flux as organic acid was 0.0893 mmol/min (or 7.44 x10⁻⁵ mol/s/m²) and the current density was 2 mA/cm² (or 20 A/m²), therefore the current efficiency was 35.91 %. Current efficiencies in the range 78-99 % were achieved in extractive fermentations [117,205,220] and the relatively low current efficiency in this study was attributed to competitive ion transfer; i.e. the transport of SO₄²⁻ (present at 20 mM), which was not measured. This suggests that the capacity for organic acid transfer by a membrane area of 200 cm² was sufficient to balance production by an *E. coli* fermentation processing 60 mmol glucose/day. Production was estimated to be *ca.* 60 mmol organic acid/day (chapter 2.2-*phase 3*). An equal rate of transport would be predicted under a current density of 2 mA/cm² and a current efficiency of 16.75 % (equation 1). This current efficiency was considered feasible given that it was half of that obtained in the simulation. In sustained *E. coli* fermentations organic acid transfer balanced production (chapter 2.2-*phase 4*, chapter 2.6).

2.5.2g Energetic analysis of a dual system using electrodialysis

Electrodialysis requires an input of electrical energy, which detracts from the net energy output of the dual system. Whether the addition of a photofermentation to the system results in a net energy profit depends upon the current efficiency, and upon the quantity of H₂ produced in the photobioreactor from the transported organic acids. The “break-even” current efficiency (BCE) denotes the current efficiency at which the energy output resulting from ED balances the electrical energy input to ED and the BCE can be calculated according to equation 2.

$$BCE (\%) = \frac{10000CFV}{Y_{theo} E_{H_2} S} \quad (\text{equation 2})$$

- BCE break even current efficiency (%)
 C valence of organic acid
 F Faraday constant, 96485
 Y_{theo} theoretical yield by photofermentation (mol H₂/mol substrate)
 E_{H_2} combustion enthalpy of H₂ (285900 J/mol)
 S substrate conversion efficiency by photofermentation (%)

For example, the BCE for butyrate with a substrate conversion of 75 % would be 18.00 %. In practice the BCE was significantly decreased due to the additional energy value of H₂ produced by electrolysis, as a side-reaction of electrolysis (Table 2.5-2). This tertiary source of H₂ would contribute to the H₂ output of the system and to the production of electrical energy by a fuel cell. In this work the energy value of electrolytic H₂ was sufficient to offset the electrical energy input by 28 % (Table 2.5-2), while the electrolytically generated O₂ could generate revenue or enrich the air supply to a PEM-FC, further augmenting electrical energy generation.

Table 2.5-2 Potentially offset electrical input through electrolytically generated H₂

| Energy output | | |
|--|-------------------------|-----------------------|
| rate of electrolytic H ₂ production | 1.56 x 10 ⁻⁶ | mol H ₂ /s |
| combustion enthalpy of H ₂ | 285900 | J/mol |
| Energy value of H ₂ | 0.446 | J/s (W) |
| Energy input | | |
| Current | 0.4 | A |
| Voltage | 4 | V |
| power | 1.6 | W (J/s) |
| output / input | 27.9 | % |

When the offset electrical input is incorporated, BCE is calculated according to equation 3.

$$BCE (\%) = \frac{10000CF(ViA - R_{H_2} E_{H_2})}{Y_{theo} E_{H_2} SiA} \quad (\text{equation 3})$$

- R_{H_2} Rate of electrolytic H₂ production (mol H₂/s)
 i current density (A/m²)
 A membrane area (m²)

For example, in this work RH_2 was 135 ml/h (1.56×10^{-6} mol/s), i was 20 A/m², A was 0.02 m² and V was typically 4 V. These values were used to generate BEC values for various organic acids (Table 2.5-3).

Table 2.5-3 ‘Break-even’ current efficiency (BCE) for organic acids

| Organic acid | Valence (C) | Y_{theo} ^α | Y_{theo}/C | BCE (%) ^β |
|--------------|-------------|-------------------------|--------------|----------------------|
| Butyrate | 1 | 10 | 10 | 12.99 |
| Propionate | 1 | 7 | 7 | 18.55 |
| Lactate | 1 | 6 | 6 | 21.64 |
| Pyruvate | 1 | 5 | 5 | 25.97 |
| Acetate | 1 | 4 | 4 | 32.47 |
| Succinate | 2 | 7 | 3.5 | 37.10 |
| Fumarate | 2 | 6 | 3 | 43.29 |
| Malate | 2 | 6 | 3 | 43.29 |

^α Y_{theo} values were reproduced from [170].

^β Values ($RH_2 = 1.56 \times 10^{-6}$ mol/s, $V = 4$ V, $S = 75$ %, $i = 20$ A/m², $A = 0.02$ m²) were used to calculate BEC according to equation 3.

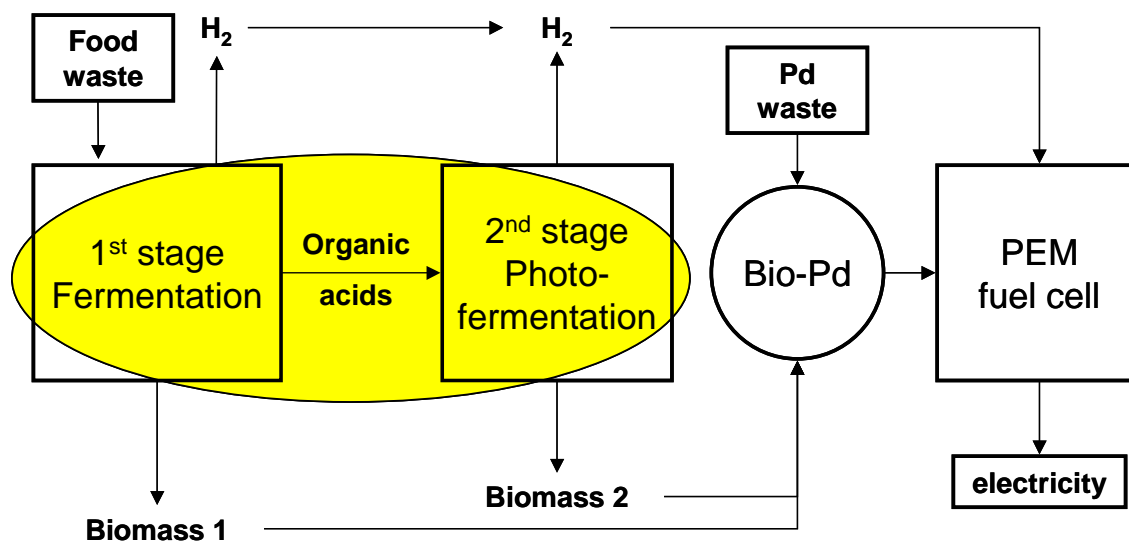
BCE decreased (i.e. becomes more energetically attractive) as the yield per valence (Y_{theo}/C) increases. As a result organic acids such as succinate and malate, normally favoured substrates for H₂ production by PNS bacteria, are less likely to result in a net energy profit, whereas butyrate would be preferred, which is a suitable substrate for *R. sphaeroides* (chapters 2.3 and 2.6). As butyrate has the lowest BEC among the organic acids examined and butyrate was the primary product of *E. coli* fermentation (chapter 2.6), a dual system combining this fermentation-type and photofermentation (e.g. by *R. sphaeroides*) would be expected to generate a net energy profit, without accounting for operating costs. A full economic assessment would be premature as the configuration of an industrial-scale dual bioreactor system is not yet finalised, hence capital and operational costs cannot be estimated. Other relevant unknowns include the cost and durability of electrodialysis membranes, ‘gate fees’ applied to feedstocks (acquired as wastes, undercutting landfill charges and tax), product values and distribution costs.

2.5.3 Conclusions

- ED was more effective in this application when operated continuously using a low current rather than intermittently, for short periods using high current.
- A current density of 2 mA/cm² was determined to be suitable, being less than 80 % of the system LCD and being sufficient to transport the anticipated organic acid flux, while opposing excessive diffusion of NH₄⁺.
- Organic acids were transported at different rates according to differences in mass, charge, concentration and ionisation. The maintenance of neutral pH in the MA chamber was moderately beneficial to organic acid transport.
- The electrical energy cost of ED was offset by the production of H₂ from the transported organic acids (by *R. sphaeroides*) and by the electrolytic production of H₂ (abiotic). For the transport of butyrate, a current efficiency of 13 % is necessary to balance the electrical energy cost.

2.6 Linking dark and light H₂ production by electrodialysis

2.6.0 Summary and introduction



Having studied the application of electrodialysis (ED) to *E. coli* fermentation (chapter 2.5) the technique was used to construct a dual system combining fermentation by *E. coli* and photofermentation by *R. sphaeroides*. Help and advice were provided by M. Wright (EKB Technology) and W. Skibar and D. Stratton-Campbell (C-Tech Innovation Ltd.). The primary conclusions were:-

- The dual system with ED achieved sustainable and continuous H₂ production monitored over 16 days from an ammonium-rich substrate. This was attributed to the transfer of organic acids to the *R. sphaeroides* culture, to the relief of organic acid toxicity on *E. coli* and to the exclusion of NH₄⁺ influx into the *R. sphaeroides* culture, such that nitrogenase activity was not inhibited.
- In practice the dual system achieved 2.4 mol H₂/mol glucose (20 % conversion of glucose to H₂), although a practical maximum yield of 10 mol H₂/mol glucose was predicted. The important sources of inefficiency were un-optimised operation of the photobioreactor and the retention of non-ionic fermentation products (i.e. ethanol). Future work will aim to overcome these bottlenecks and achieve significantly higher yields.

Several reports document dual systems combining various fermenting microorganisms and PNS bacteria, resulting in overall yields of *ca.* 8 mol H₂/mol hexose (chapter 1.2)[160].

Initial attempts to operate a dual system combining *E. coli* and *R. sphaeroides* (see chapter 2.4)[158] failed because the organic acid liquor generated by *E. coli* fermentation contained significant NH_4^+ , preventing H_2 production when the liquor was supplied to *R. sphaeroides*. Electrodialysis (ED) techniques offer a solution to this problem, having the capacity to separate the desirable organic acids from the repressive NH_4^+ , while allowing controlled quantities of NH_4^+ to pass through the anion-selective membrane (ASM) (chapter 2.5).

2.6.1 Materials & Methods

2.6.1a Dual system set-up

For dual system experiments, *E. coli* HD701 fermentations were prepared as ‘phase 4’, chapter 2.2.2c. The initial volume was 3 L and the initial concentrations of glucose and NH_4^+ were 20 mM and 1.5 mM, respectively. *R. sphaeroides* O.U. 001 was cultured as described in section 2.3.2 except that pre-culturing was performed using in 15 ml water-jacketed vials under *ca.* 300 $\mu\text{E}/\text{m}^2/\text{s}$ tungsten illumination.

The two bioreactors were operated in parallel as follows. The inoculation of the PBR took place 48 h prior to the inoculation of the fermentation vessel. The addition of feed solution (0.6 M glucose, 7.5 mM $(\text{NH}_4)_2\text{SO}_4$) to the fermentation vessel commenced 24 h following the initiation of dark fermentation at a rate of 100 ml/day to supply glucose and NH_4^+ at rates of 60 mmol/day and 1.5 mmol/day, respectively. This point coincided with the continuous addition of basal medium (1 litre/day) to the permeate vessel (Figure 2.6-a) to generate organic-acid enriched medium, which was continuously supplied to the photobioreactor (1 litre/day) from the same time-point (Figure 2.6-b, part B, open triangles). The addition of feed solution to the fermentation vessel caused little increase in culture volume due to the electroosmotic movement of water *via* ED.

Hence, the *R. sphaeroides* culture was allowed to grow in batch mode for 72 h, before the contents of the permeate vessel (containing organic acids transferred from the dark fermentation *via* ED) were continuously added to the PBR (1 l/day) and the PBR was continuously drained into the outflow vessel at the same rate, at which point the continuous addition of feed solution to the fermentation vessel also commenced.

The PBR was operated under three conditions designated Rs1-3 (Table 2.6-1). In preliminary work, the PBR was diluted with basal medium supplied directly (Rs1). Experiments designated Rs2 represent dilution with ‘empty’ medium having passed through the electrodialysis system without gaining organic acids. For Rs2 experiments, inactive membranes were fitted to the electrodialysis cell, corresponding with Ec2 experiments (above). In Rs3 experiments active electrodialysis transferred organic acids into the basal medium before it was supplied to the PBR. The *R. sphaeroides* culture was separated from the permeate chamber (MA) so that organic acid transfer could be monitored and current efficiency determined.

Table 2.6-1 Experiments

| ID | n | Description | Purpose |
|------------------|----------|-----------------------------------|--|
| Ec1 | 3 | no electrodialysis (ED) | Control – baseline H ₂ production |
| Ec2 | 4 | ED with inactive ASM | Control – DC only |
| Ec3 ^a | 2 | ED with active ASM | Organic acid transport, dual system |
| Rs1 | 1 | diluted with basal medium (no ED) | Control – no substrate |
| Rs2 | 2 | ED with inactive ASM | Control – no substrate ^b |
| Rs3 ^a | 2 | diluted with ED-permeate | Organic acid transport, dual system |

^a Ec3/Rs3 and Ec2/Rs2 experiments were performed in concert; ^b In Rs2 experiments DC was applied to the medium supplied to *R. sphaeroides* without transferring organic acids; n: number of replicate experiments; ASM: anion-selective membrane; inactive ASM: membranes were inactivated by applying a current of *ca.* 10-fold above the limiting current density of the system (10 A, 5-15 V, *ca.* 24 h).

Biomass concentration was estimated from measurements of optical density (660 nm) as described previously [158]. Culture purity was inspected regularly by serial dilution plating on nutrient agar (Oxoid, UK). Light conversion efficiency (%) was calculated by dividing the combustion enthalpy of the produced H₂ (285.9 kJ/mol) by the supplied light energy (400-950 nm) [2] (see appendix 4.1.4).

2.6 Results – A dual system using electro dialysis

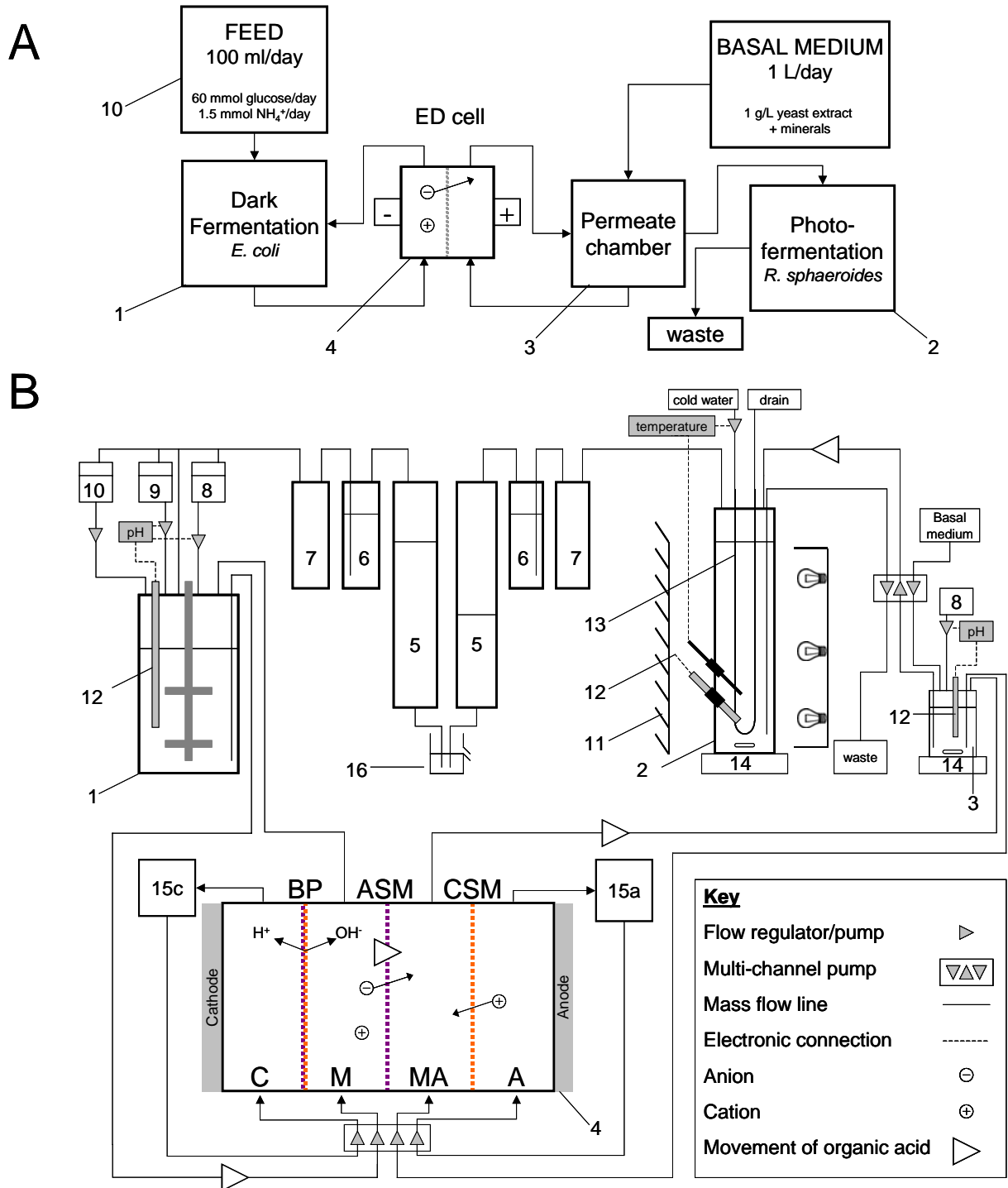


Figure 2.6-a Process scheme (A) and configuration (B) for a dual system with integrated electro dialysis.

1, fermentation vessel (3 L); 2, photobioreactor (3 L); 3, permeate vessel (1 L); 4, electro dialysis cell; 5, graduated cylinder for H_2 collection; 6, CO_2 trap (2 M NaOH with universal indicator); 7, void; 8, base titrant (3 M NaOH); 9, acid titrant (2 M H_2SO_4); 10, Feed solution; 11, tubular reflective sheath; 12, pH sensor; 13, cooling tube (stainless steel); 14, magnetic stirrer and follower; 15a/15c, anode and cathode vessels, respectively, containing 0.5 M Na_2SO_4 ; 16, anti-backflow device; BP, bi-polar membrane; ASM, anion-selective membrane; CSM, cation-selective membrane; C, cathode chamber; A, anode chamber; M, main chamber delivering organic acid from fermentation vessel (1); MA, permeate chamber supplied with basal medium and organic acids before delivery to the PBR (2). See also appendix 4.3, showing a video of the complete functioning system.

2.6.1b Electro dialysis

Thin-cell electro dialysis (ED) apparatus of a published design [89] was purchased from C-Tech Innovation Ltd. Its four chambers (C, M, MA, and A) were separated by 3 membranes; bi-polar (BP: Neosepta BP-1E), anion (ASM: Neosepta AHA), and cation (CSM: Nafion 324), respectively (Figure 2.6-a). Membranes were purchased from Eurodia Industrie, France. A fresh ASM was used in each experiment (except Ec2/Rs2). Chambers A and C (flanked by the anode and cathode, respectively) were in contact with solutions of 0.5 M Na₂SO₄, the M chamber was in contact with the *E. coli* culture and MA was in contact with the permeate vessel containing initially 1 l of a cell-free aqueous basal medium, modified from the SyA medium of [66] by omitting succinate and acetate (see appendix 4.1.2a).

Silicone rubber gaskets (1 mm thickness) were cut to expose membrane areas of 200 cm² (128 mm x 157 mm). All four chambers were flushed constantly (450 ml/min). Reynolds number (Re) was 173 (see appendix 4.1.6), suggesting laminar flow although the calculation did not account for additional turbulence due to plastic mesh occupying each chamber. A current density of 2 mA/cm² (344 mA, variable voltage) was applied throughout experiments Ec2/Rs2 and Ec3/Rs3 (Table 2.6-1). Current efficiency (or Faraday efficiency) represents the fraction of charge passed over a given time, which is attributable to the transfer of target species.

Inactive ASM were prepared for Es2/Rs2 experiments by applying a current of *ca.* 10-fold above the limiting current density of the system (10 A, 5-15 V, *ca.* 24 h) before use. Using synthetic solutions of organic acids (see chapter 2.5), negligible organic acid transport with a current efficiency of < 0.3 % was measured, whereas the use of fresh ASM resulted in current efficiencies of 36 % in parallel tests. Current efficiency was monitored during Es2/Rs2 experiments (see Results).

2.6.2 Results

2.6.2a H₂ production by *Escherichia coli*

In all experiments the rate of H₂ production was initially high and decreased over the initial 24 h as glucose was depleted (Figure 2.6-b). Upon the introduction of a constant glucose supply (60 mmol/day fed continuously) the rate of H₂ production immediately increased,

preceding a period of stable and efficient H₂ production (80 % on average). During this period, the measured concentration of glucose in the medium was zero (Figure 2.6-b, part B), hence the rate of glucose supply (60 mmol/day) was equal to the rate of glucose uptake by *E. coli*. Therefore, the rate (ml H₂/h) and yield (mol H₂/mol glucose), were directly proportional in this period, a yield of 100 % (2 mol H₂/mol glucose for *E. coli*) corresponding to a rate of 120.3 ml H₂/h, given a molar volume for H₂ at 20 °C of 24.06 l (ideal gas). This conversion was not applicable during the initial 24 h, nor when glucose was detected in the medium.

2.6 Results – A dual system using electro dialysis

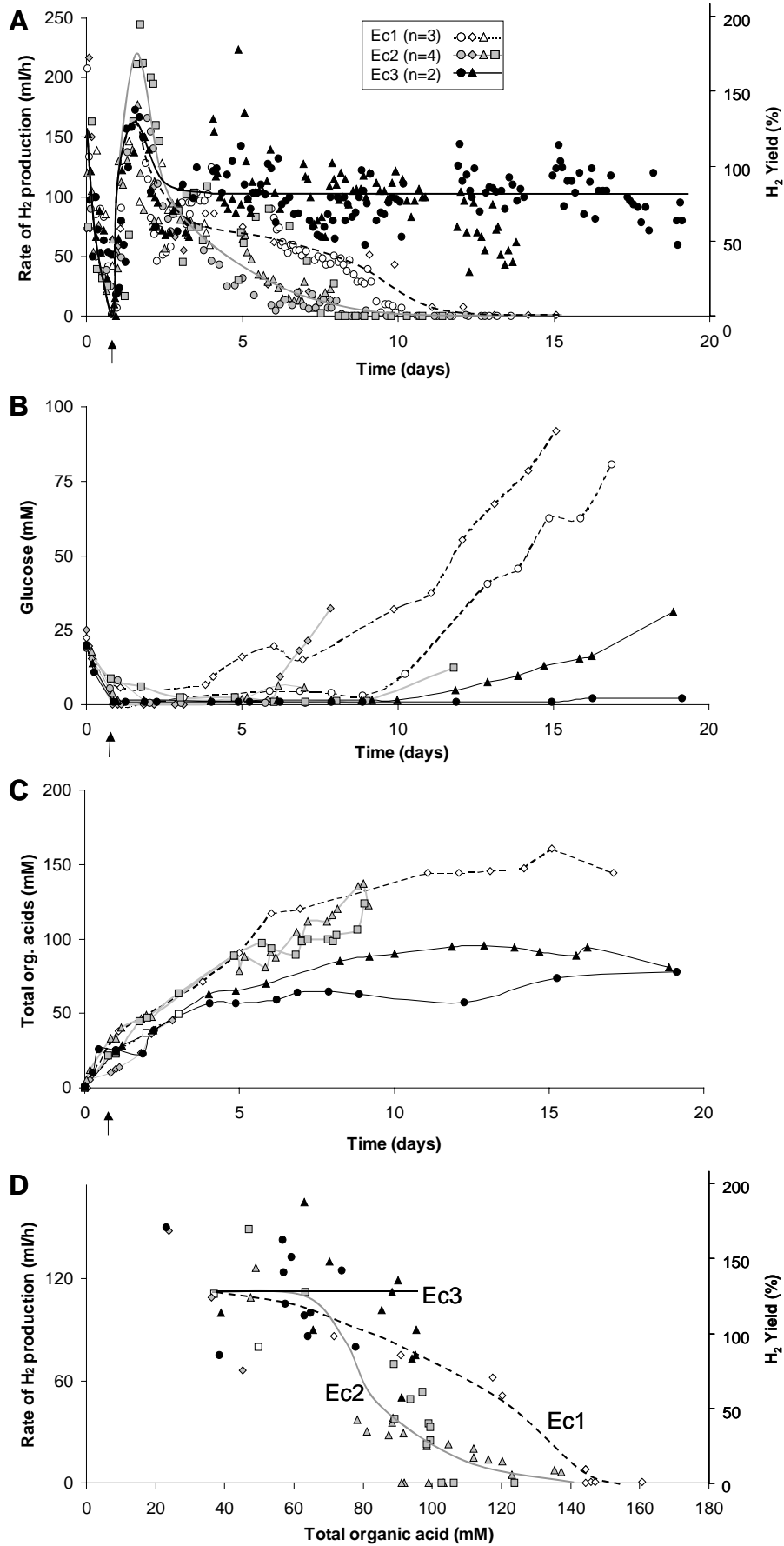


Figure 2.6-b H₂ production (A) glucose concentration (B) and organic acid concentration (C & D) in *Escherichia coli* fermentations. (Legend overleaf)

Legend to Figure 2.6-b Ec1 experiments are represented by open symbols with dotted lines, Ec2 by shaded symbols with grey lines, and Ec3 by filled symbols with black lines. The H₂ production rate of 120.3 ml/h corresponded to a yield of 2 mol H₂/mol glucose (100 %). Arrow indicates the start of glucose addition 24h after t₀. The yield scale (A) applies only between the start of glucose addition and the increase in glucose concentration for individual experiments (see text). During the operation of dual systems, the points indicated by arrows were equivalent in real time for Figures 2.6-b and 2.6-c. In D only points beyond day-2 were plotted.

The duration of efficient H₂ production was dependent upon the application of ED. In Ec1 experiments the *E. coli* culture was in contact with the ED cell but current was not applied. H₂ production remained at least 50 % efficient for *ca.* 7 days operation. Decreased efficiency of H₂ production coincided with the appearance of excess glucose (Figure 2.6-b, part B), marking a decline in culture activity, which is attributed to organic acid toxicity (see section 2.6.3).

In Ec2 experiments, the ED was operated using inactive membranes to investigate the effect of direct current (DC) on *E. coli* without causing changes in the ionic background. The efficiency of H₂ production declined below 50 % *ca.* 2-3 days sooner than in Ec1 experiments (Figure 2.6-b, part A). A direct inhibitory effect of DC on *E. coli* is considered likely as DC is known to stress (and at high voltages, destroy) bacterial cells through unknown mechanisms, perhaps through the generation of free radicals [76] and *E. coli* was also found to be particularly sensitive to low-frequency magnetic fields [50]. However, DC may also have been stimulatory to other aspects of *E. coli* activity, as the ‘spike’ in the rate of H₂ production observed reproducibly at 2-3 days was greatest in Ec2 experiments (see section 2.6.3d). A stimulation of microbial activity by DC (in the absence of product removal) was shown previously [89].

With active ED (Ec3), H₂ production remained efficient throughout the duration of the experiment (20 days, Figure 2.6-b, part A). The H₂ yield stabilised at *ca.* 80 % while the total organic acid concentration stabilised at *ca.* 80 mM (Figure 2.6-b, part C). It is proposed that the removal of organic acids prevented organic acid toxicity, as Ec3 experiments resulted in only low concentrations of organic acids, associated with high rates of H₂ production (Figure 2.6-b, part D). Conversely in Ec1/2 experiments there was a negative relationship between total organic acid concentration and the yield of H₂, such that the yield declined to 50 % when

the organic acid total reached *ca.* 120 mM for Ec1 and *ca.* 90 mM for Ec2. In other words, H₂ production continued in the absence of DC despite a background concentration of organic acids that was inhibitory in the presence of DC. This indicates that a long-term effect of DC was to exacerbate the inhibition of H₂ production by organic acids (see section 2.6.3).

2.6.2b H₂ production by *Rhodobacter sphaeroides*

In all experiments (Rs1-3) the first 72 h entailed culture growth in the photobioreactor on a growth medium containing organic acids (see materials & methods). 72 h post-inoculation (arrowed in Figure 2.6-c), the active H₂-producing cultures were diluted (HRT = 3 d) with various media (Table 2.6-1). When the diluent solution contained no organic acids and yeast extract was the only supplement (Rs1/Rs2), the residual organic acids from the growth medium washed out and H₂ production ceased by day 7 (Figure 2.6-c, part A). A similar result was observed whether the empty medium was supplied directly to the PBR (Rs1) or passed first through inactive ED system (Rs2) indicating that ED *per se* had no deleterious effects on *R. sphaeroides*.

When a synthetic mixture of organic acids was used H₂ production continued beyond day 7 with a stable substrate conversion efficiency of 32 % (chapter 2.3). A higher value (38 %) was achieved when organic acids from the *E. coli* fermentation were transported to the PBR by ED (Rs3).

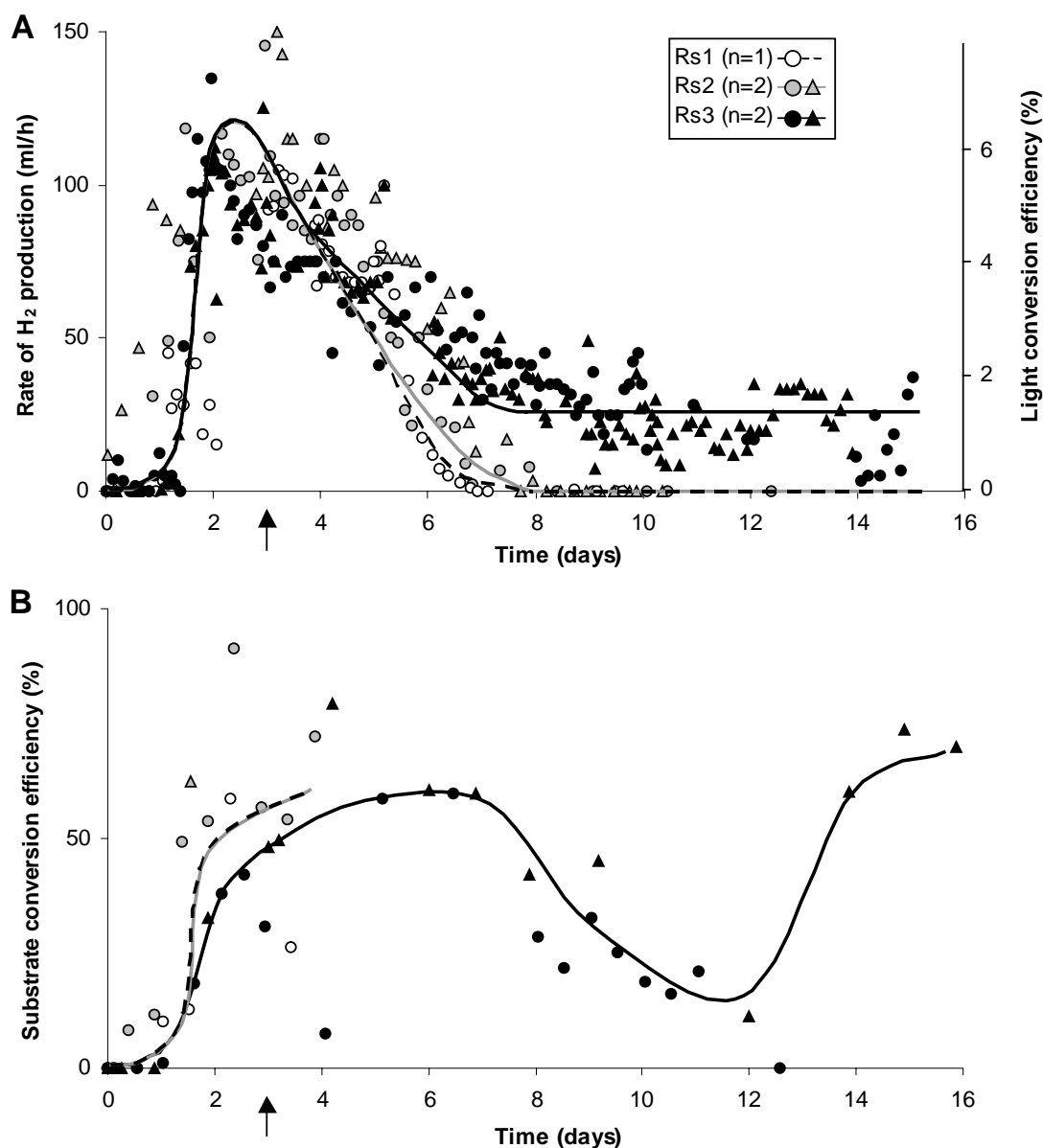


Figure 2.6-c H₂ production (A) and substrate conversion efficiency (B) by *Rhodospira rubra*.

Rs1 experiments are represented by open symbols with dotted lines, Rs2 by shaded symbols with grey lines, and Rs3 by filled symbols with black lines. The H₂ production rate of 150 ml/h corresponded to a light conversion efficiency of 7.84 % (see appendix 4.1.4). Substrate conversion efficiency (B) was calculated using the theoretical maxima of 4 mol H₂/mol acetate, 6 mol H₂/mol lactate, 7 mol H₂/mol succinate and 10 mol H₂/mol butyrate [170], based on the consumed substrate. Arrows indicate the onset of dilution after 3 days growth. During the operation of dual systems (Ec2/Rs2 and Ec3/Rs3) the dilution of both reactors commenced simultaneously at the times indicated by arrows in Figures 2.6-b and 2.6-c.

2.6.2c Electrodialysis

Rhodobacter sp. were reported to cease H₂ production in response to as little as 20 μM NH₄⁺ [90]. Further, with a background of 40 mM acetate 1.5 mM NH₄⁺ was sufficient to completely repress H₂ production in *R. sphaeroides* O.U.001 (chapter 2.3). In this study, prolonged H₂ production by *R. sphaeroides* was observed despite the presence of 15 mM NH₄⁺ in the initial feed solution. Therefore this approach, using ED, was effective in retaining NH₄⁺ in the dark fermentation while transferring fermentation products to the PBR, although a transfer rate of 2.87 μmol NH₄⁺/h was calculated (chapter 2.5), which was not measured in the dual system.

In these experiments, current efficiency followed an increasing trend from 5 % to 28 % (Figure 2.6-d), losses being attributable to competitive ion transfer, i.e. the movement of inorganic anions such as SO₄²⁻, which do not contribute to H₂ production. The increase could be attributed to the increasing concentration of organic acids in the fermentation medium (Figure 2.6-b, part C).

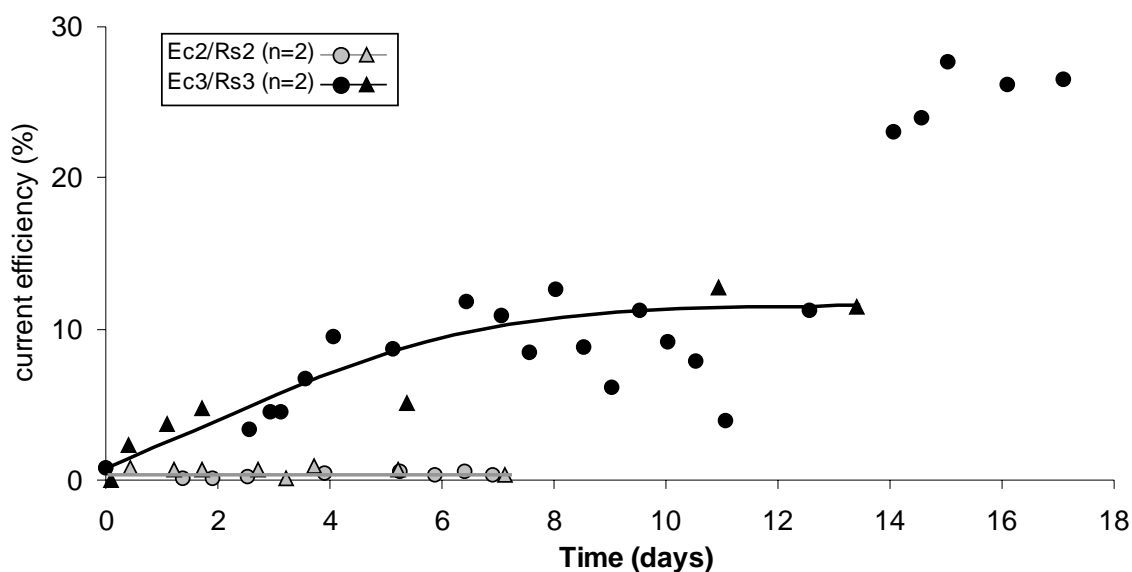


Figure 2.6-d Efficiencies of organic acid transfer in experimental dual systems.

Ec1/Rs1 experiments did not use ED, Ec2/Rs2 experiments are represented by shaded symbols with grey lines, and Ec3/Rs3 by filled symbols with black lines. Current efficiency (or Faraday efficiency) indicates the effectiveness of organic transfer and was calculated as the charge of organic acids transported divided by the charge passed over a given period. The mass transfer of organic acids was calculated from measurements of organic acid concentrations in the permeate chamber (MA) and the dilution rate (1 L/day).

In the PBR, the efficiencies of substrate conversion and utilisation were 38 % and 56-94 %, respectively (Figure 2.6-e). Consequently, the electrical energy input to ED was slightly greater than the energy value of H₂ resulting from it; i.e. the sum of H₂ from the photobioreactor and H₂ produced electrolytically (see section 2.5.2g). It was calculated that given 75 % efficient substrate conversion and complete substrate utilisation in the PBR, the threshold current efficiency required to generate sufficient H₂ to balance the energetic cost of ED would be 13 %, which is lower than the average current efficiency achieved in Ec3/Rs3 experiments (Figure 2.6-d).

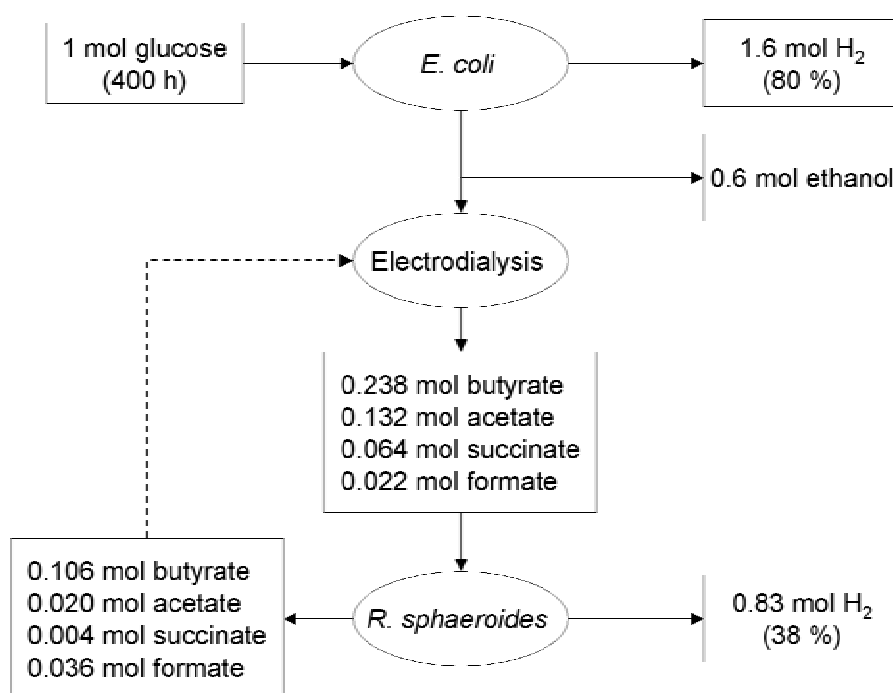


Figure 2.6-e H₂ production by a dual system with integrated electro dialysis.

All values are expressed as mol product/mol glucose, equivalent to mol product/400h. The dotted arrow illustrates the possibility to recycle unused organic acids.

Current efficiency could be improved further by the use of a cationic buffer in the fermentation medium [89], however buffers (e.g. phosphate) were excluded in this study as they would contribute to the polluting potential of waste fermentation medium and cationic buffers may represent an economic burden upon scale up. Water transport from the fermentation chamber (M) to the permeate chamber (MA) (and electrolysis) occurred at an average rate similar to that of substrate addition, obviating the need for fill-and-draw of the fermentation vessel and disposal of the resultant effluent. An additional benefit of ED was pH control. It was shown previously that bi-polar ED can double-function as a pH-stat due to

the generation of OH⁻ ion on the anode side of the bi-polar membrane [89,102,137]. In this study the demand for NaOH titrant to the fermentation vessel was completely removed by this activity of bipolar ED, and small volumes of H₂SO₄ titrant were required.

2.6.3 Discussion

2.6.3a Productivity of the dual system

The application of electrodialysis was successful in the production of H₂ by *E. coli* and *R. sphaeroides* from an initial feed containing 15 mM NH₄⁺, which if fed into a conventional system (without ED) would be inhibitory to nitrogenase-mediated H₂ production, which shut down in a background of 1 mM NH₄⁺ (chapter 2.3). The total H₂ production of the system was 261 ml H₂/h: 96 ml/h from dark fermentation, 30 ml/h from photofermentation and 135 ml/h from electrolysis of water (a side-reaction of ED).

By combining the steady-state H₂ yields from both stages with the loading rate of glucose (60 mmol/day) an overall yield of 2.4 mol H₂/mol glucose was determined (Figure 2.6-e), which is higher than would be possible using *E. coli* alone, but comparable to reported yields from some single-stage dark fermentations (chapter 1.2) [36,62]. Therefore the dual system succeeded in increasing H₂ production but significant potential for improvement remains as several reports document discontinuously operated dual systems producing *ca.* 8 mol H₂/mol glucose [6,71,80,126,206,211] (chapter 1.2). In contrast, the dual system described here tolerated NH₄⁺ in the initial feed and achieved stable and continuous operation, with the additional ED-related benefits of relief of organic acid toxicity, cell retention, water transport, and inherent pH control.

The productivity of the dual system can be dissected as follows. The dark fermentation was *ca.* 80 % efficient, whereas significant H₂-production potential was lost in the PBR resulting from incomplete substrate utilisation and inefficient substrate conversion to H₂. At steady-state (post-day 7) the average substrate conversion efficiency was 38 % in Rs3 experiments (Figure 2.6-c, part B), while on average, 94 % of succinate, 85 % of acetate and 56 % of butyrate were utilised (Figure 2.6-e). In these experiments the outflow (containing 26 % of the supplied H₂ potential) was discarded, however 100 % utilisation could be achieved in a scaled-up system in which the PBR outflow (containing valuable organic acids and

background medium components) would be returned to the permeate chamber, following cell-separation. Substrate conversion efficiencies of up to 75 % were reported for continuous cultures of APB using various substrates [25,45,162] (chapter 2.3) and the relatively low values observed here were attributed to sub-optimal culture conditions (such as substrate loading rate, hydraulic retention time, culture density and illumination). It is also possible that the Rs3 cultures were affected by sodium toxicity, although Na^+ concentrations were not monitored. Na-toxicity was identified in a mixed culture, where the use of $\text{Ca}(\text{OH})_2$ base titrant (rather than NaOH) was beneficial to dark fermentative H_2 production [97]. The ED approach utilised Na_2SO_4 in the C chamber, actively transporting cations (e.g. Na^+) across the CSM into the MA chamber. Alternatively, calcium and magnesium salts could be used in ED [30].

Given a substrate conversion efficiency of 75 % and complete substrate utilisation the overall yield would increase to 4.42 mol H_2 /mol glucose (37 % of the theoretical maximum), therefore, other factors would also be important in realising greater yields. The total concentration of organic acids in the *E. coli* medium stabilised (Figure 2.6-b, part C), indicating that ED effectively removed organic acids in balance with production. Under DC, organic acids migrated across the ASM as a result of their negative charge. Uncharged *E. coli* products (i.e. ethanol) were not transported reducing the potential for H_2 production by *R. sphaeroides*. *E. coli* produced 0.6 mol ethanol/mol glucose, which represents a potential 3.6 mol H_2 /mol glucose [54]. A potential H_2 yield of 10.05 mol H_2 /mol glucose can be predicted based on the observed dark fermentation and predicted complete transfer of organic fermentation products, and complete substrate utilisation (at 75 % conversion efficiency) in the PBR.

The transport of ethanol into the PBR was outside the scope of this study although it should be noted that alcohols are suitable substrates for H_2 production by PNS bacteria [54,71 and chapter 2.3]. The recovery of ethanol from fermentation broths by membrane distillation and molecular sieve techniques represent well-developed technology [22,167,219], hence ethanol may be transferred in a dual system by conventional methods or using an alternative process configuration as described in (see Figure 3-a).

2.6.3b Potential application of the system with alternative fermentations

E. coli produced *ca.* 0.6 mol ethanol/mol glucose, which is suitable product for conversion to H₂ by PNS bacteria [54,158] but was not separated by anion-selective ED. Alternative fermentations may be advantageous. For example, solventogenesis can be suppressed in *Clostridium acetobutylicum* fermentations producing butyrate and acetate [27,134]. However, the sensitivity of clostridial cultures to DC is unknown and, furthermore, clostridial fermentations are critically sensitive to H₂ back-pressure, producing similar H₂ yields compared to *E. coli* under practical conditions (see chapter 1.2) [40]. Lactic acid fermentation could be used, although the absence of dark H₂ production would place higher demands on efficient substrate transfer and photofermentation. Furthermore, butyrate fermentations (e.g. clostridia or *E. coli*) would be preferred over lactic acid fermentations as the theoretical H₂ yield from butyrate is higher than from lactate, resulting in a relatively low energetic cost of substrate transport (see chapter 2.5).

2.6.3c The effect of electrodialysis on *Escherichia coli*

In Ec3 experiments the total concentration of organic acids stabilised at *ca.* 80 mM, whereas H₂ production was 50 % inhibited at *ca.* 120 mM and 90 mM in experiments Ec1 and Ec2, respectively (Figure 2.6-b, part D). Therefore, an effect of applying ED to *E. coli* fermentation was the relief of organic acid toxicity, with a resultant increase in H₂ production. The relief of organic acid toxicity using ED was reported previously in *E. coli* fermentation [23] and in lactic acid fermentation [74,102]. The difference of only 10-40 mM in the stabilised concentrations of organic acids is significant, as it is known that a slight difference in the extracellular concentration of an organic acid will reflect a large difference in the cell interior, where toxicity takes effect. For example *E. coli* accumulated acetate to a cytoplasmic concentration of 240 mM, in an extracellular concentration of 8 mM and pH of 6.0 [165]. Intracellular accumulation is a result of the pH gradient across the cell membrane as the protonated fraction of the acid pool is membrane-permeable, hence the production of organic acids with lower pK_a values present a lower protonated proportion and cause less organic acid toxicity. For example *E. coli* up-regulates lactate production in response to acidic pH [32,183].

The effects of ED on cellular activity were evident not only from the rate of H₂ production but also from the rate of glucose uptake. When effective organic acid transfer was absent (Ec1 and Ec2) H₂ production declined and glucose accumulated within 9 days of operation. Conversely, when active organic acid transfer was applied (Ec3) H₂ production stabilised at approximately 80 % efficiency and the residual glucose was insignificant (Figure 2.6-b, part B).

2.6.3d The effect of direct current on *Escherichia coli*

Applying DC to *E. coli* without product removal (Ec2) shortened the period of H₂ production, but these results also provide evidence of a stimulatory effect in the short-term. Figure 2.6-c (part A) shows a reproducible spike in the rate of H₂ production at days 2-3. The production of H₂ at >100 % efficiency is attributed to the short-term uptake of lactate formed during the initial batch-mode fermentation (days 0-1) (see chapter 2.2). In Ec1 experiments the peak H₂ production rate observed was 150 ml/h, whereas rates of up to 320 ml/h were recorded for Ec2 experiments in this brief period. A further indication of the stimulatory effect of DC is the observation that DC resulted in prolonged periods of maximal glucose uptake (when the glucose concentration was negligible; Figure 2.6-b, part B) in 3 out of 4 Ec2 experiments, relative to ED-free experiments (Ec1). A similar phenomenon was described previously [89], but remains unexplained. Direct electron transfer between cells and the electrodes of the ED cell can be excluded as cells were separated from the anode and cathode by membranes.

2.6.3e Further development and application

This work represents ‘proof of concept’ for a novel system using ED to enable continuous and sustainable operation of two mutually dependent bioreactors. As individual topics, biological H₂ production and ED are well-studied, whereas the application of ED to H₂ production is a novel aspect of this study. The integration of ED resulted in two important developments; the possibility to utilise low C/N feedstocks and the possibility for sustained dark fermentation free from organic acid toxicity. There is significant potential to develop and apply this approach for energy generation in the form of H₂ production.

Although glucose/NH₄⁺ solution was used as a model feed in this study (with yeast extract supplement to the PBR), ED can be applied to fermentations using complex substrates e.g.

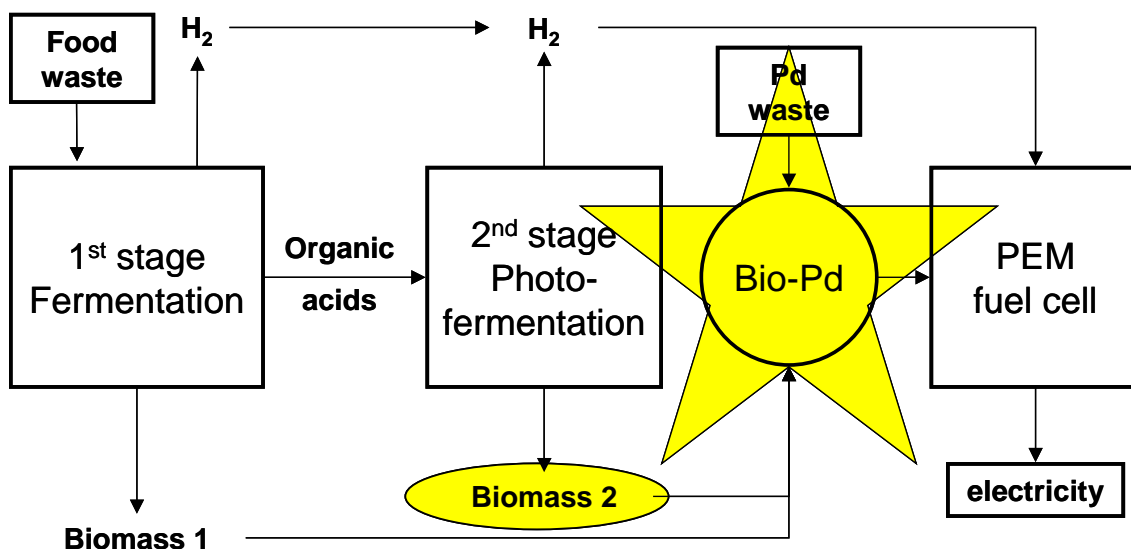
food wastes [201]. In this study, the current applied for ED was constant and an important aspect for further development would be the modulation of ED according to the requirements of the PBR and in relation to organic acid production. Using the current approach, this would entail rapid, on-line analysis of transferred species and minimal fluid retention time within the transfer system [159]. For the purpose of experimentation an artificial symbiosis was established between *E. coli* HD701 and *R. sphaeroides* but this approach could be applied using a wide range of mesophilic microbial symbioses and H₂-upregulated strains. In particular, the use of other enterobacteria or mesophilic clostridia in the dark fermentation could reduce the loss of potential H₂ to solventogenesis (in this study, ethanol), although the responses of H₂-producing fermentative bacteria to DC are little-studied.

Membrane-fouling could present a challenge upon scale up although it did not become limiting within 20 days (Ec3), and, conversely, the current efficiency increased with time (Figure 2.6-d).

The use of ED resulted in a versatile system able to produce H₂ more efficiently than a single-stage *E. coli* fermentation, from an ammonium-rich feed. However, the additional benefits of product removal, pH control, a stimulatory effect of DC and the inherent properties of cell retention and suspended solids retention suggest that the ED approach could be beneficial even where high C/N substrates are available.

2.7 Biomass-supported palladium catalysts on *Desulfovibrio* and *Rhodobacter*

2.7.0 Summary



Having investigated the potential for H₂ production by a dual bioreactor system, a potential application for excess biomass from the process was explored. This chapter describes the investigation of *Rhodobacter sphaeroides* as a matrix for the formation and support of catalytically active Pd(0) particles. Methods of catalyst production, which had been developed for *Desulfovibrio desulfuricans* were applied to *R. sphaeroides* without modification and the resultant biomass-supported catalysts were compared using example test-reactions of industrial and environmental significance.

In independent work K Deplanche, IP Mikheenko and NJ Creamer found that *E. coli* biomass was an effective catalyst support. Thus, excess biomasses from both parts of the dual H₂-producing system could constitute raw materials for the manufacture of valuable catalysts. To complete the conversion of wastes to energy, a PEM-FC was constructed using the novel bionanocatalysts to generate electricity from Bio-H₂ (chapter 2.8).

Catalytic testing was performed by the author in collaboration with K. Deplanche with methodology training from the late Dr V.S. Baxter-Plant. Mrs L. Tomkins (Centre for

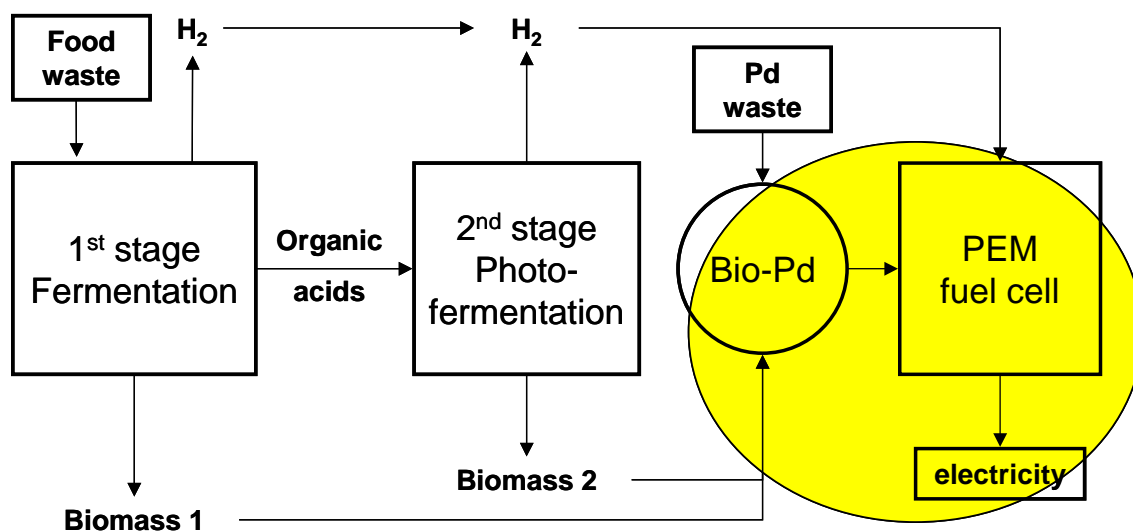
Electron Microscopy, University of Birmingham) assisted with electron microscopy. Catalyst preparation, data analysis and manuscript preparation were carried out independently by the author.

2.7.1 Article published in the Journal of Biotechnology and Bioengineering

Preliminary results were published in the Proceeding of the International Biohydrometallurgy Symposium (IBS2005), Cape Town, South Africa (reproduced in appendix 4.2.1).

2.8 Fuel cell anode construction to recycle biomass from biohydrogen production

2.8.0 Summary



In the preceding chapter (2.7) *R. sphaeroides* was found to be a suitable matrix for the biocrystallisation of Pd(0), forming a useful catalyst with comparable activity to the well-established *D. desulfuricans* material. The conceptual process (diagram above) involves the conversion of H₂ to energy using a fuel cell. This chapter focuses on the use of excess biomasses from the dual system, within the same system, to fabricate the anode catalyst of a PEM-fuel cell for generation of electricity from the two bio-H₂ streams and from the ‘electro-H₂’ stream from the electro dialysis cell (see chapter 2.5).

Electricity was generated by proton exchange membrane fuel cells (PEM-FC) with anodes constructed using bionanocatalyst. Bio-crystallised Pd(0), manufactured using outflow biomass from a continuous photobioreactor as part of a dual-bioreactor system for H₂ production, was an effective PEM-FC anode catalyst. The power outputs from PEM-FC constructed using *Rhodobacter sphaeroides* biomass was similar to that reported previously, using *E. coli* HD701. The maximum power output of “bio-fabricated” PEM-FC was 33 % that of a cell with commercial Pd(0) catalyst. The potential for catalyst production using the excess biomass from a dual system is estimated. Therefore, all elements of the proposed

system were proven in concept although optimisation and further research are required in the future development of an economically viable process.

Electrode construction and testing were performed by the author under the guidance of Dr P. Yong. Data for comparison were provided by P. Yong and I.P. Mikheenko (Figure 2.8-b).

2.8.1 Introduction to study

As detailed in chapter 1.3, polymer electrolyte membrane fuel cells (PEM-FC) are widely regarded as the most promising technology for the release of energy stored in H₂. PEM-FC employ platinum group metal (PGM) catalyst, which is problematic due to the high economic cost and ultimately limited global resources of PGM. Both issues were addressed by using bacterial cells to accelerate the reclamation of PGM from waste solutions, and bind the forming PGM particles. Once bound to relatively large bacterial cells, PGM can be concentrated easily, resulting in PGM-coated biomass. While the catalyst/biomass mixture has been shown to be effective in several important reactions [112,113], for use in PEM-FC a more electrically conductive support material is required. Therefore, the organic component must be removed by incineration [216]. It was originally thought (B. Murrer, Johnson-Matthey plc., pers. comm.) that Pd(0) would have little potential in a fuel cell but Yong *et al.* [215,216] showed that a PEM-FC constructed using palladized cells of *D. desulfuricans* produced 81 % the power of the Bio-Pt(0) equivalent and that, contrary to expectations, activity was maintained over several weeks of intermittent operation. This prompted the examination of the ability of *R. sphaeroides* to fulfil a similar function.

MEA were constructed previously [216] using bio-recovered PGM as anode catalysts. In this study the outflow biomass from a continuous H₂-producing *Rhodobacter sphaeroides* culture was salvaged for the biomineralisation of Pd, and the construction of PEM-FC anodes. The 1st stage *E. coli* biomass was retained within the vessel as a resting cell suspension, with the added fluid volume being extracted *via* the electro dialysis membrane (chapter 2.6). In contrast, the PBR operated as a chemostat, with *R. sphaeroides* biomass passing to waste.

2.8.2 Materials & Methods

2.8.2a Preparation of Bio-Pd(0)

Bio-Pd(0) was prepared as described in chapter 2.7 except that *R. sphaeroides* biomass was collected from the outflow of a continuous culture (chapter 2.6) collected over 7 days in 4 batches. As an additional modification, biomass (harvested and washed as chapter 2.7) was mixed with a model leachate solution containing 150 mg/L Pd(II) (414.69 mg/L Na₂PdCl₄, pH 2.0 with HNO₃). Bio-Pd(0) was washed three times in de-ionised water and twice in acetone, dried at room temperature and ground. The model leachate was based on a recovery efficiency of 67 % by a microwave-leaching process reclaiming PGM from solid wastes containing 0.1 % PGM w/w (A. Murray, personal communication).

2.8.2b Construction of fuel cell anode

As described previously [216] the organic component of palladized *Rhodobacter sphaeroides* biomass (*Rs*-Pd(0)) was removed by incineration. The furnace temperature was increased up to 700 °C over 4 h and then held for a further 4 h, resulting in a 92.5 % decrease in mass for palladized *Rs*-Pd samples. As the initial Pd-loading of *Rs*-Pd(0) was 5 % w/w, the resultant material was estimated to be 67 % Pd(0) and 33 % residual material (w/w). For the construction of anodes with an area of 16 cm² loaded with 1 mg Pd(0)/cm², 24 mg incinerated *Rs*-Pd was mixed with 76 mg activated carbon powder (BDH, UK) and suspended in a mixture of 1 ml H₂O and 200 µl Nafion (10 % w/v aqueous suspension, Aldrich). The resultant Nafion density was 12.5 mg/cm² and the Nafion content of the catalytic layer was 16.7 % w/w. The catalyst slurry was transferred onto Teflon-treated carbon paper (Fuel Cell Scientific, USA), spread evenly using a fine paintbrush and dried (2 h, room temperature).

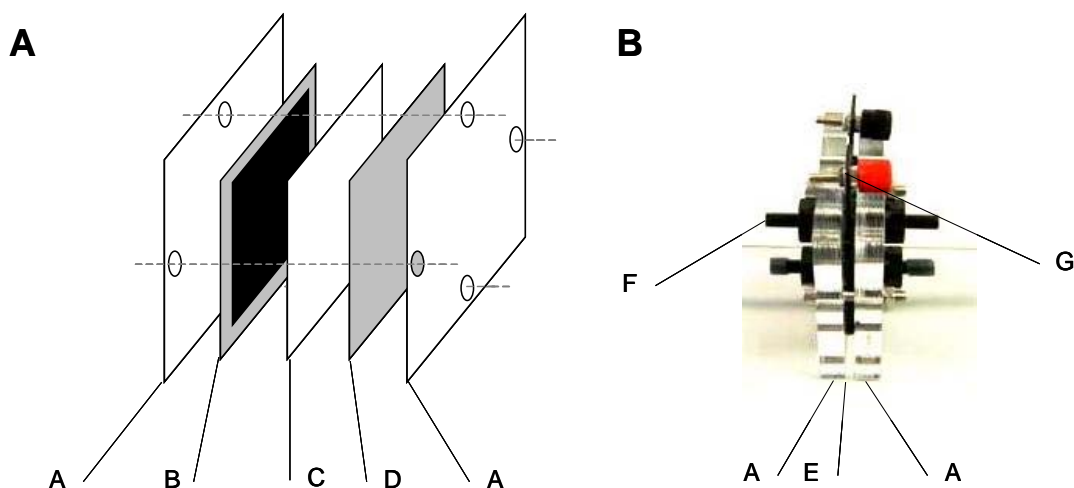


Figure 2.8-a Construction of polymer electrolyte membrane fuel cell with bio-fabricated Pd anode.

A, end-plates; B, 'bio-fabricated' Pd anode; C, Nafion sheet; D, standard Pt cathode (H-tec); E, membrane electrode assembly (MEA); F, Gas inlet; G, electrical terminals.

2.8.2c Fuel cell testing

Fabricated anodes were loaded, catalyst side facing the Nafion membrane, into a single-cell PEM-FC (no. 1919, H-tec, Germany) containing the manufacturer's Pt cathode and Nafion NRE-212 membrane (Sigma-Aldrich) (Figure 2.8-a). An electrolyser (no.1936, H-tec, Germany) supplied pure H₂ and O₂ to the anode and cathode of the PEM-FC, respectively, under *ca.* 5 cm water-pressure. For testing the PEM-FC was connected in a circuit incorporating a variable resistor. The current and voltage across the resistor were measured as resistance was varied through at least 3 cycles (0-∞ Ω).

2.8.3 Results

2.8.3a Power generation by fuel cell with ‘bio-fabricated’ anodes

Four anodes were prepared from different batches of *Rs*-Pd(0) and their power outputs were measured (Figure 2.8-b, part A). The results are inconsistent, reflecting an artefact of the biomass production method employed. *R. sphaeroides* biomass was collected discontinuously from the outflow of a continuous photobioreactor. The rate of outflow was 1 L/d and biomass was routinely harvested in batches of 2 L. Therefore, the cells were stored for up to 48 h under sub-physiological conditions (aerobic, in darkness, room temperature) before harvesting. Batch 4 was an exception as the harvested culture was collected directly from the photobioreactor as the experimental dual system was terminated and was not stored. This methodological discrepancy correlates with the efficacy of the resultant PEM-FC anodes. Batches 1-3 resulted in relatively low and inconsistent power outputs, whereas the power obtained using batch 4 was comparable to that obtained using *E. coli* HD701 (Table 2.8-1 and Figure 2.8-b, part B).

Table 2.8-1 Maximum power outputs from ‘bio-fabricated’ fuel cells

| Source of biomass * | Maximum power | | Max. catalytic efficiency g Pd/kW |
|---------------------------------|---------------|------|--------------------------------------|
| | mW | % | |
| Commercial Pd(0) av. (n=2) | 81.49 | 100 | 245.44 |
| <i>E. coli</i> HD701 av. (n=2) | 27.08 | 33.2 | 738.50 |
| <i>R. sphaeroides</i> batch 4 | 19.45 | 23.9 | 1028.49 |
| <i>R. sphaeroides</i> av. (n=4) | 6.53 | 8.0 | 3062.32 |

* Anodes were constructed using bio-Pd(0) (5 % Pd loading, w/w), manufactured using commercial Pd catalyst, *E. coli* HD701 biomass and *R. sphaeroides* biomass from the outflow of a dual H₂ producing system. Data for *E. coli* and commercial Pd were provided by P. Yong and I.P. Mikheenko. Data represent means of at least 3 measurements. SEM were less than 5 %. The electrode area was 16 cm².

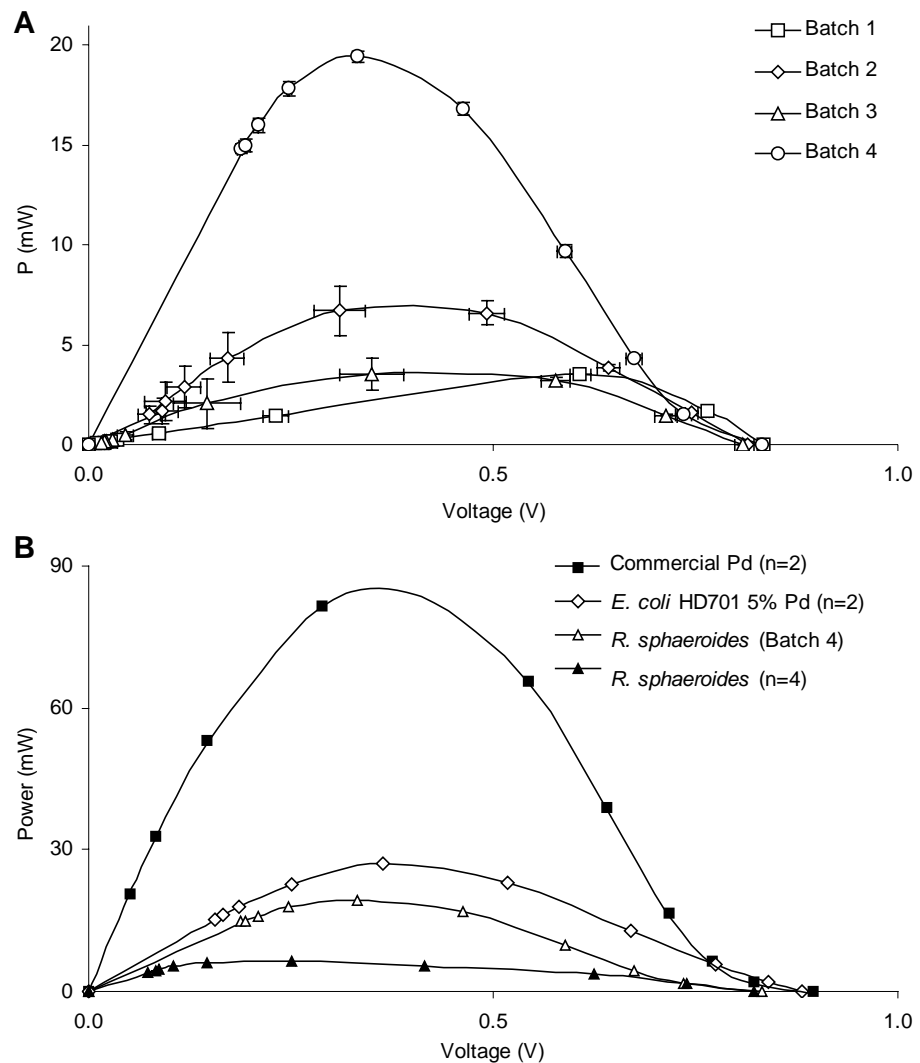


Figure 2.8-b Power output profiles of ‘bio-fabricated’ fuel cells.

Anodes were constructed using incinerated bio-Pd(0), initially 5 % Pd, w/w, manufactured using *R. sphaeroides* biomass from the outflow of a dual H₂ producing system (A) and using *E. coli* HD701 Bio-Pd(0) and using commercial Pd catalyst (B). Data for *E. coli* and commercial Pd were provided by P. Yong and I.P. Mikheenko. Data represent means \pm SEM of at least 3 measurements (A).

Previous experiments (chapter 2.7) used freshly cultured *R. sphaeroides* (and *D. desulfuricans*), and these results demonstrate the importance of the freshness of *R. sphaeroides* biomass for palladization. Therefore, the industrial production of *Rs*-Pd(0) from the output of a dual H₂-production system would be time-sensitive unless biomass can be stored without loss of activity. Refrigeration was not effective for the preservation of *E. coli* cell pellets for palladization (K. Deplanche, pers. comm.). Alternatively, a semi-continuous photobioreactor could be operated by ‘fill & draw’, providing batches of fresh culture, which would be more suitable for Bio-Pd(0) manufacture.

The maximum power output achieved using *Rs*-Pd(0) (batch 4) was broadly comparable to that achieved using *E. coli* HD701 (Table 2.8-1 and Figure 2.8-b, part B). The comparison with commercial catalyst-grade Pd powder provides a suitable reference as published values would not be applicable due to differences in the method of anode construction (see introduction). When the fuel cell was fitted with the manufacturer’s Pt anode power output was 18 % greater than that achieved using anodes home-built using commercial Pt on carbon catalyst [216].

2.8.3b Harvesting biomass from a continuous system

These results indicated the importance of using fresh biomass in Bio-Pd(0) manufacture, which potentially conflicts with the continuous outflow of biomass from the dual system. In order to eliminate the delay between emergence of biomass from the PBR and palladization, the outflow was fed directly into a Pd(II) solution. The outflow biomass concentration was reasonably stable (see Discussion), allowing the Pd loading to be roughly designed. An outflow vessel was filled with model leachate solution and then allowed to fill with outflow culture to 2 L. In this way, the biosorption step of Bio-Pd(0) manufacture was able to occur without delay.

This approach was unsuccessful due to an uncharacterised interaction between soluble, non-cellular material and Pd, resulting in the formation of a ‘Pd-X’ colloid. 63.2 % of Pd mass was not cell-bound but persisted in the supernatant following centrifugation (5-15 mg Pd(0)/L), making the supernatant clear and dark (Figure 2.8-c, part C). Consequently, the Pd(0) loading of biomass fraction was 1.8 % w/w rather than 5 % w/w. The optimal Pd-

loading for anode-fabrication is unclear, but due to the requirement for carbonisation, it is suggested that the use of higher Pd-loadings (i.e. lower organic fraction) would reduce time and energy inputs into incineration.



Figure 2.8-c The effect of medium composition on the precipitation of Pd(0).

75 ml of test-solution was mixed with 25 ml model leachate, reduced under H_2 , 20 min and allowed to settle under gravity overnight (A-C). Test solutions were pure H_2O (A), fresh *R. sphaeroides* medium (SyA) (B), and the supernatant after cell-separation from the outflow of a continuous *R. sphaeroides* culture (C). Pd(0) was absent from the first supernatant upon harvesting *Rs*-Pd(0) produced using washed cells (D).

The influence of chemical background on the precipitation of Pd(0) was investigated (Figure 2.8-c). Normal (i.e. complete) precipitation of Pd(0) was obtained in a background of pure water (Figure 2.8-c, parts A and D) and in fresh *R. sphaeroides* medium (SyA) (Figure 2.8-c, part B). Conversely, the cell-free supernatant collected from a continuous *R. sphaeroides* culture contained interfering components that prevented the precipitation of Pd(0), forming a Pd-X colloid (Figure 2.8-c, part C). This confirmed that the formation of Pd-X resulted from the presence of a soluble substance, absent from fresh medium, suggesting that it may be a product of *R. sphaeroides*. Pd-X was harvested by centrifugal filtration with 100 kDa MW cut-off (Millipore, UK). Fuel-cell construction using the harvested Pd-X was attempted, however the material failed to adhere to the support and investigation is ongoing into the use of surfactants to address this problem. Although the activity was not quantified, the harvested Pd-X was distinctly active in the decomposition of hypophosphite (chapter 2.7) and hence this may be a valuable material worthy of further study.

2.8.4 Discussion

2.8.4a Bio-fabricated Pd(0) fuel cell anode

This study compared catalysts for PEM-FC, using a reliable “vary one factor at a time” approach. As water formation at the cathode results in water balance issues [14], this would confound the investigation of catalyst quality. Therefore, a standard cathode (from the manufacturer) was used while the anode composition was varied so that the effects could be interpreted in terms of catalytic properties, rather than hydrodynamic properties.

The data indicate that Bio-Pd(0) produced using *R. sphaeroides* or *E. coli* can be 24-33 % as effective as commercial Pd catalyst as a material for PEM-FC anode fabrication. It would be anticipated that the bionanocatalysts could be produced more cheaply than the conventional materials due to the possibility of reclaiming PGM and biomass from wastes [33].

The results of the current work confirm the importance of removing competing ligands from biomass (by washing) before the biosorption of $[\text{PdCl}_4]^{2-}$ ion, which was studied previously [38]. For the preparation of cell-bound Pd(0) particles, the freshness and chemical purity of the biomass are important factors. This should be considered during the design of a pilot-scale dual system as biocatalyst production may be economically important. For industrial operation, the production of H_2 and catalyst could be reconciled by preserving the activity of the outflow biomass (e.g. by maintaining reaction conditions), by producing bionanocatalyst 24 h in shifts, or by an automated continuous harvesting and palladization system.

2.8.4b Catalyst productivity estimate

There is sufficient data for a preliminary estimate relating the scale of a dual bioreactor system for H_2 production with the potential productivity of bionanocatalyst.

With the current configuration, no excess *E. coli* biomass was produced by the dark fermentation as ED provided inherent cell retention and water transport. Likewise, a scaled-up photobioreactor would ideally utilise a cell-separation system to return solvent to the permeate chamber and biomass to the photobioreactor (Figure 2.6-a, part A). Although cell retention may initially increase the volumetric activity in both reactors, it is anticipated that optimum biomass concentrations exist. For the dark fermentation, the optimum may be very

high - where viscosity limits mixing and diffusion. However, for the photofermentation, culture density may be limited to *ca.* 2-4 g DW/L due to light limitation (self-shading) (see chapter 2.3).

Therefore, a long-term dual bioreactor system would produce excess biomass from both cultures. Their quantities are estimated based on data from the experimental system, which processed 60 mmol glucose/day. The average production rate for *E. coli* HD701 biomass was 0.60 g dw/day for a 3 L culture (Figure 2.8-d, part A). Therefore, with a Pd loading of 5 % w/w, the productivity of *Ec*-Pd(0) would be 0.21 g/day/L culture. The *R. sphaeroides* cultures eventually reached a stable biomass concentration of *ca.* 1 g/L, for 3 L culture (Figure 2.8-d, part B). As the rate of dilution was 1 L/day the biomass productivity was *ca.* 1 g/day and a Pd-loading of 5 % w/w would indicate a productivity of 0.35 g/day/L culture.

Therefore the total output can be estimated as 0.28 g catalyst/day/L total culture. Given a PGM-loading of 5 % (w/w), this productivity would reclaim 28 mg PGM/day/L culture from 0.19 L leachate/day/L culture, assuming 150 mg PGM/L leachate (A. Murray, personal communication).

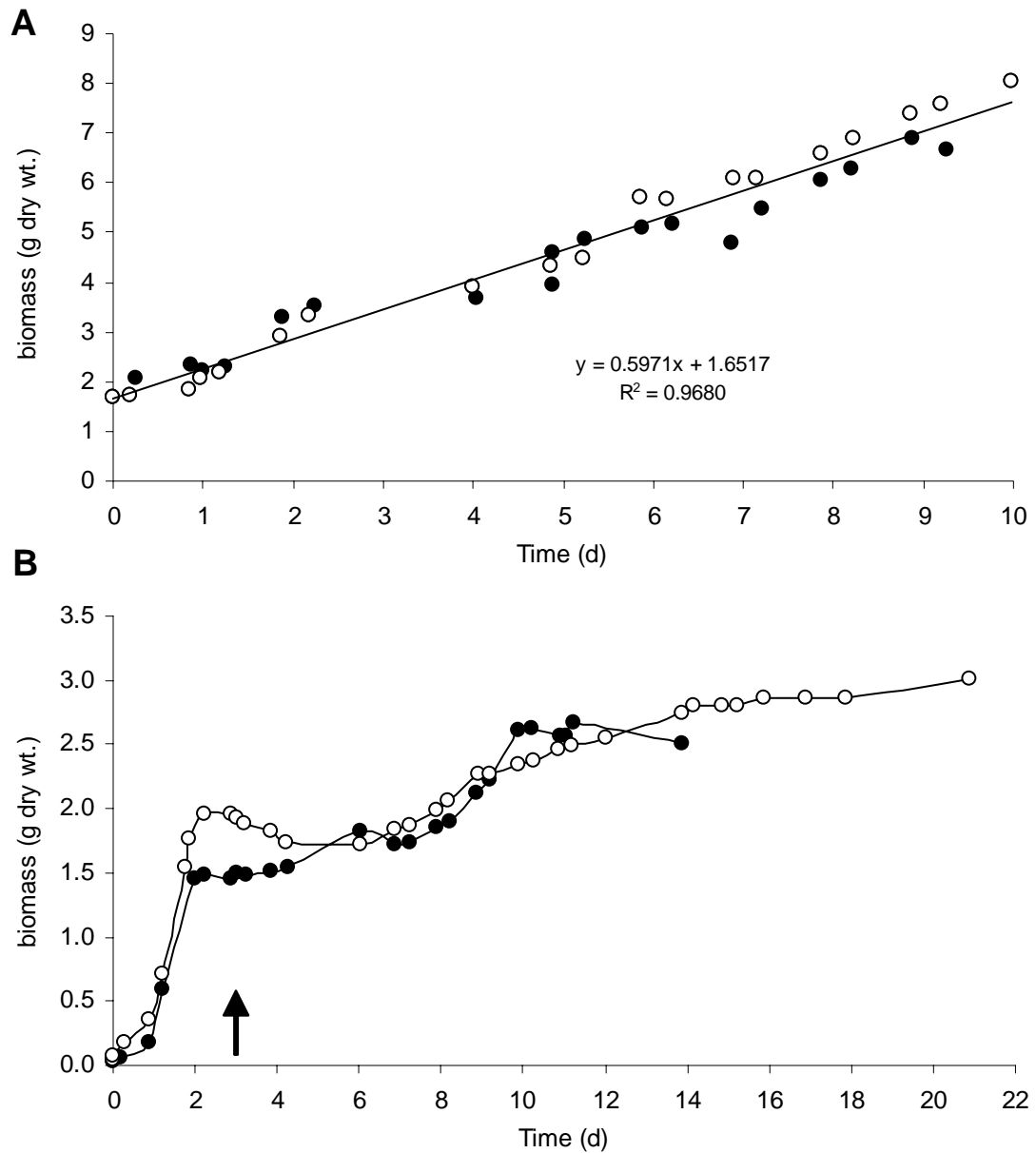


Figure 2.8-d Production of *Escherichia coli* HD701 (A) and *Rhodobacter sphaeroides* (B) biomasses by a dual-bioreactor system for H₂ production.

Data correspond with Ec3/Rs3 experiments (chapter 2.6), which were performed in duplicate (open and filled circles). Reactor volumes for *E. coli* and *R. sphaeroides* reactors were ca. 3 L. The arrow indicates the onset of dilution of the *R. sphaeroides* culture at a rate of 1 L/day.

However, these figures are subject to several caveats. For example, *E. coli* may grow more rapidly on complex medium (e.g. food wastes) containing ready sources of nitrogen (e.g. amino acids), whereas these experiments used a ‘poor’ glucose/NH₄⁺ medium (described in chapter 2.2). Furthermore, the suitability of *E. coli* biomass for palladization would be dependent upon the nature of the feedstock. A significant quantity of solids would confound cell harvesting and may also foul the reactor, possibly necessitating the separation of insoluble components from *E. coli* biomass by coarse filtering post-fermentation, or by pre-treatment of the feedstock. Palladization of waste *E. coli* after H₂ production from food wastes has not yet been attempted. The biomass output from the photobioreactor would be affected by various factors, such as the HRT, influent composition, light supply and bacterial strain, which are likely to differ after further development.

Excess catalyst would be available as a product given a productivity of 0.28 g catalyst/day/L total culture (above), which would exceed considerably, the mass of catalyst required in the construction of a PEM-FC with sufficient capacity to utilise the produced H₂, according to the following calculation. A dual system producing 8 mol H₂/mol glucose and processing 60 mmol glucose/day, would produce 0.48 mol H₂/day, with a potential energy value of 137.2 kJ. A realistic PEM-FC may operate with an efficiency of 50 % and a H₂ utilisation of 95 % [100,101]. Therefore, the produced H₂ could be converted to 65.18 kJ electrical energy/day, equivalent to a constant power of 0.754 W. Based on the basic methods and preliminary results of this study (hand-painting, 1 mg Pd/cm², 0.98-1.36 mW/cm², 739-1028 g Pd/kW), a large quantity of catalyst would be required. However, modern electrode construction techniques can produce efficiencies in the range 0.1-1 g Pd/kW [204]. Therefore, the necessary anode could be constructed using relatively insignificant quantities of catalyst and biomass, leaving a catalytically active product for alternative commercial exploitation.

The effectiveness of bio-recovered mixed PGM catalysts as substitutes for pure Pt on the anode and cathode of PEM-FC is a subject of ongoing investigation.

3 : DISCUSSION

3.0 Chapter summary and contents

This project achieved its primary goal – proof of principle for each component of a dual system for H₂ production: dark fermentation, transfer of produced organic acids, photofermentation using the transferred organic acids and the manufacture of bionanocatalyst using biomass from the dual-bioreactor system. In this section, the project outcomes and future directions are summarised (Table 3-1), the components of the system are discussed individually and the bottlenecks identified. Finally the environmental implications of the applied dual system and challenging aspects for further development are discussed.

| | |
|--|-----|
| 3.1 Dark fermentation by <i>Escherichia coli</i> | 201 |
| 3.1.1 Genetic manipulation of <i>Escherichia coli</i> for increased H ₂ production..... | 201 |
| 3.1.2 Increasing the substrate range of <i>Escherichia coli</i> | 201 |
| 3.1.3 Mass pre-culture of <i>Escherichia coli</i> | 202 |
| 3.2 Photofermentation by <i>Rhodobacter sphaeroides</i> | 203 |
| 3.2.1 Rates, yields and operating conditions | 203 |
| 3.2.2 Butyrate utilisation | 204 |
| 3.3 Integrating the dual bioreactor by electro dialysis..... | 205 |
| 3.3.1 Benefits of electro dialysis | 205 |
| 3.3.1a Electrolysis | 205 |
| 3.3.1b Butyrate fermentation and transport..... | 205 |
| 3.3.2 Demand-responsive electro dialysis | 205 |
| 3.3.3 Membrane lifespan | 206 |
| 3.3.4 Ethanol..... | 206 |
| 3.3.5 Current efficiency | 207 |
| 3.4 Biomass-supported palladium catalyst | 209 |
| 3.5 Environmental impacts | 210 |
| 3.5.1 Potential CO ₂ offsetting..... | 210 |
| 3.5.2 Apple waste scenario | 210 |
| 3.6 Prominent technical challenges for future development | 213 |
| 3.6.1 Photobioreactor development | 213 |

Table 3-1 Summary of outcomes

| Element | Outcomes | Future directions |
|----------------------------|---|--|
| Dark fermentation | <p>Stable and continuous H₂ production with 80 % efficiency using <i>E. coli</i> HD701</p> <p>Increased H₂ yield using hydrogenase mutants.</p> <p>Optimised pH.</p> <p>Improved pre-culture method.</p> <p>Characterised butyrate-type fermentation in <i>E. coli</i>.</p> | <p>Food wastes in continuous culture.</p> <p>High density fermentation.</p> <p>Strain development to further increase yield and broaden substrate range.</p> <p>Further investigation to confirm the metabolism of butyrate-type fermentation in <i>E. coli</i>.</p> <p>Prevent production of uncharged products (ethanol).</p> |
| Photo-fermentation | <p>Definition of nutritional requirements for H₂ production from acetate.</p> <p>Construction of chemostat-type photobioreactor system.</p> <p>Stable and continuous H₂ production with 1.5 % light conversion to H₂, 38 % substrate conversion to H₂ and 64 % substrate utilisation using <i>R. sphaeroides</i></p> | <p>Optimisation of continuous culture conditions to increase substrate utilisation and conversion to H₂.</p> <p>Strain development to eliminate H₂ recycling and PHB synthesis.</p> <p>Design of an industrial-scale PBR.</p> |
| Dual System | <p>Exhaustive review of previous studies on dual systems.</p> <p>Demonstration of the need for selective organic acid transfer to enable the use of nitrogen-rich substrates.</p> <p>Demonstration of organic acid transport with NH₄⁺ retention by electro dialysis.</p> <p>Stable and continuous operation of dual bioreactor system integrated by electro dialysis.</p> <p>Demonstration of control of NH₄⁺ transport <i>via</i> electro dialysis.</p> | <p>Balancing the capacity of two reactors to operate in concert.</p> <p>Control of NH₄⁺ supply to PBR in response to growth requirements.</p> <p>Development and optimisation of electro dialysis.</p> <p>Achieve separation of uncharged products (ethanol).</p> <p>Increase molar conversion towards theoretical maximum.</p> <p>Mass balance of dual system.</p> <p>De-fouling of ED membranes.</p> |
| Biomass-supported catalyst | <p>Confirmed efficacy of <i>R. sphaeroides</i>-supported Pd catalyst in environmentally and industrially valuable reactions.</p> <p>Prepared Pd catalysts using <i>R. sphaeroides</i> biomass as a product of the dual system, recycled in the fabrication of PEM-FC anodes.</p> | <p>Reconcile discontinuous catalyst preparation with continuous biomass production.</p> <p>Further characterisation of Pd-X colloid.</p> <p>Effect of strain development on the catalytic properties of resultant catalyst.</p> <p>Metal recovery from industrial leachate using <i>R. sphaeroides</i>.</p> <p>Effect of light during metal challenge</p> |

PEM-FC, polymer electrolyte membrane fuel cell; ED, electro dialysis; PBR, photobioreactor. Pd-X; uncharacterised Pd suspension (chapter 2.8).

3.1 Dark fermentation by *Escherichia coli*

3.1.1 Genetic manipulation of *Escherichia coli* for increased H₂ production

E. coli is capable of producing H₂ with a maximum yield of 2 mol H₂/mol glucose [32]. As described in chapter 2.6, stable and continuous H₂ production with a yield of 80 % (1.6 mol H₂/mol glucose) was achieved in continuous culture using strain HD701 (Δ HycA), which was also effectively deficient in lactate formation due to a switch to butyrate-type fermentation (see section 2.2.4b). Previously the genetic suppression of lactate formation resulted in improved H₂ production (Δ ldh phenotype) [119,178,179] as did the suppression of succinate formation (Δ frd phenotype). Yoshida *et al.* (2006) achieved a H₂ yield of 90 % in batch cultures using *E. coli* strain SR15, in which the formation of lactate and succinate were suppressed and FHL activity was promoted (Δ HycA, FhlA⁺⁺, Δ ldh, Δ frd phenotype). In this study (chapter 2.1) experiments using batch cultures showed that genetic manipulation to suppress H₂ recycling activity increased the H₂ yield from 38 % to 52 %. Future development would ideally combine these improvements in a single ‘super-strain’ (Δ HycA, FhlA⁺⁺, Δ ldh, Δ frd, Δ Hyd-1, Δ Hyd-2) potentially resulting in H₂ yields approaching 100 %.

3.1.2 Increasing the substrate range of *Escherichia coli*

Further strain development may be needed to enable the utilisation of certain substrates, such as sucrose. Penfold *et al.* (2004) described the transformation of *E. coli* (various strains) with plasmid pUR400 carrying sucrose-utilisation genes [147]. To achieve efficient H₂ production using sucrose-feedstocks (e.g. sugarcane juice) a H₂-overproducing strain (e.g. Δ HycA, FhlA⁺⁺, Δ ldh, Δ frd, Δ Hyd-1, Δ Hyd-2, see above) could be transformed with pUR400. Another issue is the utilisation of lactose, a capacity lacking in MC4100-derived strains including HD701 and the hydrogenase deficient strains (chapter 2.1). Wild-type *E. coli* is lac⁺, and the lac⁻ phenotype of strain MC4100 (used as parent in *E. coli* strain development) is advantageous for the purpose of genetic engineering as it permits blue/white selection on solid medium containing a marker (blue: lac⁺). Re-introduction of the lac⁺ phenotype in a future ‘super-strain’ does not represent a significant barrier. Conversely, the utilisation of more difficult substrates such as starch or lingo-cellulose by *E. coli* would require significant metabolic engineering and abiotic pre-treatment may be a more viable approach. Lignocellulosic biomass requires initial delignification by mechanical or chemical means (milling or alkaline hydrolysis) leaving cellulose and hemicellulose [31,78]. Although

cellulose-utilising microorganisms are available [139,195], hydrolysis is the rate-limiting step, hence pre-hydrolysis can be advantageous. Available hydrolytic methods include enzymatic treatment [59], acidic steam-explosion [35,153], biomimetic catalysis [109] or ohmic heat-treatment [149].

3.1.3 Mass pre-culture of *Escherichia coli*

A system is also needed for the mass culture of ‘primed’ *E. coli*, expressing the biochemical machinery for H₂ production. As demonstrated in chapter 2.1, H₂ production occurs anaerobically, therefore anaerobically grown *E. coli* is metabolically prepared for H₂ production but the anaerobic growth is very slow. A more efficient means of generating *E. coli* for H₂ production is aerobic pre-growth with sodium formate (see chapter 2.1), although further investigation is needed to optimise the formate-induction of FHL and minimise the use of sodium formate. *E. coli* culture densities of up to 50 g/l were achieved in continuous aerobic cultures [64]. An effective approach could entail a continuous aerobic pre-culture to load *E. coli* biomass progressively into an anaerobic H₂-producing reactor. The anaerobic vessel would also be fed with substrate, but may require no overflow due to the inherent cell-retention and fluid-transport properties of electro dialysis. A cost-benefit analysis is needed to investigate the induction of H₂ producing capacity in aerobically cultured *E. coli*. The induction of FHL activity in aerobically-grown *E. coli* was investigated previously [218]. The maximum FHL activity was half of that achieved in anaerobically-grown cells but only post-growth induction was investigated in this case and not the addition of formate into the aerobic growth medium as described in chapter 2.1.

3.2 Photofermentation by *Rhodobacter sphaeroides*

3.2.1 Rates, yields and operating conditions

Chapters 2.3 and 2.6 describe a photobioreactor (PBR), which was operated continuously in chemostat mode, achieving stable and continuous H₂ production from organic acids produced by *E. coli* and transported by electro dialysis. Improvements are needed in the efficiency of the photosynthetic component, which would ideally provide 70-80 % of the total bio-H₂ output, but in the experimental dual system consumed only 64 % of the supplied substrate (on the basis of carbon) and produced H₂ with a substrate conversion efficiency of 38 %, resulting in an overall contribution of only one third of the total bio-H₂. The losses in substrate conversion efficiency may be attributable to the activity of competing pathways. In this study a wild-type strain (O.U. 001) was used but, as described in chapter 1.2, significant improvements in H₂ production by PNS bacteria can be achieved through genetic manipulation, e.g. to decrease H₂ uptake activity, to prevent the formation of storage polymer and to truncate the light harvesting antennae of the photosystem in order to increase the point of light saturation (see 3.6.1). Such alterations may be necessary in order to improve the efficiency of H₂ production in the PBR. However, substrate conversion efficiencies of up to 75 % were reported for continuous cultures of wild-type PNS bacteria [25,45,162] (chapter 2.3) and the observed inefficiency may also result from sub-optimal culture conditions such as the balanced supply of light, carbon-source and nitrogen-source. Further work is required to establish the optimum conditions, e.g. with respect to the ability of ED to deliver organic acids and also a controlled amount of NH₄⁺ (for growth).

This study aimed to achieve stable and continuous H₂ production, although perfectly stable output would not be feasible in a developed system under diurnal (solar) illumination. The PBR operated as a continuously illuminated chemostat, although a fill-and-draw method may be more suitable for PNS bacteria having a relatively low specific growth rate [25] and would also be more compatible with bionanocatalyst manufacture (see 3.4). Although practically more complex, a fill-and-draw method may be more readily incorporated with diurnal illumination as the relative timings of N-source addition, medium exchange and dark periods can affect H₂ production [125].

3.2.2 Butyrate utilisation

As described in chapter 2.3 *R. sphaeroides* was grown using a medium containing a mixture of organic acids. Different organic acids were consumed to different extents, such that 99.8 % of lactate, 77.0 % of succinate, 65.7 % of acetate but only 10.9 % of butyrate were consumed. Similarly in the dual system (chapter 2.6), a mixture of organic acids (predominantly butyrate) was supplied to a chemostat-type culture, of which 93.8 % of lactate, 84.8 % of acetate and 55.5 % of butyrate were consumed. All of these substrates are known to be suitable substrates for *R. sphaeroides*, yet the relatively low uptake of butyrate is unexplained. It is known that the consumption of organic acids which are relatively oxidised compared to the cell material results in CO₂ production, whereas the utilisation of more reduced organic acids requires CO₂ uptake. For example 0.7 mol CO₂ was utilised per mol butyrate consumed, whereas 0.17 mol/mol was produced from acetate and 0.7 mol/mol was produced from succinate [184]. It is likely, therefore, that the incomplete utilisation of butyrate was, in part, due to a requirement for exogenous CO₂, although the addition of CO₂ (or bicarbonate) is not common practice for butyrate-fed photofermentations (e.g. [26]). If a CO₂ requirement can be confirmed, it would be logical to purge the PBR with the off-gas from the *E. coli* reactor (containing *ca.* 40 % CO₂) and also to incorporate headspace recirculation [66]. However, other explanations cannot be ruled out, for example the uptake mechanisms for butyrate may be less effective than those for other organic acids (e.g. lactate and succinate), or the expression of enzymes performing the decomposition of butyrate to acetyl-CoA [184] may require stimulation.

3.3 Integrating the dual bioreactor by electro dialysis

3.3.1 Benefits of electro dialysis

Electro dialysis (ED) was an effective technique for the integration of dark fermentation and photofermentation, solving the key bottleneck of ammonium inhibition of the photobioreactor, while simultaneously providing pH control, cell-retention and water extraction from the *E. coli* culture along with a tertiary H₂ stream (chapter 2.6)

3.3.1a Electrolysis

Additional H₂ resulting from electrolysis (electro-H₂) was produced in similar quantity to bio-H₂ by the experimental system. However, the ratio of bio-H₂ to electro-H₂ was low in this study due to the under-production of bio-H₂ by the photobioreactor. If the bio-H₂ yield were to improve to 8 mol H₂/mol glucose under similar conditions, then the proportion of electro-H₂ would be *ca.* 24 %. It is expected that the electro-H₂ stream would scale up proportionally with the bio-H₂ stream. Faraday's 1st law states that that 'the mass of a substance produced at an electrode during electrolysis is proportional to the quantity of electricity passed'. As the requirement for organic acid transfer would scale proportionally with the feed-processing capacity of the bio-H₂ system, the size and power of ED cell would follow, and hence the rate of electro-H₂ production.

3.3.1b Butyrate fermentation and transport

In chapter 2.5 it was found that butyrate is the primary organic acid produced by *E. coli* during long-term culture, which is beneficial because butyrate is particularly economical to transport by ED, having a very high photosynthetic H₂ production potential (10 mol H₂/mol butyrate) and a single ionic charge (chapter 2.5. Complete consumption of butyrate by the *R. sphaeroides* culture may require CO₂ addition (see section 3.2.2).

3.3.2 Demand-responsive electro dialysis

In this study a constant current was applied to the ED cell and no attempt was made to modulate ED according to the requirements of the PBR or in relation to organic acid production. It was shown (chapter 2.5.2c) that the rejection of NH₄⁺ by anion selective membranes (ASM, Neosepta AHA) is incomplete and related to the applied current. Although in this study, the nitrogen requirements of the PBR were provided using yeast

extract, there is potential to provide a metered supply of NH_4^+ to an *R. sphaeroides* culture by modulating the current applied to ED in response to growth requirements. NH_4^+ can provide a suitable nitrogen-source for H_2 producing cultures of PNS bacteria if supplied in carefully controlled quantities [125].

3.3.3 Membrane lifespan

A further observation regarding ASM was that prolonged use at high current density was detrimental to transport activity. ASMs, therefore have a lifespan, which may be very long under ideal conditions but nevertheless could significantly affect the economic feasibility of the system as ASM are very expensive (*ca.* £400/m² for Neosepta AHA). An economic analysis is to be carried out after optimisation of the process.

3.3.4 Ethanol

A significant limitation of the ED approach was the lack of ethanol transport by the ASM, which detracted a potential 3.6 mol H_2 /mol glucose from the overall yield (chapter 2.6). ASM are non-selective to non-polar molecules and it is possible that a small quantity of ethanol diffused into the permeate chamber although this was not monitored. Ethanol formation plays a key role as the primary ‘electron sink’ in anaerobic fermentation in *E. coli* [32]. Hence, to eliminate ethanol formation through metabolic engineering would be to transplant pathways, rather than genes, from another organism. Taking an example from bioethanol production (see chapter 1.2; review article section 4) membrane technology is now sufficiently advanced to provide ethanol recovery in the dual system and an additional membrane extraction step to utilise the bioethanol from *E. coli* is feasible but the economic attractiveness of this solution requires detailed investigation.

As described in chapter 2.2, alternative fermenting bacteria (e.g. clostridia) are also promising organisms for H_2 production, in which solventogenesis can be suppressed. However the enterobacteria offer the important advantages of rapid growth, (relatively) facile genetic manipulation, absence of sporulation and the possibility to eliminate H_2 uptake (which is impossible in other groups because H_2 formation and uptake are carried out by bi-directional hydrogenase). Therefore no metabolic system can be considered ideal and it may be worthwhile to attempt to supplant acetate/butyrate-type fermentation (e.g. as *Clostridium*

acetobutylicum, see chapter 2.2) into an enterobacterium such as *E. coli*. However, alternative methods for ethanol transport would be more feasible in the short-term. For example an alternative approach (Figure 3-a) could entail conventional membrane dialysis for the separation of all fermentation products (and cell retention), followed by the removal of NH_4^+ from the permeate by cation-selective ED, before supplying the remaining substrates to *R. sphaeroides*. The separated NH_4^+ and minerals could be recycled to the *E. coli* reactor or pre-cultivation. An advantage of this approach would be the facile control of NH_4^+ supply to *R. sphaeroides* by controlling the extent of NH_4^+ removal. However, membrane dialysis is known to suffer from fouling [99,181,220] and it may be difficult to prevent the diffusion of unfermented sugars along with the products. A trade-off would be sought between high dilution rate, needed to minimise the accumulation of organic acids, versus the washout of unfermented substrate and membrane fouling. Furthermore, potentially inhibitory nitrogen sources such as proteins having high molecular weight would not be separated by this means. In conclusion, 3.6 mol H_2 /mol glucose (attributable to untransported ethanol) may be a worthwhile sacrifice for the benefits of the ASM-ED approach.

3.3.5 Current efficiency

In this work, the efficiency of organic acid transfer (current efficiency) was variable, but typically greater than 13 % (see chapter 2.6); the hypothetical efficiency at which the H_2 energy resulting from ED (i.e. from electro- H_2 and photosynthetic H_2) would offset the electrical energy input into ED (the BCE, see chapter 2.4). The activity of ED may be affected by such conditions as medium composition (e.g. specific salts, cationic buffers, amino acids and proteins), culture density, cell immobilisation, improvements in ASM formulation and de-fouling. Optimisation of these factors was not attempted in this study and represents an important aspect for further development.

3.3 Discussion – The application of electro dialysis in a dual system

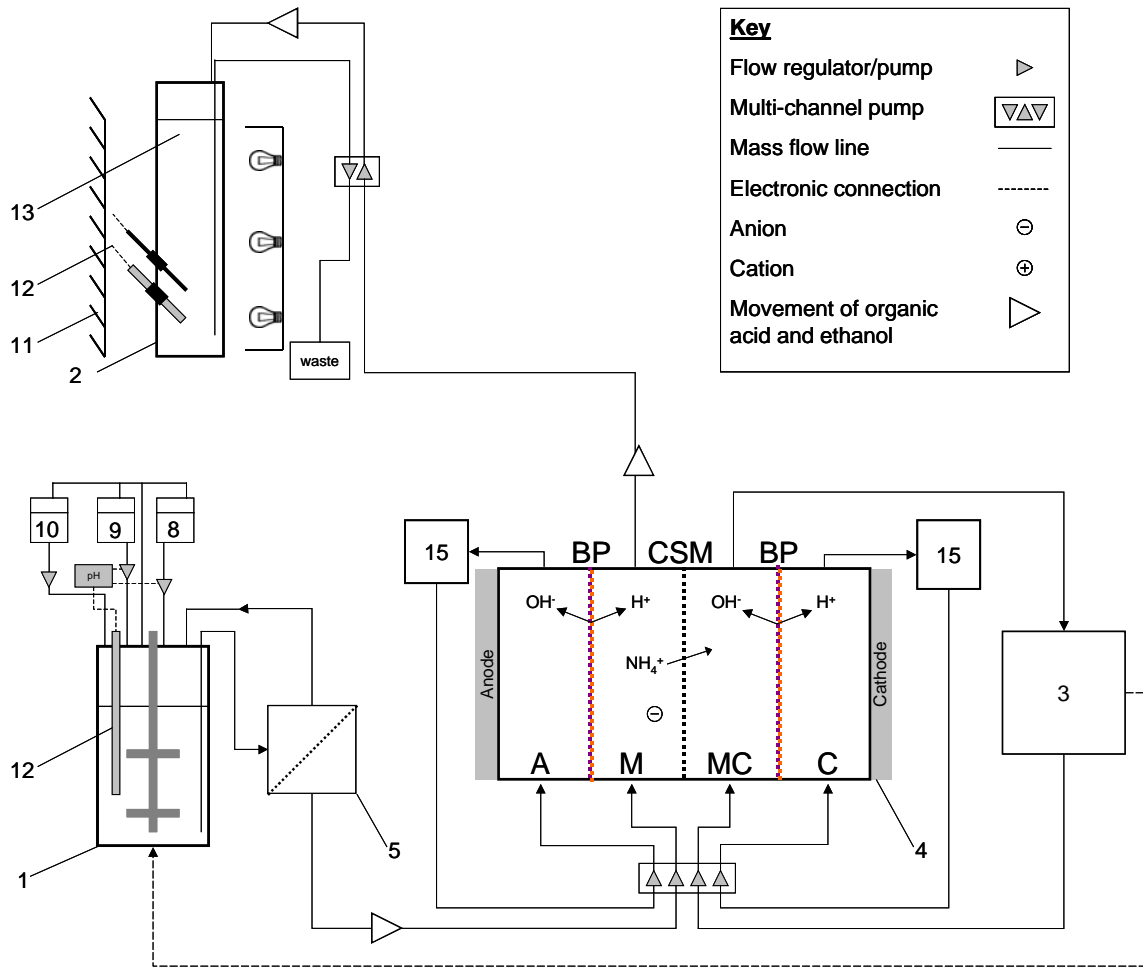


Figure 3-a An hypothetical application combining electro dialysis and membrane dialysis for the non-specific transport of fermentation products.

1, dark fermentation vessel; 2, photobioreactor; 3, permeate vessel; 4, electro dialysis cell; 5, dialysis membrane unit; 8, base titrant; 9, acid titrant; 10, feed solution; 11, tubular reflective sheath; 12, pH sensor; 13, cooling tube (stainless steel); 14, magnetic stirrer and follower; 15, electrode wash vessel (single vessel to lessen pH change); BP, bi-polar membrane; CSM, cation-selective membrane; C, cathode chamber; A, anode chamber; M, main chamber delivering organic acids, ethanol and NH_4^+ from fermentation vessel (1); MC, permeate receiving cations including NH_4^+ . For comparison with experimental configuration, see Figure 2.6-a.

3.4 Biomass-supported palladium catalyst

The dual-bioreactor system produced two kinds of biomass: *E. coli* and *R. sphaeroides* (predominantly the latter), both of which can be effective supporting biomaterials for PGM recovery and catalysis using Bio-Pd(0) [34,215]. This study represents the first investigation of bio-Pd(0) production using a photosynthetic organism, however the question of how photosynthetic metabolism might affect the pre-patterning of metal reduction was not addressed as incubations were performed in darkness, so as to adhere to a single preparation method. Further investigation of the catalytically active Pd-X colloid may also be justified (see section 2.8.3b).

The reconciliation of the necessary conditions for effective catalyst production with the continuous production of biomass is a problem, which may be resolved either *via* semi-continuous photofermentation (i.e. fill-and-draw) or by preserving the outflow biomass before catalyst manufacture, as discussed in chapter 2.8.

Rs-Pd(0) was effective in the manufacture of anode catalyst for PEM-FC and it was calculated that the excess biomass from the dual system could significantly exceed the required biomass for the production of sufficient fuel-cell catalyst for use within the process, leaving an excess for commercial catalyst production (chapter 2.8).

Issues for further investigation relevant to industrial bionanocatalyst manufacture include:-

- Supply and logistics of PGM leachates
- Adaptation of the manufacturing process to utilise continuously produced biomass, or of the dual system to provide biomass discontinuously
- Scale up of the biocatalyst manufacturing process

3.5 Environmental impacts

3.5.1 Potential CO₂ offsetting

The dual-bioreactor system for H₂ production represents a strategy for sustainable and carbon-negative energy production. The potential for carbon offsetting can be calculated based on the preliminary data obtained in this study. The system has the potential to offset CO₂ and CH₄ emissions in three ways:-

- **Offset conventional energy production.** Electricity exported to the grid would detract from the demand on power generation from fossil fuels. The CO₂ cost of energy is 0.72 kg CO₂/kWh using a coal fired power plant or 0.37 kg CO₂/kWh using a modern gas-fired power plant [187].
- **Divert waste from land-filling and avert resultant emissions.** Each tonne of biodegradable waste land-filled produces 200-400 m³ land-fill gas which is 40-45 % CO₂ and 55-60 % methane (v/v), a much more potent ‘green-house’ gas [51,164].
- **Retain C in solid state.** The process generates bacterial cell mass as a useful by-product, which is dried to produce a stable powder (*ca.* 50 % C w/w) to be used as a catalyst, preventing degradation to form CO₂. The process generates *ca.* 26.7 g dry cell mass (i.e. retains 14.3 g C and prevents the formation of 48.9 g CO₂) per mol hexose processed.

3.5.2 Apple waste scenario

A scenario was constructed to estimate the energy productivity and environmental benefits of the dual system. Fruit waste was shown to be a suitable feedstock for the system [149], hence the scenario was based on apple, which contains a high density of available sugars along with potentially useful polysaccharides, proteins and organic acids, which were not taken into account (Table 3-2).

Table 3-2 Free-sugars content of apple

| Component | Content (mol hexose/tonne apple) | Fermentable in <i>E. coli</i> |
|--------------|----------------------------------|-------------------------------|
| glucose | 122.67 | Yes |
| fructose | 335.26 | Yes |
| sucrose | 144.32 | Yes ^a |
| Total | 602.24 | |

Apple composition data were retrieved from www.food-allergens.de. Apple also contains 33.3 mol starch-hexose/tonne, excluded from the total due to the requirement for hydrolysis. Protein, lipid, fibre, amino acids and organic acids are also excluded. ^a Sucrose utilisation was achieved in *E. coli* using a sucrose-utilisation plasmid [147].

According to the constructed scenario (Table 3-3), the dual system could achieve significant environmental benefits.

Table 3-3 Scenario for H₂ production from apple waste

| | | |
|------------------------------|------------|--|
| <u>Input</u> | | |
| mass | 1 | tonne |
| hexose | 602.0 | mol |
| fraction extracted | 421.6 | mol hexose/tonne apple (70 %) ^a |
| <u>Productivity</u> | | |
| gaseous | 8 | mol H ₂ /mol hexose (projected) |
| | 3370 | mol H ₂ /tonne apple |
| | 172 | kWh/tonne apple ^b |
| | 549 | mol CO ₂ per tonne apple (14 % of total gas) ^c |
| | 24.2 | kg CO ₂ per tonne apple (14 % of total gas) ^c |
| dry cell mass | 26.7 | g dry cell mass/mol hexose (50 % C, w/w) |
| | 11.3 | kg dry cell mass/tonne apple |
| | 20.6 | kg CO ₂ fixed in biomass/tonne apple |
| <u>Offsetting</u> | | |
| power generation | 124 | kg CO ₂ /tonne apple -coal-fired plant ^d |
| | 63.7 | kg CO ₂ /tonne apple - gas-fired plant ^d |
| land-filling | 200-400 | m ³ land-fill gas/tonne apple ^e |
| | 1.15-2.59 | kg CO ₂ /tonne apple |
| | 0.570-1.25 | kg CH ₄ /tonne apple |
| <u>Totals</u> | | |
| offset CO₂ | 85.5-147 | kg CO ₂ /tonne apple |
| offset CH₄ | 0.570-1.25 | kg CH ₄ /tonne apple |
| <u>Equivalents</u> | | |
| offset GHG | 700-1300 | Km driven in a Fiat punto ^f |
| energy produced | 4 | months running a 60 W lightbulb constantly |
| | or | |
| | 1 | week running a home at 1 kW constantly |

Values are presented to 3 significant figures.

^abased on the extraction of sucrose from sugarcane

^bproduction of electricity from H₂ using a fuel cell operating at 50 % efficiency and 95 % utilisation [100].

^cwhich is not considered an emission, being derived from recently fixed CO₂.

^d0.72 kg CO₂/kWh for a coal or 0.37 kg CO₂/kWh for natural gas [187].

^elandfill gas is 40-45 % CO₂ and 55-60 % CH₄ (v/v). It is assumed that landfill gas is an emission and no recovery takes place.

^fbased on driving emissions of 136 g CO₂/km, and CH₄ having a global warming potential (GWP) of 25 (100-year basis, relative to an equal mass of CO₂) [51].

To summarise Table 3-3, processing 1 tonne of apple waste using the dual system instead of simply burying it (without landfill-gas recovery), is estimated generate sufficient power to meet the demand of a home for 1 week and to prevent greenhouse gas emissions equivalent to driving *ca.* 1000 km in a small car. However, the analysis should be interpreted with care, as further development is required before several factors can be taken into account. In particular, the scenario was based on the assumption of all produced electricity being exported to the grid because the proportion of the produced energy, needed to run the bio-H₂ system is unknown at this stage. This could be a significant detractor from the offset CO₂, which is derived partly from electricity exported to the grid to displace conventional energy production. Also, it is likely that some depreciation of the substrate would occur prior to fermentation, detracting from the quoted free-sugars content (Table 3-2), whereas the excluded components (see legend to Table 3-2) may enhance the calculated potential for H₂ production.

Further development is required preceding a complete economic analysis as summarised in Table 3-4.

Table 3-4 Technical aspects requiring development prior to an economic assessment of the dual system

| Bottleneck | Possible solutions |
|--|---|
| Low substrate conversion efficiency in PBR | Strain development (addressing HUP and PHB) Optimisation of culture conditions |
| Practicality and cost of large PBR | Use of cheap materials Light focussing from robust collectors into compact PBR |
| Limitation of H ₂ yield from dual system due to uncharged <i>E. coli</i> products (ethanol) | Alternative membrane separation (e.g. Figure 3-a) Metabolic engineering to remove ethanol from <i>E. coli</i> Alternative fermenting bacteria |

PBR, photobioreactor; HUP, H₂ uptake activity; PHB, poly-β-hydroxybutyrate (a storage polymer accumulated by *R. sphaeroides*).

3.6 Prominent technical challenges for future development

Following the development of commercially ready technology, questions relating to business and logistical aspects must be addressed. Inputs to the process requiring sourcing include sugar (e.g. from fruit waste or an energy crop), PGM leachate (e.g. from autocatalyst scrap), both of which are available, and the time for establishing supply contracts would be at pilot-scale process demonstration, but detailed consideration of these issues is beyond the remit of this study. Of more basic importance are technical bottlenecks, of which several are outlined in Table 3-4, along with possible solutions. A particularly challenging technical bottleneck is the long-term economic validity of an industrial-scale photobioreactor.

3.6.1 Photobioreactor development

Large scale industrial photobioreactors (e.g. 700 m³ [12]) have been developed for biomass production. However, the commercial application of outdoor solar photobioreactors for gaseous products is not yet evident, although this is an area of intensive research [19,31,56,104,190,192,193]. Several outdoor pilot-scale systems have been studied using cylindrical, tubular or flat-panel configurations. The flat-panel design [67] can be seen as a representative scaleable unit for a future solar-driven system, however the challenge of scale up is only beginning to be addressed.

Light is an abundant source of energy but it is diffuse (1 kW/m²) and exploitation demands large areas for light capture, which necessitates a PBR with a large surface-volume ratio. This requirement is not easily reconciled with the required mixing, gas-exchange, and control of environmental conditions (e.g. temperature and pH). However, the most significant challenge may be the economical construction and lifetime maintenance of extensive light capture surfaces, which are also sufficiently cheap, gas-impermeable, transparent and durable to function as the wall of a bioreactor. Life cycle energy analysis, an approach in which all energy inputs to the construction, operation and decommissioning of a system are accounted for, was employed in the examination of an algal H₂-producing PBR, using a tubular configuration, which is relevant to PNS bacterial H₂ production [21]. Although revealing, this study is not equivalent to an economic analysis as different forms of energy (e.g. electricity and heat) have different monetary values. The study compared glass (1.6 mm thickness), rigid acrylic (3 mm thickness) and flexible polyethylene film (0.18 mm thickness). The study

found that a favourable life cycle energy ratio (*ca.* 6) could be achieved using glass or flexible plastic film, but glass would not be practical due to its mechanical limitations. Polyethylene tubing was considered the most suitable material due to its low cost, although it would be easily damaged and weathered requiring periodic replacement, and concerns over its permeability to H₂ are currently being addressed.

A more practical approach may be to focus light into a compact PBR. Abiotic light harvesting technology may be more robust, compared to expanses of tubular or panel bioreactor, requiring mixing and environmental control. Savings in construction, maintenance and running costs of a compact PBR may offset the increased primary light capture area required due to light losses in the focussing system. This approach was advocated by other authors [40,192] and work has begun at the University of Wageningen to test a PBR using a lens to focus light and conduct it into a deep PBR through a PVC sheet (Figure 3-b) [31].

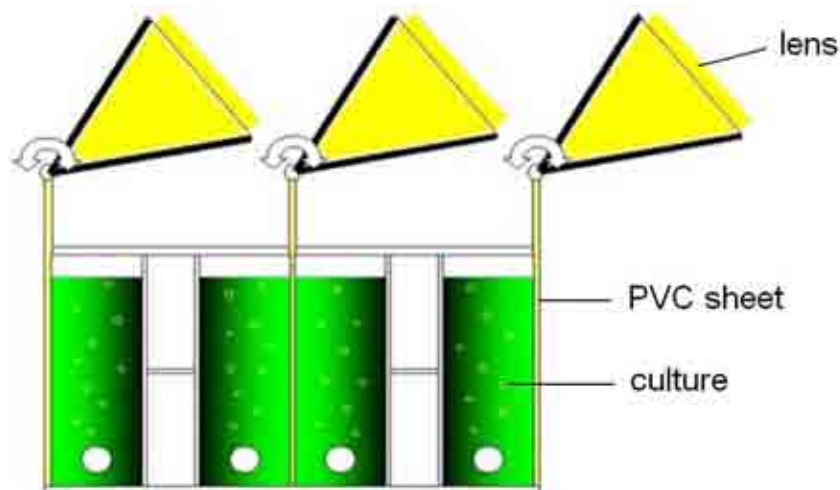


Figure 3-b Prototype light focussing photobioreactor under development at Wageningen University, Netherlands.

A lens focuses light into a PVC sheet to transmit light into deep cultures [31].

The PBR configuration outlined in Figure 3-b would facilitate solar tracking, by adjusting the angle of the focussing lens rather than the angle of the entire PBR. Experimental data is not yet available, but in theory excessive light intensity at the lens (i.e. above the saturation point of the culture) would be diffused over a larger illuminated surface area, e.g. the vertical surface of a deep PBR such as that shown. By diffusing light into a deep culture, the system may improve efficiency under excessive light intensity, however it would offer no advantage

over a solar-tracking panel or tubular PBR under sub-saturating light intensity. For this purpose the area of light capture must be larger than the area of illuminated culture surface, light capture and culture being separate components (Figure 3-c).

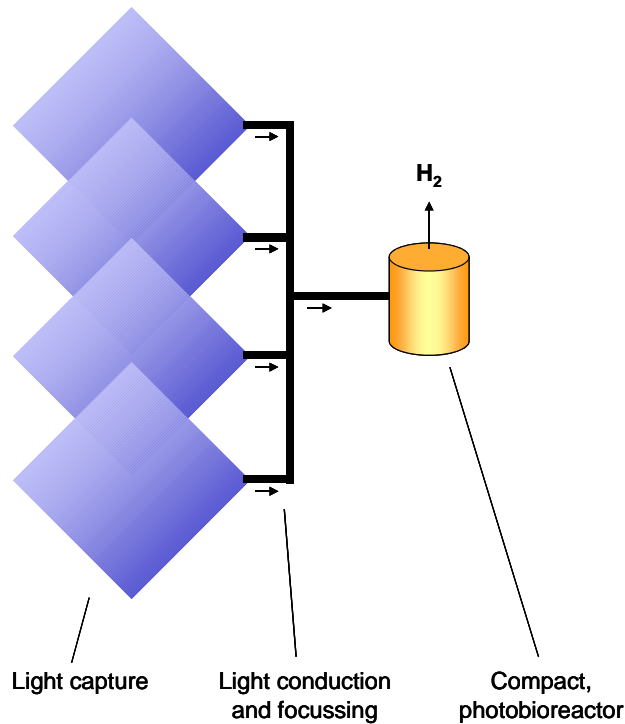


Figure 3-c Conceptual design of a light-concentrating photosynthetic system, for light intensities below saturation.

A limitation of this approach is that photosynthetic cultures have a light saturation point – a light intensity above which no further increase in productivity occurs. It would be pointless to concentrate/intensify light above the saturation point. Future work will examine the relationship between light saturation and culture density in H₂-producing cultures of PNS bacteria in order to examine the prospective advantages of light concentration.

PNS bacteria are adapted to photosynthesis at low light intensities, using large light harvesting antennae to channel diffuse light energy into the reaction centre. As a result cultures saturate at low light intensity, limiting the productivity per volume of culture. Intensive research is underway to increase the light saturation point of cultures of

photosynthetic micro-organisms, and thereby achieve, smaller denser cultures to improve the ratio of productivity-culture volume. An important approach is genetic modification to truncate light harvesting antennae [2,84,87,92,93,127,151,198], while light saturation was also improved by immobilising dense cultures in latex films [56].

In conclusion, a combination of the light concentrating approach (Figure 3-c) with an antenna-truncation strain is a promising strategy, potentially resulting in a compact, high density, high activity PBR, which could be more feasible than an expansive culture-filled system. This study has shown that the photosynthetic culture (rather than the dark fermentation), in addition to being the dominant H₂-producer, is the stage crucially limited by light availability, and future studies would focus on this.

4 : APPENDICES

4.0 Chapter contents

| | |
|---|-----|
| 4 : Appendices | 217 |
| 4.0 Chapter contents | 217 |
| 4.1 Methodology and validation..... | 218 |
| 4.1.1 Gas analysis and measurement..... | 218 |
| 4.1.1a Composition analysis – combustible gas meter (CGM) | 218 |
| 4.1.1b Fluid-displacement methods..... | 218 |
| 4.1.1c Discussion of fluid displacement methods | 220 |
| 4.1.1d Storage of gas samples | 221 |
| 4.1.1e Validation of H ₂ measurement by gas chromatography (GC)..... | 222 |
| 4.1.2 Medium compositions | 223 |
| 4.1.2a Media for the culture of <i>Rhodobacter sphaeroides</i> | 223 |
| 4.1.2b Postgate’s medium C for the growth of <i>Desulfovibrio</i> sp. (pH 7.5), per litre | 225 |
| 4.1.2c Nutrient broth for the growth of <i>Escherichia coli</i> (pH 7.0), per litre | 225 |
| 4.1.3 Biomass estimation..... | 226 |
| 4.1.4 Light conversion efficiency in photobiological H ₂ production | 227 |
| 4.1.5 Quantitative chemical analysis | 230 |
| 4.1.5a Pd(II) assay by the SnCl ₂ /HCl method | 230 |
| 4.1.5b Analysis of Pd(0) content of Bio-Pd(0)..... | 231 |
| 4.1.5c Glucose analysis by the dinitrosalicylic acid (DNSA) method | 232 |
| 4.1.5d NH ₄ ⁺ analysis by an indophenol blue method..... | 233 |
| 4.1.5e Analysis of chloride by the mercury (II) thiocyanate method..... | 235 |
| 4.1.5f Ethanol analysis by alcohol dehydrogenase (ADH) assay..... | 236 |
| 4.1.6 Reynolds number in an electro dialysis cell..... | 238 |
| 4.1.6a Fluid velocity (μ) | 238 |
| 4.1.6b Characteristic length (L)..... | 239 |
| 4.1.6c Kinematic velocity (v) | 239 |
| 4.1.7 Search results: protein-BLAST (basic local alignment search tool) | 240 |
| 4.1.7a BLAST results for <i>Euglena gracilis</i> trans-2-enoyl CoA reductase | 240 |
| 4.1.7b BLAST results for clostridial butyryl-CoA dehydrogenase | 241 |
| 4.2 Additional publications..... | 243 |
| 4.2.1 Publications in which the author played primary role..... | 243 |
| 4.2.2 Publications in which the author was involved | 266 |
| 4.2.3 Conference posters | 281 |
| 4.2.4 Conference presentations..... | 281 |
| 4.3 Video showing operational dual system..... | 284 |

4.1 Methodology and validation

4.1.1 Gas analysis and measurement

4.1.1a Composition analysis – combustible gas meter (CGM)

Samples were withdrawn from the headspace of H₂ producing cultures using a gas-tight syringe (Hamilton) and injected immediately into a CGM (GMI, UK). The system produced a numerical result related to the concentration of combustible gas in the injected sample. It was shown by GC (appendix 4.1.1e) that combustible gases other than H₂ (e.g. CH₄) were not present. This method was useful for comparing the initial production of H₂ in parallel experiments, however the device was battery-powered and could not produce consistent results. When the concentration of H₂ in the sample neared 100 %, further H₂ production could not be detected by this method, therefore useful data was produced only initially. Further, the method was inappropriate for the measurement of absolute quantities of H₂, therefore fluid displacement techniques were developed, in which the CGM was used to test qualitatively for the presence of H₂.

4.1.1b Fluid-displacement methods

Gas formed inside sealed vessels, generating positive pressure sufficient to displace fluid from a graduated container. Assuming negligible pressure differential, the volume of fluid displaced is equal to the volume of gas produced. This approach was effective in the measurement of H₂ production by cultures of *E. coli* and *R. sphaeroides* in the range 50 ml to 5 L. For 50 ml cultures of *R. sphaeroides* (Figure 4.1-a, part A) and 100 ml cultures of *E. coli* (Figure 4.1-a, part B), scrubbing solution (1-2 M NaOH) was located in the displacement cylinders (10-100 ml). For 3 L cultures a larger capacity for CO₂ absorption was anticipated. Therefore, out-gas was bubbled through 1 L of scrubbing solution before being collected over water in a 2 L collector. The separation of scrubbing and measurement minimised the use of scrubbing solution (caustic hazard) but introduced 15 cm water pressure opposing the flow of gas. *E. coli* and *R. sphaeroides* are capable of H₂ uptake and this activity is dependent on the partial pressure of H₂ (pH₂), therefore, to minimise H₂ recycling by the culture, the opposing pressure was offset by introducing negative pressure in the displacement cylinder, with a total vertical water-drop of *ca.* 30 cm (Figure 4.1-a, part C). Gas measurement was performed within ± 10 cm water pressure.

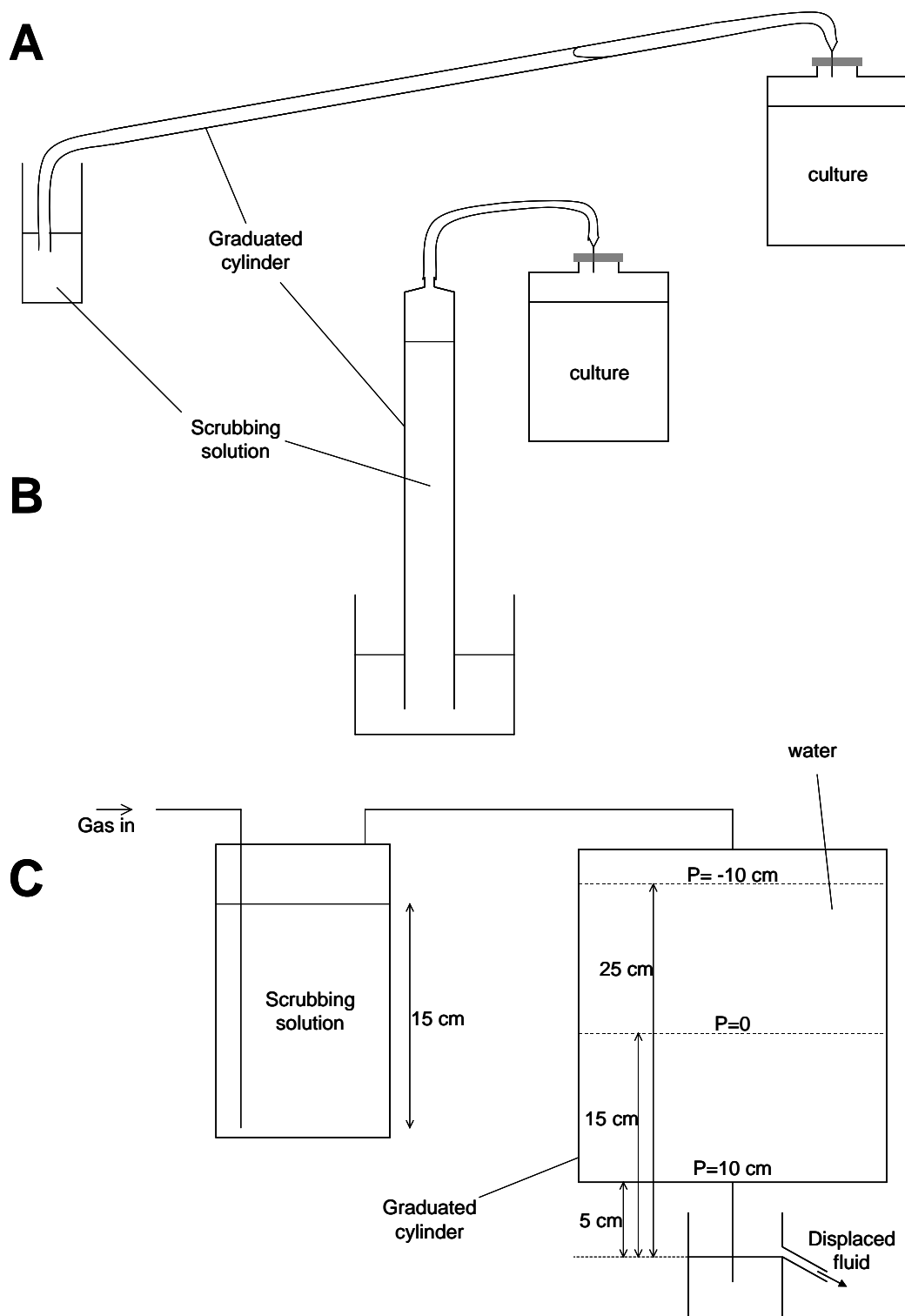


Figure 4.1-a Fluid displacement systems for the measurement of H_2 production.
 A & B, 50-200 ml cultures; C, 3- 5 L cultures. P: hydrostatic pressure.

4.1.1c Discussion of fluid displacement methods

Figure 4.1a shows how fluid displacement methods were adapted for the measurement of gas production at a wide range of rates. Data was acquired 24h using time-lapse digital photography, however the limitation of fluid displacement is that it is discontinuous; the displaced fluid must be replaced manually at intervals, creating sudden perturbations in headspace pressure which, although minimal, represent an undesirable source of error.

More sophisticated techniques include purging the reactor continuously with an inert gas such as argon, while measuring flow rates using conventional meters (accurate at high flow rates) and carrying out online composition analysis (e.g. by GC). This method would be economically unfeasible for industrial use (owing to the cost of purge gas) and would be misleading if used in experimental work due to known effects of gas-stripping on cultures, which may include the prevention of H₂ recycling (e.g. in clostridial fermentation) or the removal of CO₂ required for acetate assimilation (e.g. by certain PNS bacteria) as detailed in chapter 1.2 [66,128,136,144,196]. Ideally, low-flow gas meters (e.g. www.milligascounter.de) would be used in conjunction with data-logging equipment.

4.1.1d Storage of gas samples

The method of gas sample storage shown in Figure 4.1-b was preferred over Teflon gas bags, which cannot reliably retain H_2 for more than a few minutes. The inverted bottle was effective as glass is permanently impermeable to H_2 and the butyl rubber bung was sealed with a layer of water. Bottles were completely filled with water, which was partially displaced upon the injection of gas samples. Water was injected simultaneously, upon withdrawal of gas samples, to maintain nominal pressure, minimising contamination.

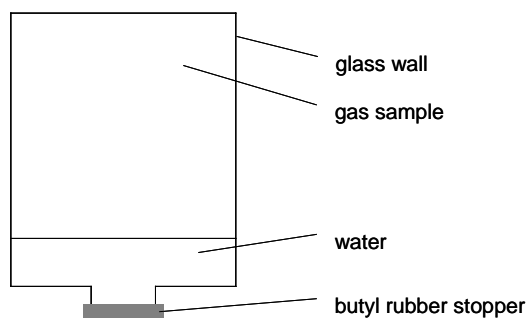


Figure 4.1-b Storage of gas samples for analysis.

4.1.1e Validation of H₂ measurement by gas chromatography (GC)

Gases were sampled from H₂ producing cultures and stored as above. The presence of H₂ and the removal of CO₂ (to <0.5 % v/v) was confirmed using a ThermoQuest gas chromatograph (TraceGC2000) fitted with a Shincarbon ST column (100/120 mesh, length: 2 m, ID: 2 mm, Shimadzu, Japan). The GC operating conditions were split 60:1, 40 °C + 15 °C/min for 10 min, and the injection volume was 1 ml.

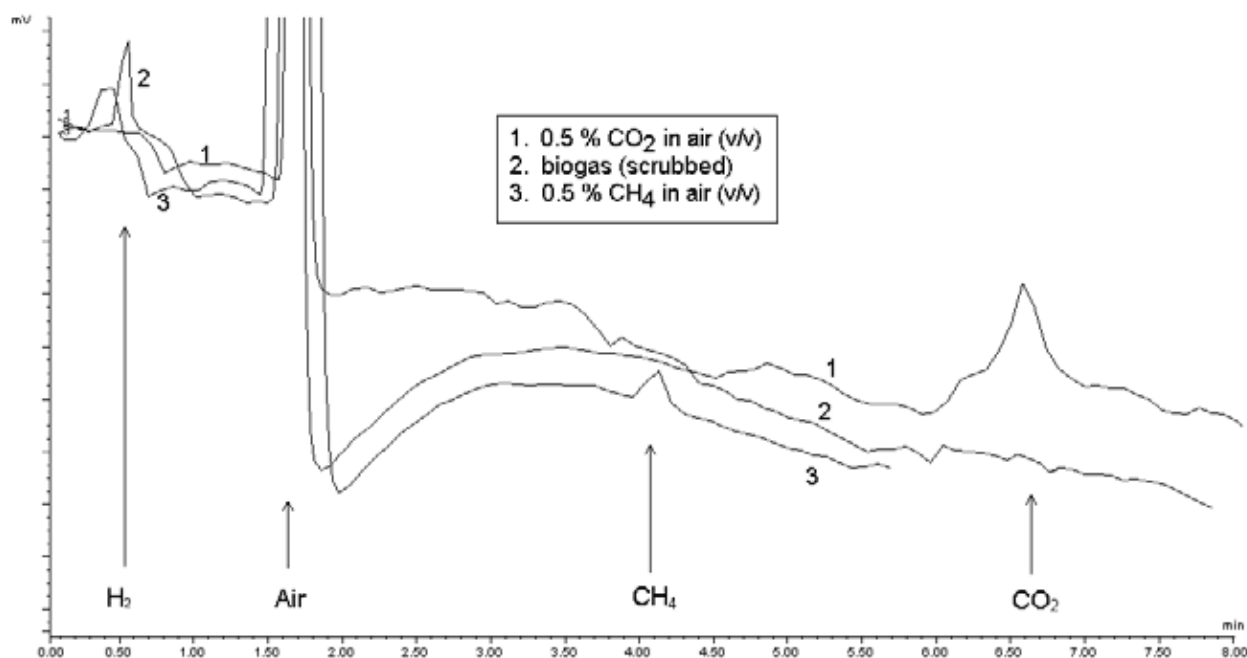


Figure 4.1-c Gas chromatogram showing the absence of CH₄ and CO₂.

CH₄ and CO₂ are excluded to less than 0.5 % v/v in bio-H₂. The sample analysis shown was taken from a continuous *R. sphaeroides* culture (chapters 2.3 and 2.6).

4.1.2 Medium compositions**4.1.2a Media for the culture of *Rhodobacter sphaeroides***

Modifications to the SyA medium described in [66] included the addition of molybdenum, a trace element necessary for the biosynthesis of MoFe nitrogenase, and hence for H₂ production [90]. External analysis of standard SyA medium (ICP-MS; inductively coupled plasma mass spectrometry, *H₂b*, Capenhurst) determined the Mo content to be 0.04 mg/l. The threshold for Mo-limitation occurred at 0.05 mg Mo/l in *R. capsulatus* [176]. Hence Mo was added to the microelements solution to increase the final concentration from 0.04 mg/L to 0.06 mg/l. A further modification was to reduce the concentrations of macronutrients in SyA medium to correspond with the fully developed (AA-c) medium of [66].

Table 4.1-1 Media for the culture of *Rhodobacter sphaeroides*

| | SyA medium | HP medium | Basal medium | Mixed org. acid medium ^δ |
|--|--------------------|--------------|-----------------|--|
| Succinate | 30 mM | - | - | 20.18 mM |
| Acetate | 0.0073 mM | - | - | 31.42 mM |
| Lactate | - | - | - | 36.97 mM |
| Formate | - | - | - | 3.56 mM |
| Yeast extract | 1 g | - | 1 g | 1 g |
| KH ₂ PO ₄ | 1.732 g | 1.732 g | 0.433 g | 0.433 g |
| K ₂ HPO ₄ | 1.466 g | 1.466 g | 0.366 g | 0.366 g |
| Macronutrient solution (20 x) ^γ | 50 ml ^β | 50 ml | 50 ml | 50 ml |
| Trace elements solution (100 x) ^γ | 10 ml ^β | 10 ml | 10 ml | 10 ml |
| Vitamins solution ^γ | 2 ml | - | 2 ml | 2 ml |
| Final pH | 6.8 | 6.8 | 6.8 | 6.8 |

Masses and volumes are per litre of final medium. ^βmodifications from [66]; ^γSolutions of macronutrients, micronutrients and vitamins were sterilised separately and added after autoclaving. ^δMixed organic acid medium simulates the effluent from a “*phase 3*” dark fermentation (see chapter 2.2) was fed to a continuous photofermentation (see chapter 2.3).

Table 4.1-2 Additives to media for the culture of *Rhodobacter sphaeroides*SyA macronutrients (20 x), per litre

| | |
|---------------------------------------|---------|
| MgSO ₄ · 7H ₂ O | 1000 mg |
| CaCl ₂ · 2H ₂ O | 500 mg |
| Sterilised by autoclaving | |

Trace elements solution (100 x), per 500 ml

| | |
|---|-----------|
| MnSO ₄ · 4H ₂ O | 1827.5 mg |
| Na ₂ EDTA · 2H ₂ O | 1051 mg |
| FeSO ₄ · 7H ₂ O | 590 mg |
| H ₃ BO ₃ (boric acid) | 140 mg |
| Na ₂ SO ₄ (anhydrous) | 19.5 mg |
| Na ₂ MoO ₄ · 2H ₂ O | 12.98 mg |
| ZnSO ₄ · 7H ₂ O | 12 mg |
| Cu(NO ₃) ₂ · 3H ₂ O | 2 mg |
| Sterilised by autoclaving | |

SyA vitamins solution (1000 x), per 20 ml

| | |
|----------------------|-------|
| Biotin | 20 mg |
| Thiamin | 20 mg |
| p-amino benzoic acid | 20 mg |
| B ₁₂ | 20 mg |
| Nicotinamide | 20 mg |
| Filter-sterilised | |

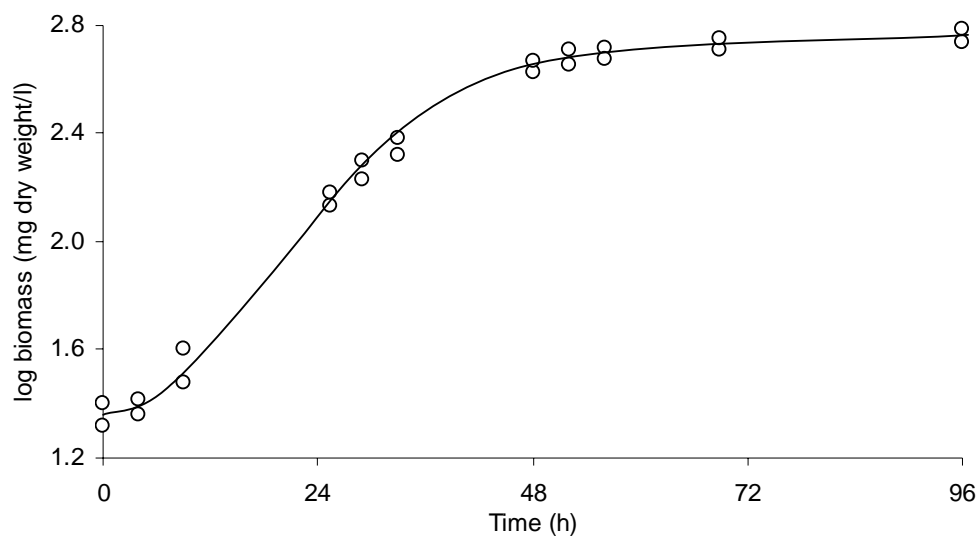


Figure 4.1-d Example growth curve for *Rhodobacter sphaeroides* O.U. 001.
R. sphaeroides was grown using SyA medium as described in chapter 2.3.

4.1.2b Postgate's medium C for the growth of *Desulfovibrio* sp. (pH 7.5), per litre

| | |
|--------------------------------------|---------|
| KH ₂ PO ₄ | 500 mg |
| NH ₄ Cl | 1000 mg |
| Na ₂ SO ₄ | 4500 mg |
| CaCl ₂ .6H ₂ O | 60 mg |
| MgSO ₄ .7H ₂ O | 60 mg |
| Yeast extract | 1000 mg |
| Sodium citrate dihydrate | 300 mg |
| FeSO ₄ .7H ₂ O | 4 mg |
| Sodium lactate | 7800 mg |
| Sterilised by autoclaving | |

4.1.2c Nutrient broth for the growth of *Escherichia coli* (pH 7.0), per litre

| | |
|---------------------------|------|
| Nutrient broth (Oxoid) | 28 g |
| Sodium formate (Sigma) | 5 g |
| Sterilised by autoclaving | |

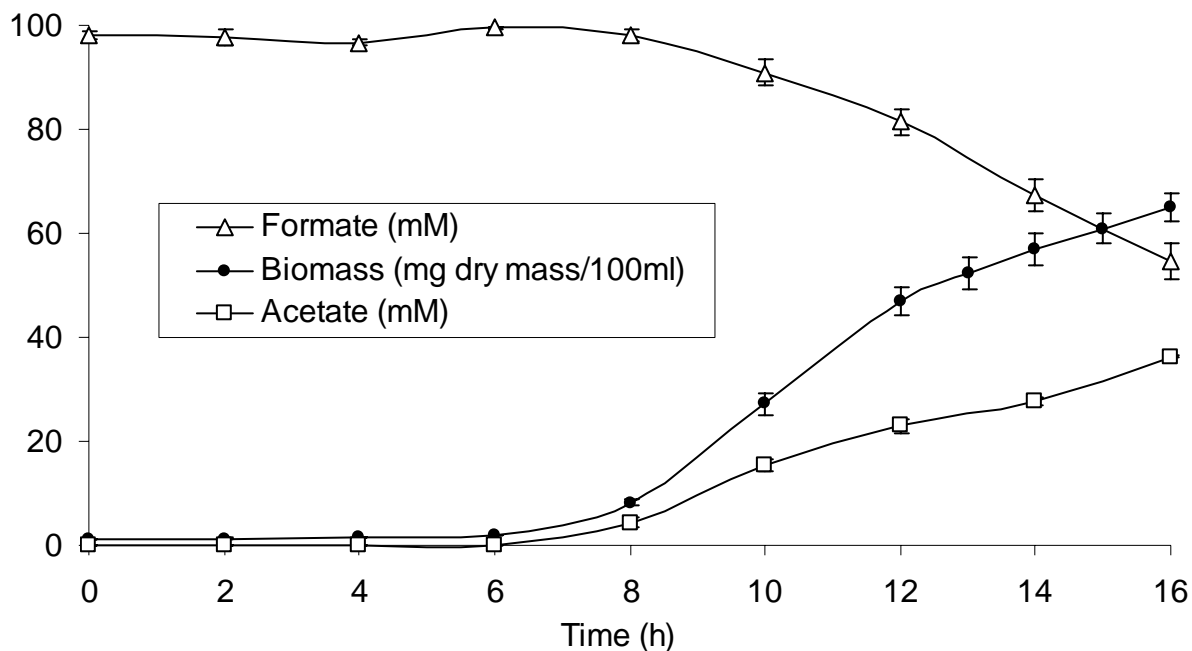


Figure 4.1-e Growth kinetics and organic acid profile for the aerobic growth of *Escherichia coli* HD701 on nutrient broth with sodium formate.

Growth was carried out as described in chapter 2.1 and organic acid analysis, as described in chapter 2.4. Means and standard errors from 4 replicate experiments are shown.

4.1.3 Biomass estimation

Biomass estimations for *E. coli* MC4100, HD701 and additional strains (chapter 2.1) were performed independently by D.W. Penfold and V. Marcadet with the same result. An OD₆₆₀ of 1 corresponded to a biomass concentration of 0.482 g/l for *E. coli*. Biomass estimations for *D. desulfuricans* were performed by D. Sanyahumbi. An OD₆₆₀ of 1 corresponded to a biomass concentration of 0.72 g/l for *D. desulfuricans*.

For *R. sphaeroides* O.U. 001, the relationship between OD₆₆₀ and culture density was investigated by the author. *R. sphaeroides* was cultivated as described in section 2.3.2a at 30 °C using SyA medium. OD₆₆₀ values were recorded for cultures (50 ml) of *R. sphaeroides*, which were subsequently harvested by centrifugation in pre-weighed containers (2400 × g; 4 °C; 20 minutes), washed twice in 50 ml deionised water and dried at 60 °C to constant mass. A linear relationship was observed when OD₆₆₀ < 1 and an OD₆₆₀ of 1 corresponded to a dry biomass concentration of 0.356 g/l.

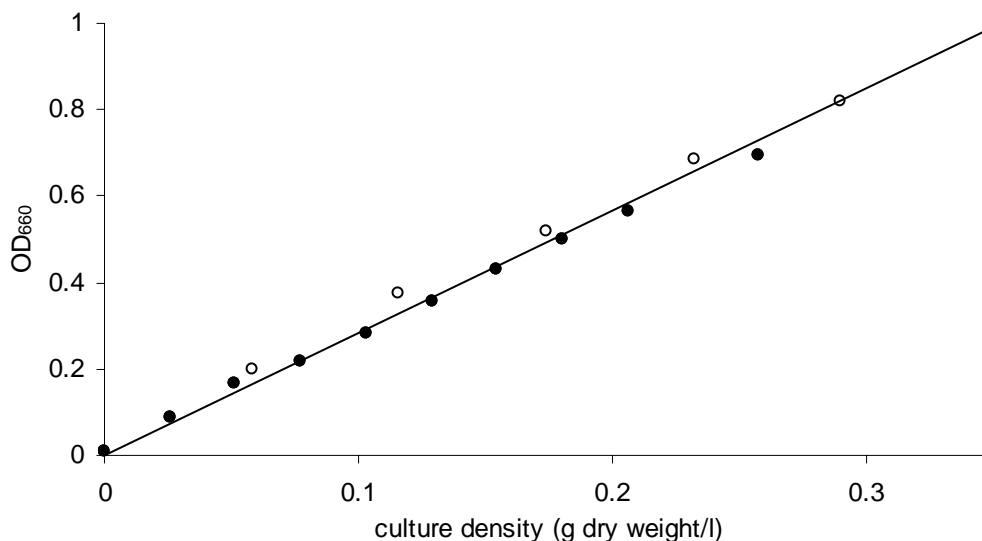


Figure 4.1-f The relationship between OD₆₆₀ and culture density in *Rhodobacter sphaeroides* O.U. 001, grown on SyA medium.

The data represent two replicate experiments, each performed in triplicate. Standard errors were within the boundaries of the symbols and are not shown.

4.1.4 Light conversion efficiency in photobiological H₂ production

A photobioreactor (PBR) supplied with a constant light intensity receives a constant supply of light energy. The proportion of that energy which is recovered in the combustion enthalpy of produced H₂ is called the light conversion efficiency.

$$\text{Light conversion efficiency (\%)} = \frac{H_2(\text{mol}) \times Y}{hv} \times 100 \quad (\text{equation 1})$$

Y combustion enthalpy of produced H₂ (285900 J/mol)
 hv light energy supplied (J)

To determine the light supply to the PBR, several factors were taken into account. The light intensity at the culture surface (i.e. the internal surface of the PBR) was measured using a specialised sensor (Skye, UK) designed to detect only photons with wavelengths in the range 400-950 nm, corresponding to the PAR (photosynthetically active radiation) range for PNS bacteria (Figure 4.1-g).

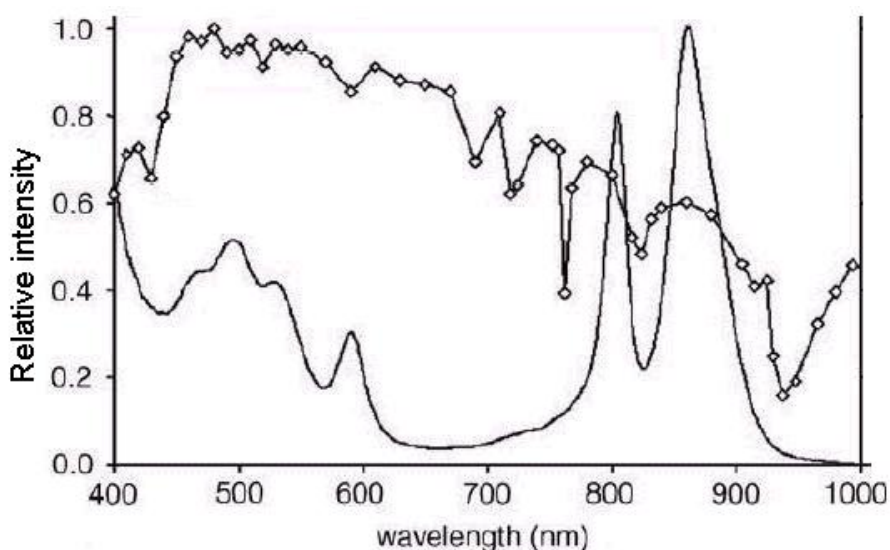


Figure 4.1-g Absorption spectrum of purple non-sulphur bacteria (solid line) and spectrum of daylight.

Taken from [2].

The light sensor produced a value in units of $\mu\text{E}/\text{m}^2/\text{s}$, where E (Einstein) is a mole of photons having wavelengths in the range 400-950 nm. To convert this value to energy (J) would be straightforward under monochromatic light (see equation 2).

$$E = \frac{Ahc}{\lambda} \quad (\text{equation 2})$$

- E Energy (J/Einstein)
- A Avogadro's number (6.602×10^{23})
- h Plank's constant (6.626×10^{-34})
- c speed of light (2.998×10^8 m/s)
- λ wavelength of monochromatic light (m)

However in practice an analysis of the emission spectrum of the light source (in this case Tungsten filament bulbs) is required in order to determine a representative wavelength to input into equation 2 (Figure 4.1-h).

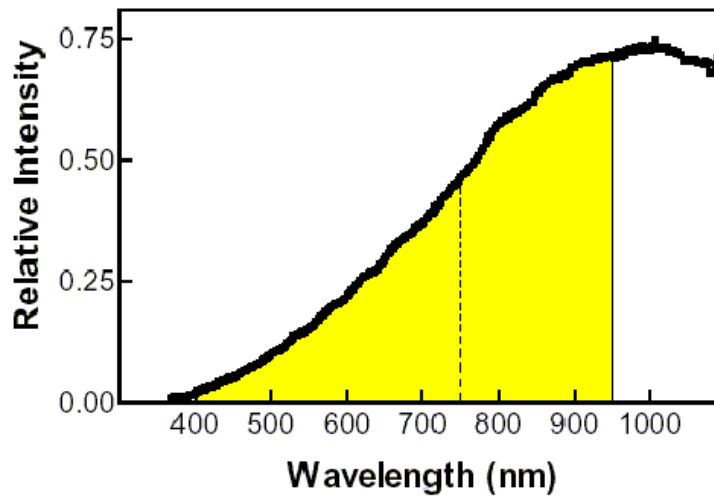


Figure 4.1-h Emission spectrum of tungsten filament within a white light bulb.

The shaded area corresponds to the part of the spectrum detected by the light sensor. The dotted line indicates the bisection of the shaded area in the x-axis [157].

The midpoint of the distribution (i.e. the representative wavelength) is the point where the emitted light (shaded area of Figure 4.1-h) is divided into two equal halves. The distribution was modelled in the x-range 400-950 using a cubic equation (author's derivation), which was

integrated to bisect the area covered by the curve. The result was 758.9 nm, (i.e. 7.589×10^{-7} m), corresponding to 157.64 kJ/E (equation 2).

In this work the PBR had an illuminated internal surface area of 0.1069 m^2 . The light intensity was measured at several points uniformly distributed points on the wetted internal surface of the vessel, under 3 x 40 W Tungsten bulbs and with the reflective sheath in position (see chapter 2.3). The average light intensity was $334.29 \text{ } \mu\text{E}/\text{m}^2/\text{s}$. Therefore the light energy supplied to the PBR was 20.217 kJ/h.

4.1.5 Quantitative chemical analysis

4.1.5a Pd(II) assay by the SnCl₂/HCl method

Application: This assay was used to confirm the complete reduction of Pd(II) in the production of Bio-Pd(0) and the separation of insoluble Pd(0) from solution. It was also used in assays of Pd content in Bio-Pd(0) (see section 4.1.5b).

Assay principle: A coloured Pd(II)-Sn(II) chloride complex forms in a conc. HCl background when the solutions are mixed [7,55].

Assay method: Samples were prepared by centrifugation or filtration to remove cells and/or interfering insoluble Pd(0). Sample volumes of 200 µl were transferred to cuvettes and 1000 µl reagent was added and mixed. Colour was allowed to develop for 30 min before the sample was mixed again and A₄₆₃ was recorded. The reagent contained 14.95 g SnCl₂ dissolved in 250 ml concentrated HCl, stored at room temperature.

Result: The relationship between Pd(II) concentration and A₄₃₆ is linear in the range: 0-200 mg/l or 0-1 mM, but in this study the assay was used only the range 0-40 mg/l. The lower limit of sensitivity was *ca.* 2 mg/l (Figure 4.1-i). Interference by components of SyA medium was excluded by repeating the assay using Pd standards dissolved in SyA medium.

Caveats & limitations: The method can be adapted for the analysis of various PGM but is applicable only for the assay of single-PGM solutions; i.e. Pd may only be assayed in the absence of other PGM. Insoluble Pd(0) is an interfering agent as Pd(0) may dissolve in the acidic reagent. This method was cross-validated using polarography by I. P. Mikheenko [123].

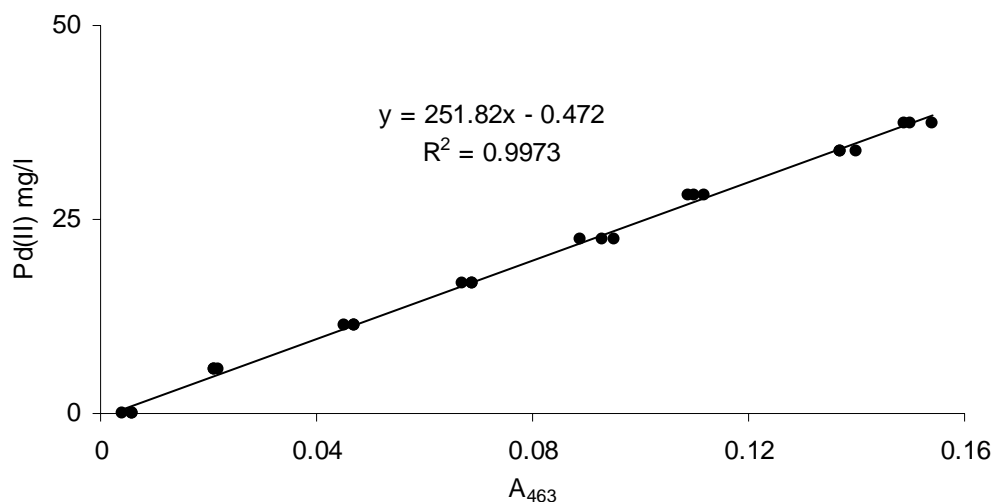


Figure 4.1-i Sample calibration curve for Pd(II) assay by the SnCl₂ method

4.1.5b Analysis of Pd(0) content of Bio-Pd(0)

Application: Accurate loading of Pd(0) on biomass is crucial to the reliable comparison of different catalysts (e.g. prepared using different biomasses, chapter 2.7). Therefore the Pd-loading was verified.

Method: Dry sample material (5-10 mg) was digested in 4.6 ml acid mixture (4.5 ml 2 M HNO₃, 0.1 ml conc. HCl, 50 °C, 2 h). Undigested organic material was subsequently removed by centrifugation (13000 x g, 4 min) and the Pd(II) concentration in the supernatant was assayed (as 4.5.1). Pure Pd powder (Sigma) was included as a standard to confirm complete oxidation of Pd(0).

Table 4.1-3 Example analysis of Pd content in Bio-Pd(0)

| Sample | mass digested (mg) | Pd(II) in supernatant (4.6 ml) | | % Pd (w/w) |
|---------------------------|--------------------|--------------------------------|------|------------|
| | | mg/l | mg | |
| Pd powder (standard) | 7.7 | 1703.99 | 7.84 | 101.80 |
| Pd powder (standard) | 7.3 | 1643.48 | 7.56 | 103.56 |
| Pd powder (standard) | 9.5 | 2040.43 | 9.39 | 98.80 |
| <i>Rs</i> -Pd(0) 25 % w/w | 4.4 | 256.44 | 1.18 | 26.81 |
| <i>Rs</i> -Pd(0) 25 % w/w | 4.1 | 225.95 | 1.04 | 25.35 |
| <i>Rs</i> -Pd(0) 50 % w/w | 3.8 | 415.67 | 1.91 | 50.32 |
| <i>Rs</i> -Pd(0) 50 % w/w | 3.9 | 412.49 | 1.90 | 48.65 |

4.1.5c Glucose analysis by the dinitrosalicylic acid (DNSA) method

Applications: Quantitative analysis of glucose in *E. coli* fermentation broths, feed solutions and effluents.

Method: Based on the method described by [24], samples were filtered, mixed with DNSA reagent in varying proportions (Table 4.1-4), boiled for 10 min, cooled on ice and the A_{570} was recorded. For the preparation of DNSA reagent, 0.25 g 3,5-dinitrosalicylic acid (DNSA) and 75 g sodium-potassium tartarate were dissolved in 50 ml 2 M NaOH overnight in a brown glass bottle, after which the volume was made up to 250 ml with de-ionised water.

Table 4.1-4 Assay range of DNSA method

| Sample vol (μ l) | Reagent vol (μ l) | Assay range (mM glucose) |
|-----------------------|------------------------|--------------------------|
| 20 | 800 | 25-250 |
| 50 | 800 | 10-100 |
| 100 | 800 | 5-50 |
| 300 | 700 | 0.5-5 |

Limitations: As the method is sensitive to all reducing sugars, the accurate quantitative analysis of glucose is dependent upon glucose being the only reducing sugar present in significant quantities. Both lower and upper limits of sensitivity apply (Table 4.1-4). DNSA reagent remains useful for up to 2 months if stored in darkness at 4 °C but decomposes gradually and calibration curves must be repeated daily.

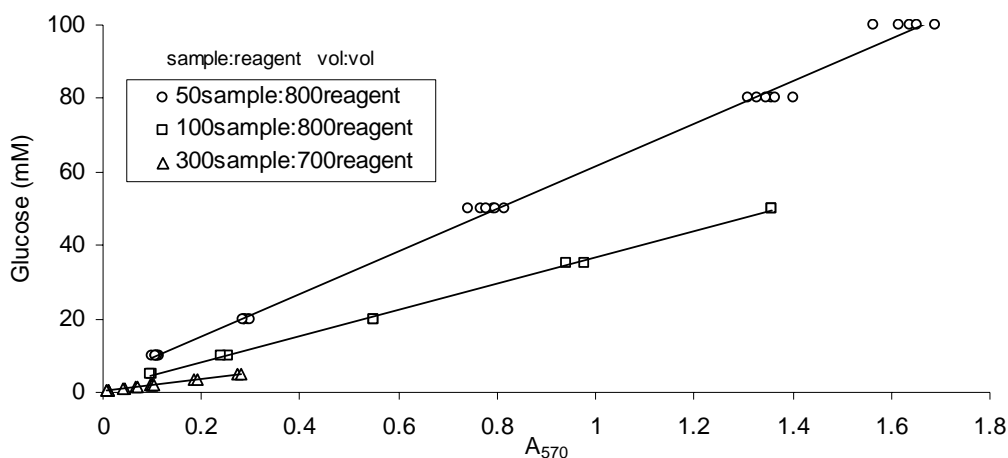


Figure 4.1-j Sample calibration curves for the analysis of glucose

4.1.5d NH₄⁺ analysis by an indophenol blue method

Applications: Quantitative analysis of NH₄⁺ in fermentation effluent (chapter 2.4) and the transfer of NH₄⁺ across anion-selective membranes (chapter 2.5).

Method: Reagents were purchased from Sigma-Aldrich (Aqual-plus kit no. 37400).

Table 4.1-5 Reagents for the analysis of NH₄⁺

| | Approximate concentration ^a |
|-----------|--|
| Reagent 1 | < 5 % NaOH > 20 % sodium tartrate-2-hydrate |
| Reagent 2 | ca. 50 % NaCl ca. 50 % Na ₂ SO ₄ <1 % dichloroisocyanuric acid-2-hydrate |
| Reagent 3 | < 5 % sodium nitroprusside-2-hydrate < 0.5 % thymol ca. 30 % ethanol |

^a all reagents in aqueous solution. Exact concentrations are proprietary.

The method was modified from the manufacturer's instructions as follows. A mixture containing 4 g reagent 2, 20 ml deionised water and 12 ml reagent 1 was prepared freshly. To 320 µl of this mixture was added 1000 µl sample ([NH₄⁺] in the range 0-200 µM), which was mixed and left for 2 min before adding 20 µl reagent 3, mixing and recording A₆₉₀.

Limitations: NH₄⁺ forms a green complex with nitroprusside and thymol in alkaline solution. Although the method is highly sensitive (range: 0-200 µM), high background concentrations of buffering agents cause interference. Potentially interfering species occurring in samples include phosphate (present in SyA medium at 20 mM) and TRIS buffer (Tris-hydroxymethyl methylamine) (used in some fermentations at 100 mM). Interference was not detected in a background of 20 mM phosphate but colour development was inhibited by 100 mM TRIS (Figure 4.1.5.4.1).

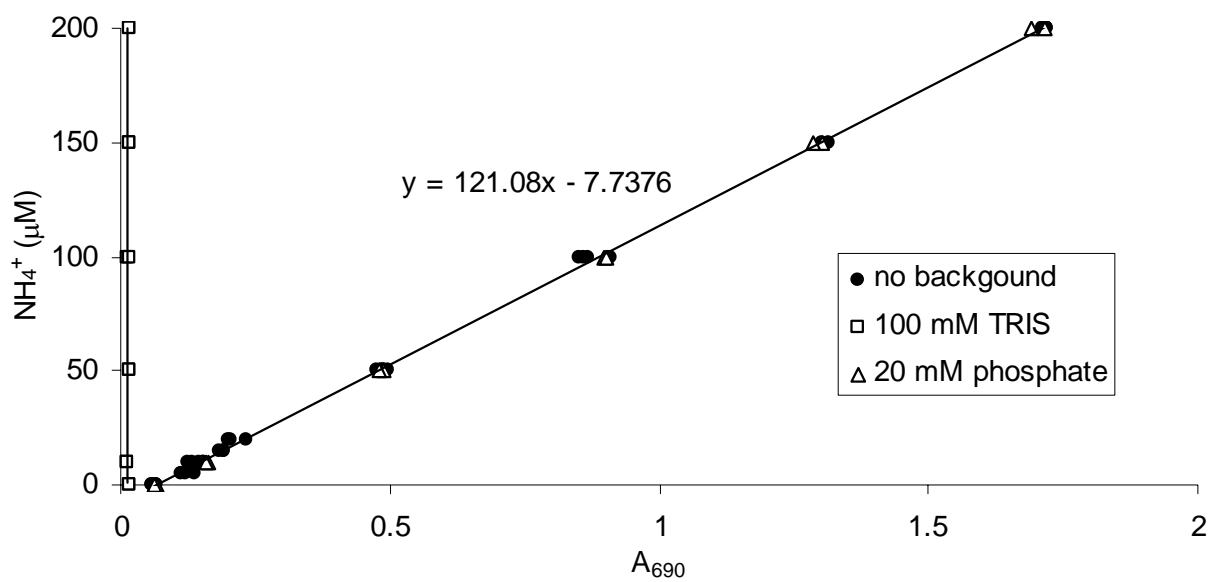


Figure 4.1-k Sample calibration curve for the analysis of NH_4^+ , validating the method for use in a background of 20 mM phosphate.

4.1.5e Analysis of chloride by the mercury (II) thiocyanate method

Application: Monitoring the reductive dehalogenation of chlorophenols and polychlorinated biphenyls by the release of Cl^- into aqueous solution (chapter 2.7).

Method: Based on the method described by [121]. To 840 μl sample, were added 80 μl Reagent A (saturated $\text{Hg}(\text{SCN})_2$ supernatant, 0.75 g/l) and 80 μl reagent B (40.4 g/l $\text{Fe}(\text{NO}_3)_3 \cdot 9\text{H}_2\text{O}$ and conc. HNO_3 , 50 % v/v). A_{460} was recorded after mixing and incubating for 10-40 min. Samples from dehalogenation experiments contained a background of MOPS buffer (20 mM sodium morpholinepropanesulfonic acid -NaOH (pH 7)) and the assay standards were prepared in the same background. All reductive dehalogenation tests were carried out in a low- Cl^- background using the highest purity reagents commercially available [9].

Limitations: Susceptible to contamination with chloride, which was excluded using negative controls.

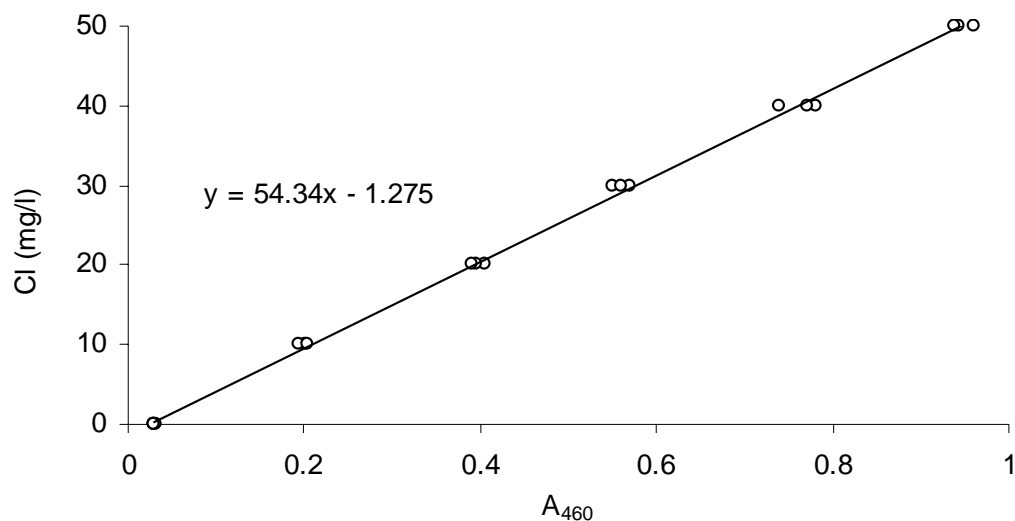
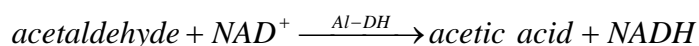
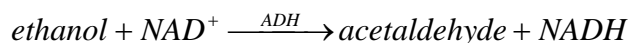


Figure 4.1-1 Sample calibration curve for the analysis of chloride.

4.1.5f Ethanol analysis by alcohol dehydrogenase (ADH) assay

Application: Monitoring ethanol production by *E. coli* and consumption by *R. sphaeroides* (chapter 2.1, 2.2).

Principle: Ethanol was oxidised to acetaldehyde (by alcohol dehydrogenase, ADH) and subsequently to acetic acid (by aldehyde dehydrogenase, Al-DH). The concomitant reduction of NAD^+ to NADH was monitored at A_{340} .



Reagents:

20 mM NAD^+ solution (pH 7.5)

Buffer A: 100 mM phosphate buffer, (0.995 g/l KH_2PO_4 , 16.33 g/l K_2HPO_4 , pH 7.5 using HCl/NaOH) with 1 g/l bovine serum albumin (as a stabilising agent).

Buffer B: 0.65 M potassium pyrophosphate (pH 9.0 using HCl/NaOH)

ADH, EC 1.1.1.1, 190 U/ml in Buffer A (Sigma, A-7011)

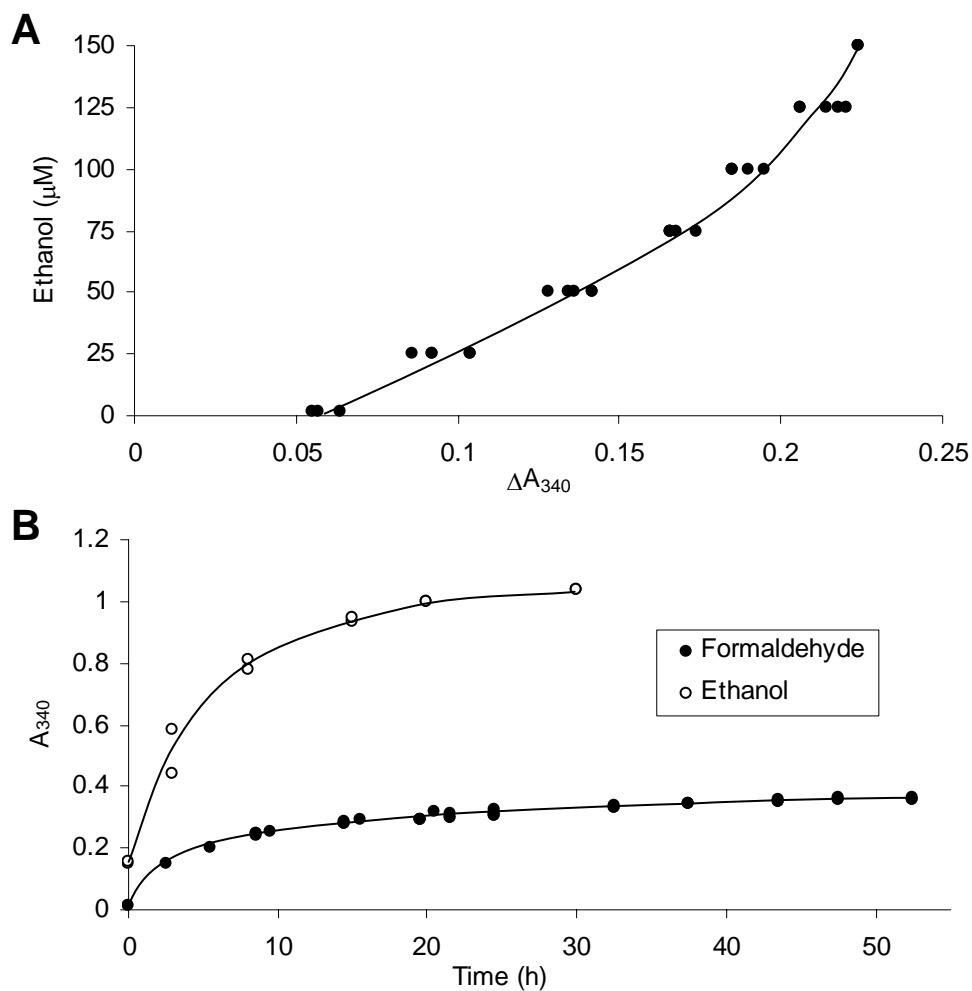
Al-DH, EC 1.2.1.5, 5.0 U/ml in Buffer A (Sigma, A-6338)

1 U ADH will oxidise 1.0 μmol ethanol to acetaldehyde per min at pH 8.8 and 25 °C.

1 U Al-DH will oxidise 1.0 μmol acetaldehyde to acetic acid per min at pH 8.0 and 25 °C.

Method: Lyophilised enzymes were resuspended in cold buffer A (4 °C) to the concentrations specified, aliquoted, and stored at –80 °C. For use enzyme suspensions were thawed and kept on ice. A pre-reaction mixture was prepared containing 23.81 ml buffer B, 23.81 ml NAD^+ solution and 0.5 ml Al-DH suspension (assay concentration: 16.18 U/l). Aldehyde was initially removed by adding 420 μl pre-reaction mixture to 1000 μl sample and incubating for 3 min. The resultant

A_{340} was recorded. The activity of Al-DH was confirmed using 100 μM formaldehyde, under assay conditions (Figure 4.1-m, part B). Ethanol was then determined from the increase in A_{340} (ΔA_{340}) following the addition of 20 μl ADH suspension (assay concentration: 2.64 U/ml) and an incubation for 3 min. Calibration curves were re-drawn for each experiment.



Limitations: Low throughput.

Figure 4.1-m Analysis of ethanol.

Sample calibration curve (A) and kinetics of the oxidation of 100 μM ethanol under assay conditions and 100 μM formaldehyde by aldehyde dehydrogenase only (B).

4.1.6 Reynolds number in an electrolysis cell

It was found (M. Wright, EKB Technolgy Ltd. pers. comm.) that limiting current density (LCD) in the electrolysis cell (chapter 2.5) was related to the turbulence of fluid flow through the cell, which is routinely represented by a dimensionless vector called Reynolds number (Re). Information on the calculation of Re was sourced from www.engineeringtoolbox.com and [142] with guidance from D. Stratton-Campbell (C-Tech Innovation Ltd.).

$$Re = \frac{\mu L}{\nu} \quad (\text{equation 1})$$

where

μ is the fluid velocity (m/s)

L is the characteristic length (m)

ν is the kinematic viscosity (m^2/s)

Using the values for μ , L and ν calculated below, Re was found to be 173, a similar value to those calculated by EKB Technology, which suggests laminar flow as Re values in excess of 10^5 – 10^6 are indicative of turbulent flow over a flat plate. However, the calculation did not account for additional turbulence due to plastic mesh occupying each chamber.

4.1.6a Fluid velocity (μ)

Fluid velocity was assumed to be similar in all four chambers of the ED cell, being created by a single 4-channel pump using identical pump-tubing (Norprene L/S 18, Cole-Parmer) for each channel. The measured flow rate of $450 \text{ cm}^3/\text{min}$ was converted to 0.0219 m/s (μ) using the length (15.70 cm) and volume (53.81 cm^3) of a single chamber of the ED cell. To determine the chamber volume occupied by fluid, the volume of an internal plastic mesh was subtracted from the total chamber volume, which was calculated from the chamber dimensions (15.70 cm , 12.35 cm , 0.32 cm). The mesh volume was determined to be $0.04 \text{ cm}^3/\text{cm}^2$ using a eureka can, and the area of mesh occupying the chamber was 193.9 cm^2 , indicating a mesh volume of 7.76 cm^3 .

4.1.6b Characteristic length (L)

Characteristic length concerns the cross-section of the vessel through which fluid flows.

$$L = \frac{4A}{P} \quad (\text{equation 2})$$

where

A is the cross-sectional area perpendicular to the direction of fluid flow (m^2)

P is the perimeter (m)

For this cell, A was 3.92 cm^2 , and P was 25.34 cm , therefore L was 0.00619 m .

4.1.6c Kinematic velocity (v)

$$v = \frac{z}{\rho} \quad (\text{equation 3})$$

where

z is the dynamic viscosity ($\text{N.s/m}^2 = \text{Pa.s} = \text{kg/m.s}$)

ρ is the fluid density ($\text{g/l} = \text{kg/m}^3$)

The dynamic viscosity for water is $801.5 \times 10^{-6} \text{ N.s/m}^2$ at $30 \text{ }^\circ\text{C}$ and the density of a typical *E. coli* culture was determined gravimetrically to be 1023.67 g/l , indicating a kinematic velocity of $0.783 \times 10^{-6} \text{ m}^2/\text{s}$.

4.1.7 Search results: protein-BLAST (basic local alignment search tool)

BLAST search results relate specifically to section 2.2.4b where interpretation is given.

4.1.7a BLAST results for *Euglena gracilis* trans-2-enoyl CoA reductase

Query: trans-2-enoyl CoA reductase of *Euglena gracilis* (UniProtKB/Swiss-Prot entry Q5EU90)

The search was limited to *Escherichia coli* (Taxid 562).

Table 4.1-6 Sequences producing significant alignments – *Euglena gracilis*

| Accession | Annotation | % identity |
|-------------|---|------------|
| NP_289367 | Putative enzyme [<i>Escherichia coli</i> O157:H7 EDL933] | 40 |
| NP_755258 | hypothetical protein ygdL [<i>Escherichia coli</i> CFT073] | 40 |
| ZP_00713503 | COG1179: Dinucleotide-utilizing enzymes involved in molybdopterin and thiamine biosynthesis family 1 [<i>Escherichia coli</i> E110019] | 40 |
| ZP_00725616 | COG1179: Dinucleotide-utilizing enzymes involved in molybdopterin and thiamine biosynthesis family 1 [<i>Escherichia coli</i> F11] | 40 |
| NP_417292 | conserved protein [<i>Escherichia coli</i> K12] | 40 |
| BAA94157 | large subunit terminase [<i>Escherichia coli</i> O157:H7] | 25 |
| NP_286986 | partial putative terminase large subunit of bacteriophage BP-933W [<i>Escherichia coli</i> O157:H7 EDL933] | 25 |
| YP_539272 | hypothetical protein UTI89_C0238 [<i>Escherichia coli</i> UTI89] | 33 |
| ZP_00725559 | COG3515: Uncharacterized protein conserved in bacteria [<i>Escherichia coli</i> F11] | 33 |
| YP_851414 | hypothetical protein APECO1_1771 [<i>Escherichia coli</i> APEC O1] | 33 |

Sequences are listed in order of decreasing similarity based both on % identity (shown) and % similarity (not shown).

4.1.7b BLAST results for clostridial butyryl-CoA dehydrogenase

Query: butyryl-CoA dehydrogenase (BCAD) of *Clostridium acetobutylicum* ATCC 824 (accession P52042).

The search was limited to *Escherichia coli* (Taxid 562).

Table 4.1-7 Sequences producing significant alignments – *Clostridium acetobutylicum*

| Accession | Annotation | % identity |
|-------------|--|------------|
| ZP_00726504 | COG1960: Acyl-CoA dehydrogenases [<i>Escherichia coli</i> F11] | 32 |
| NP_754356 | Putative acyl-CoA dehydrogenase [<i>Escherichia coli</i> CFT073] | 33 |
| YP_541217 | putative acyl-CoA dehydrogenase [<i>Escherichia coli</i> UTI89] | 33 |
| ZP_00702410 | COG1960: Acyl-CoA dehydrogenases [<i>Escherichia coli</i> E24377A] | 28 |
| ZP_00721216 | COG1960: Acyl-CoA dehydrogenases [<i>Escherichia coli</i> F11] | 28 |
| NP_288129 | crotonobetainyl-CoA dehydrogenase [<i>Escherichia coli</i> O157:H7 EDL933] | 30 |
| YP_852786 | acyl-coA dehydrogenase [<i>Escherichia coli</i> APEC O1] | 30 |
| NP_416210 | predicted acyl-CoA dehydrogenase [<i>Escherichia coli</i> K12] | 30 |
| ZP_00704000 | COG1960: Acyl-CoA dehydrogenases [<i>Escherichia coli</i> E24377A] | 30 |
| ZP_00924637 | COG1960: Acyl-CoA dehydrogenases [<i>Escherichia coli</i> 101-1] | 30 |
| ZP_00736180 | COG1960: Acyl-CoA dehydrogenases [<i>Escherichia coli</i> 53638] | 30 |
| NP_285938 | acyl-CoA dehydrogenase [<i>Escherichia coli</i> O157:H7 EDL933] | 25 |
| Q8X7R2 | Acyl-coenzyme A dehydrogenase (ACDH) | 25 |
| AAM28523 | acyl-CoA dehydrogenase [<i>Escherichia coli</i>] | 25 |
| NP_752308 | acyl-CoA dehydrogenase [<i>Escherichia coli</i> CFT073] | 25 |
| ZP_00725541 | COG1960: Acyl-CoA dehydrogenases [<i>Escherichia coli</i> F11] | 25 |
| ZP_00717599 | COG1960: Acyl-CoA dehydrogenases [<i>Escherichia coli</i> B7A] | 25 |
| ZP_00721365 | COG1960: Acyl-CoA dehydrogenases [<i>Escherichia coli</i> E110019] | 25 |
| ZP_00924937 | COG1960: Acyl-CoA dehydrogenases [<i>Escherichia coli</i> 101-1] | 25 |
| ZP_00702595 | COG1960: Acyl-CoA dehydrogenases [<i>Escherichia coli</i> E24377A] | 25 |
| NP_414756.2 | acyl coenzyme A dehydrogenase [<i>Escherichia coli</i> K12] | 25 |
| YP_539295 | acyl-CoA dehydrogenase [<i>Escherichia coli</i> UTI89] | 25 |
| YP_851438 | acyl-CoA dehydrogenase [<i>Escherichia coli</i> APEC O1] | 25 |
| ZP_00708103 | COG1960: Acyl-CoA dehydrogenases [<i>Escherichia coli</i> HS] | 23 |
| ZP_00702165 | COG1960: Acyl-CoA dehydrogenases [<i>Escherichia coli</i> E24377A] | 23 |
| ZP_00717627 | COG1960: Acyl-CoA dehydrogenases [<i>Escherichia coli</i> B7A] | 23 |
| ZP_01699570 | acyl-CoA dehydrogenase domain protein [<i>Escherichia coli</i> B] | 23 |
| NP_313190 | putative acyl coenzyme A dehydrogenase [<i>Escherichia coli</i> O157:H7 strain Sakai] | 23 |
| NP_290817 | putative acyl coenzyme A dehydrogenase [<i>Escherichia coli</i> O157:H7 EDL933] | 23 |
| ZP_00923728 | COG1960: Acyl-CoA dehydrogenases [<i>Escherichia coli</i> 101-1] | 23 |
| ZP_00737581 | COG1960: Acyl-CoA dehydrogenases [<i>Escherichia coli</i> 53638] | 23 |

4.1 Appendices – Methodology & validation

| | | |
|-------------|---|----|
| AAC18889 | putative; homology to acyl CoA dehydrogenases and isovaleryl CoA dehydrogenases [<i>Escherichia coli</i>] | 23 |
| NP_418608.4 | isovaleryl CoA dehydrogenase [<i>Escherichia coli</i> K12] | 23 |
| YP_859856 | putative acyl-CoA dehydrogenase [<i>Escherichia coli</i> APEC O1] | 22 |
| YP_543722 | putative acyl-CoA dehydrogenase [<i>Escherichia coli</i> UTI89] | 22 |
| NP_757122 | AidB protein [<i>Escherichia coli</i> CFT073] | 22 |
| ZP_00726185 | COG1960: Acyl-CoA dehydrogenases [<i>Escherichia coli</i> F11] | 22 |
| BAA07583 | 'YafH [<i>Escherichia coli</i> W3110] | 32 |
| ZP_00714579 | COG1960: Acyl-CoA dehydrogenases [<i>Escherichia coli</i> B7A] | 30 |
| YP_540695 | respiratory nitrate reductase 2 alpha chain [<i>Escherichia coli</i> UTI89] | 36 |

Sequences are listed in order of decreasing similarity based both on % identity (shown) and % similarity (not shown).

4.2 Additional publications

The work described in this thesis has been published and disseminated as follows (chronologically).

4.2.1 Publications in which the author played primary role

- Magazine article: Redwood MD (2006) Microbial biotechnology: small bugs for big business; Green energy from chocholic microbes. Society for General Microbiology, Research Matters Magazine.
Role: author
Reproduced within appendix 4.2.1
- Conference manuscript: Redwood MD, Deplanche K, Yong P, Baxter-Plant VS, Macaskie LE. Biomass-supported palladium catalysts on *Desulfovibrio* and *Rhodobacter*. Proceedings of the 16th International Biohydrometallurgy Symposium (IBS 2005), Cape Town, S. Africa. Editors: Harrison STL, Rawlings DE, Petersen J. ISBN: 1-920051-17-1 p. 335-342
Role: author
Rreproduced within appendix 4.2.1
- Journal article: Redwood MD & Macaskie LE (2006). A two-stage, two-organism process for biohydrogen from glucose. *International Journal of Hydrogen Energy* 31(11):1514-1521
Role: author
Reproduced in chapter 2.4.
- Patent: Named inventor, British Patent Application Number 0705583.3 entitled “Apparatus and Method for Biohydrogen Production” (March 2007).
Role: inventor/co-author
Reproduced within appendix 4.2.1
- Journal article: Redwood MD, Deplanche K, Baxter-Plant VS, Macaskie LE (2008) Biomass-supported palladium catalysts on *Desulfovibrio desulfuricans* and *Rhodobacter sphaeroides*. *Biotechnol Bioeng* 99(5):1045-1054.
Role: author
Reproduced in chapter 2.7
- Journal article: Redwood MD, Mikheenko IP, Sargent F, Macaskie LE (2008) Dissecting the roles of *E. coli* hydrogenases in biohydrogen production. *FEMS Microb Lett* 278:48-55.
Role: author
Reproduced in chapter 2.1
- Invited review: Redwood MD, Paterson-Beedle M, Macaskie LE. Integrating dark and light biohydrogen production strategies: towards the hydrogen economy. *Reviews in Environmental Science and Biotechnology*, *in submission*.
Role: author
Reproduced in chapter 1.2

4.2 Appendices – Additional publications

Redwood MD (2006) Microbial biotechnology: small bugs for big business; Green energy from chocoholic microbes. Society for General Microbiology, Research Matters Magazine.

Green energy from chocoholic microbes

Sweet, yummy chocolate; loved by everybody... even by bacteria! Under special conditions feeding chocolate to bacteria forces them to produce **hydrogen**, the fabled '**fuel of the future**'. By teaming up different kinds of bacteria, Scientists at the University of Birmingham are making hydrogen from chocolate-waste. This technology could ease the need for scarce landfill sites, and cut emissions of **greenhouse gases** like methane and carbon dioxide, helping **Kyoto targets** to be met.

Industries that generate sugary waste could use hydrogen, made by bacterial teamwork (**biohydrogen**), to generate electricity on-site and cut electricity bills and waste-disposal costs.



"The tricky part is getting the bacteria to pull together, but early results are promising."

- Mark Redwood of the University of Birmingham.

While the food-processing industry is the first target, this principle could later be applied to household waste. Homes and communities could use the kind of waste that would normally go on compost heaps to reduce electricity bills.

The bacterial team would include *E. coli*, a friendly gut microbe, and the soil-living *Purple Bacteria*. As *E. coli* makes biohydrogen, it uses up the high-energy substances in the food-waste (like sugars), leaving behind low-energy substances. *Purple Bacteria* use energy from sunlight, to clean up the last of the waste, and make more biohydrogen. In this way, none of the starting material is wasted. The system is being tested using waste from a well-known chocolate company.

Hydrogen can be converted to electricity by a fuel cell, and the only waste is water, whereas burning oil and natural gas (fossil-fuels) creates greenhouse gases, acid rain and smog. This kind of alternative energy strategy is becoming increasingly important, but not just because of **global warming** and Kyoto targets. At best, we have until 2050 before demand for fossil-fuels outstrips supply, creating worldwide **economic chaos**. That is, unless alternatives like hydrogen are open to people in time.

BIOMASS-SUPPORTED PALLADIUM CATALYSTS ON *DESULFOVIBRIO* AND *RHODOBACTER*

Mark D. Redwood, Kevin Deplanche, Ping Yong, Victoria S. Baxter-Plant, Lynne E. Macaskie
School of Biosciences, University of Birmingham, Edgbaston, Birmingham, UK, B15 2TT.
l.e.macaskie@bham.ac.uk

ABSTRACT

A novel *Rhodobacter sphaeroides*-supported palladium catalyst was compared with a previously studied *Desulfovibrio desulfuricans*-supported catalyst and unsupported palladium. The cell surface localisation of palladium deposits on cells of *R. sphaeroides* was similar to previous observations of *D. desulfuricans*-bound particles but the frequency of deposits differed among equally loaded preparations.

These differences may underlie the observation of different activities of *Desulfovibrio*- and *Rhodobacter*-supported catalysts, when compared with respect to their ability to promote hydrogen release from hypophosphite and to catalyse the reductive dehalogenation of chlorinated aromatic compounds. A *Desulfovibrio*-supported preparation would be potentially more useful in the reductive dehalogenation of polychlorinated biphenyls, whereas a *Rhodobacter*-supported catalyst would be preferable for the remediation of pentachlorophenol.

Keywords: palladium, catalyst, *Rhodobacter sphaeroides*, *Desulfovibrio desulfuricans*, reductive dehalogenation, polychlorinated biphenyls.

INTRODUCTION

The application of *Rhodobacter sphaeroides* in palladium recovery from solution and in catalysis using the resulting palladised biomass was investigated in comparison with the previously studied *Desulfovibrio desulfuricans*. *R. sphaeroides* is a member of the purple non-sulphur (PNS) bacteria, the metal interactions of which were first noted by Moore *et al.* (1992) [1], with some strains exhibiting intrinsically high resistance to various metallic pollutants such as chromate [2], rhodium [1], tellurite/tellurate [1, 3, 4] and selenite/selenate [1, 5, 6].

Dissimilatory metal reduction is a widespread mode of bacterial respiration in which simple organic substrates are oxidised and metals can act as the primary or sole terminal electron acceptor. For example, *Geobacter metallireducens* can oxidise various alcohols and simple organic molecules (e.g. acetate) to reduce Fe(III) to Fe(II) or U(VI) to U(IV) [7]. Conversely, in PNS bacteria metal reduction was widely concluded to be a mechanism of detoxification to permit growth in the presence metallic ions in an oxidised form [1-6]. Since *Rhodobacter* spp. are well documented to reduce metal ions [1-6] the first objective of this study was to evaluate the ability of *R. sphaeroides* to reduce Pd(II) to Pd(0).

In nature palladium occurs as a base metal (Pd(0)) in mixed ores with other platinum group metals (PGM) and nickel. It is used extensively in automotive catalysts and in industrial reactions where PGM catalysts are necessary (e.g. hydrogenation reactions) [8]. Efficient use of catalyst is essential due to the increasing price of palladium and finite ore resources [8]. Palladium can be reclaimed from wastes (e.g. spent automotive catalytic converters and electronics scrap) by solubilising with *aqua regia*, where Pd(0) is oxidised to Pd(II) in the form of the $[PdCl_4]^{2-}$ anion to create a Pd(II)-rich leachate [9]. In order to regenerate Pd(0), a reducing mechanism is required. Soluble Pd(II) can be reduced by a suitable electron donor such as H₂ but the rate was greatly accelerated in the presence of cells of *Desulfovibrio* spp. [10]. In this process the cells became ‘palladised’ (coated with a fine layer of Pd(0) nanocrystals) and the palladised biomass was shown to be an active catalyst using various test reactions [9, 11-14].

For preparation of Bio-Pd(0) catalyst, Pd(II) was initially removed from solution by biosorption [15] and reduction of sorbed Pd(II) was initially mediated by periplasmic hydrogenases [11]. On provision of an excess of reductant, crystal growth continued until Pd(II) was completely removed from the medium. Hence, palladised biomass of a known Pd:biomass loading ratio could be produced by reducing a known mass of Pd(II) in the presence of a known mass of cells. The resultant dried palladised biomass (Bio-Pd(0)) offered improved catalytic activity when compared with unsupported Pd(0) powder prepared chemically under H₂ (Chem-Pd(0)) and when compared with finely divided Pd(0) [13, 14]. The

increased catalytic activity of Bio-Pd(0) was attributed to reduced Pd(0) particle size as the crystals accumulated on biomass had only half the diameter compared to particles of Chem-Pd(0) [13]. Smaller crystals would present a larger surface area, leading to a higher catalytic activity from a constant mass of Pd(0), and indeed a subpopulation of Pd(0) nanoparticles (~5 nm diameter) was detected magnetically [11]. The Bio-Pd(0) can thus be described as a bionanocatalyst.

Biomass-supported palladium catalysts have potential applications. Bio-Pd(0) prepared using *D. desulfuricans* was shown to be catalytically active in reductive dehalogenation reactions [10, 14]. Halogenated aromatic compounds (e.g. chlorinated phenols and biphenyls) represent a group of persistent environmental contaminants. Pentachlorophenol (PCP) is widely used as a wood preservative and as a pesticide. Polychlorinated biphenyls (PCBs) were industrially prevalent due to their stability and thermal insulation properties, and were introduced into the environment from anthropogenic sources. Although industrial use and production have ceased, PCBs persist in sediments and aquifers, leading to bioaccumulation in fish stocks and continuing damage to human health [16]. Dehalogenation is a prerequisite in the biodegradation of chlorinated aromatics because the chloride substitutions protect the aromatic rings from microbial oxygenases [17], but this process occurs only very slowly in the environment. Bio-Pd(0) was shown previously to catalyse the dechlorination of PCBs [10].

Cellular surface chemistry may influence the biosorption and hydrogenase-mediated reduction of Pd(II) [12], thus affecting the patterning and hence potentially, the properties of the resultant Bio-Pd(0). Preliminary results indicated that *R. sphaeroides* can nucleate Pd(0) and form an active catalyst, prompting a comparison of Bio-Pd(0)_{*Rhodobacter*} with Bio-Pd(0)_{*Desulfovibrio*}.

Bio-Pd(0) was prepared using *D. desulfuricans* and *R. sphaeroides* at various Pd(0) loadings (25%, 5%, 1% w/w). The cellular localisation of Pd(0) deposits was determined by transmission electron microscopy (TEM), and with the objective to compare the catalytic efficacy of Bio-Pd(0)_{*Desulfovibrio*} and Bio-Pd(0)_{*Rhodobacter*}, the respective catalytic properties were investigated in tests based on H₂ release from hypophosphite [13] and dehalogenation of chlorinated aromatic compounds [10].

MATERIALS AND METHODS

Microorganisms and culture conditions

Desulfovibrio desulfuricans (NCIMB 8307) was maintained and cultured as described previously [13]. *Rhodobacter sphaeroides* O.U.001 (DSMZ 5864) was held in stock at -80°C (in 15% glycerol v/v), revived on nutrient agar (30°C) and cultured in full sealed bottles under fluorescent illumination (39.5 μM photons m⁻² s⁻¹ measured by PAR light meter SKP200, Skye Instruments Ltd.) at 30°C using the SyA medium described in [18].

Determination of dry weight

Biomass concentration (mg dry weight cm⁻³) was calculated from optical density (660 nm) with reference to a conversion, determined previously in triplicate by recording optical densities from dense cultures after various dilutions in deionised H₂O. Cultures were washed twice by centrifugation/resuspension (2400 x g, 20 min, 4°C, 50 cm³) before drying at 60°C to constant mass.

Preparation of Bio-Pd(0)

The procedure was based on that described previously [13, 14]. Bacterial cells were harvested from the mid-logarithmic phase of growth by centrifugation (11900 x g, 10 min) and resuspended in a small volume of sterile buffer (20 mM sodium morpholinepropanesulphonic acid (MOPS) (pH 7)). Analar reagents were used throughout to reduce the chloride background in dehalogenation assays.

Aliquots of cell concentrate and Pd(II) solution (Na₂PdCl₄ Sigma) were mixed to produce the desired mass ratio. For example, in order to produce Bio-Pd(0) loaded at 25% Pd(0) (w/w), 0.1 g Pd(II) and 0.3 g cell dry weight were mixed in 0.01 mM HNO₃, pH 2. Mixtures (50-100 cm³) were sealed in 100 cm³ serum bottles with butyl rubber stoppers and aluminium tear seals, degassed under vacuum (5 min), sparged with oxygen-free N₂ (10 min) and incubated statically (30°C, 60 min) to allow biosorption of Pd(II) before sparging with H₂ (15 min) after which loss of Pd(II) was confirmed by assay (below). The preparations were harvested by centrifugation (39200 x g, 10 min) and washed three times in sterile MOPS buffer (above) and once in acetone and dried at 60°C. Chemically reduced Pd(0) (Chem-Pd(0))

was prepared in parallel without bacterial cells and with complete Pd(II) reduction requiring 60 min under H₂. Dried material was ground using a pestle and mortar before catalytic testing.

Assay for Pd(II)

Before harvesting palladised biomass, complete reduction of Pd(II) was confirmed by reading the A₄₂₀ in a variable wavelength spectrometer (Ultraspec III, Pharmacia Biotech). This assay method was validated previously using the SnCl₂ method, and polarographically [11].

Electron Microscopy

Samples of palladised biomass were washed as above, omitting the acetone wash, and prepared for examination by transmission electron microscopy (TEM) as described by Baxter-Plant et al. [10].

Evaluation of catalytic activity by the hypophosphite test reaction

The method was developed from Yong et al. [13]. For assay, each reaction contained 0.5 mg Pd(0) as a variable mass of total material dependent upon the Pd(0) fraction. The preparations were resuspended in 10 cm³ of 10 % NaH₂PO_{2(aq)}, buffered with MOPS (0.5 M, pH 8), at 25°C. After the onset of gas release the volume of H₂ generated over 30 min was measured using a water trap. The pH of reaction mixtures was unchanged after 30 min.

Assay for catalytic dehalogenation of chlorinated aromatic compounds

Dehalogenation of chlorophenols and polychlorinated biphenyls (PCBs) by Bio-Pd(0) was demonstrated previously (using formate as the reductant) [10], and has applications in remediation technology. The substrates tested are shown in Table 1. Chlorophenols and PCBs were purchased from Aldrich and QMX Laboratories Ltd., respectively, and were used at equivalent concentrations of chloride.

Table 1. Chlorinated aromatic compounds used as substrates for catalytic dehalogenation tests

| Short title | Compound | | Nominal concentration (mM)* |
|-------------|----------|--------------------------------------|-----------------------------|
| | | Systematic title | |
| 2-CP | | 2-chlorophenol | 0.500 |
| PCP | | Pentachlorophenol | 0.500 |
| PCB 28 | | 2,4,4'-trichlorobiphenyl | 0.308 |
| PCB 52 | | 2,2',5,5'-tetrachlorobiphenyl | 0.274 |
| PCB 101 | | 2,2',4,5,5'-pentachlorobiphenyl | 0.123 |
| PCB 118 | | 2,3',4,4',5-pentachlorobiphenyl | 0.123 |
| PCB 138 | | 2,2',3,4,4',5'-hexachlorobiphenyl | 0.111 |
| PCB 153 | | 2,2',4,4',5,5'-hexachlorobiphenyl | 0.111 |
| PCB 180 | | 2,2',3,4,4',5,5'-heptachlorobiphenyl | 0.051 |

* Due to their low water solubility, the aromatic substrates were used as hexane in water suspensions. The concentration shown is that in the 10 cm³ of test mixture, the actual concentration in the aqueous phase was not determined. Solubilities of PCBs in water were given in [10].

For assay, each reaction contained 2 mg of test catalyst (i.e. total material: Pd(0) and biomass component), resuspended in sterile 20 mM MOPS-NaOH buffer (pH 7) and aromatic substrate (dissolved in hexane) to a total volume of 10 cm³. After settling (5 min) a 1 cm³ sample was taken from the aqueous fraction. The reaction was started by the addition of 1 cm³ 1 M formic acid and further samples were taken at suitable intervals. Catalyst was separated from the aqueous phase by centrifugation (13000 x g, 4 min), and 0.84 cm³ of supernatant was transferred into cuvettes. Reductive dehalogenation was monitored by the release of chloride, as determined by the mercury (II) thiocyanate method, scaled down from the method of Mendam et al. [19]. A standard curve was prepared using NaCl in MOPS buffer. Assay interference by the organic components was excluded experimentally.

RESULTS

Examination of the palladised biomass under electron microscopy

R. sphaeroides was successfully palladised without modification to the procedure, as shown by the appearance of black Pd(0) deposits under TEM (Figure 1). Despite morphological differences between cells of *D. desulfuricans* and *R. sphaeroides*, Pd(0) deposits exhibited similar cell surface locations and morphologies, but the frequency of Pd(0) deposits was apparently lower on *R. sphaeroides* than on *D. desulfuricans*, despite equal Pd(0) loading weight for weight, as determined by loss of Pd(II) from the palladisation mixture in each case.

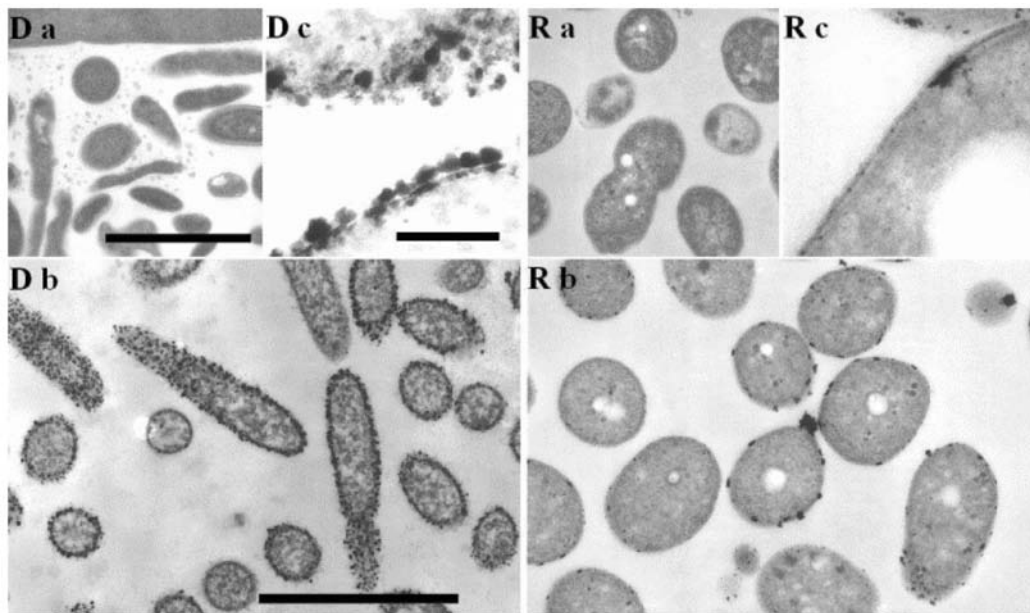


Figure 1: TEM sections of *D. desulfuricans* (*D*) and *R. sphaeroides* (*R*) palladised to 25% Pd(0) w/w
Da, Ra : non-loaded cells (bar: 2 μ m) *Db, Rb*: cells palladised at 25% w/w (bar: 2 μ m) *Dc, Rc*:
morphologies of Pd(0) deposits (bar: 0.2 μ m).

Evaluation of catalytic activity by the hypophosphite test

Hydrogen evolution from hypophosphite was used as an indicator of catalytic activity for various preparations (Figure 2). Bio-Pd(0) loaded at 1 %, 5 % and 25 % Pd(0) w/w was tested along with Chem-Pd(0) (100% Pd(0) w/w) and non-palladised biomass (0 % Pd(0) w/w).

Non-palladised biomass promoted no H₂ evolution, as did Bio-Pd(0)*Rhodobacter* and Bio-Pd(0)*Desulfovibrio* loaded at 1% Pd(0) w/w. The highest rate of H₂ generation was seen using Bio-Pd(0)*Desulfovibrio* loaded at 25% Pd(0) w/w, at more than four times the rate using Chem-Pd(0). When compared at 5% Pd(0) (w/w) the rate using Bio-Pd(0)*Desulfovibrio* was only slightly higher (1.4 times) than using the Bio-Pd(0)*Rhodobacter*, whereas at 25% Pd(0) (w/w) the rate was 2.3 times higher.

All Bio-Pd(0) preparations, loaded at 5% or 25% on *Rhodobacter* or *Desulfovibrio*, were more catalytically active than Chem-Pd(0). By this test, the most highly loaded *Desulfovibrio* preparation (25 % Pd(0) w/w) was most active, whereas a moderately loaded *Rhodobacter* preparation (5 % Pd(0) w/w) was most active. It was also observed that cells with lower loadings of Bio-Pd(0) were more readily resuspended in the reaction mixture than cells with higher loadings, which may have been a contributing factor to catalytic activity (see discussion).

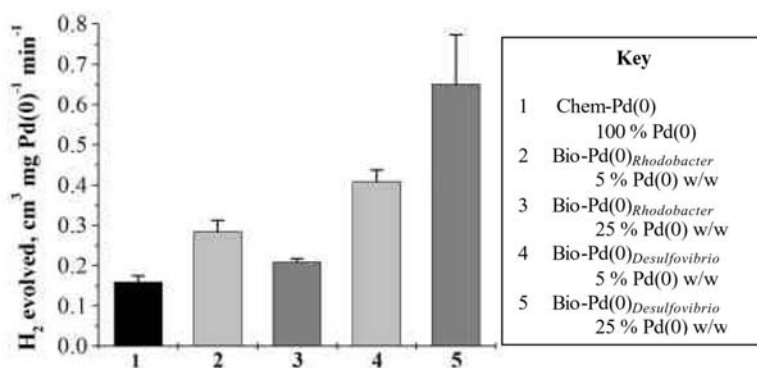


Figure 2: Rates of H₂ generation from hypophosphite by various catalytic preparations. All reactions contained 0.5 mg Pd(0). Data are means and standard errors from four experiments. No H₂ was generated using unloaded biomass or Bio-Pd(0) loaded at 1% Pd(0) w/w.

Evaluation of catalytic activity by reductive dehalogenation of chlorinated aromatic compounds

Bio-Pd(0)_{Rhodobacter}, Bio-Pd(0)_{Desulfovibrio} (25% Pd(0) w/w) and Chem-Pd(0) were tested for the capacity to catalyse reductive dechlorination of chlorophenols (2-chlorophenol and pentachlorophenol) and polychlorinated biphenyls (PCBs). Controls, i.e. non-palladised biomass and Bio-Pd(0) of each type without electron donor promoted no chloride release.

Chloride release from 2-chlorophenol (2-CP)

Constant rates of chloride release from 2-CP were observed using all three catalysts over 60 min (time course not shown). The highest chloride release (36.14 μg cm⁻³) was observed using Bio-Pd(0)_{Desulfovibrio} (Table 2). The corresponding rates using Bio-Pd(0)_{Rhodobacter} and Chem-Pd(0) were 53 % and 33% of this, respectively. On a mass of Pd(0) basis the differences between Bio-Pd(0) preparations and Chem-Pd(0) can be corrected by a factor of 4, i.e. the chloride release for Bio-Pd(0)_{Rhodobacter} and Bio-Pd(0)_{Desulfovibrio} were 12.2 and 6.5 times higher than for Chem-Pd(0), respectively.

Table 2: Chloride release from chlorophenols and PCBs

| Compound (see Table 1) | Chloride release (μg cm ⁻³) * | | |
|---------------------------|---|----------------------------------|------------------------|
| | Bio-Pd(0) _{Desulfovibrio} | Bio-Pd(0) _{Rhodobacter} | Chem-Pd(0) |
| 2-CP | 36.14 ± 2.85 | 19.31 ± 0.80 | 11.85 ± 4.87 |
| PCP | 4.65 ± 1.60 | 17.38 ± 1.93 | 0.43 ± 2.98 |
| PCB 28 | 13.18 ± 2.67 | 1.43 ± 0.71 | 5.62 ± 1.04 |
| PCB 52 | 1.02 ± 0.05 | 1.04 ± 0.41 | 0.36 ± 0.04 |
| PCB 101 | 3.93 ± 0.97 | 0.93 ± 0.27 | 0.04 ± 0.00 |
| PCB 118 | 4.29 ± 1.32 | no sig Cl ⁻ | no sig Cl ⁻ |
| PCB 138 | 1.18 ± 0.13 | no sig Cl ⁻ | no sig Cl ⁻ |
| PCB 153 | 2.55 ± 0.56 | no sig Cl ⁻ | 0.54 ± 0.02 |
| PCB 180 | 2.39 ± 0.76 | 0.46 ± 0.23 | 0.27 ± 0.02 |

* Data represent the increase in chloride concentration after 60 min for chlorophenols, and 24 hours for PCBs. Data are means ± standard errors from at least three independent experiments. Note that since the Pd:biomass ratio was 1:3, the data for Bio-Pd(0) can be multiplied by four for direct comparison with Chem-Pd(0) on a mass of Pd(0) basis. no sig Cl⁻ : significant chloride was not detected. Assay sensitivity was 0.5-100 μg Cl⁻ cm⁻³.

Chloride release from pentachlorophenol (PCP)

Table 2 shows chloride release from PCP after 1 hour, at which point the only extensive dehalogenation took place with Bio-Pd(0)*Rhodobacter*. In the case of PCP, a delay was observed for Bio-Pd(0)*Desulfovibrio* and Chem-Pd(0), the first significant chloride being detected after 1-2 hours, while Bio-Pd(0)*Rhodobacter* catalysed a similar overall extent of dechlorination, but with the first chloride release detected within 40 min (Figure 3).

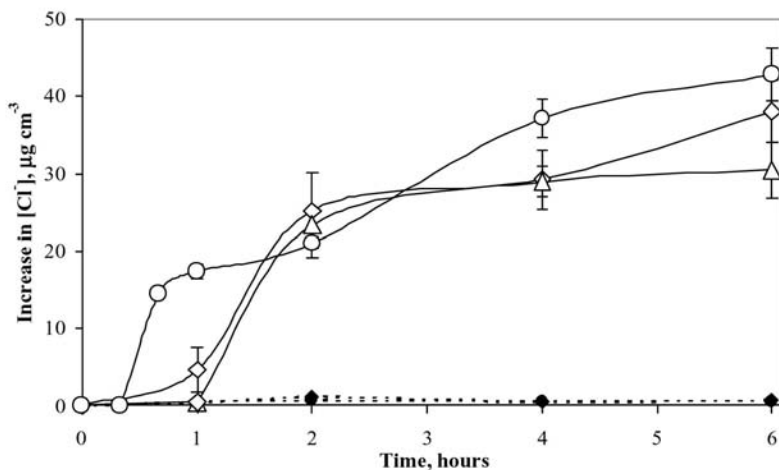


Figure 3: Reductive dehalogenation of pentachlorophenol (PCP) Pd(0) catalysts (solid lines): (◇) 25% Bio-Pd(0)*Desulfovibrio* (○) 25% Bio-Pd(0)*Rhodobacter* (△) Chem-Pd(0) Pd(0)-free controls (dashed lines): (◆) *Desulfovibrio* biomass (●) *Rhodobacter* biomass. Data represent means and standard errors from at least three independent experiments. Note that since the Pd:biomass ratio was 1:3, the data for Bio-Pd(0) can be multiplied by four for direct comparison with Chem-Pd(0) on a mass of Pd(0) basis. Error bars not shown are within the dimensions of the symbols.

After 6 hours the highest release of chloride was obtained using Bio-Pd(0)*Rhodobacter* and the corresponding value for Bio-Pd(0)*Desulfovibrio* was only slightly lower (Figure 3). On the basis of chloride release per mass of Pd(0), both Bio-Pd(0) preparations were over four times as active as Chem-Pd(0).

Chloride release from polychlorinated biphenyls (PCBs)

Chloride release from various PCBs (listed in Table 1) was determined after 24 hours (Table 2). The greatest PCB dehalogenation was observed using Bio-Pd(0)*Desulfovibrio* with PCB 28 (see Table 1). The corresponding values were 11 % and 43% of this with Bio-Pd(0)*Rhodobacter* and Chem-Pd(0), respectively. On a mass of Pd(0) basis, the extent of dehalogenation with Bio-Pd(0)*Rhodobacter* was equivalent to that observed with Chem-Pd(0), whereas Bio-Pd(0)*Desulfovibrio* was superior to Chem-Pd(0) by 9.4-fold.

This trend for the Bio-Pd(0)s was seen for the majority of the PCBs tested (Table 2), although Bio-Pd(0)*Rhodobacter* was comparable to its *Desulfovibrio* counterpart in the case of PCB 52. The controls (non-palladised biomass) exclude the possibility of chloride release from the biomass component of Bio-Pd(0). The observation of no significant chloride was seen in some tests of Bio-Pd(0)*Rhodobacter*, confirming that the background matrix was essentially chloride free and that palladisation did not permit chloride release from biomass.

These preliminary tests showed that both biomass-supported catalysts were superior to Chem-Pd(0), while Bio-Pd(0)*Desulfovibrio* was overall more effective than Bio-Pd(0)*Rhodobacter* for reductive dehalogenation of chlorinated aromatics at a loading of 25% Pd(0) w/w.

DISCUSSION

Cell-surface localisation of Pd(0) deposits was similar on cells of *R. sphaeroides* and *D. desulfuricans* (Figure 1). A periplasmic origin for Pd(0) crystals in *D. desulfuricans* was shown previously to derive from an involvement of periplasmic hydrogenases in the reduction of sorbed Pd(II) and hydrogenase activity was confirmed throughout the incubation period under H₂ [11]. The TEM study (Figure 1) demonstrated an origin for Pd(0) crystals in the periplasm of *R. sphaeroides*, suggesting that periplasm-orientated reductase activity may also initiate Pd(II) reduction in this species.

It was observed that the frequency of Pd(0) deposits was lower, and less Pd(0) was visible on cells of *R. sphaeroides* than on *D. desulfuricans*, although the ratio of Pd:biomass (w/w) was maintained constant. The TEM evidence excludes the presence of significant internal Pd(0) deposits, but it is possible that with *R. sphaeroides* a proportion of the Pd(0) deposits were below the limit of resolution.

Use of biomass as a support in catalyst preparation augmented catalytic activity, which indicates the increased availability of palladium catalytic surface. This was previously attributed to reduced particle size [13], while a further contributing factor may be the increased dispersion of the overall material and stabilisation of nanoparticles on the biomass. As the Pd(0) loading decreased, the material became more readily held in suspension (unpublished observations), which may have improved mixing in the reactors, thus increasing access to Pd(0). The evidence from Bio-Pd(0)*Rhodobacter* supports the hypothesis that an increased proportion of support could lead to increased access to Pd(0), because in the hypophosphite test, activity increased while Pd(0) loading decreased from 100% (Chem-Pd(0)) to 25% to 5% (w/w). However, for Bio-Pd(0)*Desulfovibrio* there was less activity at 5% than at 25% Pd(0) (w/w), suggesting that other factors were also important.

For catalytic testing in reductive dehalogenation of chlorinated aromatic compounds, the Bio-Pd(0) loadings were set at 25% Pd(0) (w/w). Different chlorinated aromatic compounds have different industrial uses (see introduction) and a catalyst targeting a specific waste would be highly beneficial. These studies show that in the case of PCBs *Desulfovibrio*-supported catalyst was superior, whereas in the case of pentachlorophenol, although the overall activity of both biomass-supported catalysts was similar, the Bio-Pd(0)*Rhodobacter* could offer a significant advantage for the treatment of industrial waste streams where a rapid rate would reduce the flow residence time. In contrast, for 'historical' problems such as PCP-contaminated soil, where the timescale is less important, *Rhodobacter*- and *Desulfovibrio*-supported catalysts would be equally useful.

The effect of Pd(0) loading on dehalogenation activity was not investigated, but the results of the hypophosphite test suggest these effects may be species-specific. Future studies will focus on such optimisation of the biocatalyst for PCB dehalogenation and also examine other bacterial species with metal reductase activity.

ACKNOWLEDGEMENTS

This work was supported by the BBSRC (grant No. RRAD09846 and studentship 10703) and by a Royal Society/BBSRC Industry fellowship to Prof. L. E. Macaskie. The authors would especially like to thank Mrs. L. Tomkins (Centre for Electron Microscopy, University of Birmingham) for assistance with electron microscopy.

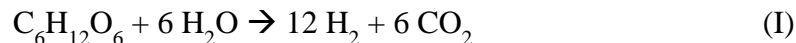
REFERENCES

- [1] Moore, M. D., Kaplan, S., J. Bacteriol., 174(5) (1992), 1505-1514.
- [2] Nepple, B. B., Kessi, J., Bachofen, R., J. Ind. Microbiol. Biotechnol., 25(4) (2000), 198-203.
- [3] Yamada, A., Miyagishima, N., Matsunaga, T., J. Mar. Biotechnol., 5(1) (1997), 46-49.
- [4] Borsetti, F., Borghese, R., Francia, F., Randi, M. R., Fedi, S., Zannoni, D., Protoplasma, 221(1-2) (2003), 153-161.
- [5] Kessi, J., Ramuz, M., Wehrli, E., Spycher, M., Bachofen, R., Appl. Environ. Microbiol., 65(11) (1999), 4734-4740.
- [6] Van Praag, E., Degli Agosti, R., Bachofen, R., Arch. Sci., 55(2) (2002), 69-80.
- [7] Lovley, D. R., Annu. Rev. Microbiol., 47((1993), 263-290.
- [8] Kendal, T., Platinum 2004, Johnson Matthey, Plc.,
- [9] Yong, P., Rowson, N. A., Farr, J. P. G., Harris, I. R., Macaskie, L. E., Environ. Technol., 24(3) (2003), 289-297.

APPARATUS AND METHOD FOR BIOHYDROGEN PRODUCTION

The present invention relates to the production of hydrogen using bacteria (biohydrogen production). More specifically, it relates to an apparatus and a method for biohydrogen production by fermentation of sugars by bacteria such as *Escherichia coli*, and photofermentation of the resulting organic acids by photoheterotrophic bacteria such as *Rhodobacter sphaeroides*. The present invention further relates to a method to improve biohydrogen production, and the uses of electric current in such methods to control ammonium transport and to improve biohydrogen production.

Biohydrogen is anticipated to play an important role in the future hydrogen economy, as it can be produced from readily available renewable substrates. Sugars are promising substrates for biological H₂ production, being readily and renewably available and potentially giving a high yield of H₂ (Equation I).



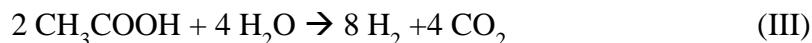
The stoichiometric yield of 12 mol H₂ per mol hexose represents the ultimate target for biohydrogen production. No single organism is capable of performing the conversion with this efficiency. In fact, the thermodynamic maximum yield for dark fermentation is 4 mol/mol (the Thauer limit) as illustrated in Equation II:

Fermentation:



In order to improve the H₂ production efficiency of the process, therefore, it is necessary to further convert the organic acids of Equation II, theoretically producing a further 8 mol of H₂:

Photofermentation:



Equations II and III describe an ideal situation in which all carbon substrate is processed along the appropriate pathways and none is diverted to the formation of biomass or alternative metabolites. In practice, fermentation will produce a range of organic compounds, according to the precise fermentation conditions used. In order to maximise the efficiency of the process, it is necessary that as many as possible of these organic compounds can be converted to produce hydrogen gas.

Similarly, although the fermentation of Equation II is shown acting on a simple hexose, in practice a sugar feed solution may also contain more complex carbohydrates. In order to maximise the efficiency of the process, it is necessary that different hexoses and more complex carbohydrates can be converted to produce hydrogen gas.

According to a first aspect of the present invention, there is provided an apparatus for biohydrogen production, comprising a cell having an anion-selective membrane dividing the cell into first and second compartments, the first compartment having a cathode, and the second compartment having an anode, wherein the first compartment is in fluid communication with a bacterial fermentation culture, and the second compartment is in fluid communication with a photoheterotrophic bacterial culture.

In one embodiment, the apparatus additionally comprises a first reactor for fermentation, in fluid communication with the first compartment of the cell. This reactor may store the majority of the bacterial fermentation culture, with culture medium from the first reactor being pumped to the first compartment of the cell and then returning to the first reactor. This allows the volume of culture medium to be varied, whilst maintaining the same design of cell. It also reduces the proportion of time for which any given bacterium is subject to the effects of the electric field within the cell; exposure to electric field is thought to reduce the viability of cell cultures.

In one embodiment, the apparatus additionally comprises a second reactor for photoheterotrophy, in communication with the second compartment of the cell. This reactor may store the majority of the photoheterotrophic bacterial culture, with culture medium from the second compartment of the cell being pumped to the second reactor, and then returning to the second compartment of the cell. As above, this allows for flexibility in the volume of culture medium used, and reduces the proportion of time for which the individual bacteria of this culture are exposed to the electric field within the cell.

According to a second aspect of the present invention there is provided a method for biohydrogen production, comprising:

- a) providing an apparatus comprising a cell having an anion-selective membrane dividing the cell into first and second compartments, the first compartment having a cathode, and the second compartment having an anode, wherein the first compartment is in fluid communication with a bacterial fermentation culture, and the second compartment is in fluid communication with a photoheterotrophic bacterial culture;
- b) supplying the bacterial fermentation culture with an aqueous solution of at least one fermentable carbohydrate, such that the bacterial fermentation culture ferments the fermentable carbohydrate and produces at least one organic acid;
- c) supplying the first compartment of the cell with culture medium from the bacterial fermentation culture;
- d) applying a potential difference between the anode and the cathode to cause the at least one organic acid to cross the anion-selective membrane from the first compartment of the cell to the second compartment of the cell;
- e) supplying the photoheterotrophic bacterial culture with fluid from the second compartment of the cell, such that the photoheterotrophic culture ferments the at least one organic acid and produces hydrogen gas;
- f) collecting hydrogen gas produced by the bacterial fermentation culture and by the photoheterotrophic bacterial culture.

This process involves a first fermentation stage, in which fermentable sugar is converted into organic acids. Although some hydrogen may be produced by this stage, the accumulation of other fermentation products (such as organic acids) can reduce or halt fermentation, even in an excess of substrate. Furthermore, the presence of the organic acids in the residual medium would present difficulties when disposing of the medium. According to the process of the present invention, therefore, organic acids produced by fermentation in the first stage are extracted from the fermentation medium (by means of the anion-selective membrane) and passed to a second photoheterotrophic stage in which the organic acids are further converted to H₂. Utilization of fermentation end-products for further H₂ production in a second stage increases the economic potential of the process by improving the H₂ yield and reducing the organic content of the final waste.

In one embodiment, the bacterial fermentation culture also produces hydrogen.

In one embodiment, the fermentation culture medium after step b) comprises dissolved ammonium. Such ammonium ions may be produced by the bacterial fermentation culture as part of the fermentation process. Alternatively, the ammonium may have been present in the initial fermentable carbohydrate solution, or may have been formed by the bacterial fermentation culture by reduction of nitrate or nitrite present in the fermentable carbohydrate solution.

Although the culture medium from the first (“fermentation”) stage of the process is able, following pH adjustment, to directly support growth of photoheterotrophic bacteria, the present inventors have surprisingly found that when the fermentation culture medium after step b) comprises ammonium, little or no hydrogen production occurs in the absence of the apparatus and method of the current invention. It is thought that nitrogenase (the enzyme thought to be responsible for H₂ production in the second, heterotrophic phase) is inhibited by the ammonium. However, by utilising the anion-selective membrane of the present invention, the majority of the ammonium is separated from the organic acids required for the second stage photoheterotrophic fermentation, allowing H₂ production to take place, as required.

One example of a membrane-equipped cell suitable for use in the present invention is described in International (PCT) Patent Application WO 2004/046351. The cell described in this document has an anion-selective membrane (Neosepta ACM) separating the Bio-Reaction Chamber (equivalent to the first compartment of the present invention) from the Product Concentrate Chamber (equivalent to the second compartment). The teaching of that document is incorporated herein by reference.

According to a third aspect of the present invention, there is provided a method for biohydrogen production, comprising:

- a) providing an apparatus comprising a cell having an anion-selective membrane dividing the cell into first and second compartments, the first compartment having a cathode, and the second compartment having an anode, wherein the first compartment is in fluid

- communication with a bacterial fermentation culture, and the second compartment is in fluid communication with a photoheterotrophic bacterial culture;
- b) supplying the bacterial fermentation culture with an aqueous solution of at least one fermentable carbohydrate, such that the bacterial fermentation culture ferments the fermentable carbohydrate and produces at least one organic acid, and the resulting culture medium comprises dissolved ammonium;
 - c) supplying the first compartment of the cell with culture medium from the bacterial fermentation culture;
 - d) applying a potential difference between the anode and the cathode to cause an electric current to flow between the anode and the cathode, and thereby to cause the at least one organic acid to cross the anion-selective membrane from the first compartment of the cell to the second compartment of the cell;
 - e) regulating the electric current flowing between the anode and the cathode such that ammonium is transferred across the anion-selective membrane from the first cell compartment to the second cell compartment;
 - f) supplying the photoheterotrophic bacterial culture with culture medium from the second compartment of the cell, such that the photoheterotrophic culture ferments the at least one organic acid and produces hydrogen gas;
 - g) collecting hydrogen gas produced by the bacterial fermentation culture and by the photoheterotrophic bacterial culture.

Although phototrophic H₂ production by anoxygenic photosynthetic bacteria (APB) is thought to be inhibited by ammonium, it is known that small quantities of a nitrogen source such as the ammonium ion are in fact essential for the growth of the bacteria. The inventors have surprisingly found that, by ensuring that the current density across the membrane is maintained within certain limits, it is possible to cause small quantities of ammonium to cross the membrane, in spite of the opposing potential difference. Thus, by regulation of the current density, it is possible to regulate the supply of ammonium ion to the bacteria in the photobioreactor and hence to maximise H₂ production.

In general, the rate of ammonium transfer decreases exponentially with increasing current density, as can be seen from Figure 3. Although generally it is desirable to maximise the current density and thereby maximise the transfer of organic acids from the first to the second compartment of the cell, in the method of this aspect of the present invention, the current is regulated to allow ammonium transport.

The precise ranges of current density will vary according to the system, but can be readily determined by the skilled man by measuring ammonium transfer for different current densities. Ammonium transfer can be measured by any appropriate method, such as for example by using the cell of the present invention without the bacterial cell cultures. The first cell compartment may then be filled with a solution of ammonium sulphate, the second cell compartment filled with an ammonium-free solution, and a known electric current passed through the cell. Samples taken from the second cell compartment at regular intervals may be tested for ammonium

concentration (for example, using the indophenol blue method, Nessler method or, for real-time measurement, an ammonium probe)

In one embodiment, the electric current flowing through the cell is varied between a maximum level at which substantially no ammonium is transferred from the first cell compartment to the second cell compartment across the anion-selective membrane, to a minimum level at which ammonium is so transferred.

The quantity of ammonium transferred from the first cell compartment to the second cell compartment in step e) should be sufficient to enable detectable growth of bacteria of the photoheterotrophic bacterial culture. Such growth may be measured by any appropriate means, such as for example by measuring optical density.

In one embodiment, the bacterial fermentation culture also produces hydrogen.

A further benefit of the methods according to the present invention is that the electrokinetic cell acts as a microfiltration unit, retaining the bacterial fermentation culture in the first stage of the process, while extracting water to maintain a constant culture volume, despite the continuous addition of feed and titrant to the culture. Water transport across the membrane occurs as a result of electro dialysis. In a single stage process, this effect would normally be considered a disadvantage, since it limits the concentration of extracted product (*e.g.* the organic acids) which is achievable. However, in the present invention, this effect helps to carry the acids to the second stage.

According to a fourth aspect of the current invention, there is provided the use of an electrical current applied through the anion-selective membrane of the apparatus of the third aspect of the present invention, in order to regulate the transfer of ammonium from the first cell compartment to the second cell compartment through the membrane.

In one embodiment, the use comprises varying the magnitude of the electric current.

According to a fifth aspect of the present invention, there is provided the use of direct electrical current to improve gaseous hydrogen production by dark fermenting bacteria capable of anaerobic fermentation of sugars to produce organic acids and hydrogen, the use comprising applying the current to a bacterial fermentation culture.

In one embodiment, the bacterial fermentation culture comprises *E. coli*.

The following optional embodiments apply to all aspects of the present invention.

As used herein, the term “bacterial fermentation culture” refers to a bacterial culture which comprises any bacterial strain capable of anaerobic fermentation of sugars to produce organic acids. In one embodiment, the bacterial fermentation culture comprises at least one bacterial strain capable of anaerobically fermenting sugars to produce organic acids and hydrogen. In a further embodiment, the bacterial fermentation culture comprises *E. coli*. In a further

embodiment still, the bacterial fermentation culture comprises the hydrogen-overproducing *E. coli* strain HD701 (M. Sauter *et al.*, Mol Microbiol 1992, vol. 6, p.1523–32). Alternatively or additionally, the properties of the bacterial culture may be altered in any manner known to the skilled man, including by genetic engineering, and may for example include genetic modifications known to increase the hydrogen production of bacterial cultures.

As used herein, the term “photoheterotrophic bacterial culture” refers to a bacterial culture which comprises any bacterial strain capable of anaerobic fermentation of organic acids under the action of light to produce hydrogen gas. Such bacteria may be known as anoxygenic photosynthetic bacteria (APB). In one embodiment, the photoheterotrophic bacterial culture comprises *R. sphaeroides*.

According to one embodiment of the present invention, hydrogen production of the photoheterotrophic bacterial culture is inhibited by presence of ammonium. This is true for all wild-type anoxygenic photosynthetic bacteria although some genetically engineered strains are known in which this behaviour is suppressed or removed.

According to one embodiment of the present invention, hydrogen gas is also collected from the cathode of the electrokinetic cell.

The inventions of the present application will now be illustrated by the following specific examples with reference to the Figures, in which:

Figure 1 represents a schematic diagram of an apparatus suitable for use in the present invention; Figure 2 shows the results of a method according to the second aspect of the present invention; Figure 3 shows the effect of current density in the electrokinetic cell on ammonium transport across an anion-selective membrane (area 200 cm²); and Figure 4 shows the results of a method according to the second aspect of the present invention.

Example 1

Apparatus

Referring to Figure 1, the biohydrogen production system 1 comprises a dark fermentation vessel 2 (6 litre, Electrolab, UK), a cell 3, and a photobioreactor 4.

Cell 3 is divided into first and second compartments 3a and 3b by means of an anion-selective membrane 10 (Neosepta AHA). The first compartment 3a is fitted with a stainless steel cathode 11, whilst the second compartment 3b is fitted with a platinum-coated anode 12; both electrodes are connected to a power supply (not shown). Culture medium from the fermentation vessel 2 is pumped through the first cell compartment 3a and then returned to the vessel 2; within the first cell compartment 3a the culture medium is protected from the cathode 11 by a bipolar membrane 13 (BP-1E). Within the bipolar membrane, the cathode 11 is immersed in a circulating solution of 0.5M sodium sulphate (not shown).

Pumps are connected to supply the fermentation vessel 2 with sugar feed 20 and pH titrants 21 as necessary.

Fluid is circulated through the second cell compartment 3b from a permeate vessel 25; within the second cell compartment 3b, the fluid is protected from the anode 12 by a cation-selective membrane 26. Within the cation-selective membrane 26, the anode 12 is immersed in a circulating solution of 0.5M sodium sulphate (not shown).

Pumps are connected to supply the permeate vessel 25 with basal medium 27 and pH titrants 21 as necessary. Basal medium 27 supplies the photobioreactor 4 with all growth requirements (including a nitrogen source) except for organic acids, which are acquired from the second cell compartment 3b.

Fluid from the permeate vessel 25 (including that which has circulated through the second cell compartment 3b) is supplied to the photobioreactor 4. Excess fluid from the photobioreactor 4 is separately discharged to waste 30.

Hydrogen gas 31 is collected from both the fermentation vessel 2 and the photobioreactor 4.

Pre-culture of *E. coli*

The H₂-overproducing strain *Escherichia coli* HD701 was kindly provided by Professor A. Böck (Lehrstuhl für Mikrobiologie, Munich, Germany) and cultured aerobically on nutrient broth (Oxoid) supplemented with 0.5 % sodium formate (w/w) (1 litre, 16 h, 200 rpm, 0.002% inoculum v/v). A standard temperature of 30 °C was upheld for all growth stages and fermentations.

Feeding regime for dark fermentation

The fermentation vessel 2 was autoclaved with 2.8 litres of aqueous fermentation medium as shown in Table 1.

| | | |
|---|----------|--|
| Na ₂ SO ₄ | 42.6 g | Sterilised as 2.8 L |
| K ₂ HPO ₄ | 10.456 g | |
| KH ₂ PO ₄ | 0.204 g | |
| (NH ₄) ₂ SO ₄ | 0.198 g | |
| 1M MgSO ₄ | 6 ml | Sterilised individually and added separately |
| trace elements solution* | 9 ml | |
| 2M glucose | 30 ml | |

Table 1: Fermentation medium (2.8 L, pH 5.5)

The fermentation vessel 2 (in fluid communication with the 1st cell compartment 3a) contained initially 2.8 litres of complete fermentation medium (above). *E. coli* cells (2 litres) were harvested from the pre-growth medium by centrifugation (4435 x g, 20 °C, 10 min) resuspended in 200 ml saline (NaCl 0.85 % (w/w), pH 7.0) and inoculated into the fermentation vessel 2.

Thus, the initial glucose concentration was 20 mM. The complete culture was purged with argon for 30 minutes before the commencement of gas measurement. Electrodialysis (400 mA, *ca.* 4V) was activated on the medium 1 hour prior to inoculation.

The permeate vessel 25 (in fluid communication with the 2nd cell compartment 3b) contained initially 1 litre of basal medium (described below).

The addition of feed solution 1 to the fermentation vessel 2 commenced 24 h following the initiation of dark fermentation (100 mL/day, 0.6 M glucose, 0.015 M (NH₄)₂SO₄). This point coincided with the continuous addition of basal medium 27 (1 litre/day) to the permeate vessel 25 to generate organic-acid enriched medium. At the same point the contents of the permeate vessel 25 were continuously supplied to the photobioreactor 4 (1 litre/day).

Pre-culture of *R. sphaeroides*

R. sphaeroides was pre-cultured in 15 mL water-jacketed vials filled with sterile succinate medium (Hoekema *et al.*, International Journal of Hydrogen Energy, 2002, vol. 27(11-12), p.1331-1333) under tungsten illumination (30 °C, 72 h).

Photobioreactor specifications

Photofermentation was carried out in a cylindrical glass photobioreactor 4 (internal diameter, 105 mm). The illuminated surface area was 0.107 m² and the average intensity of photosynthetically active radiation at the culture surface was 117.4 μE/m²/s, which was provided by 3 clear tungsten filament bulbs arranged externally along the length of the photobioreactor. The cylinder was surrounded in a reflective tube (diameter 35 cm). The culture (3.0±0.5 litre) was stirred using a magnetic stirrer and follower (1200 rpm) located at the base of the photobioreactor. A temperature of 30.0±0.2 °C was maintained using a submerged cooling coil.

Feeding/dilution regime for photofermentation

The photobioreactor 4 was autoclaved and filled with 3 litres of mixed organic acid growth medium (below), inoculated with 30 ml pre-culture (above) and sparged with argon for 30 min. After growing for 72 h, the contents of the permeate vessel 25 were continuously added to the photobioreactor 4 (1 litre/day) and the contents of the photobioreactor 4 were continuously withdrawn into the outflow vessel 30. This point coincided with the continuous addition of feed solution 1 to the fermentation vessel 2 (100 ml/day).

| | |
|---------------------------------|---------------|
| Acetate | 16 mM |
| Succinate | 14 mM |
| Lactate | 8 mM |
| Butyrate | 5 mM |
| KH ₂ PO ₄ | 1.466 g/litre |
| K ₂ HPO ₄ | 1.732 g/litre |
| Yeast extract | 1.00 g/litre |
| Vitamins solution* | 2 ml |
| Macroelements solution* | 50 ml |
| Microelements solution* | 10 ml |

Table 2: Mixed organic acid growth medium for *R. sphaeroides*

* as described by Hoekema *et al.*, International Journal of Hydrogen Energy, 2002, vol. 27(11-12), p.1331-1333

The composition of basal medium 27 was identical to that of the mixed organic acid growth medium except for the absence of organic acids (acetate, succinate, butyrate and lactate).

Figure 2 demonstrates the effect of the invention on hydrogen production in the fermentation vessel 2. Control experiments (closed squares) were carried out using a simple fermentation vessel without the electrokinetic cell of the present invention. As can be seen, hydrogen production dropped to zero after approximately 10 days. A second control (open triangles) was performed using the configuration shown in Figure 1 except that the anion selective membrane 10 was replaced with an inactive membrane (the membrane no longer transported organic acids because it was aged or fouled). Thus, under the influence of direct current without the extraction of organic acids, hydrogen production had ceased by approximately 8 days. However, in the experiment involving electrodialysis (open circles) according to the present invention, the rate of hydrogen production remained high even after approximately 20 days. The dotted line drawn at 120.3 mL/h indicates a 100 % yield - the H₂ production rate given a yield of 2 mol H₂/mol glucose and a glucose load of 60 mmol/day.

Figure 4 demonstrates the effect of the invention on hydrogen production in the photobioreactor vessel 4. Control experiments (closed squares) were performed using the configuration shown in Figure 1 except that the anion selective membrane 10 was replaced with an inactive membrane (the membrane no longer transported organic acids because it was aged or fouled). There is a peak in hydrogen production at around day 3 as the bacteria are allowed to grow in the growth medium. After day 3 the medium is diluted, as described above and hydrogen production tails off. There is very little or no hydrogen production from day 8. However, in the experiment involving electrodialysis (open circles) the hydrogen production continues beyond day 8. This can be attributed to organic acid transport across the membrane 10 and its subsequent photofermentation.

Ammonium transport

Ammonium transport across the anion-selective membrane was measured and the results are shown in Figure 3. It can be seen that the ammonium flux over 200 cm² membrane varies from

0-6.5 $\mu\text{mol}/\text{min}$ for current densities in the range 10-0 mA/cm^2 , adhering closely to an exponential function. Thus, at higher current densities, when organic acid transport is most efficient, the level of ammonium transport is very low. At lower current densities, the ammonium transport level increases up to a maximum.

Example 2:

The method of Example 1 was repeated, except that in this example the nitrogen requirements of the photofermentation were provided entirely through the transfer of ammonium ion from the first stage dark fermentation via the electro dialysis cell, rather than being added separately via the basal medium.

The apparatus shown in Figure 1 was modified by inclusion of a feedback turbidostat circuit in which a decrease in the optical density of the photoheterotrophic bacterial culture in the photobioreactor 4 prompts a period of decreased current applied to the cell 3, causing increased ammonium ion transfer through the anion-selective membrane 10. This in turn produces a period of growth, causing the turbidity of the photoheterotrophic bacterial culture to increase.

In addition, growth supplements (trace elements and vitamins) of negligible volume were supplied directly to the photobioreactor 4, in place of the supply of basal medium to the permeate vessel 25. The direct addition of growth supplements to the photobioreactor 4 means that the bacteria are not dependent on a supply from the permeate vessel 25 and so the fluid flow rate can be adjusted as required. A minimum flow rate is required in order to transport ammonium ion and organic acid from cell compartment 3b, via the permeate vessel 25 to the photobioreactor 4 but since the photobioreactor is of finite size, any excess fluid must be discharged as waste 30.

Turbidity measurements were taken to determine the required quantity of growth and hence the required quantity of ammonium. Current was then reduced to supply it over a short period, after which the current was returned to the original high setting.

In accordance with Example 1 the photofermentation was required to process an estimated 250 mmol carbon/day as a mixture of organic acids. This requires *ca.* 3.55 g *R. sphaeroides* biomass (dry weight), which is 8.73 % N (w/w) (published value). The supply of ammonium ion necessary to support this culture is dependent upon the dilution rate of the photofermentation culture. The apparatus of this experiment was designed to minimise the dilution rate of the photobioreactor, and hence minimise the necessary ammonium supply. The dilution rate is an uncontrolled variable equal to the sum of water transport via the electrokinetic cell from the dark fermentation and the addition of pH titrant to the permeate chamber. Growth supplements added to the photobioreactor are of negligible volume. A typical dilution rate would be 150 ml/day (Hydraulic retention time, HRT = 20 days), necessitating a daily nitrogen supply of 15.5 mg/day, equal to 0.763 μmol ammonium ion/min.

Nitrogen supply regime

To maximise current for organic acid transfer, the ammonium ion transfer was conducted in short periods of low current. For example a current of 0.1 mA/cm^2 would be used to supply the daily

requirement of 1.10 mmol ammonium ion in 3.04 hours, the remainder of the period being dedicated to organic acid transport employing a higher current.

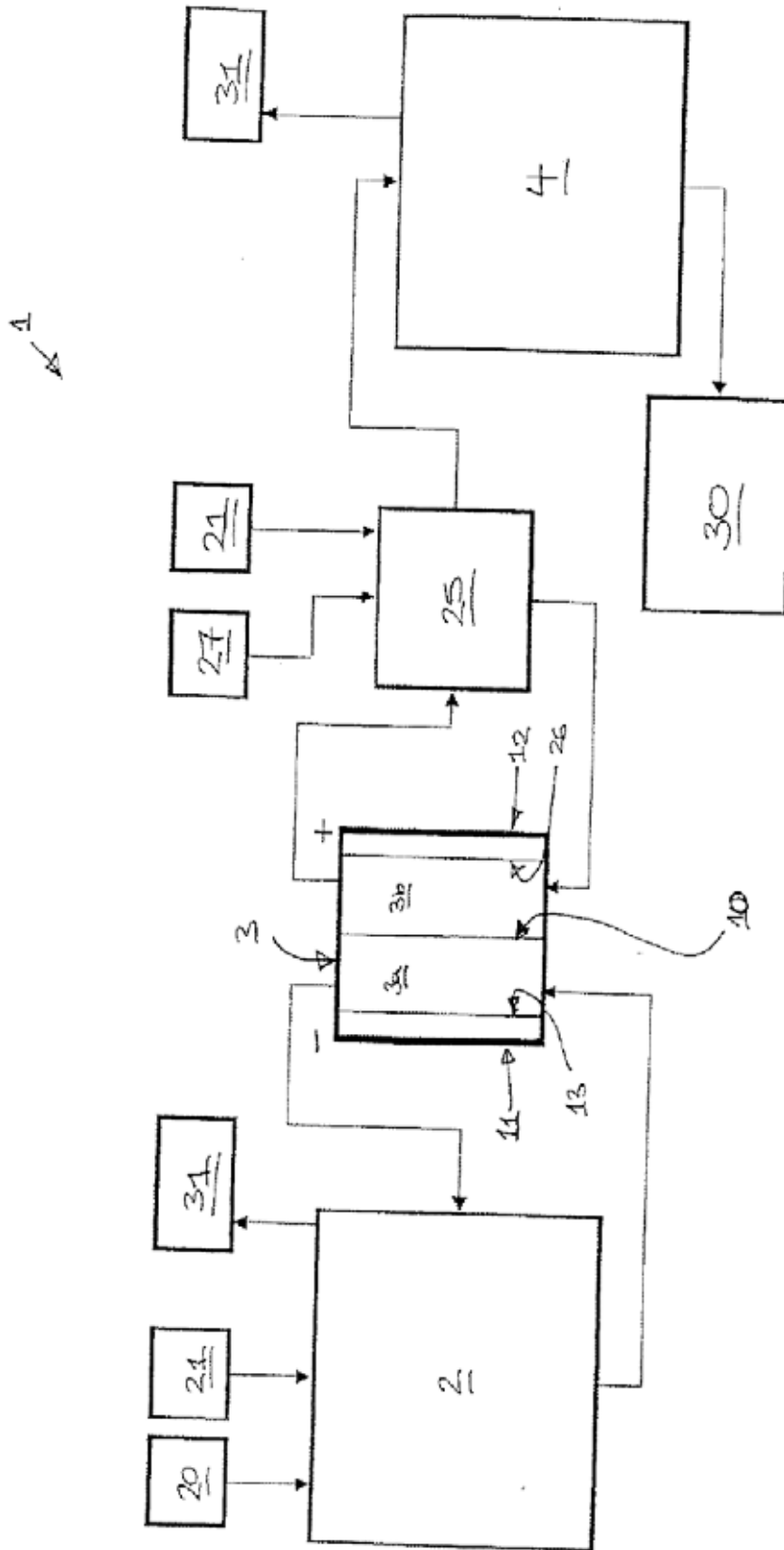


FIGURE 1.

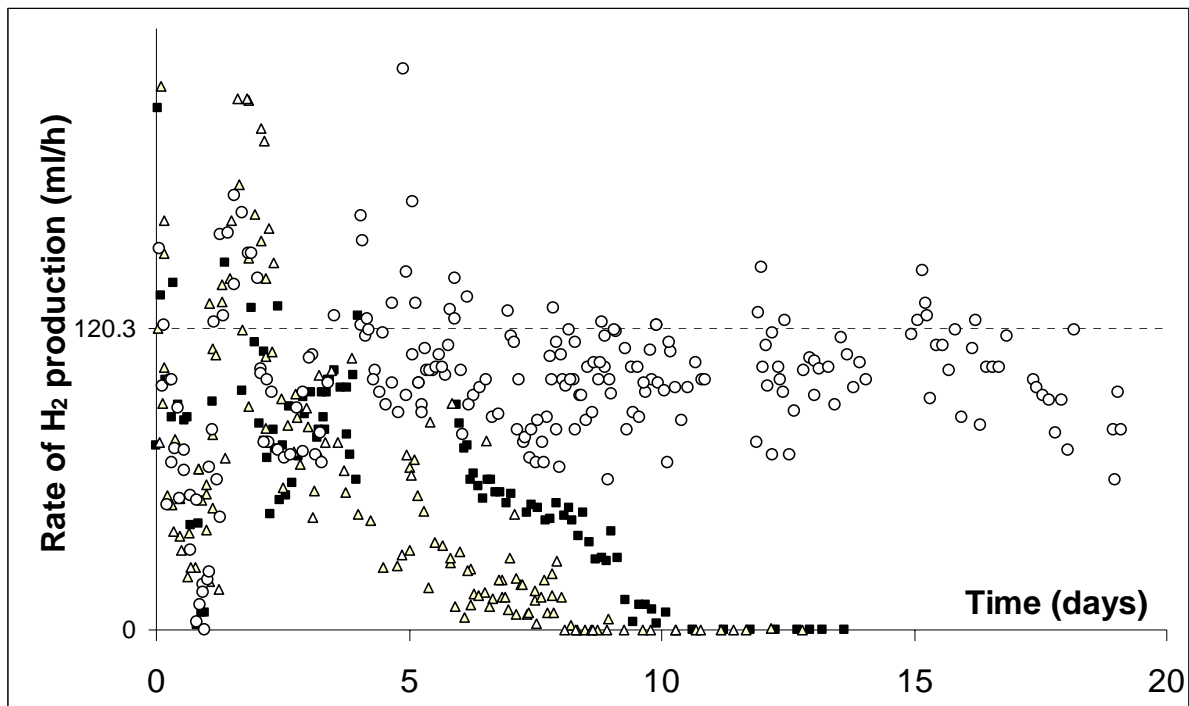


Figure 2

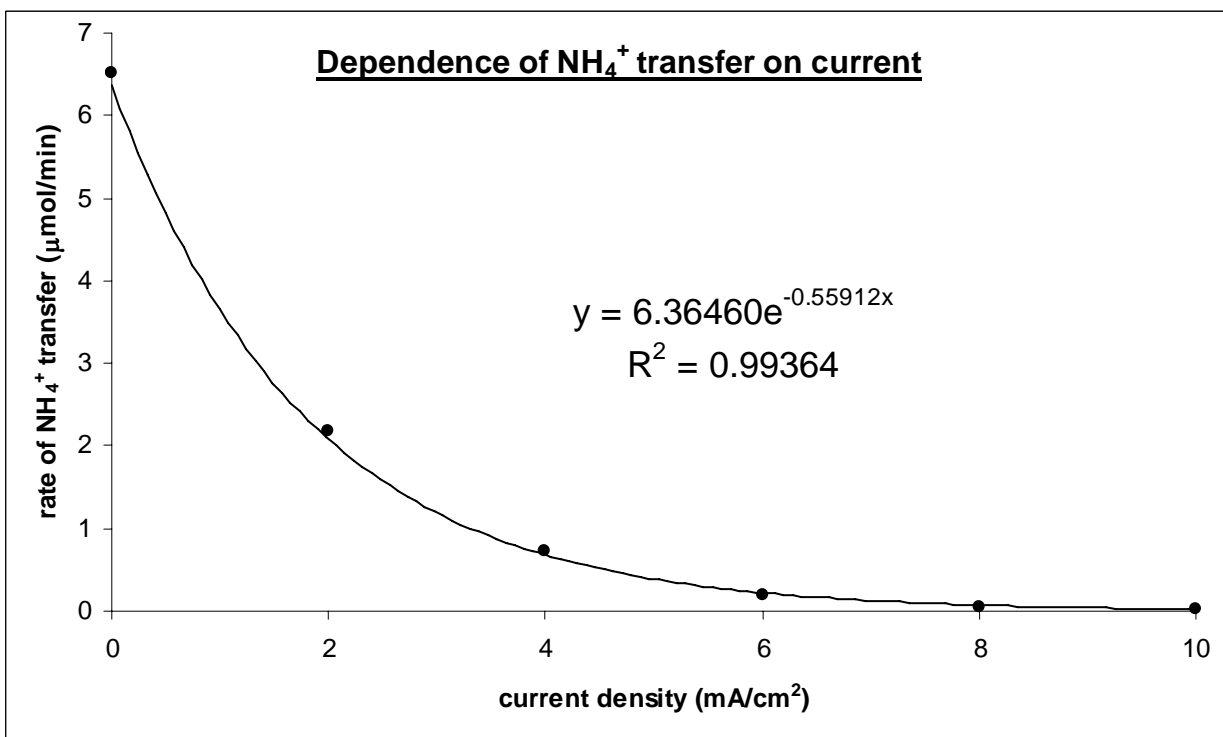


Figure 3

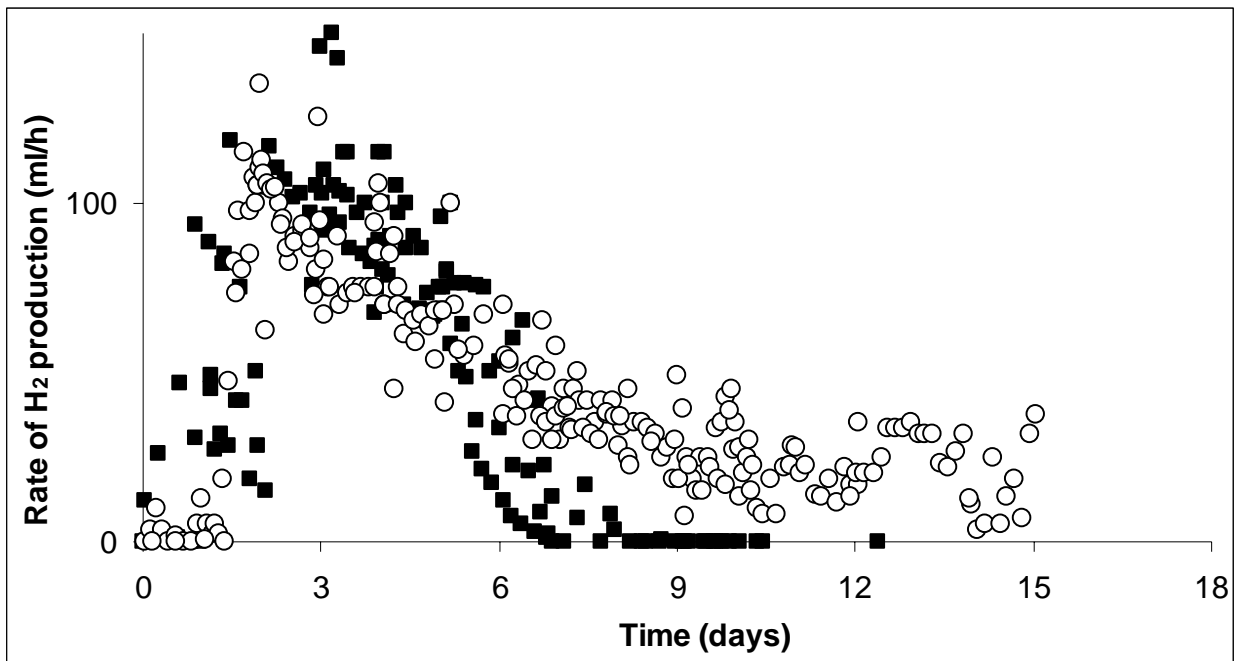


Figure 4

4.2.2 Publications in which the author was involved

- Penfold DW, Redwood MD, Yong P, Stratton-Campbell D, Skibar W, Macaske LE (2007) Microbial H₂ and electricity from wastes. Proceedings of the 7th Hydrogen - Power and Theoretical Engineering Solutions International Symposium (HyPoThESIS VII), Merida, Mexico. CICY ISBN:968-6114-21-1
Role: Assistance with GC analysis and operation of fermentations.
Authored by DW Penfold
Reproduced within section 4.2.2
- Harrad S, Robson M, Hazrati S, Baxter-Plant VS, Deplanche K, Redwood MD, Macaskie LE (2007) Dehalogenation of polychlorinated biphenyls and polybrominated diphenyl ethers using a hybrid bioinorganic catalyst. Journal of Environmental Monitoring. 9:314-318.
Role: Production of bioinorganic catalysts and carrying out dehalogenation reactions.
Authored by S Harrad
Reproduced within section 4.2.2
- Harriet Lugg, Rachel L. Sammons, Peter M. Marquis, Christopher J. Hewitt, Ping Yong, Marion Paterson-Beedle, Mark D. Redwood, Artemis Stamboulis, Mitra Kashani, Mike Jenkins and Lynne E. Macaskie. Polyhydroxybutyrate accumulation by a *Serratia* sp. Biotechnology Letters, accepted subject to minor reviewers comments
Role: Analysis of sequence data relating to butyrate metabolism (see chapter 2.2) to augment and enhance discussion.
Authored by LE Macaskie

Abstract: A strain of *Serratia* sp. showed intracellular electron-transparent inclusion bodies when incubated in the presence of citrate and glycerol 2-phosphate without nitrogen source following pre-growth under carbon-limitation in continuous culture. 1.3 mmoles of citrate were consumed per 450 mg of biomass, giving a calculated yield of maximally 55% of stored material per g of biomass dry weight. The inclusion bodies were stained with Sudan Black and Nile Red, suggesting a lipid material which was confirmed as polyhydroxybutyrate (PHB) by analysis of molecular fragments by gas chromatography and by FTIR spectroscopy of isolated bio-PHB in comparison with reference material. Multi-parameter flow cytometry in conjunction with Nile Red fluorescence, and electron microscopy, showed that not all cells contained heavy PHB bodies, suggesting the potential for increased overall yield. The economic attractiveness is enhanced by the co-production of nanoscale hydroxyapatite (HA), a possible high-value precursor for bone replacement materials.

MICROBIAL H₂ AND ELECTRICITY PRODUCTION FROM WASTES

¹D.W. PENFOLD, ¹M.D. REDWOOD, ¹P. YONG, ²D. STRATTON-CAMPBELL, ²W. SKIBAR AND ¹L.E. MACASKIE

¹ School of Biosciences, University of Birmingham, Edgbaston, Birmingham, B15 2TT, UK.

² C-Tech Innovation Ltd, Capenhurst Technology Park, Capenhurst, Chester, CH1 6EH, UK.

Keywords: *Escherichia coli*, biohydrogen, fuel cell

Abstract

HD701 was tested for its ability to utilise different food wastes for H₂ production using conditions optimised previously using 100 mM glucose at pH 5.5 and *ca.* 9 l of H₂ was produced over 47 h: a yield of ~1 mol H₂/mol glucose. H₂ was not produced from starch, cellulose or fats. Ohmic heating was evaluated as a hydrolytic method to increase the fermentable sugar content prior to fermentative bio-H₂ production. Fruit wastes were the best substrate (1.6 l of bio-H₂ in 21 h), attributable to the high reducing sugar content (292 mM). GC analysis showed only H₂ + N₂ in the off gas, and no catalyst poisons. Accordingly, bio-H₂ produced from confectionery waste supported electricity production in a PEM fuel cell. *E. coli* biomass was also used after palladisation for electrode fabrication for the PEM fuel cell, and electricity production was supported, showing potential biomass bifunctionality.

1. INTRODUCTION

1.1. From raising awareness with British Council's 'zerocarboncity' initiative to the building of the world's first sustainable city-China's Dongtan: Eco-city, the response to global warming is changing. Car companies such as BMW already manufacture hydrogen fuel cell concept cars in response to depleting reserves of fossil fuels and the need for environmentally friendly technology. To ease this transition hybrid car technology is now developed, an interim mix of current combustion and future fuel cell technology. The global response to greenhouse gas production has become more urgent since publication of the Stern Review [1,2] which concludes that if no action is taken on emissions then there is more than a 75% chance of global temperatures rising between 2-3 °C over the next 50 years causing: the global economy to shrink by as much as 20%, a decline in crop yields, particularly in Africa and a rise in sea levels which will leave more than 200 million people permanently displaced and up to 40% of species facing extinction. Against this background, green renewable energy is a topic of extensive research. Hydrogen is seen as one of the most promising contenders as its only combustion product is water and it can be directly used to produce electricity through fuel cells. One method of manufacturing this hydrogen is via microbial production from carbohydrate materials (and other biodegradable waste) via fermentation. Fermentation can thus be used to reduce the amount of waste to be land filled, in accordance with current EU directives and with the added benefit of producing a sustainable energy carrier (hydrogen).

1.2. Although numerous studies have been carried out using various microorganisms, *Escherichia coli* has been neglected even though its well-defined genetic background facilitates strain improvement for increased H₂ production. *E. coli* evolves hydrogen by dark fermentation. In the absence of external electron acceptors (oxygen, nitrate etc), it ferments available sugars into

ethanol and a range of organic acids. This causes a drop in the pH and, in a homeostatic response to this toxic acidity, the *E. coli* converts the organic acid formate into hydrogen and carbon dioxide (which is carbon neutral as it was fixed from atmospheric CO₂ into sugar by plants). An *E. coli* strain, HD701, has been identified which lacks the hyc A repressor of the formate hydrogenlyase (FHL) enzyme system responsible for cleaving formate into hydrogen and carbon dioxide and is therefore up-regulated with respect to hydrogen production [3]. Penfold *et al.* [4] showed that resting cells of *E. coli* HD701 produced H₂ from glucose solution and confectionery wastes. To increase the utility of the process, the range of utilisable substrates needs to be as broad as possible. Genes for utilisation of additional substrates and metabolic versatility can be introduced into the genetic background if required [5]. In order to determine the substrate limitations of strain HD701 this study investigates the use of household food wastes and food constituents as substrates for hydrogen production by strain HD701 and the generation of electricity using a fuel cell made with commercial components and electrodes derived from the *E. coli* biomass itself.

2. MATERIALS AND METHODS

2.1 Bacterial strains, media and pre-growth

The strain used, *E. coli* HD701, is a derivative of *E. coli* MC4100 that lacks the Hyc A regulator of the formate hydrogenlyase system (FHL) (MC4100ΔhycA) and is up-regulated with respect to H₂ evolution [4]. Cultures were maintained on nutrient agar plates (Oxoid, UK) and pre-grown in shake-flask cultures at 30 °C in nutrient broth no. 2 (Oxoid, UK) [4].

2.2 Hydrogen evolution experiments

Experiments used a 6 l fermenter (Electrolab, UK) containing 1.6 l isotonic saline (8.5g/l NaCl), overnight *E. coli* broth culture (2 l) and 400 ml of waste (as stated: 4 l final volume). Cultures were gassed with argon for 1 h and stirred continually (600 rpm) at 30 °C. The pH, (previously determined to be optimal), was maintained at 5.5 using an automated pH control system (Electrolab, UK) (1 M HCl/1 M NaOH). 1 M NaOH was used as a carbon dioxide trap. Experiments were done in duplicate; data are shown as means ± SEM. Error were within ± 5% throughout.

2.3 Sample preparation

2.3.i. Example wastes: Caramel waste was obtained and analysed as described previously[6]. It comprised: total soluble sugars (w/w) 53.0 %; total reducing sugars (w/w) 25.5 %; total protein content (w/w) 1.9 %; ammonium ion (mg/ l) 2.2. For use, the waste was diluted 1:10 into the fermenter (4 l final volume), to give a reducing sugar concentration of 140 mM. Kitchen wastes (case studies: segregated at source into fruits, vegetables and milk/milk products/bread/cakes ('sugary waste')) were collected over several days from approx. 15-20 households, together with miscellaneous segregated paper and cardboard waste, and grass cuttings. The samples were liquidised (Philips Cucina domestic liquidiser: 3-5 min). The sugary waste was used without further liquid addition and the liquid fraction was obtained by centrifugation. The fruit waste (apples, bananas, tangerines) and vegetable waste (leeks, potatoes, carrots, lettuce, cabbage) and other wastes were mixed with enough water to give a thick slurry on homogenisation. The liquid fraction was obtained by squeezing through muslin cloth (fruit waste) or by filtration (vegetable

waste and other wastes). Reducing sugar contents (determined by the dinitrosalicylic assay as described by Chaplin and Kennedy [7]) were as follows: sugary waste: 227 mM; fruit waste 292 mM; vegetable waste 60 mM; grass waste 15 mM; cardboard waste < 1 mM. For use 300 ml of each waste was diluted 1:10 into the fermenter (3 l final volume) to give reducing sugar concentrations of *ca.* 23, 29, 6 and 1.5 mM, respectively. The caramel waste stock was stored at 4 °C; the high sugar content (1.4M) prevented spoilage. The other waste homogenates were stored frozen in a domestic freezer until use (within 1-2 weeks).

2.3. (ii). *Model food waste:* 18kg of food (comprising a mixture of potatoes, carrots, lettuce, white bread and bananas and 4.5l milk) was liquidised using a waste disposal unit with water added to form a slurry. The final volume was 33 l. A 400 ml sample (unheated) was used in the bioreactor. The remainder was heated in an ohmic heater at C-Tech Innovation Ltd.

2.3. (iii). *Real food waste:* Food (vegetables, cake, and fruit) collected from staff at C-Tech Innovation Ltd. was prepared as above- 40.4kg of waste was used and the final volume was 61 l. Reducing sugars were analysed in all wastes according to Chaplin and Kennedy [7].

2.4. GC analysis

Gas samples were stored under glass and over a small volume (<5ml) of water. 1 ml samples were withdrawn using a gas-tight syringe and injected into a gas chromatograph fitted with a shincarbon ST column (micropacked, length: 2m, ID: 1mm, Resteck) and a thermal conductivity detector TCD). The carrier gas was helium (485 ml min⁻¹) and the oven temperature was held at 40 °C for the first 4 min, increased by 10 °C min⁻¹ up to 150 °C, and held for 5 min.

2.5. Preparation of palladised biomass for electrodes, and electrode preparation

Cells of *E. coli* HD701 were harvested and palladised as described previously [6]. The ‘bio-Pd’ (5% Pd (0)/biomass w/w) was harvested by centrifugation and washed with deionised water three times and then with acetone. Samples were dried at room temperature and then transferred to 10 ml alumina ceramic crucibles. The crucibles were transferred to a furnace with a temperature control program. The temperature was increased gradually from room temperature to 700 °C within 4 h and held at 700 °C for a further 4 h. The samples were cooled to room temperature in the furnace. Reference material, treated in parallel, was commercial Pd powder (submicron, Aldrich Chem. Co, Germany). Reference Pd (0) and bio-manufactured Pd(0) (20 mg of each, as metal) were mixed separately with pure activated carbon powder (80 mg; BDH Chemicals Ltd, UK). Nafion[®] (0.21ml; 10 wt % in water, Sigma-Aldrich) and water (0.2 ml) were added to each sample containing 20% of Pd and 80% of carbon (plus the residual biomass component). The sample was mixed well and applied homogeneously by painting onto 16 cm² teflon treated carbon paper (Fuel Cell Scientific, USA), and dried at room temperature.

2.6. Testing Pd-electrodes in a proton exchange membrane (PEM) fuel cell system

A fuel cell system (“ECO” H₂/O₂ fuel cell, H-tec, Hydrogen Energy Systems, Luebeck, Germany) was used to test the laboratory-made electrodes (i.e., containing commercial Pd powder (C-Pd) and bio-manufactured Pd from *E-coli* HD701 (E-Pd). A standard Pt electrode (as supplied by the manufacturer) was used as the cathode for all the tests. The ECO H₂/O₂ unit contains a spotlight, a PEM electrolyser (where H₂ and O₂ are produced by the electrolysis of water, using solar power or artificial illumination) and a PEMFC Kit (a self-assembly fuel cell). The electrolysed H₂ and O₂ are fed into the PEM fuel cell via the anode (H₂ stream) and cathode

(O₂ stream). Current (I) and voltage (V) were measured and recorded against resistance (R) from R= ∞ to R= 0 Ω gradually as described by Voigt *et al.* [8]. P (output power in watts (W)) = I (current in amperes (A)) x V (voltage in volts (V)).

2.7. Bioenergy generating system

The proton exchange membrane (PEM) fuel cell (above) was connected to a motorised fan (H-tec, Germany). Bio-H₂ from fermentation of caramel waste was fed into the fuel cell through a 1 M NaOH carbon dioxide trap. The assembly was used to generate electricity with an electrical load. [9].

3. RESULTS AND DISCUSSION

3.1. Model Food constituents

3.1.1. Previous studies have established that the biohydrogen process can be used with simple sugars such as glucose and fructose and industrial confectionery waste as substrates for hydrogen production [4]. However, for the process to have commercial application, a wider substrate base needs to be identified. A range of food constituent surrogates was therefore tested to evaluate the potential for using household food-waste for hydrogen production by *E. coli* HD701 (Table 1).

Table 1. Hydrogen evolved from various food constituents

| Food constituent | Volume of H ₂ evolved (ml) | Time course (h) |
|--------------------------|---------------------------------------|-----------------|
| Tryptone (6.25 g/l) | 1380 | 50 |
| Lactose (18 g/l) | 0 | 50 |
| Maltose (18 g/l) | 3635 | 53 |
| Maltodextrin (18 g/l) | 3840 | 50 |
| Cellulose (18 g/l) | 0 | 96 |
| Pectin (18 g/l) | 1480 | 26 |
| Fats/fatty acids (18g/l) | 0 | 53 |
| Glycerol (100 mM) | 2950 | 70 |
| Starch (14 g/l) | 0 | 70 |

Starch, cellulose and fats did not promote any hydrogen production after 95 and 53 h, respectively. This was not unexpected since *E. coli* does not possess exocellular enzymes to degrade β-glucan linkages (cellulose) and its debranching activity towards 1, 6-α-linkages (starch branch points) is low (if present at all) and the native polymers are too large to enter the cells. Lactose could not be utilised since *E. coli* HD701 is a *lac*⁻ strain [3].

3.1.2. Since *E. coli* strain HD701 was unable to use starch as a substrate for biohydrogen production, commercially available amylase and isoamylase (debranching enzyme) were tested in an upstream reactor for their ability to break down starch into a utilisable form for the *E. coli*. Using published methods it was shown that the commercial amylase was highly active (0.5 mmol of reducing sugar released/min/unit of enzyme). However, the reducing sugar produced from starch (14g/l) hydrolysis was only 17 mM over one hour using 100 U of amylase. Addition of this hydrolysate to the hydrogen-evolving reactor (final reducing sugar concentration of 1.7 mM) gave 80 ml of hydrogen over a period of 10 h. Upstream enzymatic hydrolysis of waste would

clearly limit concentration of available sugar and also the rate of hydrolysis of available polyglucose. Therefore, ohmic heating was evaluated—as an alternative hydrolytic method in subsequent processes involving food wastes (see later).

3.1.3. Both maltodextrins and maltose are hydrolysis products of starch. Using the same mass of these as was used as glucose in previous experiments (72 g/reactor), *ca.* 4 l of hydrogen was evolved from both compounds, less than half the total volume as obtained previously from glucose [D.W. Penfold, unpublished]. The optimum pH for H₂ evolution from glucose was pH 5.5 (D.W. Penfold, unpublished) but since other studies have shown that the *mal* genes are upregulated at alkaline pH [10, 11] more work is needed to obtain the optimum pH for maltodextrin utilisation.

3.1.4. Approximately 3 l of hydrogen was evolved from 100 mM glycerol after 78 h but with a lag of *ca.* 24 h before onset of hydrogen production. Addition of 10 mM glycerol to the preculture completely prevented hydrogen production. This experiment was repeated in duplicate with the same result being obtained in all cases. This lag could be attributed to inhibition of glycerol kinase by the presence of glucose. Consequently *E. coli* may not utilise glycerol until all of the glucose is consumed. However, the cause of the complete inhibition of hydrogen production by addition of glycerol to the preculture requires further investigation

3.1.5. A similar lag was observed with tryptone (produced from the tryptic digest of casein). Twenty five grams of tryptone was added per reactor and this resulted in *ca.* 1.4 l (1380 ± 220 ml) hydrogen being evolved over 50 h after a lag phase of 8 h. The presence of a nitrogenous compound causes the formation of amines as suggested by an observed increase in pH into alkalinity (pH 9.5). Hydrogen production occurred after cessation of the increase in pH and readjustment of the pH to neutrality.

3.2. Biohydrogen production from sample wastes

3.2.1. As seen in above, enzymatic pre-hydrolysis of the complex carbohydrates did not liberate simple sugars at a rate sufficiently high to sustain effective H₂ production. Thermal treatment techniques are able to break down complex wastes to smaller molecules and therefore ohmic heating was used as a potential alternative pre-treatment method. This method overcomes the problem of uneven heat distribution associated with conventional heating processes (caused by them only heating the surface of the product) by generating internal heat within the product. Ohmic heating is a direct method of heating where an alternating current is passed through the sample and the resistance of the sample causes it to heat up. Alternating current is used to prevent electrolysis of the sample. Comparison of unheated and treated food wastes was therefore carried out in the study of bio-H₂ production from real waste samples (Table 2)

Table 2. Free reducing sugar content and hydrogen production from waste

| Sample | Free reducing sugar (mM) | Volume of H₂ (ml) | Time (hours) |
|--|---------------------------------|-------------------------------------|---------------------|
| Untreated milk, milk products, bread (sugary waste) | 228 | 2750 | 28 |
| Heat treated milk, milk products, bread (sugary waste) | 260 | 990 | 28 |
| Untreated vegetable waste | 60 | 800 | 23 |
| Heat treated vegetable waste | 137 | 500 | 23 |
| Untreated fruit waste | 292 | 3570 | 70 |
| Heat treated fruit waste | 303 | 1570 | 70 |
| Untreated paper and cardboard waste | 0.5 | 10 | 29 |
| Heat treated paper and cardboard waste | 0.8 | 0 | 29 |
| Untreated grass waste | 15 | 505 | 52 |
| Heat treated grass waste | 28 | 5 | 52 |
| Industrial caramel waste | 1400 | 3100 | 10 |

Using sugary waste the heating process resulted in a change of colour of the solution from a whitish colour to a brown colour. Reducing sugar assays on the treated and untreated waste showed the reducing sugar concentration of the treated and untreated waste to be *ca.* 260 and 230 mM, respectively. The saturating concentration producing the maximal velocity of H₂ production from a glucose solution was 100 mM (final concentration in the reactor), demonstrated using glucose [4]. Hydrogen evolution from the sugary waste samples was monitored. After 28 h, this was approximately 2.75 and 1 l (Table 2). Therefore, despite the liberation of additional sugar, ohmic-heat treatment of the waste solution supported less than half the volume of hydrogen production compared to the untreated sample. One possible reason for the lower amount of hydrogen produced from the treated waste is caramelisation of the sugars in the heating process, which is well known to be growth inhibitory [12]. The same effect was seen in all of the wastes examined (Table 2) where bio-H₂ production from the ohmically-treated samples was approx. halved, except for the grass waste where the inhibition was almost complete.

3.2.2. The best substrate for volumetric hydrogen production was fruit waste (untreated) with *ca.* 3.5 l of hydrogen evolved over 50 h, as expected since this contained the highest free sugar (Table 2).

3.2.3. Vegetable and grass wastes supported less hydrogen production as expected according to their lower free sugar contents (and paper/ cardboard waste none at all). Despite the release of additional sugar by ohmic heat treatment no benefit of this approach was realised in any of the samples tested. It was concluded that further work is required to establish the optimum conditions for ohmic heat treatment concomitant with the lowest production of inhibitory agents. Incorporation of ascorbic acid (a free radical scavenger) after ohmic heating had no beneficial effect and the inhibitory agent(s) remain unidentified [12].

3.2.4. GC analysis of head gases

Hydrogen production from heat-treated and untreated model and real waste was investigated. Apart from argon, hydrogen was the only gas detected. GC analysis of the gas evolved from the heat-treated model waste showed that less hydrogen was present than in the unheated waste. This is consistent with previous heat-treated results in this study where less hydrogen was evolved via an effect presumed to be a result of caramelisation [12]. Furthermore, GC analysis of gas

produced from the unheated real waste and both the heat-treated/untreated model waste confirmed that only hydrogen, nitrogen and argon were present. The absence of carbon dioxide validated the efficacy of the 1 M NaOH scrubber.

3.2.5. Use of biohydrogen in a fuel cell

Since culture head gas contained H₂ and CO₂, and no catalyst poisons (CO, H₂S) detectable by GC analysis (above) it was tested directly for use in a fuel cell. Biohydrogen generated from both glucose and confectionery waste by *E. coli* HD701 was used in conjunction with proton exchange membrane (PEM) fuel cell (connected to a motorised fan) to investigate if the gas could be used to generate electricity (Figure 1). Sufficient electricity (Table 3) was produced to power the fan for approximately 15 h. Notably, the system was found to work effectively without a NaOH scrub showing that CO₂ was not inhibitory to fuel cell action.

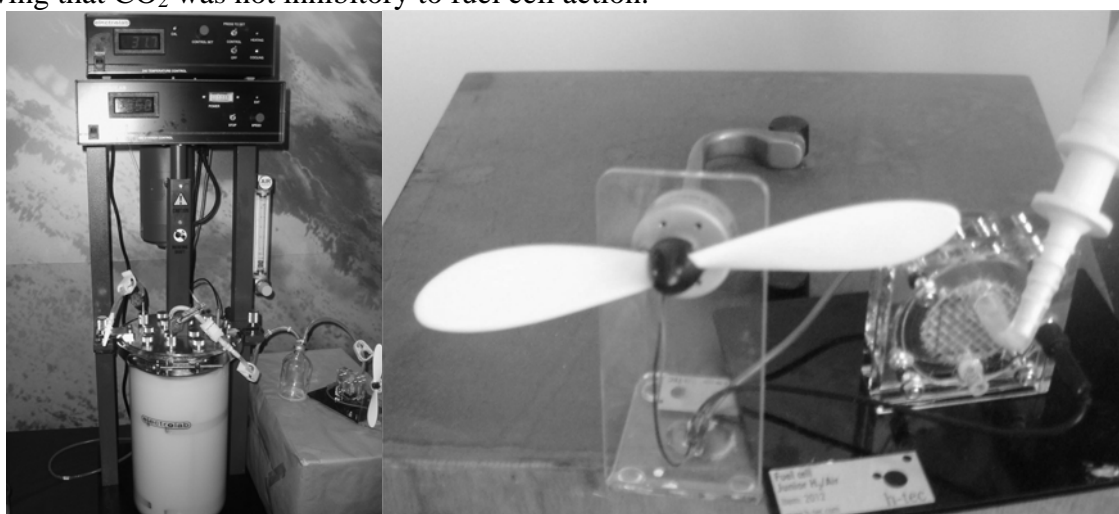


Figure 1. Bio-H₂ production at the expense of caramel waste using the bioreactor with exit gas passed into a proton exchange membrane (PEM) fuel cell (left) and the PEM fuel cell (right) which comprises anodic and cathodic layers comprising precious metal (usually Pt) nanocatalyst on carbon particles. H₂ is oxidised; e⁻ are used for the electric current and H⁺ passes through the proton conducting layer to make water (with air) at the cathode. The working system is shown at <http://www.biochemsoctrans.org/bst/033/0076/bst0330076.htm>.

3.2.6. Use of palladised *E. coli* HD701 as fuel cell electrode material

For sustainability a process should be ‘zero discharge’ and spent biomass would comprise a high BOD waste for landfilling or other disposal. PEM fuel cells contain precious metals in the catalytic electrodes; the function of the anodic layer is to split H₂ to provide electrons to power the electrical load (Figure 1). Other studies have shown that *E. coli* can be used to scavenge precious metals from industrial wastes and scrap [13]. In a final series of tests the ability of *E. coli* strain HD701 to support palladium metal nanoparticles and function as a catalyst in a PEM fuel cell was evaluated as shown in Figure 2 and Table 3. These preliminary studies showed that the *E. coli*-Pd (0) supported electricity production, although this was lower than that obtained using commercial Pd (0) powder (Figure 2). The power output (Table 3) was 33% of the commercial reference. However other studies [14] have shown that palladium supported on another type of Gram negative biomass perform comparable to commercial fuel cell materials

[14] and that the efficacy is critically dependent on the preparation conditions for each biomass type (unpublished work). The preliminary tests with *E. coli* are sufficiently promising to warrant further development.

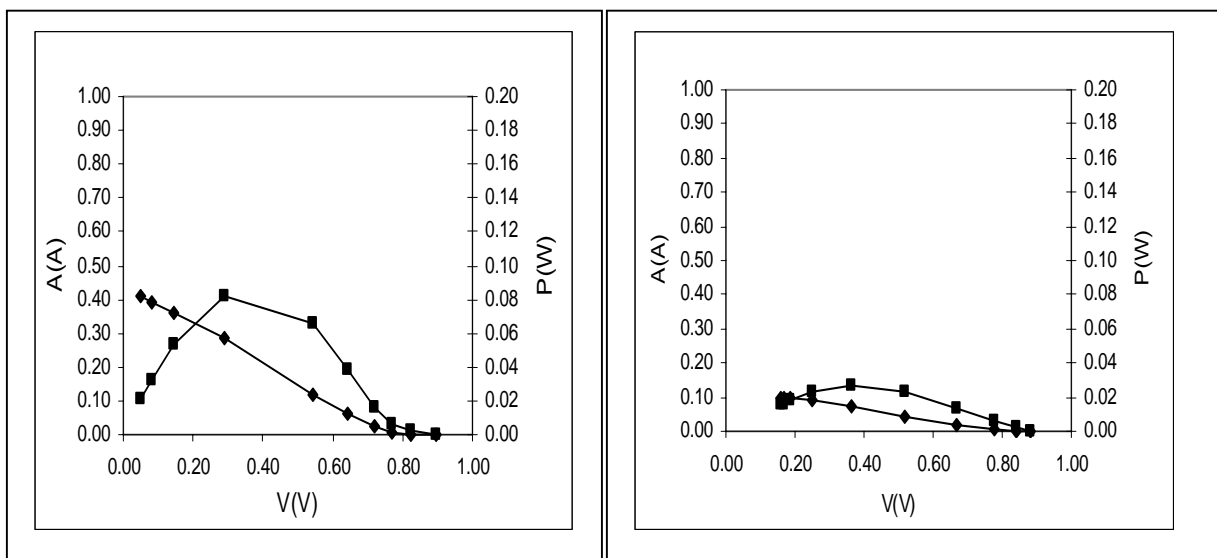


Figure 2. Comparison of performance of anodes: (left) prepared with commercial Pd powder (submicron, Aldrich Chem. Co Germany) (C-Pd); and (right) prepared with bio-Pd from *E. coli* HD701. (E-Pd) The commercial cathode used in all experiments was provided with the ECO H_2/O_2 fuel cell system. All experiments were done twice with two separate preparations and the agreement was within 5%, ■: power (P). ◆: current (A).

Table 3. Maximum Power generation ($R = 1 \Omega$) using commercial Pd (0) and palladised cells of *E. coli* HD701

| Anode (H_2) | Cathode | Power _{max} |
|-----------------|---------|----------------------|
| C-Pd(0) | Std-Pt | 0.081 |
| E-Pd(0) | Std-Pt | 0.027 |

4. CONCLUSIONS

This feasibility study indicates that the biohydrogen production process can be used for clean hydrogen production that can support a fuel cell. It has shown that the majority of food waste constituents tested can be used for hydrogen production apart from (ligno) cellulosics and fats. However, additional experiments need to be carried out to realise the potential benefits of ohmic heating on real food wastes. Biohydrogen supports electricity production using a PEM fuel cell and the biomass can also be further processed into PEM fuel cell electrode materials towards process sustainability

5. ACKNOWLEDGEMENTS

This work was funded by DEFRA (contract No NTFUN2) and by the Royal Society (Industrial Fellowship and Brian Mercer Senior Award for Innovation to LEM). The authors wish to thank

Professor A. Böck (Lehrstuhl für Mikrobiologie der Universität, Munich, Germany) for permission to use *E. coli* HD701, Dr. G. Thompson (School of Civil Engineering, The University of Birmingham, England) for analysis of caramel waste and Cadbury Trebor Bassett Ltd for provision of the caramel waste.

6. REFERENCES

- [1] Stern N. The Stern review report. http://www.hm-treasury.gov.uk/independent_reviews/stern_review_economics_climate_change/stern_review_report.cfm
- [2] Brown C, Cornwell R, and McCarthey M. The Day that Changed the Climate. The Independent: special issue 31st October 2006.
- [3] Sauter M, Bohm R and Bock A. (1992) Mutational analysis of the operon (*hyc*) determining hydrogenase 3 formation in *Escherichia coli*. Mol. Microbiol. 6: 1523–1532.
- [4] Penfold DW, Forster C and Macaskie LE. (2003) Increased hydrogen production by *Escherichia coli* strain HD701 in comparison with the wildtype parent strain MC4100. Enz. Microb. Technol.32: 185-189.
- [5] Penfold DW and Macaskie LE. (2004) Production of H₂ from sucrose by *Escherichia coli* strains carrying the pUR400 plasmid, which encodes invertase activity. Biotechnol. Lett. 26: 1879 – 1883.
- [6] Humphries AC, Penfold DW and Macaskie LE. (2006) Cr (VI) reduction by bio- and bioinorganic catalysis via use of bio-H₂: a sustainable approach for remediation of wastes. J Chem. Technol. Biotechnol. in press.
- [7] Chaplin MF and Kennedy JF. (1986) Carbohydrate analysis a practical approach. (eds.). Oxford: IRL Press, p 3.
- [8] Voigt C, Hoeller S, and Kueter U. (2005) Fuel Cell Technology for Classroom Instruction. Wasserstoff-Energie-Systeme Gmb, Luebeck, ISBN 3-9810227-1-8.
- [9] Penfold, DW and Macaskie LE. (2006) Integrated bioreactor and fuel cell for electricity biomanufacture. <http://www.biochemsoctrans.org/bst/033/0076/bst0330076.htm>.
- [10] Chagneau C, Heyde M, Alonso S, Portalier R and Laloi P. (2001) External pH-dependent expression of the maltose regulon and *ompF* gene in *Escherichia coli* is affected by the level of glycerol kinase, encoded by *glpK*. J. Bacteriol. 183: 5675-5683.
- [11] Hayes EH, Wilks JC, Sanfilippo P, Yohannes E, Tate DP, Jones BD, Radmacher MD, BonDurant SS and Slonczewski JL. (2006) Oxygen limitation modulates pH regulation of catabolism and hydrogenases, multi-drug transporters and envelope composition in *Escherichia coli* K-12. BMC Microbiology. 6: 89-107.
- [12] Byrd JJ, Cheville AM, Bose JL, and Kaspar CW. (1999) Lethality of a H₂- and phosphate-catalyzed glucose by-product to *Escherichia coli* O157:H7 and partial protection conferred by the *rpoS* regulon. Appl. Environ. Microbiol. 65: 2396–2401.
- [13] Mabbett AN, Sanyahumbi D., Yong P. and Macaskie LE. (2006) Biorecovered precious metals from industrial wastes: single step conversion of a mixed metal liquid wastes to a bioinorganic catalyst with environmental application. Environ Sci. Technol. 40: 1015-1021.
- [14] Yong P, Paterson-Beedle M, Mikheenko IP and Macaskie LE. (2007) From biomineralisation to fuel cells: biomanufacture of Pt and Pd nanocrystals for fuel cell electrode catalyst. Biotechnol. Lett. in press.

4.2.3 Conference posters

- International Hydrogen Energy Congress (IHEC), July 2005, Istanbul, Turkey,
Title: A two-organism system for biohydrogen from glucose
Reproduced within section 4.2.3

- HYdrogen POWer and THEoretical Engineering SolutIonS (HYPOTHESIS VII), March 2007, Merida, Mexico.
Title: Microbial Hydrogen and Energy Production
Reproduced within section 4.2.3

4.2.4 Conference presentations

- Conference speaker: Redwood MD, Penfold DW and Macaskie LE. Microbial production of hydrogen and energy. in: Recovering value from liquid and solid wastes. 4th July 2007, Sheffield, UK. www.aqua-enviro.net
 - Process strategies
 - Mechanisms and organisms
 - Potential for energy generation

- Conference speaker: HYdrogen POWer and THEoretical Engineering SolutIonS (HYPOTHESIS VII), March 2007, Merida, Mexico.
Title: Microbial Hydrogen and Energy Production (see poster)

A two-stage system for biohydrogen from glucose



Paper number: 203 Mark D. Redwood, David W. Penfold and Lynne E. Macaskie
 e-mail: mdr391@bham.ac.uk address: School of Biosciences, University of Birmingham, Edgbaston, Birmingham B15 2TT.

1 : Introduction

Hydrogen (H₂) is likely to play a key role in the future energy economy. H₂ is not an energy source but an energy vector, acting as a store for the abundant energy which is available from renewable sources such as organic wastes. Sugars found in organic wastes are promising substrates for H₂ production, yielding a maximum of 12 moles H₂ per mole hexose.



Fermentation (e.g. by *Escherichia coli*) is a prevalent approach as H₂ can be produced at a high rate and on a large scale. However, the yield is thermodynamically limited to 4 mol H₂ per mol hexose. The remaining energy is used by the cell to dissipate reducing power in the formation of organic end-products.

This poses two challenges:

- Remediation of *E. coli* fermentation waste to be acceptable for final discharge.
- Extraction of remaining energy bound in fermentation end-products (as H₂).

Purple non-sulphur bacteria (e.g. *Rhodobacter* spp.) have the metabolic capacity to address both problems. Members of this group are capable of photoheterotrophy, whereby anoxygenic photosynthesis captures light energy to oxidise simple organic compounds (e.g. fermentation end-products). H₂ is produced under nitrogen-limitation as a by-product of nitrogenase activity. Hence, the removal of fixed nitrogen sources (e.g. ammonia) is prerequisite to H₂ formation. [1,2]

4 : Experiment

Hypothesis 1:
R. sphaeroides can remove organic compounds from fermentation waste

Hypothesis 2:
R. sphaeroides can produce H₂ at the expense of fermentation waste

Controlled factors

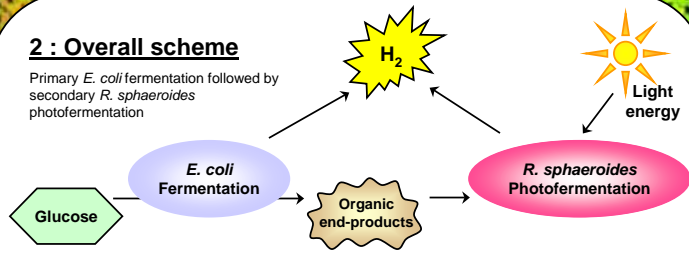
Bacteria : *R. sphaeroides* O.U.001 (DSMZ 5864) grown on succinate at 30 °C.
Test medium : Fermentation waste supernatant, diluted 50% with H₂O, filter-sterilised.
Inoculum : 5% v/v of a 4 g/L (dry mass) suspension of log-phase cells (to 0.2 g/L).
Light : 10 μE/m²/s (47 W/m²) photosynthetically active radiation fluorescent lamps.
Reactors : 200 mL anaerobic bottles, stirred magnetically.
Atmosphere : Anaerobic (under argon).

Measured variables

H₂ formation : by displacement of 1 M NaOH from a graduated glass tube.
pH change : in twice-daily samples.
Culture growth : OD₆₆₀ converted to g dry weight/L using a determined calibration.
Analysis of growth media : Supernatants were stored at -20 °C before analyses: anion HPLC for organic acids and NO₂/NO₃; colorimetric dinitrosalicylic acid assay for glucose [3]; colorimetric Nessler assay for ammonia [4]; colorimetric bicinchoninic acid assay for protein (Sigma procedure TPR0562).

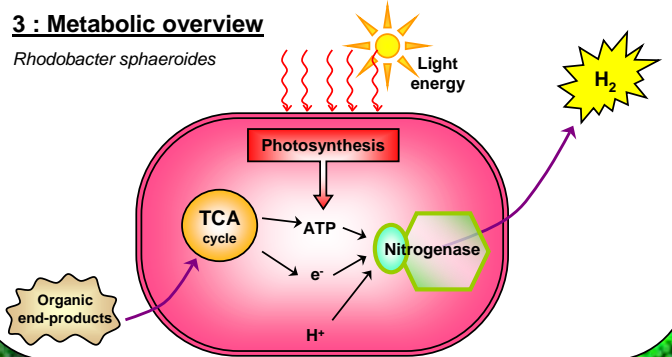
2 : Overall scheme

Primary *E. coli* fermentation followed by secondary *R. sphaeroides* photofermentation



3 : Metabolic overview

Rhodobacter sphaeroides



5 : Properties of fermentation waste (supernatant)

Fermentation of glucose was performed over 24 hours at 30 °C by *E. coli* HD701 [5]. 60% of glucose was fermented (leaving a residual glucose concentration of 40 mM)

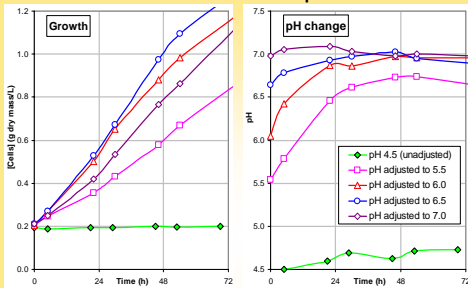
Fermentation end-products

- | | |
|-------------------------|---|
| • ethanol (2 C) : 20 mM | • pH : ~ 4.5 |
| • organic acids | • low turbidity |
| acetate (2 C) : 20 mM | • ammonia : 4.4 mM (nil NO ₃ , nil NO ₂) |
| lactate (3 C) : 15 mM | • protein : 2.30 g/L |
| succinate (4 C) : 3 mM | • chloride : 1.63 g/L (46 mM) |
| | • phosphate : 5.2 mM |

The properties of low turbidity, high organics content and high nitrogenous content make fermentation waste a promising substrate for cultivation of *R. sphaeroides*.

6 : Results and discussion

Growth of *R. sphaeroides* on fermentation liquor and effect of initial pH

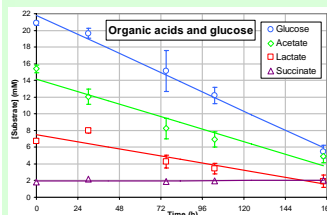


Left: Growth of *R. sphaeroides* on liquor from *E. coli* fermentation adjusted to different pHs prior to inoculation

Right: pH profile during growth starting at different pHs.

R. sphaeroides grew rapidly on fermentation liquor after the pH was increased from 4.5 to at least 5.5 (Growth rate: 0.20 g/L/day). The growth-associated neutralisation of pH, improved the disposability of the liquor.

Removal of glucose and organic acids



| | Units | Initial rate of removal (units/h/g dry cell mass) |
|-----------|-------|---|
| Glucose | mM | 2.388 |
| Acetate | mM | 2.774 |
| Lactate | mM | 0.875 |
| Ammonia | mM | 0.042 |
| Protein | g/l | 0 |
| Succinate | mM | 0 |

Glucose and acetate were the two primary carbon sources in this experiment, while lactate was removed at a lower rate and succinate was not consumed.

Hydrogen production

Theoretical expectation of H₂ production : The acetate, lactate and succinate present in 1 L fermentation waste could yield 0.194 mol (4.83 L) H₂.

Observed H₂ production : Despite removal of organic acids, H₂ formation was not observed using fermentation liquor. A positive control was performed using a synthetic medium lacking nitrogenous components, but containing glucose, ethanol and organic acids in identical concentrations to the fermentation waste. H₂ was produced at a rate of 124 mL H₂/L culture/day (10.5 mL/h/g dry mass).

Interpretation : The lack of H₂ evolution from fermentation liquor was attributed to the presence of fixed nitrogen sources. Repressive concentrations of ammonia were present in the fermentation liquor (along with significant protein) and the rate of ammonia removal was insufficient to overcome repression of nitrogenase activity.

Outlook : A high feedstock C/N ratio is necessary for photoheterotrophic H₂ production due to repression of the nitrogenase system in the presence of fixed nitrogen sources. The problem of a low C/N ratio (or excessive nitrogen) may be overcome by the use of denitrification techniques, two-stage photobioreactors [6], or mutant/engineered strains [7].

7 : Conclusions

R. sphaeroides was able to grow on fermentation waste (after slight increase of pH), simultaneously removing organic components and neutralising the pH, to render the medium more suitable for disposal into the environment. Nitrogenase activity (H₂ production) was inhibited by the high nitrogen content, but was shown in nitrogen-free medium. Future work will aim to meet the second objective via the use of nitrogenase derepressed mutants.

8 : References



- [1] Hillmer P & Gest H (1977) *J. Bacteriol.* 129(2):724-731.
- [2] Koku H et al. (2002) *International J. Hydrogen Energy.* 27:1315-1329.
- [3] Chaplin MF & Kennedy JF (1986) *Carbohydrate analysis: a practical approach.* IRL Press, Oxford.
- [4] Mendam J et al. (2000). *Vogel's Textbook of Quantitative Chemical Analysis* 6th Edn. Longman, New York.
- [5] Penfold DW et al. (2003) *Enzyme and Microbial Technology.* 2003. 33(2-3):185-189.
- [6] Fascetti E & Todini O (1995). *Appl. Microbiol. Biotechnol.* 44 (3-4):300-305.
- [7] Zinchenko VV (1991) *Genetika* 27(6):991-999.

Microbial Hydrogen and Energy Production



Mark D. Redwood, David W. Penfold and Lynne E. Macaskie e-mail: mdredwood@googlemail.com address: School of Biosciences, University of Birmingham, Edgbaston, Birmingham B15 2TT.

Problem: No single microorganism can achieve total conversion of sugars to hydrogen. **Objective:** To develop a two stage artificial symbiosis for efficient and continuous production of hydrogen from sugary wastes

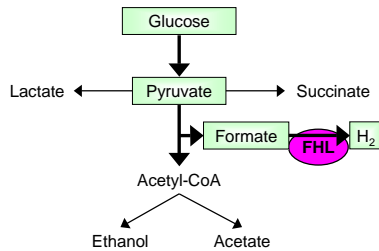
Dark Fermentation

- *Escherichia coli* HD701 (derived from MC4100)
- Genotype: $\Delta hycA$
- Phenotype: H_2 -overproduction
- Fermenter volume : 3-5 L
- Fed-batch/continuous operation
- Dilution rate: 100 mL/day
- Load: 60 mmol glucose/day (or sugary waste)
- pH controlled at 5.50



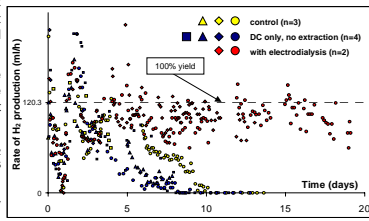
Metabolic overview : Mixed acid fermentation

Glucose $\rightarrow H_2$ + organic acids



H_2 production by *E. coli* HD701

- Control experiments represent conventional dark fermentation without electrodiolysis. H_2 production stopped by day 10 due to organic acid toxicity.
- 'DC only' experiments used an inactive membrane in the cell to investigate the effect of direct current on *E. coli* without electrodiolysis.
- With functioning electrodiolysis H_2 production was stable and continuous due to the removal of organic acids.
- 120.3 mL/h represents 100% efficiency given a maximum yield of 2 mol H_2 /mol glucose.



Conclusions

Stage 1 dark fermentation = 1.6 mol H_2 /mol sugar, plus waste organic acids

Stage 2 photofermentation = Consumption of stage 1 organic acids to make additional H_2

Acknowledgements

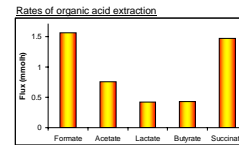
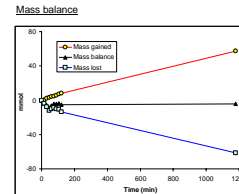
The authors thank Dr IP Mikheenko and Dr P Yong for their help and advice.

We acknowledge with thanks the support of EPSRC, BBSRC and the Royal Society and the help of C-tech Innovation Ltd and EKB Technology Ltd.

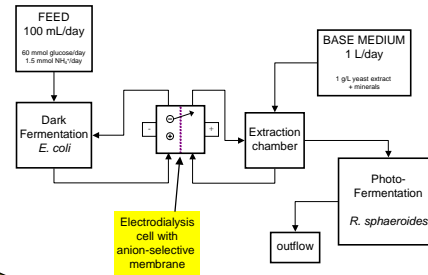
Organic Acid Transfer

Electrodiolysis

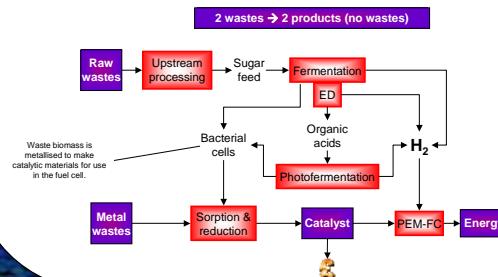
- Transfer of organic acids from *E. coli* fermenter to *R. sphaeroides* photobioreactor to maximise H_2 -yield (mol/mol).
- Organic acids migrate from cathode to anode under a direct current (2 mA/cm²).
- An anion-selective membrane (Neosepta AHA) separates the *E. coli* fermentation from the extraction chamber.
- The extraction rate varies for different organic acids. Depending on the molecular mass and charge.
- Succinate, a 4-carbon divalent organic acid is transported as quickly as formate, a 1-carbon monovalent organic acid.



Experimental process

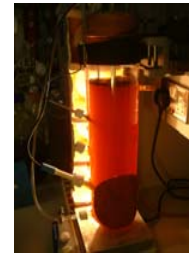


Process summary



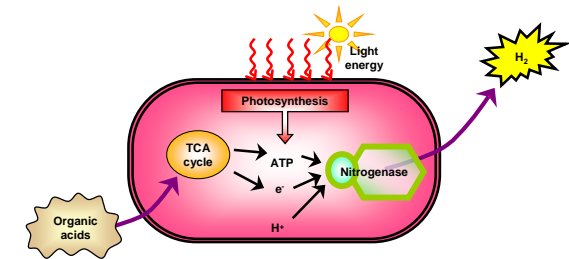
Photofermentation

- *Rhodobacter sphaeroides* O.U.001
- A wild-type strain (DSMZ 5864)
- 30 °C, Tungsten illumination
- Continuous operation
- Photobioreactor volume: 3 L
- Dilution rate: 1 L/day
- Load: variable (dependent upon electrodiolysis)



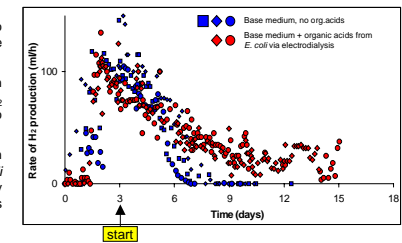
Metabolic overview: Photofermentation

Organic acids + light energy $\rightarrow H_2$ + CO_2



H_2 production by *R. sphaeroides*

- *R. sphaeroides* was cultured to establish a H_2 -producing culture before dilution started after day 3.
- When the culture was diluted with a medium lacking organic acids, H_2 production ceased by day 8 due to the washout of organic acids.
- When the culture was diluted with a medium enriched with *E. coli* fermentation products crossed by electrodiolysis, H_2 production was stable and continuous.



Summary

The combination of dark fermentation and photofermentation increases the volume of hydrogen generated and eliminates the disposal issue of organic acid residues from a single-stage dark fermentation. The two bioreactions are kept separate because they function optimally under different environmental conditions. The method of transferring fermentation products between reactors is crucial. Electrodiolysis actively removes organic acids from the fermentation culture, while restricting the passage of ammonium ion which would inhibit nitrogenase-mediated H_2 production in the photofermentation.

The integrated dual system to produce hydrogen energy from glucose is a laboratory-scale model for a potentially applicable industrial process. The integrated electrodiolysis makes the process adaptable to the use of any sugary feedstock, and the process also produces two kinds of biomass which are both useful for the production of PEM-fuel cell catalyst.

4.3 Video showing operational dual system

The recording (located on the enclosed disc) corresponds to the dual system as described in chapter 2.6 and illustrated in Figure 2.6-a. Narrative to video: The opening view focuses on the *E. coli* fermenter, also showing the permeate chamber (MA) in the foreground. The view moves right to show the illuminated PBR (*R. sphaeroides* culture) with the reflective tube in place. Next, the view moves up and right to show the two large H₂ collection vessels (see Figure 4.1-a, part C), with a digital camera positioned for time-lapse photography. Looking down, we see the plastic container for the PBR outflow, containing red culture. The view then zooms out to show the dual bioreactor system. Next we look left to see the power supply providing 400 mW to the electro dialysis cell below, and also the 4-channel pump circulating solutions and *E. coli* culture to the 4 chambers of the electro dialysis cell. Next, the recording shows a bio-fabricated PEM-FC connected to the fuel-cell testing apparatus (see chapter 2.8), generating power from H₂ to run an electric fan. Finally, we step back to view the entire assembly.

5 : BIBLIOGRAPHY

References of published or submitted works are included within those sections, which forming the main text of chapters 1.2, 2.1, 2.4 and 2.7.

1. 2006 Fuel Cell Industry Survey, New Energy for World Markets. PricewaterhouseCoopers www.pwc.com/ca/eng/ins-sol/survey-rep/fcis_06.pdf.
2. Akkerman I, Janssen M, Rocha J, and Wijffels RH (2002) Photobiological hydrogen production: photochemical efficiency and bioreactor design. *Int J Hydrogen Energy* 27(11-12):1195-1208.
3. Albers H and Gottschalk G (1976) Acetate metabolism in *Rhodospseudomonas gelatinosa* and several other *Rhodospirillaceae*. *Arch Microbiol* 111:45-49.
4. Alipui OD, Zhang D, and Schulz H (2002) Direct hydration of 3-octynoyl-CoA by crotonase: a missing link in Konrad Bloch's enzymatic studies with 3-alkynoyl thioesters. *292(5):1171-1174*.
5. Armitage JP, Kelly DP, and Sockett RE, Flagellate motility, behavioral responses and active transport in Purple Nonsulfur Bacteria, in *Anoxygenic Photosynthetic Bacteria*, R.E. Blankenship, M.T. Madigan, and C.E. Bauer, Editors. 1995. p. 1005-1028.
6. Asada Y and Miyake J (1999) Photobiological hydrogen production (Review). *J Biosci Bioeng* 88(1):1-6.
7. Ayres GH and Meyer AS (1951) Spectrophotometric study of the platinum(IV)-tin(II) chloride system. *Anal Chem* 23:299-304.
8. Battaile KP, Mohsen A-WA, and Vockley J (1996) Functional role of the active site glutamate-368 in rat short-chain acyl-CoA dehydrogenase. *Biochem* 35:15356-63.
9. Baxter-Plant V, Mikheenko IP, and Macaskie LE (2003) Sulphate-reducing bacteria, palladium and the reductive dehalogenation of chlorinated aromatic compounds. *Biodegrad* 14(2):83-90.
10. Baxter-Plant VS, Mikheenko IP, Robson M, Harrad SJ, and Macaskie LE (2004) Dehalogenation of chlorinated aromatic compounds using a hybrid bioinorganic catalyst on cells of *Desulfiovibrio desulfuricans*. *Biotechnol Lett* 26(24):1885-1890.
11. Becker DF, Fuchs JA, Banfield DK, Funk WD, MacGillivray RT, and Stankovich MT (1993) Characterization of wild-type and an active-site mutant in *Escherichia coli* of short-chain acyl-CoA dehydrogenase from *Megasphaera elsdenii*. *Biochem Eng J* 32(40):10736-10742.
12. Benemann JR (2000) Hydrogen production by microalgae. *J Appl Phycol* 12:291-300.
13. Bennet GN and Rudolph FB (1995) The central metabolic pathway from acetyl-CoA to butyryl-CoA in *Clostridium acetobutylicum*. *FEMS Microbiol Lett* 17:241-249.
14. Berg P, Promislow K, Saint-Pierre J, Stumper J, and Wettonc B (2004) Water management in PEM fuel cells. *J Electrochem Soc* 151(3):A341-A353.
15. Biebl H and Pfennig N, Isolation of members of the family *Rhodospirillaceae*, in *The Prokaryotes*, M.P. Starr, et al., Editors. 1981, Springer. p. 267-273.
16. Binstock JF and Schulz H (1981) Fatty acid oxidation complex from *Escherichia coli*. *Methods Enzymol* 71 Pt C:403-411.
17. Blackwood AC, Neish AC, and Ledingham GA (1956) Dissimilation of glucose at controlled pH values by pigmented and non-pigmented strains of *Escherichia coli*. *J Bacteriol* 72:497-499.

18. Booth IR (1985) Regulation of cytoplasmic pH in bacteria. *Microbiol Rev* 49(4):359-378.
19. Borodin VB, Tsygankov AA, Rao KK, and Hall DO (2000) Hydrogen production by *Anabaena variabilis* PK84 under simulated outdoor conditions. *Biotechnol Bioeng* 69(5):478-485.
20. Borsetti F, Borghese R, Francia F, Randi MR, Fedi S, and Zannoni D (2003) Reduction of potassium tellurite to elemental tellurium and its effect on the plasma membrane redox components of the facultative phototroph *Rhodobacter capsulatus*. *Protoplasma* 221(1-2):153-161.
21. Burgess G and Fernandez-Velasco JG (2007) Materials, operational energy inputs, and net energy ratio for photobiological hydrogen production. *Int J Hydrogen Energy* 32:1255-1234.
22. Chandel AK, Chan ES, Rudravaram R, Narusu ML, Rao LV, and Ravindra P (2007) Economics and environmental impact of bioethanol production technologies: an appraisal. *Biotechnol Mol Biol Rev* 2(1):14-32.
23. Chang Y-HD, Grodzinsky AJ, and Wang DIC (1995) Augmentation of mass transfer through electrical means for hydrogel-entrapped *Escherichia coli* cultivation. *Biotechnol Bioeng* 48:149-157.
24. Chaplin MF, Monosaccharides (section 2.2.2), in *Carbohydrate analysis: a practical approach*, M.F. Chaplin and J.F. Kennedy, Editors. 1986, IRL Press at Oxford University press, UK. p. 324.
25. Chen C-Y, Lee C-M, and Chang J-S (2006) Feasibility study on bioreactor strategies for enhanced photohydrogen production from *Rhodospseudomonas palustris* WP3-5 using optical-fiber-assisted illumination systems. *Int J Hydrog Energy* 31:2345-2355.
26. Chen C-Y, Lu W-B, Wu J-F, and Chang J-S (2007) Enhancing the phototrophic hydrogen production of *Rhodospseudomonas palustris* via statistical experimental design. *Int J Global Energy Iss* 32:940-949.
27. Chen X, Sun Y, Xiu Z, Li X, and Zhang D (2006) Stoichiometric analysis of biological hydrogen production by fermentative bacteria. *Int J Hydrogen Energy* 31:539-549.
28. Cherrington CA, Hinton M, Mead GC, and Chopra I (1991) Organic acids: chemistry, antibacterial activity and practical applications. *Adv Microb Physiol* 32:87-708.
29. Chlanda FP, Lee LTC, and Liu K-J (1976) Bipolar membranes and method of making same. US Patent 4,116,889.
30. Chukwu UN and Cheryan M (1999) Electrodialysis of acetate fermentation broths. *Appl Biochem Biotechnol Spring*, 77-79:485-499.
31. Claassen PAM and De Vrije T project participants BWP II (2006) Hydrogen from biomass. BWP II project, public report. Agrotechnology and Food Sciences Group. ISBN:90-8585-023-1: Wageningen.
32. Clark DP (1989) The fermentation pathways of *Escherichia coli*. *FEMS Microbiol Rev* 5(3):223-234.
33. Creamer NJ, Baxter-Plant VS, Henderson J, Potter M, and Macaskie LE (2006) Palladium and gold removal and recovery from precious metal solutions and electronic scrap leachates by *Desulfovibrio desulfuricans*. *Biotechnol Lett* 28(18):1475-84.
34. Creamer NJ, Mikheenko IP, Deplanche K, Yong P, Wood J, Pollman K, Selenska-Pobell S, and Macaskie LE (2007) A novel hydrogenation and hydrogenolysis catalyst using palladized biomass of Gram negative and Gram positive bacteria. *Adv Mat Res* 20-21:603-606.

35. Datar R, Huang J, Maness P-C, Mohagheghi A, Czernik S, and Chornet E (2007) Hydrogen production from the fermentation of corn stover biomass pretreated with a steam-explosion process. *Int J Hydrogen Energy* 32:932-939.
36. Davila-Vazquez G, Arriaga S, Alatrisme-Mondragon F, de Leon-Rodriguez A, Rosales-Colunga LM, and Razo-Flores E (2007) Fermentative biohydrogen production: trends and perspectives. *Rev Environ Sci Biotechnol* in press
37. De Luca G, De Philip P, Dermoun Z, Rousset M, and Vermeglio A (2001) Reduction of technetium(VII) by *Desulfovibrio fructosovorans* is mediated by the nickel-iron hydrogenase. *Appl Environ Microbiol* 37(10):4583-4587.
38. de Vargas I, Macaskie LE, and Guibal E (2004) Biosorption of palladium and platinum by sulfate-reducing bacteria. *J Chem Technol Biotechnol* 79(1):49-56.
39. de Vargas I, Sanyahumbi D, Ashworth MA, Hardy CM, and Macaskie LE. Use of X-ray photoelectron spectroscopy to elucidate the mechanism of palladium and platinum biosorption by *Desulfovibrio desulfuricans* biomass. in 16th International Biohydrometallurgy Symposium. 2005. Cape Town, S. Africa: Published by 16th Int. Biohydrometallurgy Symp. Cape Town. p. 605-616. 1-92-0051-17-1 2005.
40. de Vrije T and Claassen PAM, Dark hydrogen fermentations, in Bio-methane & Biohydrogen, J.H. Reith, R.H. Wijffels, and H. Barten, Editors. 2003, Dutch Biological Hydrogen Foundation: Petten, Netherlands. p. 103-123.
41. Dittrich CR, Bennet GN, and San K-Y (2005) Characterisation of the acetate-producing pathways in *Escherichia coli*. *Biotechnol Prog* 21:1062-1067.
42. Djordjevic S, Pace CP, Stankovich MT, and Kim JJ (1995) Three-dimensional structure of butyryl-CoA dehydrogenase from *Megasphaera elsdenii*. *Biochem* 34(7):2163-2171.
43. Eroğlu I, Aslan K, Gündüz U, Yücel M, and Türker L. Continuous hydrogen production by *R. sphaeroides* O.U 001. in International Conference on Biological Hydrogen Production. 1997. Waikoloa, Hawaii: Plenum Press, New York. p. 143.
44. Eroğlu I, Aslan K, Gündüz U, Yücel M, and Türker L (1999) Substrate consumption rates for hydrogen production by *Rhodobacter sphaeroides* in a column photobioreactor. *J Biotechnol* 70:103-113.
45. Fascetti I and Todini O (1995) *Rhodobacter sphaeroides* RV cultivation and hydrogen production in a one- and two-stage chemostat. *Appl Microbiol Biotechnol* 44:300-305.
46. Feigenbaum J and Schulz H (1975) Thiolases of *Escherichia coli*: purification and chain length specificities. *J Bacteriol* 122(2):407-411.
47. Fidaleo M and Moresi M (2005) Modeling of sodium acetate recovery from aqueous solutions by electrodialysis. *Biotechnol Bioeng* 91(5):556-568.
48. Filatova LV, Berg IA, Krasil'nikova EN, and Ivanovskii RN (2005) A study of the mechanism of acetate assimilation in purple nonsulfur bacteria lacking the glyoxylate shunt: Enzymes of the citramalate cycle in *Rhodobacter sphaeroides*. *Microbiol*, Translated from *Mikrobiologiya* 74(3):270-278 (translated from *Mikrobiologiya* 74(3):319).
49. Filatova LV, Berg IA, Krasil'nikova EN, Tsygankov AA, Laurinavichene TV, and Ivanovskii RN (2005) A study of the mechanism of acetate assimilation in purple nonsulfur bacteria lacking the glyoxylate shunt: Acetate assimilation in *Rhodobacter sphaeroides*. *Microbiol*, Translated from *Mikrobiologiya* 74(3):265-269 (translated from *Mikrobiologiya* 74(3):313).
50. Fojt L, Strasak L, Vetterl V, and Smarda J (2004) Comparison of the low-frequency magnetic field effects on bacteria *Escherichia coli*, *Leclercia adecarboxylata* and *Staphylococcus aureus*. *Bioelectrochem* 63(1-2):337-41.

51. Forster P, Ramaswamy V, Artaxo P, Berntsen T, Betts R, Fahey DW, Haywood J, Lean J, Lowe DC, Myhre G, Nganga J, Prinn R, Raga G, Schulz M, and Van Dorland R, Changes in atmospheric constituents and in radiative forcing, in *Climate Change 2007: The Physical Science Basis. Contribution of Working Group I to the Fourth Assessment Report of the Intergovernmental Panel on Climate Change*, S. Solomon, et al., Editors. 2007: Cambridge University Press, Cambridge, UK and New York, USA.
52. Franchi E, Tosi C, Scolla G, Penna GD, Rodriguez F, and Pedroni PM (2004) Metabolically engineered *Rhodobacter sphaeroides* RV strains for improved biohydrogen photoproduction combined with disposal of food wastes. *Mar Biotechnol* 6:552-565.
53. Freeman A, Woodley JM, and Lilly MD (1993) *In situ* product removal as a tool for bioprocessing. *Biotechnol (NY)* 11(9):1007-12.
54. Fuji T, Tarusawa M, Miyanaga M, Kiyota S, Watanabe T, and Yabuki M (1987) Hydrogen production from alcohols, malate and mixed electron donors by *Rhodospseudomonas* sp. No. 7. *Agric Biol Chem* 51(1):1-7.
55. Gaston C, *Dosages absorptiométriques des éléments minéraux*. 1978, Masson, Paris.
56. Gosse JL, Engel BJ, Rey FE, Harwood CS, Scriven LE, and Flickinger MC (2007) Hydrogen production by photoreactive nanoporous latex coatings of nongrowing *Rhodospseudomonas palustris* CGA009. *Biotechnol Prog* 23(1):124-130.
57. Grot WG, Laminates of support material and fluorinated polymer containing pendant side chains containing sulfonyl groups. US Patent 3,770,567. 1973.
58. Grove WR (1838) On a new voltaic combination. *Philosophical Magazine and Journal of Science* 13:430.
59. Hahn-Hägerdal B, Galbe M, Gorwa-Grauslund MF, Liden G, and Zacchi G (2006) Bio-ethanol - the fuel of tomorrow from the residues of today. *Trends Biotechnol* 24(12):549-556.
60. Hall TA (1999) BioEdit: a user-friendly biological sequence alignment editor and analysis program for Windows 95/98/NT. *Nucl Acids Symp Ser* 41:95-98.
61. Hallenbeck PC, Integration of hydrogen evolving systems with cellular metabolism: The molecular biology and biochemistry and electron transport factors and associated reductases., in *Biohydrogen II : An Approach to Environmentally Acceptable Technology*, J. Miyake, T. Matsunaga, and A. San Pietro, Editors. 1997, Pergamon. p. 171-181.
62. Hallenbeck PC (2005) Fundamentals of the fermentative production of hydrogen. *Water Sci Technol* 52(1-2):21-29.
63. He GQ, Kong Q, Chen QH, and Ruan H (2005) Batch and fed-batch production of butyric acid by *Clostridium butyricum* ZJUCB. *J Zhejiang Univ Sci B* 6(11):1076-80.
64. Hewitt CJ, Caron GN-V, Axelsson B, McFarlane CM, and Nienow AW (2000) Studies related to the scale up of high-cell-density *E. coli* fed-batch fermentations using multiparameter flow cytometry: Effect of a changing microenvironment with respect to glucose and dissolved oxygen concentration. *Biotechnol Bioeng* 70(4):381-390.
65. Hillmer P and Gest H (1977) H₂ metabolism in the photosynthetic bacterium *Rhodospseudomonas capsulata*: Production and utilisation of H₂ by resting cells. *J Bacteriol* 129(2):732-739.
66. Hoekema S, Bijmans M, Janssen M, Tramper J, and Wijffels RH (2002) A pneumatically agitated flat-panel photobioreactor with gas re-circulation: anaerobic photoheterotrophic cultivation of a purple non-sulfur bacterium. *Int J Hydrogen Energy* 27(11-12):1331-1338.

67. Hoekema S, Douma RD, Janssen M, Tramper J, and Wijffels RH (2006) Controlling light-use by *Rhodobacter capsulatus* continuous cultures in a flat-panel photobioreactor. *Biotechnol Bioeng* 95(4):613-26.
68. Hoffmeister M, Piotrowski M, Nowitzki U, and Martin W (2005) Mitochondrial trans-2-enoyl-CoA reductase of wax ester fermentation from *Euglena gracilis* defines a new family of enzymes involved in lipid synthesis. *J Biol Chem* 280(6):4329-4338.
69. Huang C, Xu T, Zhang Y, Xue Y, and Chen G (2007) Application of electro dialysis to the production of organic acids: State-of-the-art and recent developments. *J Memb Sci* 288:1-12.
70. Hustede E, Steinbuchel A, and Schlegel HG (1993) Relationship between the photoproduction of hydrogen and the accumulation of PHB in nonsulfur purple bacteria. *Appl Microbiol Biotechnol* 39(1):87-93.
71. Ike A, Kawaguchi H, Hirata K, and Miyamoto K, Hydrogen photoproduction from starch in algal biomass, in *Biohydrogen II : An Approach to Environmentally Acceptable Technology*, J. Miyake, T. Matsunaga, and A. San Pietro, Editors. 2001, Pergamon. p. 53-61.
72. Ingraham J, Effect of temperature, pH, water activity, and pressure on growth, in *Escherichia coli* and *Salmonella Typharium*, F.C. Niedhardt, Editor. 1987, Am. Soc. Microbiol.: Washington DC. p. 1543-1554.
73. Iram SH and Cronan JE (2006) The β -oxidation systems of *Escherichia coli* and *Salmonella enterica* are not functionally equivalent. *J Bacteriol* 188(2):599-608.
74. Ishizaki A, Nomura Y, and Iwahara M (1990) Built-in electro dialysis batch culture, a new approach to release of end product inhibition. *J Ferment Bioeng* 70:108-113.
75. Ivanovskii RN, Krasil'nikova EN, and Berg IA (1997) The mechanism of acetate assimilation in the purple nonsulfur bacterium *Rhodospirillum rubrum* lacking isocitrate lyase. *Microbiol* 66(6):621-626 (translated from *Mikrobiologiya* 153:399).
76. Jackman SA, Maini G, Sharman AK, and Knowles CJ (1999) The effects of direct electric current on the viability and metabolism of acidophilic bacteria. *Enz Microb Technol* 24:316-324.
77. Jiang GR, Nikolova S, and Clark DP (2001) Regulation of the *ldhA* gene, encoding the fermentative lactate dehydrogenase of *Escherichia coli*. *Microbiology* 147(Pt 9):2437-46.
78. Kapdan IK and Kargi F (2006) Bio-hydrogen production from waste materials. *Enz Microb Technol* 38:569-582.
79. Katsuda T, Arimoto T, Igarashi K, Azuma M, Kato J, Takakuwa S, and Ooshima H (2000) Light intensity distribution in the externally illuminated cylindrical photobioreactor and its application to hydrogen production by *Rhodobacter capsulatus*. *Biochem Eng J* 5:157-164.
80. Kawaguchi H, Hashimoto K, Hirata K, and Miyamoto K (2001) H₂ production from algal biomass by a mixed culture of *Rhodobium marinum* A-501 and *Lactobacillus amylovorus*. *J Biosci Bioeng* 91(3):277-282.
81. Kendal T (2006) *Platinum Review. 2006*, Published by Johnson Matthey Plc., www.platinum.matthey.com/publications.
82. Kendal T (2007) *Platinum Review. 2007*, Published by Johnson Matthey Plc., www.platinum.matthey.com/publications.
83. Kessi J, Ramuz M, Wehrli E, Spycher M, and Bachofen R (1999) Reduction of selenite and detoxification of elemental selenium by the phototrophic bacterium *Rhodospirillum rubrum*. *Appl Environ Microbiol* 65(11):4734-4740.

84. Kim E-J, Kim J-S, Kim M-S, and Lee JK (2006) Effect of changes in the level of light harvesting complexes of *Rhodobacter sphaeroides* on the photoheterotrophic production of hydrogen. *Int J Hydrogen Energy* 31:531-538.
85. Kim JJP and Wu J (1988) Structure of the medium-chain acyl-CoA dehydrogenase from pig-liver mitochondria at 3-A resolution. *PNAS USA* 85(18):6677-6681.
86. Kim JS, Ito K, and Takahashi H (1980) The relationship between nitrogenase activity and hydrogen evolution in *Rhodospseudomonas palustris*. *Agric Biol Chem* 44(4):827-833.
87. Kim NJ, Lee JK, and Lee CJ (2004) Pigment reduction to improve photosynthetic productivity of *Rhodobacter sphaeroides*. *J Gen Microbiol* 1692(28):607-16.
88. Kirkpatrick C, Maurer LM, Oyelakin NE, Yoncheva YN, Maurer R, and Slonczewski JL (2001) Acetate and formate stress: Opposite responses in the proteome of *Escherichia coli*. *J Bacteriol* 183(21):6466-6477.
89. Knowles CJ, Jackman S, A., Li H, Mustacchi R, and Sunderland G, Control of biocatalysis reactions (2004) International Patent No. WO 2004/046351 A1, World Intellectual Property Organisation. p. 41.
90. Koku H, Eroğlu I, Gündüz U, Yücel M, and Türker L (2002) Aspects of the metabolism of hydrogen production by *Rhodobacter sphaeroides*. *Int J Hydrogen Energy* 27:1315-1329.
91. Koku H, Eroğlu I, Gündüz U, Yücel M, and Türker L (2003) Kinetics of biological hydrogen production by the photosynthetic bacterium *Rhodobacter sphaeroides* O.U. 001. *Int J Hydrogen Energy* 28(381-388)
92. Kondo T, Arakawa M, Wakayama T, and Miyake J (2002) Hydrogen production by combining two types of photosynthetic bacteria with different characteristics. *Int J Hydrogen Energy* 27(11-12):1303-1308.
93. Kondo T, Wakayama T, and Miyake J (2006) Efficient hydrogen production using a multi-layered photobioreactor and a photosynthetic bacterium mutant with reduced pigment. *Int J Hydrogen Energy* 31(11):1522-1526.
94. Kornberg HL and Madsen NB (1958) The Metabolism of C₂ Compounds in Microorganisms; 3. synthesis of malate from acetate via the glyoxylate cycle. *Biochem J* 68:549.
95. Korolev S, Koroleva O, Petterson K, Gu M, Collart F, Dementieva I, and Joachimiak A (2002) Autotracing of *Escherichia coli* acetate CoA-transferase alpha-subunit structure using 3.4 Å MAD and 1.9 Å native data. *Acta Crystallogr D Biol Crystallogr* 58(Pt 12):2116-2121.
96. Kurokawa T and Shigeharu T (2005) Effects of formate on fermentative hydrogen production by *Enterobacter aerogenes*. *Mar Biotechnol* 7:112-118.
97. Kyazze G, Dinsdale R, Guwy AJ, Hawkes FR, Premier GC, and Hawkes DL (2007) Performance characteristics of a two-stage dark fermentative system producing hydrogen and methane continuously. *Biotechnol Bioeng* 97(4):759-770.
98. Larminie J and Dicks A, Fuel cell systems explained, 2nd ed. second ed. ed. 2003: John Wiley & Sons, Chichester, Sussex, UK.
99. Lee K-S, Lin P-J, Fangchiang K, and Chang J-S (2007) Continuous hydrogen production by anaerobic mixed microflora using a hollow-fiber microfiltration membrane reactor. *Int J Hydrogen Energy* 32:950-957.
100. Levin DB, Pitt L, and Love M (2004a) Biohydrogen production: prospects and limitations to practical application. *Int J Hydrogen Energy* 29:173-185.

101. Levin DB (2004b) Re: Biohydrogen production: prospects and limitations to practical application-Erratum. *Int J Hydrogen Energy* 29:1425-1426.
102. Li H, Mustacchi R, Knowles CJ, Skibar W, Sunderland G, Dalrymple I, and Jackman S, A. (2004) An electrokinetic bioreactor: using direct electric current for enhanced lactic acid fermentation and product recovery. *Tetrahedron* 60:655-661.
103. Liessens J and Verstraete W (1986) Selective inhibitors for continuous non-axenic hydrogen production by *Rhodobacter capsulatus*. *J Appl Bacteriol* 61(6):547-557.
104. Lindblad P, Christensson K, Lindberg P, Fedorov A, Pinto F, and Tsygankov A (2002) Photoproduction of H₂ by wildtype *Anabaena* PCC 7120 and a hydrogen uptake deficient mutant: from laboratory experiments to outdoor culture. *Int J Hydrogen Energy* 27(11-12):1271-1281.
105. Litzter S and G. M (2004) PEM fuel cell electrodes. *J Pow Sour* 130:61-76.
106. Liu X, Zhu Y, and Yang ST (2006) Butyric acid and hydrogen production by *Clostridium tyrobutyricum* ATCC 25755 and mutants. *Enz Microb Technol* 38:521-528.
107. Lloyd JR, Lovley DR, and Macaskie LE (2003) Biotechnological application of metal-reducing microorganisms. *Adv Appl Microbiol* 53:85-119.
108. Lovley DR (1993) Dissimilatory Metal Reduction. *Annu Rev Microbiol* 47:263-290.
109. Lu Y and Mosier NS (2007) Biomimetic catalysis for hemicellulose hydrolysis in corn stover. *Biotechnol Prog* 23(1):116-23.
110. Ludden PW and Roberts GP (2002) Nitrogen fixation by photosynthetic bacteria. *Photosynth Res* 73(1-3):115-118.
111. Mabbett A, N., Sanyahumbi D, Yong P, and Macaskie LE (2006) Biorecovered precious metals from industrial wastes: single step conversion of mixed metal liquid waste to a bioinorganic catalyst with environmental application. *Environ Sci Technol* 40:1015-1021.
112. Mabbett AN, Yong P, Baxter-Plant VS, Mikheenko IP, Farr JPG, and Macaskie LE. Effective reduction and removal of Cr(VI) and reductive dehalogenation of chlorophenol by hybrid bioinorganic catalytic processes. in *Biohydrometallurgy: Fundamentals, Technology and Sustainable Development, Part B*. 2001. Ouro Preto, Minas Gerais, Brazil. p. 335-342. ISBN: 0-444-50623-3.
113. Macaskie LE, Baxter-Plant VS, Creamer NJ, Humphries AC, Mikheenko IP, Mikheenko PM, Penfold DW, and Yong P (2005) Applications of bacterial hydrogenases in waste decontamination, manufacture of novel bionanocatalysts and in sustainable energy. *Biochem Soc Trans* 33(Pt 1):76-9.
114. Macaskie LE, Creamer NJ, Essa AM, and Brown NL (2007) A new approach for the recovery of precious metals from solution and from leachates derived from electronic scrap. *Biotechnol Bioeng* 96(4):631-9.
115. Macy JM, Michel T, A., and Kirsch DG (1989) Selenate reduction by a *Pseudomonas species*: a new mode of anaerobic respiration. *FEMS Microbiol Lett* 61(1-2):195-198.
116. Madigan MT, Martinko JM, and Parker J, Brock *Biology of Microorganisms*. 9th ed. 2000: Prentice Hall.
117. Madzingaidzo L, Danner H, and Braun R (2002) Process development and optimisation of lactic acid purification using electrodialysis. *J Biotechnol* 96(3):223-239.
118. Marchler-Bauer A, Anderson JB, Derbyshire MK, DeWeese-Scott C, Gonzales NR, Gwadz M, Hao L, He S, Hurwitz DI, Jackson JD, Ke Z, Krylov D, J. LC, Liebert CA, Liu C, Lu F, Lu S, Marchler GH, Mullokandov M, Song JS, Thanki N, Yamashita RA, Yin JJ, Zhang D, and Bryant SH (2007) CDD: a conserved domain database for interactive domain family analysis. *Nucleic Acids Res* 35:D237-240.

119. Mat-Jan F, Alam KY, and Clark DP (1989) Mutants of *Escherichia coli* deficient in the fermentative lactate dehydrogenase. *J Bacteriol* 171(1):342-348.
120. McLaggan D, Naprstek J, Buurman ET, and Epstein W (1994) Interdependence of K⁺ and glutamate accumulation during osmotic adaptation of *Escherichia coli*. *J Biol Chem* 269(3):1911-1917.
121. Mendam J, Denney RC, Barnes JD, and Thomas M, Vogel's Textbook of Quantitative Chemical Analysis 6th Edn. 2000.
122. Mendoza D, Morales F, Escudero R, and Walter J (1999) Magnetization studies in quasi two-dimensional palladium nanoparticles encapsulated in a graphite host. *J Phys - Condensed Matt* 11(28):L317-L322.
123. Mikheenko IP (2004) Nanoscale Palladium Recovery, PhD Thesis, University of Birmingham.
124. Mikheenko IP, Mikheenko PM, Dementin S, Rousset M, and Macaskie LE. Nanoengineering of ferromagnetic palladium in hydrogenase negative mutants of *Desulfovibrio fructosovorans*. in 16th International Biohydrometallurgy Symposium. 2005. Cape Town, S. Africa: Published by 16th Int. Biohydrometallurgy Symp. Cape Town. p. 605-616. 1-92-0051-17-1 2005.
125. Miyake J, Tomizuka N, and Kamibayashi A (1982) Prolonged photo-hydrogen production by *Rhodospirillum rubrum*. *J Ferment Technol* 60(3):199-203.
126. Miyake J, Mao X-Y, and Kawamura S (1984) Photoproduction of hydrogen from glucose by a co-culture of a photosynthetic bacterium and *Clostridium butyricum*. *J Ferment Technol* 62(6):531-535.
127. Miyake J, Miyake M, and Asada Y (1999) Biotechnological hydrogen production: research for efficient light conversion. *J Biotechnol* 70:89-101.
128. Mizuno O, Dinsdale R, Hawkes FR, Hawkes DL, and Noike T (2000) Enhancement of hydrogen production from glucose by nitrogen gas sparging. *Bioresour Technol* 73:59-65.
129. Moon PJ, Parulekar SJ, and Tsai S-P (1998) Competitive anion transport in desalting mixtures of organic acids by batch electrodialysis. *J Memb Sci* 141:75-89.
130. Moore MD and Kaplan S (1992) Identification of intrinsic high-level resistance to rare earth oxides and oxyanions in members of the class *Proteobacteria* - characterization of tellurite, selenite, and rhodium sesquioxide reduction in *Rhodobacter sphaeroides*. *J Bacteriol* 174(5):1505-1514.
131. Mustacchi R, Knowles CJ, Li H, Dalrymple I, Sunderland G, Skibar G, and Jackman SA (2005a) The effect of whole cell immobilisation on the biotransformation of benzonitrile and the use of direct electric current for enhanced product removal. *Biotechnol Bioeng* 91(4):436-440.
132. Mustacchi R, Knowles CJ, Li H, Dalrymple I, Sunderland G, Skibar W, and Jackman S, A. (2005b) Enhanced biotransformations and product recovery in a membrane bioreactor through application of a direct current. *Biotechnol Bioeng* 89(1):18-23.
133. Nakada E, Asada Y, Arai T, and Miyake J (1995) Light penetration into cell suspensions of photosynthetic bacteria and relation to hydrogen production. *J Ferment Bioeng* 80(1):53-57.
134. Nath K and Das D (2004) Improvement of fermentative hydrogen production: various approaches. *Appl Microbiol Biotechnol* 65(5):520-529.
135. Nepple BB, Kessi J, and Bachofen R (2000) Chromate reduction by *Rhodobacter sphaeroides*. *J Ind Microbiol Biotechnol* 25(4):198-203.

136. Nielsen AM, Amandusson H, Bjorklund R, Dannetun H, Ejlertsson J, Ekedahl L-G, Lundstrom I, and Svensson BH (2001) Hydrogen production from organic waste. *Int J Hydrogen Energy* 26:547-550.
137. Nomura Y, Iwahara M, and Hongo M (1988) Acetic acid production by an electro dialysis fermentation method with a computerized control system. *Appl Environ Microbiol* 54(1):137-142.
138. Noparatnaraporn N, Takenko K, and Sasaki K, Hydrogen and poly-(hydroxy) alkanolate production from organic acids by photosynthetic bacteria, in *Biohydrogen II : An Approach to Environmentally Acceptable Technology*, J. Miyake, T. Matsunaga, and A. San Pietro, Editors. 1997, Pergamon. p. 33-40.
139. Odom JM and Wall JD (1983) Photoproduction of H₂ from cellulose by an anerobic bacterial culture. *Appl Environ Microbiol* 45(4):1300-1305.
140. Oh Y-K, Seol E-H, Kim M-S, and Park S (2004) Photoproduction of hydrogen from acetate by a chemoheterotrophic bacterium *Rhodospseudomonas palustris* P4. *Int J Hydrogen Energy* 29:1115-1121.
141. Ordal EJ and Halvorson HO (1939) A comparison of hydrogen production from sugars and formic acid by normal and variant strains of *Escherichia coli*. *J Bacteriol* 38:199-220.
142. Orlandi P, ed. *Fluid flow phenomena: a numerical toolkit*. Fluid mechanics and its applications. 2000, Kluwer, London.
143. Park SJ and Lee SY (2003) Identification and characterization of a new enoyl coenzyme A hydratase involved in biosynthesis of medium-chain-length polyhydroxyalkanoates in recombinant *Escherichia coli*. *J Bacteriol* 185(18):5391-5397.
144. Park W, Hyun SH, Oh SE, Logan BE, and Kim IS (2005) Removal of headspace CO₂ increases biological hydrogen production. *Environ Sci Technol* 39(12):4416-4420.
145. Pawar S and Schulz H (1981) The structure of the multienzyme complex of fatty acid oxidation from *Escherichia coli*. *J Biol Chem* 256(8):3894-9.
146. Penfold DW, Forster CF, and Macaskie LE (2003) Increased hydrogen production by *Escherichia coli* strain HD701 in comparison with the wild-type parent strain MC4100. *Enz Microb Technol* 33(2-3):185-189.
147. Penfold DW and Macaskie LE (2004) Production of H₂ from sucrose by *Escherichia coli* strains carrying the pUR400 plasmid, which encodes invertase activity. *Biotechnol Lett* 26:1879-1883.
148. Penfold DW, Sargent F, and Macaskie LE (2006) Inactivation of the *Escherichia coli* K-12 twin arginine translocation system promotes increased hydrogen production. *FEMS Microbiol Lett* 262:135-137.
149. Penfold DW, Redwood MD, Yong P, Stratton-Campbell D, Skibar W, and Macaskie LE (2007) Microbial H₂ and electricity from wastes, *Proceedings of the 7th Hydrogen - Power and Theoretical Engineering Solutions International Symposium (HyPoThESIS VII)*, Merida, Mexico. CICY ISBN:968-6114-21-1.
150. Peters JE, Thate TE, and Craig NL (2003) Definition of the *Escherichia coli* MC4100 genome by use of a DNA array. *J Bacteriol* 185(6):2017-2021.
151. Polle JEW, Kanakagiri S, Jin E, Masuda T, and Melis A (2002) Truncated chlorophyll antenna size of the photosystems - a practical method to improve microalgal productivity and hydrogen production in mass culture. *Int J Hydrogen Energy* 27(11-12):1257-1264.
152. Portalier R and Stoeber F (1982) D-Mannonate and D-altronate-NAD dehydrogenases from *Escherichia coli*. *Methods Enzymol* 89 Pt D:210-218.

153. Ramos LP (2003) The chemistry involved in the steam treatment of lignocellulosic materials. *Quim. Nova.* 26(6):863-871.
154. Randerson J (2003) (Energy Special) Hydrogen: The clean green energy dream. *New Scientist* 179(2408):8-11.
155. Raymond L, Wei-Hwa H, and Peter SF (1992) In situ electrode formation on a Nafion membrane by chemical platinization. *J Electrochem Soc* 139(1):15-23.
156. Reahl ER. Half a century of desalination with electro dialysis. www.gewater.com. 2007.
157. Rechtsteiner GA and Ganske JA (1998) Using natural and artificial light sources to illustrate quantum mechanical concepts. *Chem Educat* 3(4):1-4.
158. Redwood MD and Macaskie LE (2006) A two-stage, two-organism process for biohydrogen from glucose. *Int J Hydrogen Energy* 31(11):1514-1521.
159. Redwood MD and Macaskie LE, Method and apparatus for biohydrogen production. British Patent Application No. 0705583.3. 2007a: UK.
160. Redwood MD, Paterson-Beedle M, and Macaskie LE (2007b) Integrating dark and light biohydrogen production strategies: towards the hydrogen economy. *Rev Environ Sci Bio/Technol* in submission
161. Richard HT and Foster JW (2003) Acid resistance in *Escherichia coli*. *Adv Appl Microbiol* 52:167-86.
162. Rocha JS, Barbosa MJ, and Wijffels RH, Hydrogen production by photoheterotrophic bacteria: Culture media, yields and efficiencies, in *Biohydrogen II : An Approach to Environmentally Acceptable Technology*, J. Miyake, T. Matsunaga, and A. San Pietro, Editors. 2001, Pergamon. p. 3-32.
163. Roddy D Making a viable fuel cell industry happen in the Tees Valley. *Fuel Cells Bulletin* January 2004:10-12.
164. Rodhe H (1990) A comparison of the contribution of various gases to the greenhouse effect. *Science* 248(4960):1217-1219.
165. Roe AJ, McLaggan D, Davidson I, O'Byrne C, and Booth IR (1998) Perturbation of anion balance during inhibition of growth of *Echerichia coli* by weak acids. *J Bacteriol* 180(4):767-722.
166. Roe AJ, O'Byrne C, McLaggan D, and Booth IR (2002) Inhibition of *Escherichia coli* growth by acetic acid: a problem with methionine biosynthesis and homocysteine toxicity. *Microbiology* 148(Pt 7):2215-2222.
167. Rogers PL, Jeon YJ, and Svenson CJ (2005) Application of biotechnology to industrial sustainability. *Trans IChemE Part B* 83(B6):499-503.
168. Rossman R, Sawers RG, and Bock A (1991) Mechanism of regulation of the formate-hydrogenlyase pathway by oxygen, nitrate, and pH: definition of the formate regulon. *Mol Microbiol* 5(11):2807-2814.
169. Sasikala K, Ramana CV, and Rao PR (1992) Photoproduction of hydrogen from the waste water of a distillery by *Rhodobacter sphaeroides* O.U. 001. *Int J Hydrogen Energy* 17(1):23-27.
170. Sasikala K, Ramana CV, Rao PR, and Kovacs KL (1995) Anoxygenic phototrophic bacteria : Physiology and advances in hydrogen production technology. *Adv Appl Microbiol* 38:211-295.
171. Sato K, Nishina Y, and Shiga K (2003) Purification of electron-transferring flavoprotein from *Megasphaera elsdenii* and binding of additional FAD with an unusual absorption spectrum. *J Biochem (Tokyo)* 134(5):719-729.

172. Sauter M, Bohm R, and Bock A (1992) Mutational analysis of the operon (*hyc*) determining hydrogenase-3 formation in *Escherichia coli*. *Mol Microbiol* 6(11):1523-1532.
173. Sawers G (1994) The hydrogenases and formate dehydrogenases of *Escherichia coli*. *Antonie Van Leeuwenhoek* 66(1-3):57-88.
174. Sawers RG (2005) Formate and its role in hydrogen production in *Escherichia coli*. *Biochem Soc Trans* 33:42-46.
175. Shi X-Y and Yu Q-H (2006) Continuous production of hydrogen from mixed volatile fatty acids with *Rhodospseudomonas capsulata*. *Int J Hydrogen Energy* 31:1641-1647.
176. Siemann S, Schneider K, Oley M, and Muller A (2003) Characterization of a tungsten-substituted nitrogenase isolated from *Rhodobacter capsulatus*. *Biochem* 42(13):3846-3857.
177. Skibinski DA, Golby P, Chang YS, Sargent F, Hoffman R, Harper R, Guest JR, Attwood MM, Berks BC, and Andrews SC (2002) Regulation of the hydrogenase-4 operon of *Escherichia coli* by the σ^{54} -dependent transcriptional activators FhlA and HyfR. *J Bacteriol* 184(23):6642-6653.
178. Sode K, Watanabe M, Makimoto H, and Tomiyama M (1999) Construction and characterisation of fermentative lactate dehydrogenase *E. coli* mutant and its potential for bacterial hydrogen production. *Appl Biochem Biotechnol* 77-79:317-323.
179. Sode K, Yamamoto S, and Tomiyama M, Metabolic engineering approaches for the improvement of bacterial hydrogen production based on *Escherichia coli* mixed acid fermentation, in *Biohydrogen II : An Approach to Environmentally Acceptable Technology*, J. Miyake, T. Matsunaga, and A. San Pietro, Editors. 2001, Pergamon. p. 195-204.
180. Sopian K, Ramli W, and Daud W (2006) Challenges and future developments in proton exchange membrane fuel cells. *Renewable Energy* 31:719-727.
181. Splendiani A, Nicolella C, and Livingston AG (2003) A novel biphasic extractive membrane bioreactor for minimization of membrane-attached biofilms. *Biotechnol Bioeng* 83(1):8-19.
182. Stephenson M and Stickland LH (1932) Hydrogenlyases: Bacterial enzymes liberating molecular hydrogen. *Bacteriol J* 26:712-724.
183. Stokes JL (1949) Fermentation of glucose by suspensions of *Escherichia coli*. *J Bacteriol* 57:147-158.
184. Tabita FR, The biochemistry and metabolic regulation of carbon metabolism and CO₂ fixation in purple bacteria, in *Anoxygenic Photosynthetic Bacteria*, R.E. Blankenship, M.T. Madigan, and C.E. Bauer, Editors. 1995. p. 885-914.
185. Taniyama T, Ohta E, and Sato T (1997) Observation of 4d ferromagnetism in free-standing Pd fine particles. *Europhys Lett* 38(3):195-200.
186. Taylor GH, *Organic chemistry for students of biology and medicine* 3rd Ed. 1987: Longman, Essex, England.
187. Teske S, Zervos A, and Schäfer O. Energy [R]evolution www.greenpeace.org/raw/content/international/press/reports/energyrevolutionreport.pdf. Jan 2007.
188. Thomas CE, James BD, Lomax FD, and Kuhn IF (2000) Fuel options for the fuel cell vehicle: hydrogen, methanol or gasoline? *Int J Hydrogen Energy* 25(6):551-567.
189. Thorpe C and Kim JJ (1995) Structure and mechanism of action of the acyl-CoA dehydrogenases. *FASEB J* 9(9):718-725.

190. Tsygankov A (2007) Nitrogen-fixing cyanobacteria: A review. *Appl Biochem Microbiol* 43(3):250.
191. Tsygankov AA, Fedorov AS, Laurinavichene TV, Gogotov IN, Rao KK, and Hall DO (1998) Actual and potential rates of hydrogen photoproduction by continuous culture of the purple non-sulphur bacterium *Rhodobacter capsulatus*. *Appl Microbiol Biotechnol* 49(1):102-107.
192. Tsygankov AA (2001) Laboratory scale photobioreactors. *Appl Biochem Microbiol* 37(4):333-341.
193. Tsygankov AA, Fedorov AS, Kosourov SN, and Rao KK (2002) Hydrogen production by cyanobacteria in an automated outdoor photobioreactor under aerobic conditions. *Biotechnol Bioeng* 80(7):777-83.
194. Turkarslan S, Yiğit OD, Aslan K, Eroğlu I, and Gündüz U. Photobiological hydrogen production by *R. sphaeroides* O.U 001 by utilisation of waste water from milk industry. in *International Conference on Biological Hydrogen Production*. 1997. Waikoloa, Hawaii: Plenum Press, New York. p. 143.
195. Ueno Y, Kawai T, Sato S, Otsuka S, and Morimoto S (1995) Biological production of hydrogen from cellulose by natural anaerobic microflora. *J Ferment Bioeng* 97(4):395-397.
196. Valdez-Vazquez I, Rios-Leal E, Carmona-Martinez A, Munoz-Paez KM, and Poggi-Varaldo HM (2006) Improvement of biohydrogen production from solid wastes by intermittent venting and gas flushing of batch reactors headspace. *Environ Sci Technol* 40:3509-3415.
197. van Praag E, Degli Agosti R, and Bachofen R (2002) Selenite reduction and uptake hydrogenase activity in *Rhodospirillum rubrum*. *Arch Sci* 55(2):69-80.
198. Vasilyeva L, Miyake M, Khatipov E, Wakayama T, Sekine M, Hara M, Nakada E, Asada Y, and Miyake J (1999) Enhanced hydrogen production by a mutant of *R. sphaeroides* having an altered light-harvesting system. *J Biosci Bioeng* 87(5):619-624.
199. Vignais PM, Toussaint B, and Colbeau A, Regulation of hydrogenase gene expression, in *Anoxygenic Photosynthetic Bacteria*, R.E. Blankenship, M.T. Madigan, and C.E. Bauer, Editors. 1995, Springer Netherlands. p. 1175-1190.
200. Walter A and Gutknecht J (1984) Monocarboxylic acid permeation through lipid bilayer-membranes. *J Memb Biol* 77(3):255-264.
201. Wang Q, Cheng G, Sun X, and Jin B (2006) Recovery of lactic acid from kitchen garbage fermentation broth by four-compartment configuration electro dialyzer. *Process Biochem* 41:152-158.
202. Warnecke T and Gill RT (2005) Organic acid toxicity, tolerance, and production in *Escherichia coli* biorefining applications. *Microb Cell Fact* 4:25.
203. Wasewar KL (2005) Separation of lactic acid: Recent advances. *Chem Biochem Eng Q* 19(2):159-172.
204. Wee J-H, Lee K-Y, and Kim SH (2007) Fabrication methods for low-Pt-loading electrocatalysts in proton exchange membrane fuel cell systems. *J Pow Sour* 165:667.
205. Wee YJ, Yun JS, Lee YY, Zeng AP, and Ryu HW (2005) Recovery of lactic acid by repeated batch electro dialysis and lactic acid production using electro dialysis wastewater. *J Biosci Bioeng* 99(2):104-108.
206. Weetall HH, Sharma BP, and Detar CC (1989) Photometabolic production of hydrogen from organic substrates by free and immobilised mixed cultures of *Rhodospirillum rubrum* and *Klebsiella pneumoniae*. *Biotechnol Bioeng* 23:605-614.

207. Wilson MS and Gottesfeld S (1992) Thin-film catalyst layers for polymer electrolyte fuel cell electrodes. *J Appl Electrochem* 22(1):1-7.
208. Xu T (2005) Ion exchange membranes: State of their development and perspective. *J Memb Sci* 263:1-29.
209. Yamada A, Miyagishima N, and Matsunaga T (1997) Tellurite removal by marine photosynthetic bacteria. *J Mar Biotechnol* 5(1):46-49.
210. Yetis M, Gündüz U, Eroğlu I, Yücel M, and Türker L (2000) Photoproduction of hydrogen from sugar refinery wastewater by *Rhodobacter sphaeroides* O.U. 001. *Int J Hydrogen Energy* 25:1035-1041.
211. Yokoi H, Saitsu A, Uchida H, Hirose J, Hayashi S, and Takasaki Y (2001) Microbial hydrogen production from sweet potato starch residue. *J Biosci Bioeng* 91(1):58-63.
212. Yong P, Farr JPG, Harris IR, and Macaskie LE (2002) Palladium recovery by immobilized cells of *Desulfovibrio desulfuricans* using hydrogen as the electron donor in a novel electrobioreactor. *Biotechnol Lett* 24(3):205-212.
213. Yong P, Rowson NA, Farr JPG, Harris IR, and Macaskie LE (2002) Bioreduction and biocrystallization of palladium by *Desulfovibrio desulfuricans* NCIMB 8307. *Biotechnol Bioeng* 80(4):369-379.
214. Yong P, Rowson NA, Farr JPG, Harris IR, and Macaskie LE (2003) A novel electrobiotechnology for the recovery of precious metals from spent automotive catalysts. *Environ Technol* 24(3):289-297.
215. Yong P, Mikheenko IP, and Macaskie LE (2007) A novel fuel cell catalyst for clean energy production based on a bionanocatalyst. *Adv Mat Res* 20-21:655-658.
216. Yong P, Paterson-Beedle M, Mikheenko IP, and Macaskie LE (2007) From bio-mineralisation to fuel cells: biomanufacture of Pt and Pd nanocrystals for fuel cell electrode catalyst. *Biotechnol Lett* 29:539-544.
217. Yoshida A, Nishimura T, Kawaguchi H, Inui M, and Yukawa H (2005) Enhanced hydrogen production from formic acid by formate hydrogen lyase-overexpressing *Escherichia coli* strains. *Appl Environ Microbiol* 71(11):6762-6768.
218. Yoshida A, Nishimura T, Kawaguchi H, Inui M, and Yukawa H (2007) Efficient induction of formate hydrogen lyase of aerobically grown *Escherichia coli* in a three-step biohydrogen production process. *Appl Microbiol Biotechnol* 74:754-760.
219. Zacchi G and Axelsson A (1989) Economic evaluation of preconcentration in product and of ethanol from dilute sugar solutions. *Biotechnol Bioeng* 34:223-233.
220. Zelic B, Gostovic S, Vuorilehto K, Vasic-Racki D, and Takors R (2004) Process strategies to enhance pyruvate production with recombinant *Escherichia coli*: From repetitive fed-batch to *in situ* product recovery with fully integrated electrodialysis. *Biotechnol Bioeng* 85(6):638-646.
221. Zhang S-T, Matsuoka H, and Toda K (1993) Production and recovery of propionic and acetic acids in electrodialysis culture of *Propionibacterium shermanii*. *J Ferment Bioeng* 75:276-282.